Geometric integration applied to moving mesh methods and degenerate Lagrangians

Thesis by

Tomasz M. Tyranowski

In Partial Fulfillment of the Requirements

for the Degree of

Doctor of Philosophy

California Institute of Technology

Pasadena, California

2014

(Defended September 26, 2013)

Mojej Mamie

"Necessitas in loco, spes in virtute, salus in victoria."

Stanisław Żółkiewski

Acknowledgments

Dear Reader, the thesis you are about to read is the end product of my life and work at Caltech. What an amazing adventure it has been! I will certainly remember this time as the most formative years of my life. The fantastically culturally diverse environment of Caltech has helped me redefine myself as an adult individual and acquire a better understanding of who I am and where I come from. The interaction with many amazing people and exposition to a broad spectrum of views, opinions, and persuasions have given me a new perspective on my own system of values—I have reinforced my beliefs on some issues, formed new ones, and completely changed on others. I am very thankful for this enlightening experience. And for the virtually always sunny skies of California!

Fate, however, has not spared me some difficult moments. Without doubt the greatest blow, both personally and professionally, was the death of my advisor, Jerrold E. Marsden. Jerry was the reason I came to Caltech. I had first met him during one of my summer internships at Caltech, and at that time I decided that if I got into graduate school here, I wanted to work in his group. I was very happy when he agreed to be my advisor. I was fascinated by the research ongoing in his group. I loved the interplay between geometry, physics, and computations. I will remember Jerry as a great mind, an extremely knowledgeable person, and an excellent teacher. His differential geometry course was the most demanding, yet the most rewarding class I have ever taken. Jerry was also very kind and approachable, and he always had time when I wanted to talk to him. Even though I did not get a chance to interact with him as much as I wanted, I continue to learn from him through his prolific body of work, papers, and textbooks. It is beyond me how he found time to write all those wonderful things. I feel greatly honored to be able to call myself one of his students.

Jerry's passing greatly affected my well-being, and left me somewhat disillusioned and worried about my future. It is thanks to a number of people that I have successfully

completed my studies. First and foremost, I would like to express my gratitude to my co-advisor, Mathieu Desbrun, for his invaluable help, support, and all the great advice he has given me over the years. And for all the Polish-French jokes we shared.

I also would like to thank my defense committee members, James L. Beck, Thomas Y. Hou, and Houman Owhadi, for their comments, which greatly improved the final version of this thesis, and suggestions on the possible extensions of my work.

I would like to acknowledge a number of other people whose insights to varying degrees influenced my research. I thank Ernst Hairer, Michael Holst, Eva Kanso, Melvin Leok, Patrick Mullen, Tudor Ratiu, Ari Stern, and Abigail Wacher for useful discussions and remarks. I feel particularly indebted to Joris Vankerschaver. Joris, thank you for your friendly support, and all the scientific and non-scientific conversations we had. I think that putting me in touch with you was the best thing Jerry ever did for me.

The CMS department has been running smoothly thanks to the brilliant and super-friendly administrative staff. My sincere thanks to Jeri Chittum, Sydney Garstang, Maria Lopez, and Sheila Shull. Special thanks to Sydney for answering my countless questions about punctuation and writing style.

Next, I would like to thank my fellow ACM students and colleagues: Patrick Sanan, Michael McCoy, Gemma Mason, Melissa Yeung, Fernando de Goes, Keenan Crane, Peyman Tavallali, Eldar Akhmetgaliyev, Dzhelil Rufat, Yong Sheng Soh, Alex Gittens, Richard Chen, and Theodore Dikaliotis. Thank you for all the conversations we had, whether it was last week, or a few years back.

My life here would have been utterly miserable without friends. Thank you all for sharing laughs with me, for cheering me up when I was feeling down, and for all the crazy stuff we did together (yay, skydiving!). In no particular order, I would like to thank Paula Popescu, Esperanza Linares, Vaclav Cvicek, Aleksander Kubica, Aron Varga, Tadek Prochwicz, Justyna Jarzębińska, Marcin Machura, Mateusz Koreń, Marek Rams, and Wojtek Makowiecki; very special thanks to my dear ballroom dance buddies: Chieh-feng Chang, Devvrath Khatri, Hannah Hoersting, Shang-Lin Chen, Caitlin Scott, Wendy Mercer, Wendy Li, Megan & Robert Nissen, Neil Halelamien, Kevin Mooney, Branimir Ćaćić, Amanda Shing, Jay Daigle, Hari Narayanan, Artemis Ailianou, Sarah Gustafson, and David Levitan.

I would like to express my appreciation and gratitude to Marie Nacua, Helen Sok, and Yelena Tuzova. Thank you for your friendship, and above all, for restoring my faith in

people.

Last but not least, I owe a debt of gratitude to my mother, Urszula Tyranowska, for her continual love and support. Mom, thank you for all the sacrifices you made in your life, so I could pursue my dreams. I don't know how I am ever going to repay you. *Mamo, dziękuję Ci za wszystko!*

Abstract

Moving mesh methods (also called r-adaptive methods) are space-adaptive strategies used for the numerical simulation of time-dependent partial differential equations. These methods keep the total number of mesh points fixed during the simulation, but redistribute them over time to follow the areas where a higher mesh point density is required. There are a very limited number of moving mesh methods designed for solving field-theoretic partial differential equations, and the numerical analysis of the resulting schemes is challenging. In this thesis we present two ways to construct r-adaptive variational and multisymplectic integrators for (1+1)-dimensional Lagrangian field theories. The first method uses a variational discretization of the physical equations and the mesh equations are then coupled in a way typical of the existing r-adaptive schemes. The second method treats the mesh points as pseudo-particles and incorporates their dynamics directly into the variational principle. A user-specified adaptation strategy is then enforced through Lagrange multipliers as a constraint on the dynamics of both the physical field and the mesh points. We discuss the advantages and limitations of our methods. The proposed methods are readily applicable to (weakly) non-degenerate field theories—numerical results for the Sine-Gordon equation are presented.

In an attempt to extend our approach to degenerate field theories, in the last part of this thesis we construct higher-order variational integrators for a class of degenerate systems described by Lagrangians that are linear in velocities. We analyze the geometry underlying such systems and develop the appropriate theory for variational integration. Our main observation is that the evolution takes place on the primary constraint and the 'Hamiltonian' equations of motion can be formulated as an index 1 differential-algebraic system. We then proceed to construct variational Runge-Kutta methods and analyze their properties. The general properties of Runge-Kutta methods depend on the 'velocity' part of the Lagrangian. If the 'velocity' part is also linear in the position coordinate, then we

show that non-partitioned variational Runge-Kutta methods are equivalent to integration of the corresponding first-order Euler-Lagrange equations, which have the form of a Poisson system with a constant structure matrix, and the classical properties of the Runge-Kutta method are retained. If the 'velocity' part is nonlinear in the position coordinate, we observe a reduction of the order of convergence, which is typical of numerical integration of DAEs. We also apply our methods to several models and present the results of our numerical experiments.

Contents

List of Figures

List of Tables

Chapter 1

Introduction

The main purpose of this thesis is to design, analyze, and implement variational and multisymplectic integrators for Lagrangian partial differential equations with space-adaptive meshes. We combine geometric numerical integration and r-adaptive methods for the numerical solution of PDEs, and we show that these two fields are compatible—mostly due to the fact that in r-adaptation the number of mesh points remains constant and we can treat them as additional pseudo-particles whose dynamics is coupled to the dynamics of the physical field of interest.

Variational integrators

Geometric (or structure-preserving) integrators are numerical methods that preserve geometric properties of the flow of a differential equation (see [23], [42], [57]). This class encompasses symplectic integrators for Hamiltonian systems, variational integrators for Lagrangian systems, and numerical methods on manifolds, including Lie group methods and integrators for constrained mechanical systems. The main motivation for developing structure-preserving algorithms lies in the fact that they show excellent numerical behavior, especially for long-time integration of equations possessing geometric properties. Geometric integrators proved to be extremely useful for numerical computations in astronomy, molecular dynamics, mechanics, and theoretical physics.

An important class of structure-preserving integrators are *variational integrators* for Lagrangian systems ([23], [41]). This type of integrators is based on discrete variational principles. The variational approach provides a unified framework for the analysis of many symplectic algorithms and is characterized by a natural treatment of the discrete Noether

theorem, as well as forced, dissipative, and constrained systems. Variational integrators were first introduced in the context of finite-dimensional mechanical systems, but later Marsden & Patrick & Shkoller [39] generalized this idea to field theories. Variational integrators have since then been successfully applied in many computations, for example in elasticity ([36]), electrodynamics ([59]), or fluid dynamics ([47]). The existing variational integrators so far have been developed on static, mostly uniform spatial meshes.

Moving mesh methods

Adaptive meshes used for the numerical solution of partial differential equations fall into three main categories: h-adaptive, p-adaptive, and r-adaptive. R-adaptive methods, which are also known as *moving mesh methods* ([7], [28]), keep the total number of mesh points fixed during the simulation, but relocate them over time. These methods are designed to minimize the error of computations by optimally distributing the mesh points, contrasting with h-adaptive methods, for which the accuracy of the computations is obtained via insertion and deletion of mesh points. Moving mesh methods are a large and interesting research field of applied mathematics, and their role in modern computational modeling is growing. Despite the increasing interest in these methods in recent years, they are still in a relatively early stage of development compared to the more matured h-adaptive methods.

There are three logical steps to r-adaptation:

- Discretization of the physical PDE;
- Mesh adaptation strategy;
- Coupling the mesh equations to the physical equations.

The key ideas of this thesis regard the first and the last step. Following the general spirit of variational integrators, we discretize the underlying action functional rather than the PDE itself, and then derive the discrete equations of motion. We base our adaptation strategies on the equidistribution principle and the resulting moving mesh partial differential equations (MMPDEs). We interpret MMPDEs as constraints, which allows us to consider *novel* ways of coupling them to the physical equations. Note that we will restrict our explanations to one time and one space dimension for the sake of simplicity. As an application example we apply our space-adaptive methods to the Sine-Gordon equation.

Lagrangians linear in velocities

We further attempt to extend these r-adaptive methods to degenerate field theories, e.g., the nonlinear Schrödinger equation. The main difficulty is the fact that upon spatial discretization the nonlinear Schrödinger equation turns into a (finite-dimensional) mechanical system whose Lagrangian is linear in velocities. Low-order variational time integrators for such systems were proposed in [56] and [65], but due to stiffness, space-adaptive methods usually require higher-order integration. Therefore, in the last part of this thesis we turn our attention to Lagrangians linear in velocities, develop general variational integration theory, and construct variational partitioned Runge-Kutta methods for such systems.

Theoretical aspects of variational integration are well understood in the case when the Lagrangian describing the considered system is regular, that is, when the corresponding Legendre transform is (at least locally) invertible. However, the corresponding theory for degenerate Lagrangian systems is less developed. The analysis of degenerate systems becomes a little more cumbersome, because the Euler-Lagrange equations may cease to be second order, or may not even make any sense at all. In the latter case one needs to determine if there exists a submanifold of the configuration bundle TQ on which consistent equations of motion can be derived. This can be accomplished by applying the Dirac theory of constraints or the pre-symplectic constraint algorithm (see [18], [38]).

A particularly simple case of degeneracy occurs when the Lagrangian is linear in velocities. In that case, the dynamics of the system is defined on the configuration manifold Q itself, rather than its tangent bundle TQ, provided some regularity conditions are satisfied. Such systems arise in many physical applications, including interacting point vortices in the plane (see [45], [56], [65]), or partial differential equations such as the nonlinear Schrödinger ([16]), KdV ([11], [19]) or Camassa-Holm equations ([8], [9]). In Chapter 7 we show how certain Poisson systems can be recast as Lagrangian systems whose Lagrangians are linear in velocities. Therefore, our approach offers a new perspective on geometric integration of Poisson systems, which often arise as semi-discretizations of some integrable nonlinear partial differential equations, e.g., the Toda or Volterra lattice equations, and play an important role in the modeling of many physical phenomena (see [13], [33], [60]).

Outline and contributions

This thesis is organized as follows. In Chapter 2 and Chapter 3 we present an overview of geometric integration and moving mesh methods, respectively. Chapters 4-7 constitute the main contributions of the thesis. In Chapter 4 we propose two general ideas on how to combine geometric integration and moving mesh methods, namely the control-theoretic and the Lagrange multiplier strategies, and construct several r-adaptive variational integrators. In Chapter 5 we show how similar integrators can be be constructed using the covariant formalism of multisymplectic field theory. In Chapter 6 we apply our integrators to the Sine-Gordon equation and we present our numerical results. In Chapter 7 we analyze systems with Lagrangians linear in velocities, investigate how the theory of variational integration differs from the non-degenerate case, and then proceed to construct variational partitioned Runge-Kutta schemes for such systems. We summarize our work in Chapter 8 and discuss several directions in which it can be extended. Chapters 4-6 were published in [63], and Chapter 7 in [64].

Chapter 2

Background: Geometric integration

In this chapter we review the basics of geometric mechanics, multisymplectic field theory and geometric numerical integration. We focus on the most important aspects which are critical for the understanding of the later chapters of this thesis. We refer the interested reader to literature for proofs and more details.

2.1 Hamiltonian mechanics

Let Q be the n-dimensional configuration manifold of a system. The evolution of a Hamiltonian system is defined on the cotangent bundle T^*Q, also called the *phase space*. Let q^μ denote local coordinates on Q, where $\mu = 1, \dots, n$, and let (q^μ, p_μ) denote the corresponding canonical coordinates on T^*Q. A Hamiltonian system is defined by specifying a smooth function $H : T^*Q \longrightarrow \mathbb{R}$, the so-called Hamiltonian.

The cotangent bundle T^*Q possesses an intrinsic symplectic structure. We first define the canonical Cartan one-form $\Theta : T^*Q \longrightarrow T^*T^*Q$ by the formula

$$\Theta(\omega) = (\pi_{T^*Q})^*\omega \tag{2.1.1}$$

for any $\omega \in T^*Q$, where $\pi_{T^*Q} : T^*Q \longrightarrow Q$ is the cotangent bundle projection, and $(\pi_{T^*Q})^*$ denotes the pull-back by π_{T^*Q}. In canonical coordinates we have

$$\Theta = p_\mu dq^\mu, \tag{2.1.2}$$

where summation over repeated Greek indices is implied. The canonical symplectic two-

form is then defined by

$$\Omega = -d\Theta = dq^\mu \wedge dp_\mu. \tag{2.1.3}$$

A vector field $Z : T^*Q \longrightarrow TT^*Q$ on the cotangent bundle is called *Hamiltonian*, if it satisfies the equation

$$i_Z\Omega = dH, \tag{2.1.4}$$

where $i_Z\Omega$ is the interior product of Z and Ω (also denoted by $Z \lrcorner \Omega$), i.e., the one-form such that $i_Z\Omega \cdot V = \Omega(Z, V)$ for any vector field V on T^*Q. The *Hamiltonian equations* for H are the system of differential equations satisfied by the flow $F_t^H : T^*Q \longrightarrow T^*Q$ for Z, that is,

$$\frac{d}{dt}F_t^H = Z \circ F_t^H. \tag{2.1.5}$$

If in canonical coordinates $(q^\mu(t), p_\mu(t)) = F_t^H(\bar{q}^\mu, \bar{p}_\mu)$ for some initial condition $(\bar{q}^\mu, \bar{p}_\mu)$, then the Hamiltonian equations take the well-known form

$$\begin{aligned} \dot{q}^\mu &= \frac{\partial H}{\partial p_\mu}, \\ \dot{p}_\mu &= -\frac{\partial H}{\partial q^\mu}. \end{aligned} \tag{2.1.6}$$

The most important properties of Hamiltonian systems are summarized in the following theorems.

Theorem 2.1.1. *The flow F_t^H for* (2.1.6) *preserves the Hamiltonian, that is, $H \circ F_t^H = H$ for all $t \in \mathbb{R}$.*

Theorem 2.1.2. *The flow F_t^H for* (2.1.6) *is symplectic, that is,*

$$(F_t^H)^*\Omega = \Omega, \qquad \forall t \in \mathbb{R}. \tag{2.1.7}$$

Expressed in canonical coordinates, the symplecticity condition takes the form

$$(DF_t^H)^T \begin{pmatrix} 0 & I \\ -I & 0 \end{pmatrix} DF_t^H = \begin{pmatrix} 0 & I \\ -I & 0 \end{pmatrix}, \qquad \forall t \in \mathbb{R}, \tag{2.1.8}$$

where DF_t^H denotes the Jacobian of the local coordinate representative of the flow F_t^H, and I is the $n \times n$ identity matrix.

We refer the reader to [23] and [38] for the proofs of these theorems and more information on Hamiltonian systems.

2.2 Symplectic integrators for Hamiltonian systems

2.2.1 Basic definitions

The purpose of the numerical integration of the Hamiltonian system (2.1.6) is to determine an approximate solution at the discrete set of times $t_k = kh$, where h is the time step and $k = 0, 1, 2, \ldots$ A numerical scheme is defined by specifying a map $F_h : T^*Q \longrightarrow T^*Q$ which approximates the exact Hamiltonian flow F_h^H. Let us consider canonical coordinates, and for brevity denote $q = (q^1, \ldots, q^n)$ and $p = (p_1, \ldots, p_n)$. Given the initial condition $(q_0, p_0) \in T^*Q$, the numerical solution is defined by the iteration

$$(q_{k+1}, p_{k+1}) = F_h(q_k, p_k), \tag{2.2.1}$$

where (q_k, p_k) approximates the exact solution at time $t = t_k$. Of particular interest is the rate at which F_h converges to F_h^H as $h \longrightarrow 0$. One usually considers a *local error* (error made after one step) and a *global error* (error made after many steps). We will assume the following definitions (see [23], [24], [26], [41]).

Definition 2.2.1. *A numerical scheme for the Hamiltonian system* (2.1.6) *defined by the map F_h is of order r if there exists an open set $U \subset T^*Q$ and constants $C > 0$ and $\bar{h} > 0$ such that*

$$\left\| F_h(q,p) - F_h^H(q,p) \right\| \leq C h^{r+1} \tag{2.2.2}$$

for all $(q,p) \in U$ and $h \leq \bar{h}$.

Definition 2.2.2. *A numerical scheme for the Hamiltonian system* (2.1.6) *defined by the map F_h is convergent of order r if there exists an open set $U \subset T^*Q$ and constants $C > 0$, $\bar{h} > 0$ and $\bar{T} > 0$ such that*

$$\left\| (F_h)^K(q,p) - F_T^H(q,p) \right\| \leq Ch^{r+1}, \tag{2.2.3}$$

where $h = T/K$, for all $(q,p) \in U$, $h \leq \bar{h}$, and $T \leq \bar{T}$.

Under some smoothness assumptions, one can show that if the method F_h is of order r, then it is also convergent of order r (see [24]).

The symplectic structure of Hamiltonian systems has many important physical and mathematical consequences, therefore it is beneficial to preserve it in numerical computations as well. This gives rise to the class of *symplectic integrators*.

Definition 2.2.3. *A numerical scheme for the Hamiltonian system* (2.1.6) *defined by the map F_h is called symplectic if in canonical coordinates F_h satisfies the condition*

$$(DF_h)^T \begin{pmatrix} 0 & I \\ -I & 0 \end{pmatrix} DF_h = \begin{pmatrix} 0 & I \\ -I & 0 \end{pmatrix}, \tag{2.2.4}$$

where DF_h denotes the Jacobian of the numerical flow F_h, and I is the $n \times n$ identity matrix.

Example: Symplectic Euler scheme. The so-called symplectic Euler scheme is a simple integrator for (2.1.6) and is given by the formula

$$\begin{aligned} q_{k+1} &= q_k + h\frac{\partial H}{\partial p}(q_{k+1}, p_k), \\ p_{k+1} &= p_k - h\frac{\partial H}{\partial q}(q_{k+1}, p_k). \end{aligned} \tag{2.2.5}$$

This system of equations implicitly defines F_h: given (q_k, p_k), it has to be solved (using Newton's method for instance) for (q_{k+1}, p_{k+1}). It can be shown that the symplectic Euler method is symplectic and first-order accurate (see [23]).

2.2.2 Runge-Kutta methods

Higher-order symplectic integrators can be constructed as Runge-Kutta and partitioned Runge-Kutta methods. Let us review Runge-Kutta methods first.

Definition 2.2.4. *Let b_i, a_{ij} $(i,j = 1,\dots,s)$ be real numbers and let $c_i = \sum_{j=1}^{s} a_{ij}$. An s-stage Runge-Kutta method for the Hamiltonian system* (2.1.6) *is defined by*

$$\begin{aligned}
\dot{Q}_i &= \frac{\partial H}{\partial p}(Q_i, P_i), && i = 1,\dots,s,\\
\dot{P}_i &= -\frac{\partial H}{\partial q}(Q_i, P_i), && i = 1,\dots,s,\\
Q_i &= q_k + h\sum_{j=1}^{s} a_{ij}\dot{Q}_j, && i = 1,\dots,s,\\
P_i &= p_k + h\sum_{j=1}^{s} a_{ij}\dot{P}_j, && i = 1,\dots,s,\\
q_{k+1} &= q_k + h\sum_{i=1}^{s} b_i\dot{Q}_i,\\
p_{k+1} &= p_k + h\sum_{i=1}^{s} b_i\dot{P}_i.
\end{aligned} \tag{2.2.6}$$

If $a_{ij} = 0$ for $i \le j$, then the method is called *explicit*, and the internal stages Q_i, P_i, $\dot{Q}_i$, and $\dot{P}_i$ are determined by a series of explicit assignments. Otherwise the method is called *implicit*, and the system (2.2.6) has to be simultaneously solved for all Q_i, P_i, $\dot{Q}_i$, and $\dot{P}_i$ before one can compute q_{k+1} and p_{k+1}. The coefficients a_{ij}, b_i, and c_i are often arranged into a table, the so-called Butcher's tableau of the Runge-Kutta method,

$$\begin{array}{c|ccc}
c_1 & a_{11} & \cdots & a_{1s}\\
\vdots & \vdots & & \vdots\\
c_s & a_{s1} & \cdots & a_{ss}\\
\hline
 & b_1 & \cdots & b_s
\end{array} \tag{2.2.7}$$

Verner's method of order 6 is an example of an 8-stage explicit Runge-Kutta method (see Table 2.1). The 3-stage Radau IIA scheme is implicit and fifth order (see Table 2.2). This method is also *stiffly accurate*, that is, its coefficients satisfy $a_{sj} = b_j$ for $j = 1,\dots,s$, so the numerical value of the solution at the new time step is equal to the value of the last internal stage, which is beneficial when solving differential-algebraic equations. The Radau IIA

0							
$\frac{1}{6}$	$\frac{1}{6}$						
$\frac{4}{15}$	$\frac{4}{75}$	$\frac{16}{75}$					
$\frac{2}{3}$	$\frac{5}{6}$	$-\frac{8}{3}$	$\frac{5}{2}$				
$\frac{5}{6}$	$-\frac{165}{64}$	$\frac{55}{6}$	$-\frac{425}{64}$	$\frac{85}{96}$			
1	$\frac{12}{5}$	-8	$\frac{4015}{612}$	$-\frac{11}{36}$	$\frac{88}{255}$		
$\frac{1}{15}$	$-\frac{8263}{15000}$	$\frac{124}{75}$	$-\frac{643}{680}$	$-\frac{81}{250}$	$\frac{2484}{10625}$	0	
1	$\frac{3501}{1720}$	$-\frac{300}{43}$	$\frac{297275}{52632}$	$-\frac{319}{2322}$	$\frac{24068}{84065}$	0	$\frac{3850}{26703}$
	$\frac{3}{40}$	0	$\frac{875}{2244}$	$\frac{23}{72}$	$\frac{264}{1955}$	0	$\frac{125}{11592}$ $\quad$ $\frac{43}{616}$

Table 2.1: Verner's method of order 6

$\frac{4-\sqrt{6}}{10}$	$\frac{88-7\sqrt{6}}{360}$	$\frac{296-169\sqrt{6}}{1800}$	$\frac{-2+3\sqrt{6}}{225}$
$\frac{4+\sqrt{6}}{10}$	$\frac{296+169\sqrt{6}}{1800}$	$\frac{88+7\sqrt{6}}{360}$	$\frac{-2-3\sqrt{6}}{225}$
1	$\frac{16-\sqrt{6}}{36}$	$\frac{16+\sqrt{6}}{36}$	$\frac{1}{9}$
	$\frac{16-\sqrt{6}}{36}$	$\frac{16+\sqrt{6}}{36}$	$\frac{1}{9}$

Table 2.2: The 3-stage Radau IIA method of order 5

methods are in general known for their excellent stability properties when applied to stiff differential equations (see [26]). Of particular interest to us is the family of Gauss methods, whose first three members are shown in Table 2.3. The 1-stage Gauss method is also known as the *midpoint rule*.

The following general convergence results can be proved (see [23], [26]).

Theorem 2.2.5. *The s-stage Gauss method is of order* $2s$.

Theorem 2.2.6. *The s-stage Radau IIA method is of order* $2s-1$.

The Hamiltonian equations (2.1.6) have a natural partitioned structure, namely the q and the p variables. The idea of partitioned Runge-Kutta methods is to take two different Runge-Kutta methods, and apply the first one to the q variables, and the other to the p variables.

$\frac{1}{2}$	$\frac{1}{2}$
	1

$\frac{1}{2}-\frac{\sqrt{3}}{6}$	$\frac{1}{4}$	$\frac{1}{4}-\frac{\sqrt{3}}{6}$
$\frac{1}{2}+\frac{\sqrt{3}}{6}$	$\frac{1}{4}+\frac{\sqrt{3}}{6}$	$\frac{1}{4}$
	$\frac{1}{2}$	$\frac{1}{2}$

$\frac{1}{2}-\frac{\sqrt{15}}{10}$	$\frac{5}{36}$	$\frac{2}{9}-\frac{\sqrt{15}}{15}$	$\frac{5}{36}-\frac{\sqrt{15}}{30}$
$\frac{1}{2}$	$\frac{5}{36}+\frac{\sqrt{15}}{24}$	$\frac{2}{9}$	$\frac{5}{36}-\frac{\sqrt{15}}{24}$
$\frac{1}{2}+\frac{\sqrt{15}}{10}$	$\frac{5}{36}+\frac{\sqrt{15}}{30}$	$\frac{2}{9}+\frac{\sqrt{15}}{15}$	$\frac{5}{36}$
	$\frac{5}{18}$	$\frac{4}{9}$	$\frac{5}{18}$

Table 2.3: Gauss methods of order 2, 4, and 6

Definition 2.2.7. *Let b_i, a_{ij} and $\bar{b}_i$, $\bar{a}_{ij}$ $(i,j=1,\dots,s)$ be the coefficients of two Runge-Kutta methods. An s-stage partitioned Runge-Kutta method for the Hamiltonian system* (2.1.6) *is defined by*

$$\begin{aligned}
\dot{Q}_i &= \frac{\partial H}{\partial p}(Q_i,P_i), && i=1,\dots,s,\\
\dot{P}_i &= -\frac{\partial H}{\partial q}(Q_i,P_i), && i=1,\dots,s,\\
Q_i &= q_k + h\sum_{j=1}^{s} a_{ij}\dot{Q}_j, && i=1,\dots,s,\\
P_i &= p_k + h\sum_{j=1}^{s} \bar{a}_{ij}\dot{P}_j, && i=1,\dots,s,\\
q_{k+1} &= q_k + h\sum_{i=1}^{s} b_i\dot{Q}_i,\\
p_{k+1} &= p_k + h\sum_{i=1}^{s} \bar{b}_i\dot{P}_i.
\end{aligned} \tag{2.2.8}$$

The symplectic Euler method (2.2.5) is an example of a partitioned Runge-Kutta method, where the implicit Euler scheme $b_1=1$, $a_{11}=1$ is combined with the explicit Euler scheme $\bar{b}_1=1$, $\bar{a}_{11}=0$. Of particular interest to us are the Lobatto IIIA-IIIB pairs, that is, partitioned Runge-Kutta methods combining the Lobatto IIIA and Lobatto IIIB schemes (see Table 2.4, Table 2.5, and Table 2.6). The 2-stage Lobatto IIIA-IIIB is also known as *Störmer-Verlet*.

The following convergence result can be proved (see [23], [26]).

Theorem 2.2.8. *The s-stage Lobatto IIIA-IIIB method is of order $2s-2$.*

0	0	0
1	$\frac{1}{2}$	$\frac{1}{2}$
	$\frac{1}{2}$	$\frac{1}{2}$

$\frac{1}{2}$	$\frac{1}{2}$	0
$\frac{1}{2}$	$\frac{1}{2}$	0
	$\frac{1}{2}$	$\frac{1}{2}$

Table 2.4: Lobatto IIIA-IIIB pair of order 2

0	0	0	0
$\frac{1}{2}$	$\frac{5}{24}$	$\frac{1}{3}$	$-\frac{1}{24}$
1	$\frac{1}{6}$	$\frac{2}{3}$	$\frac{1}{6}$
	$\frac{1}{6}$	$\frac{2}{3}$	$\frac{1}{6}$

0	$\frac{1}{6}$	$-\frac{1}{6}$	0
$\frac{1}{2}$	$\frac{1}{6}$	$\frac{1}{3}$	0
1	$\frac{1}{6}$	$\frac{5}{6}$	0
	$\frac{1}{6}$	$\frac{2}{3}$	$\frac{1}{6}$

Table 2.5: Lobatto IIIA-IIIB pair of order 4

0	0	0	0	0
$\frac{5-\sqrt{5}}{10}$	$\frac{11+\sqrt{5}}{120}$	$\frac{25-\sqrt{5}}{120}$	$\frac{25-13\sqrt{5}}{120}$	$\frac{-1+\sqrt{5}}{120}$
$\frac{5+\sqrt{5}}{10}$	$\frac{11-\sqrt{5}}{120}$	$\frac{25+13\sqrt{5}}{120}$	$\frac{25+\sqrt{5}}{120}$	$\frac{-1-\sqrt{5}}{120}$
1	$\frac{1}{12}$	$\frac{5}{12}$	$\frac{5}{12}$	$\frac{1}{12}$
	$\frac{1}{12}$	$\frac{5}{12}$	$\frac{5}{12}$	$\frac{1}{12}$

0	$\frac{1}{12}$	$\frac{-1-\sqrt{5}}{24}$	$\frac{-1+\sqrt{5}}{24}$	0
$\frac{5-\sqrt{5}}{10}$	$\frac{1}{12}$	$\frac{25+\sqrt{5}}{120}$	$\frac{25-13\sqrt{5}}{120}$	0
$\frac{5+\sqrt{5}}{10}$	$\frac{1}{12}$	$\frac{25+13\sqrt{5}}{120}$	$\frac{25-\sqrt{5}}{120}$	0
1	$\frac{1}{12}$	$\frac{11-\sqrt{5}}{24}$	$\frac{11+\sqrt{5}}{24}$	0
	$\frac{1}{12}$	$\frac{5}{12}$	$\frac{5}{12}$	$\frac{1}{12}$

Table 2.6: Lobatto IIIA-IIIB pair of order 6

Symplecticity. In this thesis we are mainly interested in symplectic Runge-Kutta methods. The following criterion for symplecticity holds (see [23], [26], [42], [57]).

Theorem 2.2.9. *If the coefficients of a partitioned Runge-Kutta method* (2.2.8) *satisfy*

$$\begin{aligned} b_i\bar{a}_{ij} + \bar{b}_j a_{ji} &= b_i\bar{b}_j, \qquad i,j = 1,\dots,s, \\ b_i &= \bar{b}_i, \qquad i = 1,\dots,s, \end{aligned} \tag{2.2.9}$$

then it is symplectic.

Note that the Runge-Kutta method (2.2.6) is a special case of a partitioned method with $\bar{a}_{ij} = a_{ij}$ and $\bar{b}_i = b_i$, therefore Theorem 2.2.9 is applicable in that case, too. Consequently, we have:

Theorem 2.2.10. *The Gauss methods are symplectic.*

Theorem 2.2.11. *The Lobatto IIIA-IIIB methods are symplectic.*

2.2.3 Backward error analysis

Consider a system of ordinary differential equations

$$\dot{y} = f(y). \tag{2.2.10}$$

A numerical method F_h produces a sequence of approximations y_0, y_1, y_2, ..., such that $y_k - y(kh) = O(h^{r+1})$, where r is the (global) order of the method (cf. Definition 2.2.2). The idea of backward error analysis is to search for a *modified differential equation* of the form

$$\dot{\tilde{y}} = f(\tilde{y}) + hf_2(\tilde{y}) + h^2 f_3(\tilde{y}) + \dots, \tag{2.2.11}$$

such that $y_k = \tilde{y}(kh)$, and study how this equation is different from (2.2.10).

The true power of symplectic integrators for Hamiltonian equations is revealed through their backward error analysis: a symplectic integrator for the Hamiltonian system (2.1.6) defines the *exact* flow for a nearby Hamiltonian system, whose Hamiltonian can be expressed as the asymptotic series

$$\tilde{H}(q,p) = H(q,p) + hH_2(q,p) + h^2H_3(q,p) + \ldots, \tag{2.2.12}$$

that is, the modified differential equation (2.2.11) is also Hamiltonian. Owing to this fact, under some additional assumptions, symplectic numerical schemes nearly conserve the original Hamiltonian $H(q,p)$ over exponentially long time intervals (see [23] for details).

2.3 Lagrangian mechanics

We will now review the Lagrangian description of mechanics. Unlike in the Hamiltonian approach, the dynamics of a Lagrangian system is defined on the tangent bundle TQ. Let $(q^\mu, \dot{q}^\mu)$, where $\mu = 1, 2, ..., n$, denote local bundle coordinates on TQ. The system is described by defining the Lagrangian $L : TQ \longrightarrow \mathbb{R}$ and the corresponding action functional

$$S[q(t)] = \int_a^b L\big(q^\mu(t), \dot{q}^\mu(t)\big)\, dt. \tag{2.3.1}$$

The dynamics is obtained through Hamilton's principle, which seeks the curves $q(t)$ for which the functional $S[q(t)]$ is stationary under variations of $q(t)$ with fixed endpoints, i.e., we seek $q(t)$ such that

$$dS[q(t)] \cdot \delta q(t) = \frac{d}{d\epsilon}\bigg|_{\epsilon=0} S[q_\epsilon(t)] = 0 \tag{2.3.2}$$

for all $\delta q(t)$ with $\delta q(a) = \delta q(b) = 0$, where $q_\epsilon(t)$ is a smooth family of curves satisfying $q_0 = q$ and $\frac{d}{d\epsilon}\big|_{\epsilon=0} q_\epsilon = \delta q$. By using integration by parts, the Euler-Lagrange equations follow as

$$\frac{\partial L}{\partial q^\mu} - \frac{d}{dt}\frac{\partial L}{\partial \dot{q}^\mu} = 0. \tag{2.3.3}$$

The Lagrangian defines the Legendre transformation $\mathbb{F}L : TQ \longrightarrow T^*Q$, which is the fiber derivative of L, and is intrinsically defined by

$$\mathbb{F}L(v_q) \cdot w_q = \frac{d}{d\epsilon}\bigg|_{\epsilon=0} L(v_q + \epsilon w_q), \tag{2.3.4}$$

where $v_q, w_q \in T_qQ$. In local bundle coordinates we have

$$\mathbb{F}L(q^\mu, \dot{q}^\mu) = \left(q^\mu, \frac{\partial L}{\partial \dot{q}^\mu}\right), \tag{2.3.5}$$

that is,

$$p_\mu = \frac{\partial L}{\partial \dot{q}^\mu}. \tag{2.3.6}$$

If $\mathbb{F}L$ is a local diffeomorphism, then L is said to be *regular*. If $\mathbb{F}L$ is actually a global diffeomorphism of TQ and T^*Q, then we say L is *hyperregular*. Otherwise L is called *degenerate*. The Legendre transform allows to introduce a symplectic structure on TQ. We define the Lagrangian two-form

$$\Omega_L = (\mathbb{F}L)^*\Omega, \tag{2.3.7}$$

where Ω was defined in (2.1.3). If L is regular, then Ω_L is a symplectic form, i.e., it is closed and non-degenerate. If L is degenerate, then Ω_L also becomes degenerate and is then called *pre-symplectic*. We further define the energy $E : TQ \longrightarrow \mathbb{R}$ associated with the Lagrangian L as

$$E(v_q) = \mathbb{F}L(v_q) \cdot v_q - L(v_q), \tag{2.3.8}$$

where $v_q \in T_qQ$. In local bundle coordinates this takes the form

$$E(q^\mu, \dot{q}^\mu) = \frac{\partial L}{\partial \dot{q}^\nu}\dot{q}^\nu - L(q^\mu, \dot{q}^\mu). \tag{2.3.9}$$

We are now in a position to introduce the notion of a Lagrangian vector field. By definition, a Lagrangian vector field $Z : TQ \longrightarrow TTQ$ satisfies the equation

$$i_Z\Omega_L = dE. \tag{2.3.10}$$

Theorem 2.3.1. *The flow $F_t^L : TQ \longrightarrow TQ$ of a Lagrangian vector field Z preserves the energy associated with the Lagrangian, that is, $E \circ F_t^L = E$ for all $t \in \mathbb{R}$.*

If the Lagrangian L is regular, then there exists a unique vector field Z satisfying (2.3.10), and its flow F_t^L satisfies the Euler-Lagrange equations (2.3.3). Moreover, one can

prove the following result.

Theorem 2.3.2. *If the Lagrangian L is regular, then the flow $F_t^L : TQ \longrightarrow TQ$ of the Lagrangian vector field Z is symplectic on TQ, that is, $(F_t^L)^*\Omega_L = \Omega_L$ for all $t \in \mathbb{R}$.*

If the Lagrangian L is hyperregular, then it is possible to relate Lagrangian mechanics on TQ to Hamiltonian mechanics on T^*Q by defining the Hamiltonian $H = E \circ (\mathbb{F}L)^{-1}$. We then have the following equivalence result.

Theorem 2.3.3. *Let L be the hyperregular Lagrangian, and $H = E \circ (\mathbb{F}L)^{-1}$ the corresponding Hamiltonian. If F_t^L is the flow of the Lagrangian vector field Z on TQ and F_t^H the flow of the Hamiltonian vector field Z_H on T^*Q, then the relationship between the evolution on the tangent and cotangent bundles is given by*

$$Z = (\mathbb{F}L)^* Z_H, \qquad F_t^L = (\mathbb{F}L)^{-1} \circ F_t^H \circ \mathbb{F}L. \tag{2.3.11}$$

In coordinates this means that the Hamiltonian equations (2.1.6) are equivalent to the Euler-Lagrange equations (2.3.3). This becomes more evident if one rewrites the Euler-Lagrange equations in the implicit Hamiltonian form as

$$\begin{aligned} p_\mu &= \frac{\partial L}{\partial \dot{q}^\mu}(q, \dot{q}), \\ \dot{p}_\mu &= \frac{\partial L}{\partial q^\mu}(q, \dot{q}). \end{aligned} \tag{2.3.12}$$

If the Lagrangian is hyperregular, then the first equation can be solved for $\dot{q}$ in terms of q and p. This relationship can be then substituted in the second equation, and the whole system will take the form (2.1.6). If the Lagrangian is only regular, then Theorem 2.3.3 has a local character, i.e., the relation between the Lagrangian and Hamiltonian pictures holds in some open neighborhoods of the tangent and cotangent bundles.

If the Lagrangian is degenerate, then the solutions of (2.3.10) may not be unique, or may not even exist at all. In that case one needs to use, e.g., the pre-symplectic constraint algorithm (see [18]) to determine if there is any submanifold of TQ on which (2.3.10) can be solved.

More information on the geometry of Lagrangian systems and variational principles can be found in [38] and [18].

2.4 Variational integrators for Lagrangian systems

2.4.1 Discrete Mechanics

As indicated in Section 2.2, the main purpose of symplectic integration is to preserve at the discrete level the symplectic structure underlying continuous Hamiltonian systems. Similarly, the central idea of variational integration is to preserve the variational structures of Lagrangian systems. This leads to so-called Discrete Mechanics and the underlying idea of discretization due to Veselov. For a Veselov-type discretization we consider the discrete state space $Q \times Q$, which serves as a discrete approximation of the tangent bundle (see [41]). We define a discrete Lagrangian L_d as a smooth map $L_d : Q \times Q \longrightarrow \mathbb{R}$ and the corresponding discrete action

$$S = \sum_{k=0}^{N-1} L_d(q_k, q_{k+1}). \tag{2.4.1}$$

The variational principle now seeks a sequence q_0, q_1, ..., q_N that extremizes S for variations holding the endpoints q_0 and q_N fixed. The Discrete Euler-Lagrange equations follow

$$D_2 L_d(q_{k-1}, q_k) + D_1 L_d(q_k, q_{k+1}) = 0. \tag{2.4.2}$$

Assuming that these equations can be solved for q_{k+1}, i.e., L_d is non-degenerate, they implicitly define the discrete Lagrangian map $F_{L_d} : Q \times Q \longrightarrow Q \times Q$ such that

$$F_{L_d}(q_{k-1}, q_k) = (q_k, q_{k+1}). \tag{2.4.3}$$

Let $(q^\mu, \bar{q}^\mu)$ denote local coordinates on $Q \times Q$. We can define the discrete Legendre transforms $\mathbb{F}L_d^+, \mathbb{F}L_d^- : Q \times Q \longrightarrow T^*Q$, which in local coordinates on $Q \times Q$ and T^*Q are respectively given by

$$\begin{aligned} \mathbb{F}^+ L_d(q, \bar{q}) &= \big(\bar{q}, D_2 L_d(q, \bar{q})\big), \\ \mathbb{F}^- L_d(q, \bar{q}) &= \big(q, -D_1 L_d(q, \bar{q})\big), \end{aligned} \tag{2.4.4}$$

where $q = (q^1, \ldots, q^n)$ and $\bar{q} = (\bar{q}^1, \ldots, \bar{q}^n)$. The Discrete Euler-Lagrange equations (2.4.2) can be equivalently written as

$$\mathbb{F}^+ L_d(q_{k-1}, q_k) = \mathbb{F}^- L_d(q_k, q_{k+1}). \tag{2.4.5}$$

Using either of the transforms, one can define the discrete Lagrange two-form on $Q \times Q$ by $\omega_{L_d} = (\mathbb{F}^{\pm} L_d)^* \tilde{\Omega}$, which in coordinates gives

$$\omega_{L_d} = \frac{\partial^2 L_d}{\partial q^\mu \partial \bar{q}^\nu} dq^\mu \wedge d\bar{q}^\nu. \tag{2.4.6}$$

It then follows that the discrete flow F_{L_d} is symplectic, i.e., $F_{L_d}^* \omega_{L_d} = \omega_{L_d}$.

Using the Legendre transforms we can pass to the cotangent bundle and define the discrete Hamiltonian map $\tilde{F}_{L_d} : T^*Q \longrightarrow T^*Q$ by

$$\tilde{F}_{L_d} = \mathbb{F}^{\pm} L_d \circ F_{L_d} \circ (\mathbb{F}^{\pm} L_d)^{-1}. \tag{2.4.7}$$

This map is also symplectic, i.e., $\tilde{F}_{L_d}^* \Omega = \Omega$, where Ω is the canonical symplectic form on T^*Q. Using (2.4.4), the discrete Euler-Lagrange equations (2.4.2) can be equivalently rewritten in the position-momentum formulation on T^*Q as

$$\begin{aligned} p_k &= -D_1 L_d(q_k, q_{k+1}), \\ p_{k+1} &= D_2 L_d(q_k, q_{k+1}). \end{aligned} \tag{2.4.8}$$

This system implicitly defines the discrete Hamiltonian map: given (q_k, p_k), one can solve (2.4.8) for (q_{k+1}, p_{k+1}).

2.4.2 Correspondence between discrete and continuous systems

To relate discrete and continuous mechanics it is necessary to introduce a timestep $h \in \mathbb{R}$. If the continuous Lagrangian L is non-degenerate, it is possible to define a particular choice of discrete Lagrangian which gives an exact correspondence between discrete and continuous systems (see [41]), the so-called *exact discrete Lagrangian*.

Definition 2.4.1. *The exact discrete Lagrangian L_d^E for the non-degenerate Lagrangian $L : TQ \longrightarrow \mathbb{R}$ is*

$$L_d^E(q,\bar{q}) = \int_0^h L\big(q_E(t),\dot{q}_E(t)\big)\,dt, \tag{2.4.9}$$

for sufficiently small h and $\bar{q}$ sufficiently close to q, where $q_E(t)$ is the solution to (2.3.3) *that satisfies the boundary conditions $q_E(0) = q$ and $q_E(h) = \bar{q}$.*

The discrete Legendre transforms $\mathbb{F}^{\pm}L_d^E$ associated with L_d^E can be related to the continuous Legendre transform $\mathbb{F}L$.

Theorem 2.4.2. *A regular Lagrangian L and the corresponding exact discrete Lagrangian L_d^E have Legendre transforms related by*

$$\begin{aligned}\mathbb{F}^{+}L_d^E(q,\bar{q}) &= \mathbb{F}L(q_E(h),\dot{q}_E(h)),\\ \mathbb{F}^{-}L_d^E(q,\bar{q}) &= \mathbb{F}L(q_E(0),\dot{q}_E(0)),\end{aligned} \tag{2.4.10}$$

for sufficiently small h and $\bar{q}$ sufficiently close to q, where $q_E(t)$ is the solution to (2.3.3) *that satisfies the boundary conditions $q_E(0) = q$ and $q_E(h) = \bar{q}$.*

Solving the discrete Euler-Lagrange equations (2.4.2) associated with L_d^E yields the discrete trajectory $q_0, q_1, \ldots$ such that q_k coincides with the exact solution of the continuous Euler-Lagrange equations (2.3.3) at time $t_k = kh$. This important property can be summarized in the following theorem, which we cite after [41].

Theorem 2.4.3. *Consider a regular Lagrangian L, its corresponding exact discrete Lagrangian L_d^E, and the pushforward of both the continuous and discrete systems to T^*Q, yielding a Hamiltonian system with Hamiltonian H and a discrete Hamiltonian map $\tilde{F}_{L_d^E}$, respectively. Then, for a sufficiently small timestep h, the flow of the Hamiltonian system equals the discrete Hamiltonian map, that is,*

$$F_h^H = \tilde{F}_{L_d^E}. \tag{2.4.11}$$

For a given continuous system described by the regular Lagrangian L, a variational integrator is constructed by choosing a discrete Lagrangian L_d which approximates the exact discrete Lagrangian L_d^E. The precision of this approximation can be measured by defining the order of accuracy of the discrete Lagrangian.

Definition 2.4.4. *A discrete Lagrangian $L_d : Q \times Q \longrightarrow \mathbb{R}$ is of order r if there exists an open subset $U \subset TQ$ with compact closure and constants $C > 0$ and $\bar{h} > 0$ such that*

$$\left| L_d\big(q(0), q(h)\big) - L_d^E\big(q(0), q(h)\big) \right| \leq C h^{r+1} \tag{2.4.12}$$

for all solutions $q(t)$ of the Euler-Lagrange equations (2.3.3) with initial conditions $(q(0), \dot{q}(0)) \in U$ and for all $h \leq \bar{h}$.

As discussed in Section 2.4.1, the discrete Lagrangian L_d defines the discrete Hamiltonian map $\tilde{F}_{L_d}$ on the cotangent bundle T^*Q. This map is a numerical scheme for the Hamiltonian system corresponding to the Lagrangian L (cf. Theorem 2.3.3), and so Definition 2.2.1 and Definition 2.2.2 apply. If the Lagrangian L is regular, then one can show that the discrete Lagrangian L_d is of order r if and only if the associated discrete Hamiltonian map $\tilde{F}_{L_d}$ is of order r (see [41]).

Example: Symplectic Euler scheme revisited. Consider a regular Lagrangian L and the following discrete Lagrangian

$$L_d(q, \bar{q}) = h L\Big(\bar{q}, \frac{\bar{q} - q}{h}\Big). \tag{2.4.13}$$

One can check that this discrete Lagrangian is first-order. A variational numerical integrator is obtained by forming the discrete Euler-Lagrange equations (2.4.8). It is straightforward to verify that these equations are equivalent to (2.2.5), i.e., the symplectic Euler scheme, where the Hamiltonian H and the Lagrangian L are related as in Theorem 2.3.3.

2.4.3 Variational partitioned Runge-Kutta methods

To construct higher-order variational integrators, one may consider a class of partitioned Runge-Kutta methods similar to partitioned Runge-Kutta methods for Hamiltonian systems. We will construct an s-stage variational partitioned Runge-Kutta integrator for the regular Lagrangian L by considering the discrete Lagrangian

$$L_d(q, \bar{q}) = h \sum_{i=1}^{s} b_i L(Q_i, \dot{Q}_i), \tag{2.4.14}$$

where the internal stages Q_i, $\dot{Q}_i$, $i = 1, \ldots, s$, satisfy the relation

$$Q_i = q + h\sum_{j=1}^{s} a_{ij}\dot{Q}_j, \tag{2.4.15}$$

and are chosen so that the right-hand side of (2.4.14) is extremized under the constraint

$$\bar{q} = q + h\sum_{i=1}^{s} b_i\dot{Q}_i. \tag{2.4.16}$$

A variational integrator is then obtained by forming the corresponding discrete Euler-Lagrange equations (2.4.8). We have the following result:

Theorem 2.4.5. *The s-stage variational partitioned Runge-Kutta method based on the discrete Lagrangian* (2.4.14) *with the coefficients* a_{ij} *and* b_i *is equivalent to the following partitioned Runge-Kutta method applied to the implicit Hamiltonian equations* (2.3.12)*:*

$$\begin{aligned}
P_i &= \frac{\partial L}{\partial \dot{q}}(Q_i, \dot{Q}_i), && i = 1, \dots, s,\\
\dot{P}_i &= \frac{\partial L}{\partial q}(Q_i, \dot{Q}_i), && i = 1, \dots, s,\\
Q_i &= q + h\sum_{j=1}^{s} a_{ij}\dot{Q}_j, && i = 1, \dots, s,\\
P_i &= p + h\sum_{j=1}^{s} \bar{a}_{ij}\dot{P}_j, && i = 1, \dots, s,\\
\bar{q} &= q + h\sum_{j=1}^{s} b_j\dot{Q}_j,\\
\bar{p} &= p + h\sum_{j=1}^{s} b_j\dot{P}_j,
\end{aligned} \tag{2.4.17}$$

where the coefficients satisfy the condition

$$b_i\bar{a}_{ij} + b_j a_{ji} = b_i b_j, \qquad \forall i, j = 1, \dots, s, \tag{2.4.18}$$

and (q, p) *denote the current values of position and momentum,* $(\bar{q}, \bar{p})$ *denote the respective values at the next time step, and* Q_i, $\dot{Q}_i$, P_i, $\dot{P}_i$ *are the internal stages.*

If the Lagrangian L is regular, then (2.4.17) is equivalent to the symplectic partitioned Runge-Kutta method (2.2.6), where H and L are related as in Theorem 2.3.3. We therefore have that the Gauss and Lobatto IIIA-IIIB methods discussed in Section 2.2.2 are

variational (cf. Theorem 2.2.10 and Theorem 2.2.11).

More information on variational integrators can be found in [41].

2.5 Constrained mechanical systems

Below we present a short overview of how the theory discussed in the previous sections applies to constrained mechanical systems and variational integration of such systems.

2.5.1 Lagrangian and Hamiltonian descriptions of constrained systems

Suppose we have a Lagrangian system with a configuration manifold Q and a regular Lagrangian $L : TQ \longrightarrow \mathbb{R}$, but we restrict the allowable configurations of the system to the submanifold $N = g^{-1}(0) \subset Q$, where $g : Q \longrightarrow \mathbb{R}^d$ is the *constraint function* and we assume 0 is a regular value of g (so that N is indeed a submanifold; see [38]). Note that, if $i : N \longrightarrow Q$ is the inclusion map, then $Ti : TN \longrightarrow TQ$ provides a canonical way to embed TN in TQ, and TN can be regarded as a submanifold of TQ. In fact, in a local bundle chart on TQ we have the characterization

$$TN = \Big\{ (q, \dot{q}) \in TQ \;\Big|\; g(q) = 0 \text{ and } Dg(q)\dot{q} = 0 \Big\}, \tag{2.5.1}$$

where $Dg(q)$ denotes the Jacobi matrix of the (local representative of) constraint function $g(q)$. We can therefore consider the restricted Lagrangian system with the configuration manifold N and the Lagrangian $L^N = L|_{TN}$, and the theory presented in Section 2.3 can be directly applied. However, it is often more elegant and convenient to consider this restricted system as a constrained version of the larger system defined on Q. It is particularly useful in numerical computations when Q has a vector space structure, which is easier to handle than the possibly nonlinear structure of the constraint submanifold N.

It can be shown that if L is regular, so is L^N (see [41]). Therefore, TN can be endowed with the Lagrangian symplectic form Ω_{L^N}, as explained in Section 2.3, and this form is preserved by the flow of the Lagrangian vector field associated with L^N. It can be further shown that this symplectic structure on TN is compatible with the symplectic structure on TQ, that is, $\Omega_{L^N} = (Ti)^* \Omega_L$, where Ω_L is the Lagrangian form on TQ.

The action functional for the unconstrained system is given by (2.3.1). This functional

is defined on the set of all smooth curves $\mathcal{C}(Q) = \{q : [a,b] \longrightarrow Q\}$, that is, $S : \mathcal{C}(Q) \longrightarrow \mathbb{R}$. The action functional $S^N : \mathcal{C}(N) \longrightarrow \mathbb{R}$ for the Lagrangian L^N is given by an analogous formula. Since $N \subset Q$ and $TN \subset TQ$ are submanifolds, we have $S^N = S|_{\mathcal{C}(N)}$. The dynamics of the constrained system is given by Hamilton's principle, i.e., extremizing S^N. To consider this dynamics in the embedding space, we further introduce the augmented configuration manifold $Q \times \mathbb{R}^d$ and the augmented Lagrangian $L_C : T(Q \times \mathbb{R}^d) \longrightarrow \mathbb{R}$ defined by

$$L_C(q, \lambda, \dot{q}, \dot{\lambda}) = L(q, \dot{q}) - \langle \lambda, g(q) \rangle, \tag{2.5.2}$$

where $\lambda \in \mathbb{R}^d$ denotes the vector of Lagrange multipliers and $\langle ., . \rangle$ is the standard scalar product on $\mathbb{R}^d$. The corresponding augmented action functional $S_C : \mathcal{C}(Q) \times \mathcal{C}(\mathbb{R}^d) \longrightarrow \mathbb{R}$ is given by

$$S_C\big[q(t), \lambda(t)\big] = \int_a^b L_C\big(q(t), \lambda(t), \dot{q}(t), \dot{\lambda}(t)\big)\, dt = S[q(t)] - \int_a^b \big\langle \lambda(t), g(q(t)) \big\rangle\, dt. \tag{2.5.3}$$

The relation between the dynamics of the restricted system on N and the augmented system on $Q \times \mathbb{R}^d$ is given by the following theorem (see [38]).

Theorem 2.5.1 (**Lagrange multiplier theorem).** *The following statements are equivalent:*

1. *The curve $q : \mathbb{R} \longrightarrow N \subset Q$ is an extremum of S^N;*
2. *The pair of curves $q : [a,b] \longrightarrow Q$ and $\lambda : [a,b] \longrightarrow \mathbb{R}^d$ is an extremum of S_C.*

The curves extremizing the augmented action functional S_C satisfy the Euler-Lagrange equations associated with L_C, the so-called *constrained* Euler-Lagrange equations,

$$\begin{aligned} \frac{\partial L}{\partial q^\mu} - \frac{d}{dt}\frac{\partial L}{\partial \dot{q}^\mu} &= \Big\langle \lambda, \frac{\partial g}{\partial q^\mu} \Big\rangle, \\ g(q) &= 0. \end{aligned} \tag{2.5.4}$$

Deriving the equations of motion for constrained Hamiltonian systems is a little more cumbersome. Suppose we have a Hamiltonian system with the Hamiltonian $H : T^*Q \longrightarrow \mathbb{R}$,

but we restrict the dynamics to the constraint submanifold $N = g^{-1}(0) \subset Q$ as before. The main complication is the fact that there is no canonical way of embedding T^*N in T^*Q, and it is not obvious how to define an appropriate Hamiltonian H^N on T^*N. However, if the Hamiltonian H is hyperregular, that is, there exists a corresponding hyperregular Lagrangian L on TQ, as in Theorem 2.3.3, then one can realize T^*N as a symplectic submanifold of T^*Q by defining the embedding $\eta : T^*N \longrightarrow T^*Q$ as $\eta = \mathbb{F}L \circ Ti \circ (\mathbb{F}L^N)^{-1}$. Using canonical coordinates on T^*Q, we have the following characterization

$$\eta(T^*N) = \left\{ (q,p) \in T^*Q \;\middle|\; g(q) = 0 \text{ and } Dg(q)\frac{\partial H}{\partial p} = 0 \right\}. \tag{2.5.5}$$

It is straightforward to show that the canonical symplectic form Ω^N on T^*N is then compatible with the canonical symplectic form Ω on T^*Q, that is, $\Omega^N = \eta^*\Omega$. We can further take $H^N = H \circ \eta$. The Hamiltonian equations on T^*N will be defined by (2.1.4), and the theory discussed in Section 2.1 directly applies. However, it is again useful to consider the dynamics of this constrained system in the embedding space. We have the natural embedding $T\eta : TT^*N \longrightarrow TT^*Q$, so the Hamiltonian vector field Z^N on T^*N can be regarded as a vector field on $\eta(T^*N)$. This leads to the following constrained equations on motion on T^*Q:

$$\begin{aligned} \dot{q}^\mu &= \frac{\partial H}{\partial p_\mu}, \\ \dot{p}_\mu &= -\frac{\partial H}{\partial q^\mu} - \left\langle \lambda, \frac{\partial g}{\partial q^\mu} \right\rangle, \\ g(q) &= 0, \end{aligned} \tag{2.5.6}$$

where λ again denotes Lagrange multipliers. If the Lagrangian L is hyperregular, then (2.5.6) and (2.5.4) are equivalent, as in Theorem 2.3.3.

For more information on the geometry of constrained Lagrangian and Hamiltonian systems we refer the reader to [38].

2.5.2 Variational integrators for constrained systems

Variational integration of constrained Lagrangian systems follows the main ideas presented in Section 2.4. We start with a regular discrete Lagrangian $L_d : Q \times Q \longrightarrow \mathbb{R}$. The discrete

dynamics is restricted to the constraint submanifold $N \times N \subset Q \times Q$, where $N = g^{-1}(0) \subset Q$ as before. We consider the augmented discrete state space $(Q \times \mathbb{R}^d) \times (Q \times \mathbb{R}^d)$ and the augmented discrete Lagrangian $L_d^C : (Q \times \mathbb{R}^d) \times (Q \times \mathbb{R}^d) \longrightarrow \mathbb{R}$,

$$L_d^C(q, \lambda, \bar{q}, \bar{\lambda}) = L_d(q, \bar{q}) - \langle \lambda, g(q) \rangle. \tag{2.5.7}$$

The discrete Euler-Lagrange equations (2.4.2) for L_d^C yield

$$\begin{aligned} D_2 L_d(q_{k-1}, q_k) + D_1 L_d(q_k, q_{k+1}) &= Dg(q_k)^T \lambda_k, \\ g(q_{k+1}) &= 0, \end{aligned} \tag{2.5.8}$$

where Dg denotes the Jacobi matrix of the constraint function g, and λ_k denotes the column vector of Lagrange multipliers. If q_{k-1}, q_k are known, then (2.5.8) can be solved for q_{k+1} and λ_k.

The discrete Lagrangian L_d is chosen to approximate the exact discrete Lagrangian for L. However, the exact discrete Lagrangian for a constrained system is not simply the standard exact discrete Lagrangian (2.4.9) restricted to the constraint submanifold $N \times N$, as that would be the action along an unconstrained trajectory. Instead, the constrained exact discrete Lagrangian $L_d^{N,E} : N \times N \longrightarrow \mathbb{R}$ is defined by

$$L_d^{N,E}(q, \bar{q}) = \int_0^h L^N\big(q_E(t), \dot{q}_E(t)\big)\, dt, \tag{2.5.9}$$

where $q_E(t)$ is the solution to the constrained Euler-Lagrange equations (2.5.4) satisfying the boundary conditions $q_E(0) = q$ and $q_E(h) = \bar{q}$.

Lobatto IIIA-IIIB pair. Higher-order variational integrators for constrained systems can be constructed as in Section 2.4.3: a variational Runge-Kutta method for a constrained Lagrangian system described by a regular Lagrangian L is equivalent to a symplectic partitioned Runge-Kutta method applied to the constrained Hamiltonian equations (2.5.6).

Consider a Hamiltonian system $H : T^*Q \longrightarrow \mathbb{R}$ with the holonomic constraint $g : Q \longrightarrow \mathbb{R}^d$, and two Runge-Kutta methods with the coefficients a_{ij}, b_i and $\bar{a}_{ij}$, $\bar{b}_i$, respectively. An s-stage *constrained partitioned Runge-Kutta method* is the map

$$F_h : \eta(T^*N) \ni (q,p) \longrightarrow (\bar{q},\bar{p}) \in \eta(T^*N), \tag{2.5.10}$$

implicitly defined by the system of equations

$$\dot{Q}_i = \frac{\partial H}{\partial p}(Q_i,P_i), \qquad i=1,\dots,s, \tag{2.5.11a}$$

$$\dot{P}_i = -\frac{\partial H}{\partial q}(Q_i,P_i) - Dg(Q_i)^T\Lambda_i, \qquad i=1,\dots,s, \tag{2.5.11b}$$

$$0 = g(Q_i), \qquad i=1,\dots,s, \tag{2.5.11c}$$

$$Q_i = q + h\sum_{j=1}^{s} a_{ij}\dot{Q}_j, \qquad i=1,\dots,s, \tag{2.5.11d}$$

$$P_i = p + h\sum_{j=1}^{s} \bar{a}_{ij}\dot{P}_j, \qquad i=1,\dots,s, \tag{2.5.11e}$$

$$\bar{q} = q + h\sum_{i=1}^{s} b_i\dot{Q}_i, \tag{2.5.11f}$$

$$\bar{p} = p + h\sum_{i=1}^{s} \bar{b}_i\dot{P}_i, \tag{2.5.11g}$$

$$0 = Dg(\bar{q})\frac{\partial H}{\partial p}(\bar{q},\bar{p}), \tag{2.5.11h}$$

where Q_i, $\dot{Q}_i$, P_i, $\dot{P}_i$ and Λ_i are the internal stages of the method. However, this system is not solvable for an arbitrary choice of the Runge-Kutta methods—note we have only $(4s+2)n+sd$ unknowns (the internal stages and $\bar{q}$, $\bar{p}$), but $(4s+2)n+(s+1)d$ equations. It can be shown that (2.5.11) is solvable if one chooses the coefficients of the s-stage Lobatto IIIA-IIIB method (see Section 2.2.2). For the Lobatto IIIA-IIIB schemes we have $a_{1j} = 0$ for $j = 1,\dots,s$ (cf. Table 2.4, Table 2.5, and Table 2.6), therefore in (2.5.11d) we have $Q_1 = q$. If we assume $g(q) = 0$, i.e., the initial position is consistent with the constraint, then d equations in (2.5.11c) for $i = 1$ are automatically satisfied, and the whole system becomes solvable. Further, the Lobatto IIIA-IIIB schemes satisfy $a_{sj} = b_j$ for $j = 1,\dots,s$, so from (2.5.11d) and (2.5.11f) we have $\bar{q} = Q_s$, and consequently, by (2.5.11c), we also have $g(\bar{q}) = 0$, i.e., the new position of the system is consistent with the constraint. This result, together with (2.5.11h), means that $(\bar{q},\bar{p}) \in \eta(T^*N)$, that is, (2.5.11) indeed defines an integrator for the constrained Hamiltonian system. The following theorem can be proved (see [31], [23]).

Theorem 2.5.2. *The s-stage constrained Lobatto IIIA-IIIB scheme* (2.5.11) *is symplectic*

on $\eta(T^*N)$ and convergent of order $2s-2$.

If one defines the discrete Lagrangian $L_d : Q \times Q \longrightarrow \mathbb{R}$ as

$$L_d(q,\bar{q}) = h\sum_{i=1}^{s} b_i L(Q_i, \dot{Q}_i), \tag{2.5.12}$$

where Q_i and $\dot{Q}_i$ satisfy (2.5.11), then the resulting variational integrator will be equivalent to the constrained Lobatto IIIA-IIIB scheme, where L and H are related as in Theorem 2.3.3.

More information on variational and symplectic integration of constrained mechanical systems can be found in [23], [26], and [41].

2.6 Field theory and multisymplectic geometry

In the previous sections we focused on finite-dimensional mechanics. Here we turn our attention to field theories and review their underlying multisymplectic geometry. Multisymplectic geometry provides a covariant formalism for the study of field theories in which time and space are treated on equal footing.

Multisymplectic geometry. Let $\mathcal{X}$ be an oriented manifold representing the $(n+1)$-dimensional spacetime with local coordinates $(x^0, x^1, \ldots, x^n) \equiv (t, x)$, where $x^0 \equiv t$ is time and $(x^1, \ldots, x^n) \equiv x$ are space coordinates. Physical fields are sections of a configuration fiber bundle $\pi_{\mathcal{X}Y} : Y \longrightarrow \mathcal{X}$, that is, continuous maps $\phi : \mathcal{X} \longrightarrow Y$ such that $\pi_{\mathcal{X}Y} \circ \phi = \mathrm{id}_{\mathcal{X}}$. This means that for every $(t,x) \in \mathcal{X}$, $\phi(t,x)$ is in the fiber over (t,x), which is $Y_{(t,x)} = \pi^{-1}_{\mathcal{X}Y}((t,x))$. The evolution of the field takes place on the first jet bundle J^1Y, which is the analog of TQ for mechanical systems. J^1Y is the affine bundle over Y with the fibers J^1_yY defined as

$$J^1_yY = \left\{ \vartheta : T_{(t,x)}\mathcal{X} \to T_yY \;\middle|\; T\pi_{\mathcal{X}Y} \circ \vartheta = \mathrm{id}_{T_{(t,x)}\mathcal{X}} \right\} \tag{2.6.1}$$

for $y \in Y_{(t,x)}$, where the linear maps ϑ represent the tangent mappings $T_{(t,x)}\phi$ for local sections ϕ such that $\phi(t,x) = y$. The local coordinates (x^μ, y^a) on Y induce the coordinates $(x^\mu, y^a, v^a{}_\mu)$ on J^1Y. Intuitively, the first jet bundle consists of the configuration bundle Y, and of the first partial derivatives of the field variables with respect to the independent variables. Let $\phi(x^0, \ldots, x^n) = (x^0, \ldots, x^n, y^1, \ldots, y^m)$ in coordinates and let $v^a{}_\mu = y^a{}_{,\mu} =$

$\partial y^a/\partial x^\mu$ denote the partial derivatives. We can think of J^1Y as a fiber bundle over $\mathcal{X}$. Given a section $\phi : \mathcal{X} \longrightarrow Y$, we can define its first jet prolongation

$$j^1\phi : \mathcal{X} \ni (t,x) \longrightarrow T_{(t,x)}\phi \in J^1Y, \tag{2.6.2}$$

in coordinates given by

$$j^1\phi(x^0, x^1, \ldots, x^n) = (x^0, x^1, \ldots, x^n, y^1, \ldots, y^m, y^1{}_{,0}, \ldots, y^m{}_{,n}), \tag{2.6.3}$$

which is a section of the fiber bundle J^1Y over $\mathcal{X}$. For higher-order field theories we consider higher-order jet bundles, defined iteratively by $J^2Y = J^1(J^1Y)$ and so on. The local coordinates on J^2Y are denoted $(x^\mu, y^a, v^a{}_\mu, w^a{}_\mu, \kappa^a_{\mu\nu})$. The second jet prolongation $j^2\phi : \mathcal{X} \longrightarrow J^2Y$ is given in coordinates by $j^2\phi(x^\mu) = (x^\mu, y^a, y^a{}_{,\mu}, y^a{}_{,\mu}, y^a{}_{,\mu,\nu})$.

Lagrangian dynamics. Lagrangian density for first order field theories is defined as a map $\mathcal{L} : J^1Y \longrightarrow \mathbb{R}$. The corresponding action functional is

$$S[\phi] = \int_{\mathcal{U}} \mathcal{L}(j^1\phi)\, d^{n+1}x, \tag{2.6.4}$$

where $\mathcal{U} \subset \mathcal{X}$. Hamilton's principle seeks fields $\phi(t,x)$ that extremize S, that is,

$$\left.\frac{d}{d\lambda}\right|_{\lambda=0} S[\eta_Y^\lambda \circ \phi] = 0 \tag{2.6.5}$$

for all η_Y^λ that keep the boundary conditions on $\partial\mathcal{U}$ fixed, where $\eta_Y^\lambda : Y \longrightarrow Y$ is the flow of a vertical vector field V on Y. This leads to the Euler-Lagrange equations

$$\frac{\partial\mathcal{L}}{\partial y^a}(j^1\phi) - \frac{\partial}{\partial x^\mu}\left(\frac{\partial\mathcal{L}}{\partial v^a{}_\mu}(j^1\phi)\right) = 0, \tag{2.6.6}$$

where Einstein's summation convention is used.

Multisymplectic form formula. Given the Lagrangian density $\mathcal{L}$ one can define the Cartan $(n+1)$-form $\Theta_\mathcal{L}$ on J^1Y, in local coordinates given by

$$\Theta_\mathcal{L} = \frac{\partial\mathcal{L}}{\partial v^a{}_\mu} dy^a \wedge d^n x_\mu + \left(\mathcal{L} - \frac{\partial\mathcal{L}}{\partial v^a{}_\mu} v^a{}_\mu\right) d^{n+1}x, \tag{2.6.7}$$

where $d^n x_\mu = \partial_\mu \lrcorner d^{n+1}x$. The multisymplectic $(n+2)$-form is then defined by

$$\Omega_{\mathcal{L}} = -d\Theta_{\mathcal{L}}. \tag{2.6.8}$$

Let $\mathcal{P}$ be the set of solutions of the Euler-Lagrange equations, that is, the set of sections ϕ satisfying (2.6.5) or (2.6.6). For a given $\phi \in \mathcal{P}$, let $\mathcal{F}$ be the set of first variations, that is, the set of vector fields V on J^1Y such that $(t,x) \to \eta_Y^\epsilon \circ \phi(t,x)$ is also a solution, where η_Y^ϵ is the flow of V. The multisymplectic form formula states that if $\phi \in \mathcal{P}$ then for all V and W in $\mathcal{F}$,

$$\int_{\partial\mathcal{U}} (j^1\phi)^* \big(j^1V \lrcorner j^1W \lrcorner \Omega_{\mathcal{L}}\big) = 0, \tag{2.6.9}$$

where j^1V is the jet prolongation of V, that is, the vector field on J^1Y whose flow is the first jet prolongation of the flow η_Y^ϵ for V, i.e.,

$$j^1V = \left.\frac{d}{d\epsilon}\right|_{\epsilon=0} j^1\eta_Y^\epsilon. \tag{2.6.10}$$

The local representation is given by

$$j^1V = \Big(V^\mu, V^a, \frac{\partial V^a}{\partial x^\mu} + \frac{\partial V^a}{\partial y^b} v^b{}_\mu - v^a{}_\nu \frac{\partial V^\nu}{\partial x^\mu}\Big), \tag{2.6.11}$$

where $V = (V^\mu, V^a)$ in local coordinates. The multisymplectic form formula is the multisymplectic counterpart of the fact that in finite-dimensional mechanics, the flow of a mechanical system consists of symplectic maps, as discussed in Section 2.1 and Section 2.3.

Higher-order field theories. For a k^{th}-order Lagrangian field theory with the Lagrangian density $\mathcal{L} : J^kY \longrightarrow \mathbb{R}$, analogous geometric structures are defined on $J^{2k-1}Y$. In particular, for a second-order field theory the multisymplectic $(n+2)$-form $\Omega_{\mathcal{L}}$ is defined on J^3Y and a similar multisymplectic form formula can be proven. If the Lagrangian density does not depend on the second order time derivatives of the field, it is convenient to define the subbundle $J_0^2Y \subset J^2Y$ such that $J_0^2Y = \{\vartheta \in J^2Y \,|\, \kappa^a_{00} = 0\}$.

For more information about the geometry of jet bundles, see [58]. The multisymplectic formalism in field theory is discussed in [21]. The multisymplectic form formula for first-order field theories is derived in [39], and generalized for second-order field theories in [34].

Higher-order field theory is considered in [20].

2.7 Multisymplectic variational integrators

Veselov-type discretization. Veselov-type discretization can be generalized to multisymplectic field theory. We take $\mathcal{X} = \mathbb{Z} \times \mathbb{Z} = \{(j,i)\}$, where for simplicity we consider $\dim \mathcal{X} = 2$, i.e., $n = 1$. The configuration fiber bundle is $Y = \mathcal{X} \times \mathscr{F}$ for some smooth manifold $\mathscr{F}$. The fiber over $(j,i) \in \mathcal{X}$ is denoted Y_{ji} and its elements y_{ji}. A rectangle $\square$ of $\mathcal{X}$ is an ordered 4-tuple of the form $\square = \big((j,i),(j,i+1),(j+1,i+1),(j+1,i)\big) = (\square^1,\square^2,\square^3,\square^4)$. The set of all rectangles in $\mathcal{X}$ is denoted $\mathcal{X}^\square$. A point (j,i) is touched by a rectangle if it is a vertex of that rectangle. Let $\mathcal{U} \subset \mathcal{X}$. Then $(j,i) \in \mathcal{U}$ is an interior point of $\mathcal{U}$ if $\mathcal{U}$ contains all four rectangles that touch (j,i). The interior $\operatorname{int}\mathcal{U}$ is the set of all interior points of $\mathcal{U}$. The closure $\operatorname{cl}\mathcal{U}$ is the union of all rectangles touching the interior points of $\mathcal{U}$. The boundary of $\mathcal{U}$ is defined by $\partial\mathcal{U} = (\mathcal{U} \cap \operatorname{cl}\mathcal{U}) \backslash \operatorname{int}\mathcal{U}$. A section of Y is a map $\phi : \mathcal{U} \subset \mathcal{X} \to Y$ such that $\phi(j,i) \in Y_{ji}$. We can now define the discrete first jet bundle of Y as

$$\begin{aligned} J^1Y &= \left\{ (y_{ji}, y_{j\,i+1}, y_{j+1\,i+1}, y_{j+1\,i}) \;\middle|\; (j,i) \in \mathcal{X},\, y_{ji}, y_{j\,i+1}, y_{j+1\,i+1}, y_{j+1\,i} \in \mathscr{F} \right\} \\ &= \mathcal{X}^\square \times \mathscr{F}^4. \end{aligned} \tag{2.7.1}$$

Intuitively, the discrete first jet bundle is the set of all rectangles together with four values assigned to their vertices. Those four values are enough to approximate the first derivatives of a smooth section with respect to time and space using, for instance, finite differences. The first jet prolongation of a section ϕ of Y is the map $j^1\phi : \mathcal{X}^\square \to J^1Y$ defined by $j^1\phi(\square) = (\square, \phi(\square^1), \phi(\square^2), \phi(\square^3), \phi(\square^4))$. For a vector field V on Y, let V_{ji} be its restriction to Y_{ji}.

Discrete Euler-Lagrange equations. Define a discrete Lagrangian $L : J^1Y \to \mathbb{R}$, $L = L(y_1, y_2, y_3, y_4)$, where for convenience we omit writing the base rectangle. The associated discrete action is given by

$$S[\phi] = \sum_{\square \subset \mathcal{U}} L \circ j^1\phi(\square).$$

The discrete variational principle seeks sections that extremize the discrete action, that is, mappings $\phi(j,i)$ such that

$$\left.\frac{d}{d\lambda}\right|_{\lambda=0} S[\phi_\lambda] = 0 \tag{2.7.2}$$

for all vector fields V on Y that keep the boundary conditions on $\partial\mathcal{U}$ fixed, where $\phi_\lambda(j,i) = F_\lambda^{V_{ji}}(\phi(j,i))$ and $F_\lambda^{V_{ji}}$ is the flow of V_{ji} on $\mathscr{F}$. This is equivalent to the discrete Euler-Lagrange equations

$$\begin{aligned}\frac{\partial L}{\partial y_1}(y_{ji}, y_{j\,i+1}, y_{j+1\,i+1}, y_{j+1\,i}) + \frac{\partial L}{\partial y_2}(y_{j\,i-1}, y_{ji}, y_{j+1\,i}, y_{j+1\,i-1}) + \\ + \frac{\partial L}{\partial y_3}(y_{j-1\,i-1}, y_{j-1\,i}, y_{ji}, y_{j\,i-1}) + \frac{\partial L}{\partial y_4}(y_{j-1\,i}, y_{j-1\,i+1}, y_{j\,i+1}, y_{ji}) = 0\end{aligned} \tag{2.7.3}$$

for all $(j,i) \in \operatorname{int}\mathcal{U}$, where we adopt the convention $\phi(j,i) = y_{ji}$.

Discrete multisymplectic form formula. In analogy to the Veselov discretization of mechanics, we can define four 2-forms Ω_L^l on J^1Y, where $l = 1,2,3,4$ and $\Omega_L^1 + \Omega_L^2 + \Omega_L^3 + \Omega_L^4 = 0$, that is, only three 2-forms of these forms are independent. The 4-tuple $(\Omega_L^1, \Omega_L^2, \Omega_L^3, \Omega_L^4)$ is the discrete analog of the multisymplectic form $\Omega_{\mathcal{L}}$. We refer the reader to the literature for details, e.g. [39]. By analogy to the continuous case, let $\mathcal{P}$ be the set of solutions of the discrete Euler-Lagrange equations (2.7.3). For a given $\phi \in \mathcal{P}$, let $\mathcal{F}$ be the set of first variations, that is, the set of vector fields V on J^1Y defined as in the continuous case. The discrete multisymplectic form formula then states that if $\phi \in \mathcal{P}$, then for all V and W in $\mathcal{F}$,

$$\sum_{\substack{\square \\ \square \cap \mathcal{U} \neq \varnothing}} \left(\sum_{\substack{l \\ \square^l \in \partial\mathcal{U}}} \left[(j^1\phi)^*(j^1V \lrcorner j^1W \lrcorner \Omega_L^l) \right](\square) \right) = 0, \tag{2.7.4}$$

where the jet prolongations are defined to be

$$j^1V(y_{\square^1}, y_{\square^2}, y_{\square^3}, y_{\square^4}) = \left(V_{\square^1}(y_{\square^1}), V_{\square^2}(y_{\square^2}), V_{\square^3}(y_{\square^3}), V_{\square^4}(y_{\square^4})\right). \tag{2.7.5}$$

The discrete form formula (2.7.4) is in direct analogy to the multisymplectic form formula (2.6.9) that holds in the continuous case.

Discrete Lagrangian. Given a continuous Lagrangian density $\mathcal{L}$ one chooses a corresponding discrete Lagrangian as an approximation

$$L(y_{\square^1}, y_{\square^2}, y_{\square^3}, y_{\square^4}) \approx \int_{\overline{\square}} \mathcal{L} \circ j^1 \bar{\phi}\, dx\, dt, \tag{2.7.6}$$

where $\overline{\square}$ is the rectangular region of the continuous spacetime that contains $\square$ and $\bar{\phi}(t,x)$ is the solution of the Euler-Lagrange equations corresponding to $\mathcal{L}$, with the boundary values at the vertices of $\square$ corresponding to $y_{\square^1}$, $y_{\square^2}$, $y_{\square^3}$, and $y_{\square^4}$.

Higher-order discrete field theory. The discrete second jet bundle J^2Y can be defined by considering ordered 9-tuples

$$\begin{aligned}\boxplus &= \big((j-1,i-1),(j-1,i),(j-1,i+1),(j,i-1),\\ &\qquad\qquad (j,i),(j,i+1),(j+1,i-1),(j+1,i),(j+1,i+1)\big)\\ &= (\boxplus^1,\boxplus^2,\boxplus^3,\boxplus^4,\boxplus^5,\boxplus^6,\boxplus^7,\boxplus^8,\boxplus^9)\end{aligned} \tag{2.7.7}$$

instead of rectangles $\square$, and the discrete subbundle J^2_0Y can be defined by considering 6-tuples

$$\begin{aligned}\boxminus &= \big((j,i-1),(j,i),(j,i+1),(j+1,i+1),(j+1,i),(j+1,i-1)\big)\\ &= (\boxminus^1,\boxminus^2,\boxminus^3,\boxminus^4,\boxminus^5,\boxminus^6).\end{aligned} \tag{2.7.8}$$

Similar constructions then follow and a similar discrete multisymplectic form formula can be derived for a second order field theory.

Multisymplectic variational integrators for first order field theories are introduced in [39], and generalized for second-order field theories in [34].

Chapter 3

Background: Moving mesh methods

In this chapter we review r-adaptive methods for time-dependent partial differential equations, also known as moving mesh methods. As mentioned in Chapter 1, even though it is still in a relatively early stage of development, the field of moving mesh methods is already quite large, with many applications studied and research directions investigated. It is beyond the scope of this chapter to review the full spectrum of topics related to moving mesh methods. Instead, we focus only on one-dimensional problems in space, and we highlight only the most important aspects that will later allow us to put our approach to mesh adaptation in context. For a comprehensive summary of the field we refer the reader to [28] and [7], and the references therein.

For clarity, we will consider a concrete example, namely Burgers' equation

$$\frac{\partial u}{\partial t} + u\frac{\partial u}{\partial X} = \nu\frac{\partial^2 u}{\partial X^2}, \tag{3.0.1}$$

where $u = u(X,t)$ satisfies the boundary conditions $u(0,t) = u_L$ and $u(X_{max},t) = u_R$, and we will discuss how r-adaptive meshes can be applied to this model.

3.1 Discretization of the PDE on a nonuniform mesh

The first logical step of r-adaptation is the discretization of the physical PDE on a nonuniform mesh. It is often convenient to introduce a suitable coordinate transformation. Specifically, we assume for the moment that a time-dependent coordinate transformation $X : [0, X_{max}] \times \mathbb{R} \longrightarrow [0, X_{max}]$, $X = X(x,t)$, is given, where X represents the spatial coor-

dinate in the physical domain, and x denotes the spatial coordinate in the computational domain. This transformation is chosen such that the solution in the transformed variable,

$$\varphi(x,t) = u(X(x,t),t), \tag{3.1.1}$$

is smooth, and can be accurately approximated on a uniform mesh in the computational domain. A finite difference discretization of Burgers' equation on this uniform mesh can be derived using the so-called *quasi-Lagrange approach*. We transform (3.0.1) to the computational domain and derive the corresponding PDE for $\varphi(x,t)$. By the chain rule we have

$$\begin{aligned} u_X(X(x,t),t) &= \frac{\varphi_x(x,t)}{X_x(x,t)}, \\ u_{XX}(X(x,t),t) &= \frac{1}{X_x(x,t)}\left(\frac{\varphi_x(x,t)}{X_x(x,t)}\right)_x, \\ u_t(X(x,t),t) &= \varphi_t(x,t) - \frac{\varphi_x(x,t)}{X_x(x,t)}X_t(x,t), \end{aligned} \tag{3.1.2}$$

where subscripts denote differentiation with respect to appropriate variables. Burgers' equation becomes

$$\varphi_t - \frac{\varphi_x}{X_x}X_t + \varphi\frac{\varphi_x}{X_x} = \frac{\nu}{X_x}\left(\frac{\varphi_x}{X_x}\right)_x. \tag{3.1.3}$$

Let us discretize this equation in the computational domain by considering the uniformly spaced mesh points $x_i = i \cdot \Delta x$ for $i = 0, 1, \ldots, N+1$, where $\Delta x = X_{max}/(N+1)$. Denote $X_i(t) = X(x_i,t)$ and $y_i(t) = \varphi(x_i,t)$. Note that $X_i(t)$ describes the position of the i-th mesh point in the physical space at time t. The spatial derivatives can be approximated using finite differences, for instance

$$\varphi_x(x_i,t) \approx \frac{y_{i+1}-y_i}{\Delta x}, \qquad X_x(x_i,t) \approx \frac{X_{i+1}-X_i}{\Delta x}. \tag{3.1.4}$$

The semi-discretization of (3.1.3) becomes

$$\dot{y}_i - \frac{y_{i+1}-y_i}{X_{i+1}-X_i}\dot{X}_i + y_i\frac{y_{i+1}-y_i}{X_{i+1}-X_i} = \nu\frac{\frac{y_{i+2}-y_{i+1}}{X_{i+2}-X_{i+1}} - \frac{y_{i+1}-y_i}{X_{i+1}-X_i}}{X_{i+1}-X_i}. \tag{3.1.5}$$

If the functions $X_i(t)$ are known, then (3.1.5), together with the boundary conditions $y_0 = u_L$ and $y_{N+1} = u_R$, forms a system of ordinary differential equations for $y_1, \ldots, y_N$, and can be integrated in time using any numerical scheme. However, in practice we usually do not know the mesh point trajectories ahead of time, and we would like the mesh to dynamically adapt to the changes in the solution. We will therefore need additional equations describing the evolution of the mesh itself. An approach based on the equidistribution principle is discussed in the next section.

3.2 Moving mesh partial differential equations

3.2.1 Equidistribution principle

The concept of equidistribution is the most popular paradigm of r-adaptation (see [7], [28]). Given a continuous mesh density function $\rho(X)$, the equidistribution principle seeks to find a mesh $0 = X_0 < X_1 < ... < X_{N+1} = X_{max}$ such that the following holds

$$\int_0^{X_1} \rho(X)\, dX = \int_{X_1}^{X_2} \rho(X)\, dX = ... = \int_{X_N}^{X_{max}} \rho(X)\, dX, \tag{3.2.1}$$

that is, the quantity represented by the density function is equidistributed among all cells. In the continuous setting we will say that the reparametrization $X = X(x)$ equidistributes $\rho(X)$ if

$$\int_0^{X(x)} \rho(X)\, dX = \frac{x}{X_{max}}\sigma, \tag{3.2.2}$$

where $\sigma = \int_0^{X_{max}} \rho(X)\, dX$ is the total amount of the equidistributed quantity. Differentiate this equation with respect to x to obtain

$$\rho(X(x))\frac{\partial X}{\partial x} = \frac{1}{X_{max}}\sigma. \tag{3.2.3}$$

It is still a global condition in the sense that σ has to be known. For computational purposes it is convenient to differentiate this relation again and consider the following partial differential equation (also called moving mesh PDE, or MMPDE)

$$\frac{\partial}{\partial x}\Big(\rho(X(x))\frac{\partial X}{\partial x}\Big) = 0 \tag{3.2.4}$$

with the boundary conditions $X(0) = 0$, $X(X_{max}) = X_{max}$. An example discretization of this MMPDE on a uniform mesh in the computational domain can be

$$\frac{1}{\Delta x}\Big(\frac{\rho_{i+1}+\rho_i}{2}\frac{X_{i+1}-X_i}{\Delta x} - \frac{\rho_i+\rho_{i-1}}{2}\frac{X_i-X_{i-1}}{\Delta x}\Big) = 0, \tag{3.2.5}$$

where $\rho_i = \rho(X(x_i))$. Together with the boundary conditions $X_0 = 0$ and $X_{N+1} = X_{max}$, (3.2.5) provides a way to dynamically adapt the mesh in (3.1.5), as will be discussed in Section 3.3.

The choice of the mesh density function $\rho(X)$ is typically problem-dependent and the subject of much research. A popular example is the generalized solution arclength given by

$$\rho = \sqrt{1+\alpha^2\Big(\frac{\partial u}{\partial X}\Big)^2} = \sqrt{1+\alpha^2\Big(\frac{\varphi_x}{X_x}\Big)^2}, \tag{3.2.6}$$

where α is an adjustable scaling parameter. It is often used to construct meshes that can follow moving fronts with locally high gradients ([7], [28]). With this choice, equation (3.2.4) is equivalent to

$$\alpha^2\varphi_x\varphi_{xx} + X_xX_{xx} = 0, \tag{3.2.7}$$

assuming $X_x > 0$, which we demand anyway. A finite difference discretization on the mesh $x_i = i \cdot \Delta x$ gives us the set of contraints

$$g_i(y_1,...,y_N,X_1,...,X_N) =$$
$$\alpha^2(y_{i+1}-y_i)^2 + (X_{i+1}-X_i)^2 - \alpha^2(y_i-y_{i-1})^2 - (X_i-X_{i-1})^2 = 0, \tag{3.2.8}$$

with the previously defined y_i's and X_i's. Another popular example is the curvature-based mesh density

$$\rho = \sqrt[4]{1+\alpha^2\Big(\frac{\partial^2 u}{\partial X^2}\Big)^2}. \tag{3.2.9}$$

The resulting mesh is denser in the areas of high curvature in the solution. In some applications the curvature-based density function gives significantly more accurate results than the arclength density function, although it may be computationally more costly and prone to

instabilities. Yet another example are mesh density functions based on scaling invariance. Scaling invariance is an important property of a broad class of partial differential equations whose solutions blow up in finite time. Such blowups typically occur on increasingly smaller length scales and application of adaptive meshes greatly improves the accuracy of numerical computations. One may choose a density function such that the resulting MMPDE remains invariant under the same scaling, for instance

$$\rho = u^{\gamma}, \tag{3.2.10}$$

where γ is an appropriately chosen coefficient related to the scaling symmetry of the physical PDE.

3.2.2 Mesh smoothing

The main idea of moving mesh methods is to concentrate the mesh points in the areas where higher accuracy is required, for instance in the areas where the function $u(X,t)$ is not smooth or varies rapidly. This may be achieved by considering the equidistribution principle and the related partial differential equation (3.2.4). However, the mesh density function ρ computed this way may also change abruptly, which may introduce significant stiffness and slow down numerical computations. In order to improve the efficiency and accuracy of the computations one may apply certain smoothing techniques.

Spatial smoothing. It is a common practice in computations involving moving mesh methods to smooth out the mesh density function in space at each timestep, so that the MMPDE is easier to integrate and the resulting mesh is smoother. Smoothing the mesh density, e.g. by some local averaging procedure, can considerably improve the performance and accuracy of computations, as the iterations of the method may converge faster and larger time steps may be applied. A simple example is given by weighted averaging, i.e.,

$$\begin{aligned} \rho_i &:= \frac{1}{4}\rho_{i-1} + \frac{1}{2}\rho_i + \frac{1}{4}\rho_{i+1}, \qquad\qquad i = 1, \ldots, N, \\ \rho_0 &:= \frac{1}{2}\rho_0 + \frac{1}{2}\rho_1, \\ \rho_{N+1} &:= \frac{1}{2}\rho_N + \frac{1}{2}\rho_{N+1}, \end{aligned} \tag{3.2.11}$$

where := denotes the assignment operation. Several sweeps of this procedure may be applied at each integration step.

More generally, a smoothed density function $\tilde{\rho}$ can be obtained by using an elliptic operator, such as the Laplacian, or an approximation to it. For instance, one can consider the boundary value problem

$$\begin{aligned} \Big(1 - \beta^{-2}\frac{d^2}{dx^2}\Big)\tilde{\rho} &= \rho, \\ \frac{d\tilde{\rho}}{dx}(0) = \frac{d\tilde{\rho}}{dx}(X_{max}) &= 0, \end{aligned} \tag{3.2.12}$$

where $\beta > 0$ is a parameter which can be fine-tuned, and ρ and $\tilde{\rho}$ are regarded as functions of x. For a given ρ, the new mesh density $\tilde{\rho}$ will have higher regularity. For more information see [29].

Temporal smoothing. The equidistribution principle leads to the boundary value problem (3.2.4), which does not involve time derivatives of the time-dependent coordinate transformation $X(x,t)$. As a result, the semi-discretizations (3.2.5) or (3.2.8) are a set of algebraic constraints, which, when coupled to the semi-discretization (3.1.5), form a set of differential-algebraic equations (DAEs), as will be discussed in Section 3.3. There are several advantages of modifying (3.2.4), so that it contains the mesh speed. First of all, a semi-discretization will then give a set of ODEs, which are numerically easier to handle than DAEs. In addition, including the mesh speed in the mesh equations allows for the introduction of a certain level of temporal smoothing for mesh movement. In order to construct such modifications, it is convenient to consider the inverse coordinate transformation, that is, $x = x(X,t)$. The MMPDE (3.2.4) is then transformed into

$$\frac{\partial}{\partial X}\left(\frac{1}{\rho(X,t)}\frac{\partial x}{\partial X}\right) = 0 \tag{3.2.13}$$

with the boundary conditions $x(0,t) = 0$ and $x(X_{max},t) = X_{max}$. It is easy to see that the solution to this problem is a minimizer of the functional

$$I\big[x(X,t)\big] = \frac{1}{2}\int_0^{X_{max}} \frac{1}{\rho(X,t)}\left(\frac{\partial x}{\partial X}\right)^2 dX, \tag{3.2.14}$$

that is, (3.2.13) is equivalent to $\delta I/\delta x = 0$ with appropriate boundary conditions. As a way to introduce the mesh speed, we can consider the *gradient flow equation*, which has the form

$$\frac{\partial x}{\partial t} = -\frac{P}{\epsilon}\frac{\delta I}{\delta x}, \tag{3.2.15}$$

where P is some positive-definite differential operator, and $\epsilon > 0$ is a user-specified parameter that controls the response time of mesh movement to changes in $\rho(X,t)$. The theoretical advantage of using the inverse transformation $x = x(X,t)$ is the fact that the functional (3.2.14) is quadratic and the associated PDE (3.2.13) is linear, which makes the analysis of existence, uniqueness, and well-posedness easier. However, it is not practical in computations, since $x(X,t)$ does not directly specify the location of the mesh points in the physical domain. Let us transform back to the formulation with the reparametrization $X = X(x,t)$. The gradient flow equation takes the form

$$\frac{\partial X}{\partial t} = \frac{1}{\epsilon}\frac{\partial X}{\partial x}P\left(\rho\frac{\partial X}{\partial x}\right)^{-2}\left(\frac{\partial X}{\partial x}\right)^{-1}\frac{\partial}{\partial x}\left(\rho\frac{\partial X}{\partial x}\right), \tag{3.2.16}$$

By choosing various P's, we can obtain different modifications of (3.2.4). For instance, for $P = (\rho X_x)^2$ we get the so-called MMPDE5 (see [27])

$$\text{(MMPDE5):} \qquad \frac{\partial X}{\partial t} = \frac{1}{\epsilon}\frac{\partial}{\partial x}\left(\rho\frac{\partial X}{\partial x}\right), \tag{3.2.17}$$

whereas for

$$P = -\left(\frac{\partial X}{\partial x}\right)^{-1}\left(\frac{\partial}{\partial x}\rho\frac{\partial}{\partial x}\right)^{-1}\left(\rho\frac{\partial X}{\partial x}\right)^{2}\frac{\partial X}{\partial x} \tag{3.2.18}$$

we obtain

$$\text{(MMPDE4):} \qquad \frac{\partial}{\partial x}\left(\rho\frac{\partial X_t}{\partial x}\right) = -\frac{1}{\epsilon}\frac{\partial}{\partial x}\left(\rho\frac{\partial X}{\partial x}\right), \tag{3.2.19}$$

and

$$P = -\left(\frac{\partial X}{\partial x}\right)^{-1}\left(\frac{\partial^2}{\partial x^2}\right)^{-1}\left(\rho\frac{\partial X}{\partial x}\right)^{2}\frac{\partial X}{\partial x} \tag{3.2.20}$$

results in

$$\text{(MMPDE6):} \qquad \frac{\partial^2 X_t}{\partial x^2} = -\frac{1}{\epsilon}\frac{\partial}{\partial x}\left(\rho\frac{\partial X}{\partial x}\right), \tag{3.2.21}$$

where $X_t \equiv \partial X/\partial t$ is the mesh speed. We may refer to the equidistribution relation (3.2.4) as MMPDE0. Note that MMPDE4-6 all contain the left-hand side term of MMPDE0, that is,

$$\frac{1}{\epsilon}\frac{\partial}{\partial x}\left(\rho\frac{\partial X}{\partial x}\right). \tag{3.2.22}$$

This term is zero if the mesh equidistributes the quantity represented by ρ. When it is non-zero, then it provides a driving force that draws the mesh back to equidistribution. This can be interpreted as attraction and repulsion pseudoforces which prevent the mesh points from collapsing or crossing each other.

Discretization of MMPDEs on a uniform mesh in the computational domain can be done in a way similar to (3.2.5) or (3.2.8). For instance, for MMPDE5 we may consider the following semi-discretization

$$\epsilon\dot{X}_i = \frac{1}{\Delta x}\Big(\frac{\rho_{i+1}+\rho_i}{2}\frac{X_{i+1}-X_i}{\Delta x} - \frac{\rho_i+\rho_{i-1}}{2}\frac{X_i-X_{i-1}}{\Delta x}\Big). \tag{3.2.23}$$

If we use the generalized arclength density (3.2.6), a similar discretization of MMPDE5 may take the form

$$\epsilon\dot{X}_i = \frac{1}{\Delta x^2}\frac{\alpha^2(y_{i+1}-y_i)^2 + (X_{i+1}-X_i)^2 - \alpha^2(y_i-y_{i-1})^2 - (X_i-X_{i-1})^2}{\sqrt{(y_{i+1}-y_{i-1})^2 + (X_{i+1}-X_{i-1})^2}}, \tag{3.2.24}$$

or simply $\epsilon\dot{X}_i = g_i(y_1, ..., y_N, X_1, ..., X_N)$, if one absorbs some positive terms into the definition of ϵ, where g_i was defined in (3.2.8). Note that (3.2.23) or (3.2.24) form a set of ODEs, unlike (3.2.5) or (3.2.8).

Information about other types of MMPDEs can be found in [27] and [30].

3.3 Coupling the mesh equations to the physical equations

The last logical step of an r-adaptive method consists of coupling the mesh equations discussed in Section 3.2 to the physical equations discussed in Section 3.1. This can be

achieved in two general ways, either by using the *quasi-Lagrange approach* or the *rezoning approach*. For the quasi-Lagrange approach, the physical PDE and the mesh equation can be further solved *simultaneously* or *alternately*. In this thesis we use only the simultaneous quasi-Lagrange approach, but for completeness we present a short overview of each strategy.

3.3.1 Quasi-Lagrange approach

In the quasi-Lagrange strategy, the mesh points are considered to move continuously in time. The physical time derivatives are therefore transformed into derivatives along the mesh trajectories, as in (3.1.2), and the physical PDE (3.0.1) is transformed into (3.1.3). This transformed PDE is then solved together with the mesh equation, say (3.2.4) or (3.2.17), for both the physical solution and the mesh configuration. This system can be integrated in time either simultaneously or alternately.

Simultaneous solution. The semi-discretization (3.1.5) of Burgers' equation and the semi-discretization (3.2.5) together form the differential-algebraic system

$$\begin{aligned} \dot{y}_i - \frac{y_{i+1}-y_i}{X_{i+1}-X_i}\dot{X}_i + y_i\frac{y_{i+1}-y_i}{X_{i+1}-X_i} &= \nu\frac{\frac{y_{i+2}-y_{i+1}}{X_{i+2}-X_{i+1}} - \frac{y_{i+1}-y_i}{X_{i+1}-X_i}}{X_{i+1}-X_i}, \\ 0 &= \frac{1}{\Delta x}\Big(\frac{\rho_{i+1}+\rho_i}{2}\frac{X_{i+1}-X_i}{\Delta x} - \frac{\rho_i+\rho_{i-1}}{2}\frac{X_i-X_{i-1}}{\Delta x}\Big), \end{aligned} \tag{3.3.1}$$

which needs to be solved for the functions $y_i(t)$ and $X_i(t)$, where $i = 1, \ldots, N$ and $y_0(t) = u_L$, $y_{N+1}(t) = u_R$, $X_0(t) = 0$, $X_{N+1}(t) = X_{max}$. This can be done with the help of an appropriate numerical DAE solver (see [6], [26], [22]). If we consider the MMPDE5 (3.2.17) instead, we obtain the following ODE system

$$\begin{aligned} \dot{y}_i - \frac{y_{i+1}-y_i}{X_{i+1}-X_i}\dot{X}_i + y_i\frac{y_{i+1}-y_i}{X_{i+1}-X_i} &= \nu\frac{\frac{y_{i+2}-y_{i+1}}{X_{i+2}-X_{i+1}} - \frac{y_{i+1}-y_i}{X_{i+1}-X_i}}{X_{i+1}-X_i}, \\ \epsilon\dot{X}_i &= \frac{1}{\Delta x}\Big(\frac{\rho_{i+1}+\rho_i}{2}\frac{X_{i+1}-X_i}{\Delta x} - \frac{\rho_i+\rho_{i-1}}{2}\frac{X_i-X_{i-1}}{\Delta x}\Big), \end{aligned} \tag{3.3.2}$$

which can be solved using any ODE solver.

The main advantage of this approach is the fact it is conceptually simple. Moreover, since at each time step we solve the equations simultaneously for $y_i(t)$ and $X_i(t)$, the mesh

responds promptly to any change occurring in the physical solution. However, the coupling between the mesh and the physical solution is highly nonlinear, even if one considers a linear PDE instead of Burgers' equation. As a result, (3.3.1) and (3.3.2) are more difficult and expensive to solve. This is the main reason why simultaneous solution has been limited mainly to one-dimensional problems in space.

Alternate solution. In order to decouple the mesh equations from the physical equations, one may try to solve them separately. Suppose we are looking for a solution at the discrete set of times $0 = t_0 < t_1 < t_2 < \ldots$, where the increments $\Delta t_n = t_{n+1} - t_n$ do not have to be uniform over the integration interval, and denote $y_i^n = y_i(t_n)$ and $X_i^n = X_i(t_n)$. The idea of the alternate solution procedure is to first generate a mesh X^{n+1} at the new time level using the mesh and the physical solution (X^n, y^n) at the current time level, and then solve for the physical solution y^{n+1} at the new time level. As an example, consider the following discretization of (3.3.2):

$$\epsilon \frac{X_i^{n+1} - X_i^n}{\Delta t_n} = \frac{1}{\Delta x}\left(\frac{\rho_{i+1}^n + \rho_i^n}{2} \frac{X_{i+1}^{n+1} - X_i^{n+1}}{\Delta x} - \frac{\rho_i^n + \rho_{i-1}^n}{2} \frac{X_i^{n+1} - X_{i-1}^{n+1}}{\Delta x} \right), \tag{3.3.3a}$$

$$\begin{aligned} \frac{y_i^{n+1} - y_i^n}{\Delta t_n} &- \frac{1}{2}\left(\frac{y_{i+1}^n - y_i^n}{X_{i+1}^n - X_i^n} + \frac{y_{i+1}^{n+1} - y_i^{n+1}}{X_{i+1}^{n+1} - X_i^{n+1}} \right) \frac{X_i^{n+1} - X_i^n}{\Delta t_n} \\ &+ \frac{1}{2}\left(y_i^n \frac{y_{i+1}^n - y_i^n}{X_{i+1}^n - X_i^n} + y_i^{n+1} \frac{y_{i+1}^{n+1} - y_i^{n+1}}{X_{i+1}^{n+1} - X_i^{n+1}} \right) \\ &= \frac{1}{2}\nu \left(\frac{\frac{y_{i+2}^n - y_{i+1}^n}{X_{i+2}^n - X_{i+1}^n} - \frac{y_{i+1}^n - y_i^n}{X_{i+1}^n - X_i^n}}{X_{i+1}^n - X_i^n} + \frac{\frac{y_{i+2}^{n+1} - y_{i+1}^{n+1}}{X_{i+2}^{n+1} - X_{i+1}^{n+1}} - \frac{y_{i+1}^{n+1} - y_i^{n+1}}{X_{i+1}^{n+1} - X_i^{n+1}}}{X_{i+1}^{n+1} - X_i^{n+1}} \right). \end{aligned} \tag{3.3.3b}$$

We see that equation (3.3.3a) is decoupled and can be solved for the new mesh (M), i.e. X_i^{n+1}. The new mesh can be then substituted into (3.3.3b), and the equation can be solved for the updated physical solution (P), i.e. y_i^{n+1}. This is referred to as the MP procedure.

The main advantage of the alternate solution procedure is the fact that the mesh and physical equations decouple, and each can be solved more efficiently. However, the new mesh X^{n+1} adapts only to the current physical solution y^n, which introduces a time lag in mesh movement. This may cause instabilities in the computations if the mesh is not generated accurately enough at one time step. As a consequence, much smaller time steps Δt_n may be required.

3.3.2 Rezoning approach

In the rezoning strategy the mesh points are considered to move in a discontinuous fashion in time. Let us briefly describe this procedure. Suppose that at time t_n we have the physical solution y^n and the mesh X^n. The physical solution $\tilde{y}^{n+1}$ at the new time level is computed by holding the mesh X^n fixed. Naturally, the updated physical solution $\tilde{y}^{n+1}$ on the mesh X^n will not, in general, satisfy the equidistribution principle. Using the values $\tilde{y}_0^{n+1}, \ldots, \tilde{y}_{N+1}^{n+1}$ and the mesh points $X_0^n, \ldots, X_{N+1}^n$, the physical solution is interpolated, and a new equidistributing mesh X^{n+1} and corresponding y^{n+1} are then computed, for instance by solving (3.2.4). Interpolation of the physical solution is a crucial step for the success of this approach, and often has to be done in a special way. We refer the interested reader to [28] for more information.

Chapter 4

R-adaptive variational integrators

In this chapter we propose two ideas on how moving mesh methods can be applied in geometric integration of Lagrangian partial differential equations. Let us consider a (1+1)-dimensional scalar field theory with the action functional

$$S[\phi] = \int_0^{T_{max}} \int_0^{X_{max}} \mathcal{L}(\phi, \phi_X, \phi_t)\, dX\, dt, \tag{4.0.1}$$

where $\phi : [0, X_{max}] \times [0, T_{max}] \longrightarrow \mathbb{R}$ is the field and $\mathcal{L} : \mathbb{R} \times \mathbb{R} \times \mathbb{R} \longrightarrow \mathbb{R}$ its Lagrangian density. For simplicity, we assume the following fixed boundary conditions

$$\begin{aligned} \phi(0,t) &= \phi_L, \\ \phi(X_{max},t) &= \phi_R. \end{aligned} \tag{4.0.2}$$

In order to further consider moving meshes, let us perform a change of variables $X = X(x,t)$ such that for all t the map $X(.,t) : [0, X_{max}] \longrightarrow [0, X_{max}]$ is a 'diffeomorphism'—more precisely, we only require that $X(.,t)$ is a homeomorphism such that both $X(.,t)$ and $X(.,t)^{-1}$ are piecewise C^1. In the context of mesh adaptation the map $X(x,t)$ is going to represent the spatial position at time t of the mesh point labeled by x. Define $\varphi(x,t) = \phi(X(x,t),t)$. Then the partial derivatives of ϕ are $\phi_X(X(x,t),t) = \varphi_x/X_x$ and $\phi_t(X(x,t),t) = \varphi_t - \varphi_x X_t/X_x$. Plugging these equations in (4.0.1) we get

$$S[\phi] = \int_0^{T_{max}} \int_0^{X_{max}} \mathcal{L}\Big(\varphi, \frac{\varphi_x}{X_x}, \varphi_t - \frac{\varphi_x X_t}{X_x}\Big) X_x\, dx\, dt =: \tilde{S}[\varphi], \tilde{S}[\varphi, X] \tag{4.0.3}$$

where the last equality defines two modified, or 'reparametrized', action functionals. For the first one, $\tilde{S}$ is considered as a functional of φ only, whereas in the second one we also treat it as a functional of X. This leads to two different approaches to mesh adaptation, which we dub the *control-theoretic* strategy and the *Lagrange multiplier* strategy, respectively.

The 'reparametrized' field theories defined by $\tilde{S}[\varphi]$ and $\tilde{S}[\varphi, X]$ are both intrinsically covariant; however, it is convenient for computational purposes to work with a space-time split and formulate the field dynamics as an initial value problem. Therefore, in this chapter we take the view of infinite dimensional manifolds of fields as configuration spaces, and develop the control-theoretic and Lagrange multiplier strategies in that setting. It allows us to discretize our system in space first and consider time discretization later on. It is clear from our exposition that the resulting integrators are variational. In Chapter 5 we show how similar integrators can be constructed using the covariant formalism of multisymplectic field theory.

4.1 Control-theoretic approach to r-adaptation

At first glance, it appears that the simplest and most straightforward way to construct an r-adaptive variational integrator would be to discretize the physical system in a similar manner to the general approach to variational integration, i.e., discretize the underlying variational principle (see Section 2.4 and Section 2.7), and then derive the mesh equations and couple them to the physical equations in a way typical of the existing r-adaptive algorithms (see Section 3.3). We explore this idea in this section and show that it indeed leads to space adaptive integrators that are variational in nature. However, we also show that those integrators do not exhibit the behavior expected of geometric integrators, such as good energy conservation.

4.1.1 Reparametrized Lagrangian

For the moment let us assume that $X(x,t)$ is a known function. We denote by $\xi(X,t)$ the function such that $\xi(.,t) = X(.,t)^{-1}$, that is $\xi(X(x,t),t) = x$ [1]. We thus have $\tilde{S}[\varphi] = S[\varphi(\xi(X,t),t)]$.

[1] We allow a little abuse of notation here: X denotes both the argument of ξ and the change of variables $X(x,t)$. If we wanted to be more precise, we would write $X = h(x,t)$.

Proposition 4.1.1. *Extremizing $S[\phi]$ with respect to ϕ is equivalent to extremizing $\tilde{S}[\varphi]$ with respect to φ.*

Proof. The variational derivatives of S and $\tilde{S}$ are related by the formula

$$\delta\tilde{S}[\varphi]\cdot\delta\varphi(x,t) = \delta S[\varphi(\xi(X,t),t)]\cdot\delta\varphi(\xi(X,t),t). \tag{4.1.1}$$

Suppose $\phi(X,t)$ extremizes $S[\phi]$, i.e., $\delta S[\phi]\cdot\delta\phi = 0$ for all variations $\delta\phi$. Given the function $X(x,t)$, define $\varphi(x,t) = \phi(X(x,t),t)$. Then, by the formula above we have $\delta\tilde{S}[\varphi] = 0$, so φ extremizes $\tilde{S}$. Conversely, suppose $\varphi(x,t)$ extremizes $\tilde{S}$, that is, $\delta\tilde{S}[\varphi]\cdot\delta\varphi = 0$ for all variations $\delta\varphi$. Since we assume $X(.,t)$ is a homeomorphism, we can define $\phi(X,t) = \varphi(\xi(X,t),t)$. Note that an arbitrary variation $\delta\phi(X,t)$ induces the variation $\delta\varphi(x,t) = \delta\phi(X(x,t),t)$. Then we have $\delta S[\phi]\cdot\delta\phi = \delta\tilde{S}[\varphi]\cdot\delta\varphi = 0$ for all variations $\delta\phi$, so $\phi(X,t)$ extremizes $S[\phi]$.

□

The corresponding instantaneous Lagrangian $\tilde{L} : Q\times W\times\mathbb{R}\longrightarrow\mathbb{R}$ is

$$\tilde{L}[\varphi,\varphi_t,t] = \int_0^{X_{max}} \tilde{\mathcal{L}}(\varphi,\varphi_x,\varphi_t,t)\,dx \tag{4.1.2}$$

with the Lagrangian density

$$\tilde{\mathcal{L}}(\varphi,\varphi_x,\varphi_t,x,t) = \mathcal{L}\Big(\varphi,\frac{\varphi_x}{X_x},\varphi_t-\frac{\varphi_x X_t}{X_x}\Big)X_x. \tag{4.1.3}$$

The function spaces Q and W must be chosen appropriately for the problem at hand, so that (4.1.2) makes sense. For instance, for a free field we will have $Q = H^1([0,X_{max}])$ and $W = L^2([0,X_{max}])$. Since $X(x,t)$ is a function of t, we are looking at a time-dependent system. Even though the energy associated with (4.1.2) is not conserved, the energy of the original theory associated with (4.0.1)

$$E = \int_0^{X_{max}} \Big(\phi_t\frac{\partial\mathcal{L}}{\partial\phi_t}(\phi,\phi_X,\phi_t) - \mathcal{L}(\phi,\phi_X,\phi_t)\Big)\,dX \tag{4.1.4}$$

$$= \int_0^{X_{max}} \Big[\Big(\varphi_t-\frac{\varphi_x X_t}{X_x}\Big)\frac{\partial\mathcal{L}}{\partial\phi_t}\Big(\varphi,\frac{\varphi_x}{X_x},\varphi_t-\frac{\varphi_x X_t}{X_x}\Big) - \mathcal{L}\Big(\varphi,\frac{\varphi_x}{X_x},\varphi_t-\frac{\varphi_x X_t}{X_x}\Big)\Big]X_x\,dx \tag{4.1.5}$$

is conserved. To see this, note that if $\phi(X,t)$ extremizes $S[\phi]$ then $dE/dt = 0$ (computed from (4.1.4)). Trivially, this means that $dE/dt = 0$ when formula (4.1.5) is invoked as well. Moreover, as we have noted earlier, $\phi(X,t)$ extremizes $S[\phi]$ iff $\varphi(x,t)$ extremizes $\tilde{S}[\varphi]$. This means that the energy (4.1.5) is constant on solutions of the reparametrized theory.

4.1.2 Spatial Finite Element discretization

We begin with a discretization of the spatial dimension only, thus turning the original infinite-dimensional problem into a time-continuous finite-dimensional Lagrangian system. Let $\Delta x = X_{max}/(N+1)$ and define the reference uniform mesh $x_i = i \cdot \Delta x$ for $i = 0, 1, ..., N+1$, and the corresponding piecewise linear finite elements

$$\eta_i(x) = \begin{cases} \frac{x - x_{i-1}}{\Delta x}, & \text{if } x_{i-1} \le x \le x_i, \\ -\frac{x - x_{i+1}}{\Delta x}, & \text{if } x_i \le x \le x_{i+1}, \\ 0, & \text{otherwise.} \end{cases} \tag{4.1.6}$$

We now restrict $X(x,t)$ to be of the form

$$X(x,t) = \sum_{i=0}^{N+1} X_i(t)\eta_i(x) \tag{4.1.7}$$

with $X_0(t) = 0$, $X_{N+1}(t) = X_{max}$ and arbitrary $X_i(t)$, $i = 1, 2, ..., N$ as long as $X(.,t)$ is a homeomorphism for all t. In our context of numerical computations, the functions $X_i(t)$ represent the current position of the i^{th} mesh point. Define the finite element spaces

$$Q_N = W_N = \text{span}(\eta_0, ..., \eta_{N+1}) \tag{4.1.8}$$

and assume that $Q_N \subset Q$, $W_N \subset W$. Let us denote a generic element of Q_N by φ and a generic element of W_N by $\dot{\varphi}$. We have the decompositions

$$\varphi(x) = \sum_{i=0}^{N+1} y_i\eta_i(x), \qquad \dot{\varphi}(x) = \sum_{i=0}^{N+1} \dot{y}_i\eta_i(x). \tag{4.1.9}$$

The numbers $(y_i, \dot{y}_i)$ thus form natural (global) coordinates on $Q_N \times W_N$. We can now approximate the dynamics of system (4.1.2) in the finite-dimensional space $Q_N \times W_N$. Let us consider the restriction $\tilde{L}_N = \tilde{L}|_{Q_N \times W_N \times \mathbb{R}}$ of the Lagrangian (4.1.2) to $Q_N \times W_N \times \mathbb{R}$. In the chosen coordinates we have

$$\tilde{L}_N(y_0, ..., y_{N+1}, \dot{y}_0, ..., \dot{y}_{N+1}, t) = \tilde{L}\Big[\sum_{i=0}^{N+1} y_i\eta_i(x), \sum_{i=0}^{N+1} \dot{y}_i\eta_i(x), t\Big]. \tag{4.1.10}$$

Note that, given the boundary conditions (4.0.2), y_0, y_{N+1}, $\dot{y}_0$, and $\dot{y}_{N+1}$ are fixed. We will thus no longer write them as arguments of $\tilde{L}_N$.

The advantage of using a finite element discretization lies in the fact that the symplectic structure induced on $Q_N \times W_N$ by $\tilde{L}_N$ is strictly a restriction (i.e., a pull-back) of the (pre-)symplectic structure[2] on $Q \times W$. This establishes a direct link between symplectic integration of the finite-dimensional mechanical system $(Q_N \times W_N, \tilde{L}_N)$ and the infinite-dimensional field theory $(Q \times W, \tilde{L})$

4.1.3 DAE formulation and time integration

We are now going to consider time integration of the Lagrangian system $(Q_N \times W_N, \tilde{L}_N)$. If the functions $X_i(t)$ are known, then one can perform variational integration in the standard way, that is, define the discrete Lagrangian $\tilde{L}_d : \mathbb{R} \times Q_N \times \mathbb{R} \times Q_N \to \mathbb{R}$ and solve the corresponding discrete Euler-Lagrange equations (see Section 2.4 and [41], [23]). Let $t_n = n \cdot \Delta t$ for $n = 0, 1, 2, \ldots$ be an increasing sequence of times and $\{y^0, y^1, \ldots\}$ the corresponding discrete path of the system in Q_N. The discrete Lagrangian L_d is an approximation to the exact discrete Lagrangian L_d^E, such that

$$\tilde{L}_d(t_n, y^n, t_{n+1}, y^{n+1}) \approx \tilde{L}_d^E(t_n, y^n, t_{n+1}, y^{n+1}) \equiv \int_{t_n}^{t_{n+1}} \tilde{L}_N(y(t), \dot{y}(t), t)\, dt, \tag{4.1.11}$$

where $y^n = (y_1^n, ..., y_N^n)$, $y^{n+1} = (y_1^{n+1}, ..., y_N^{n+1})$, and $y(t)$ is the solution of the Euler-Lagrange equations corresponding to $\tilde{L}_N$, with the boundary values $y(t_n) = y^n$, $y(t_{n+1}) = y^{n+1}$. Depending on the quadrature we use to approximate the integral in (4.1.11), we obtain different types of variational integrators. As will be discussed below, in r-adaptation one has to deal with stiff differential equations or differential-algebraic equations, therefore higher-order integration in time is required. We are going to employ variational partitioned Runge-Kutta methods (see Section 2.4.3). An s-stage Runge Kutta method is constructed by choosing

[2] In most cases the symplectic structure of $(Q \times W, \tilde{L})$ is only weakly-nondegenerate; see [18]

$$\tilde{L}_d(t_n, y^n, t_{n+1}, y^{n+1}) = (t_{n+1} - t_n) \sum_{i=1}^{s} b_i \tilde{L}_N(Y_i, \dot{Y}_i, t_i), \tag{4.1.12}$$

where $t_i = t_n + c_i(t_{n+1} - t_n)$, the right-hand side is extremized under the constraint $y^{n+1} = y^n + (t_{n+1} - t_n) \sum_{i=1}^{s} b_i \dot{Y}_i$, and the internal stage variables Y_i, $\dot{Y}_i$ are related by $Y_i = y^n + (t_{n+1} - t_n) \sum_{j=1}^{s} a_{ij} \dot{Y}_j$. It can be shown that the variational integrator with the discrete Lagrangian (4.1.12) is equivalent to an appropriately chosen symplectic partitioned Runge-Kutta method applied to the Hamiltonian system corresponding to $\tilde{L}_N$ (see Section 2.4.3 and [41], [23]). With this in mind we turn our semi-discrete Lagrangian system $(Q_N \times W_N, \tilde{L}_N)$ into the Hamiltonian system $(Q_N \times W_N^*, \tilde{H}_N)$ via the standard Legendre transform (see Section 2.3)

$$\tilde{H}_N(y_1, ..., y_N, p_1, ..., p_N; X_1, ..., X_N, \dot{X}_1, ..., \dot{X}_N) = \sum_{i=1}^{N} p_i \dot{y}_i - \tilde{L}_N(y_1, ..., y_N, \dot{y}_1, ..., \dot{y}_N, t), \tag{4.1.13}$$

where $p_i = \partial \tilde{L}_N / \partial \dot{y}_i$, and we explicitly state the dependence on the positions X_i and velocities $\dot{X}_i$ of the mesh points. The Hamiltonian equations take the form[3]

$$\begin{aligned} \dot{y}_i &= \frac{\partial \tilde{H}_N}{\partial p_i}\Big(y, p; X(t), \dot{X}(t)\Big), \\ \dot{p}_i &= -\frac{\partial \tilde{H}_N}{\partial y_i}\Big(y, p; X(t), \dot{X}(t)\Big). \end{aligned} \tag{4.1.14}$$

Suppose that the functions $X_i(t)$ are C^1 and H_N is smooth as a function of the y_i's, p_i's, X_i's, and $\dot{X}_i$'s (note that these assumptions are used for simplicity, and can be easily relaxed if necessary, depending on the regularity of the considered Lagrangian system). Then the assumptions of Picard's theorem are satisfied and there exists a unique C^1 flow $F_{t_0,t} = (F^y_{t_0,t}, F^p_{t_0,t}) : Q_N \times W_N^* \to Q_N \times W_N^*$ for (4.1.14). This flow is symplectic.

However, in practice we do not know the X_i's and we in fact would like to be able to adjust them 'on the fly', based on the current behavior of the system. We are going to do that by introducing additional constraint functions $g_i(y_1, ..., y_N, X_1, ..., X_N)$ and demanding

[3]It is computationally more convenient to directly integrate the implicit Hamiltonian system $p_i = \partial \tilde{L}_N / \partial \dot{y}_i$, $\dot{p}_i = \partial \tilde{L}_N / \partial y_i$, but as long as system (4.0.1) is at least weakly-nondegenerate there is no theoretical issue with passing to the Hamiltonian formulation, which we do for the clarity of our exposition.

that the conditions $g_i = 0$ be satisfied at all times[4]. The choice of these functions may be based on the equidistribution principle, as discussed in Section 3.2; for instance we may take (3.2.8). This leads to the following differential-algebraic system of index 1 (see [6], [26], [22])

$$\begin{aligned}
\dot{y}_i &= \frac{\partial \tilde{H}_N}{\partial p_i}\Big(y, p; X, \dot{X}\Big), \\
\dot{p}_i &= -\frac{\partial \tilde{H}_N}{\partial y_i}\Big(y, p; X, \dot{X}\Big), \\
0 &= g_i(y, X), \\
y_i(t_0) &= y_i^{(0)}, \\
p_i(t_0) &= p_i^{(0)}
\end{aligned} \tag{4.1.15}$$

for $i = 1, ..., N$. Note that an initial condition for X is fixed by the constraints. This system is of index 1, because one has to differentiate the algebraic equations once with respect to time in order to reduce it to an implicit ODE system. In fact, the implicit system will take the form

$$\begin{aligned}
\dot{y} &= \frac{\partial \tilde{H}_N}{\partial p}\Big(y, p; X, \dot{X}\Big), \\
\dot{p} &= -\frac{\partial \tilde{H}_N}{\partial y}\Big(y, p; X, \dot{X}\Big), \\
0 &= \frac{\partial g}{\partial y}(y, X)\dot{y} + \frac{\partial g}{\partial X}(y, X)\dot{X}, \\
y(t_0) &= y^{(0)}, \\
p(t_0) &= p^{(0)}, \\
X(t_0) &= X^{(0)},
\end{aligned} \tag{4.1.16}$$

where $X^{(0)}$ is a vector of arbitrary initial condition for the X_i's. Suppose again that H_N is a smooth function of y, p, X, and $\dot{X}$. Futhermore, suppose that g is a C^1 function of y, X, and $\frac{\partial g}{\partial X} - \frac{\partial g}{\partial y}\frac{\partial^2 H_N}{\partial \dot{X} \partial p}$ is invertible with its inverse bounded in a neighborhood of the

[4]In the context of Control Theory the constraints $g_i = 0$ are called *strict static state feedback*. See [46].

exact solution.[5] Then, by the Implicit Function Theorem equations (4.1.16) can be solved explicitly for $\dot{y}$, $\dot{p}$, $\dot{X}$ and the resulting explicit ODE system will satisfy the assumptions of Picard's theorem. Let $(y(t), p(t), X(t))$ be the unique C^1 solution to this ODE system (and hence to (4.1.16)). We have the trivial result:

Proposition 4.1.2. *If $g(y^{(0)}, X^{(0)}) = 0$, then $(y(t), p(t), X(t))$ is a solution to (4.1.15).*[6]

In practice we would like to integrate system (4.1.15). A question arises regarding in what sense is this system symplectic, and in what sense a numerical integration scheme for this system can be regarded as variational. Let us address these issues.

Proposition 4.1.3. *Let $(y(t), p(t), X(t))$ be a solution to (4.1.15) and use this $X(t)$ to form the Hamiltonian system (4.1.14). Then we have that*

$$y(t) = F^y_{t_0,t}(y^{(0)}, p^{(0)}), \qquad p(t) = F^p_{t_0,t}(y^{(0)}, p^{(0)})$$

and

$$g\Big(F^y_{t_0,t}(y^{(0)}, p^{(0)}), X(t)\Big) = 0,$$

where $F_{t_0,t}(\hat{y}, \hat{p})$ is the symplectic flow for (4.1.14).

Proof. Note that the first two equations of (4.1.15) are the same as (4.1.14), therefore $(y(t), p(t))$ trivially satisfies (4.1.14) with the initial conditions $y(t_0) = y^{(0)}$ and $p(t_0) = p^{(0)}$. Since the flow map $F_{t_0,t}$ is unique, we must have $y(t) = F^y_{t_0,t}(y^{(0)}, p^{(0)})$ and $p(t) = F^p_{t_0,t}(y^{(0)}, p^{(0)})$. Then we also must have that $g\Big(F^y_{t_0,t}(y^{(0)}, p^{(0)}), X(t)\Big) = 0$, that is, the constraints are satisfied along one particular integral curve of (4.1.14) that passes through $(y^{(0)}, p^{(0)})$ at t_0.

□

Suppose we now would like to find a numerical approximation of the solution to (4.1.14) using an s-stage partitioned Runge-Kutta method with coefficients a_{ij}, b_i, $\bar{a}_{ij}$, $\bar{b}_i$, c_i (see Section 2.2.2 and [24], [23]). The numerical scheme will take the form

[5] Again, these assumptions can be relaxed if necessary.

[6] Note that there might be other solutions, as for any given $y^{(0)}$ there might be more than one $X^{(0)}$ that solves the constraint equations.

$$
\begin{aligned}
\dot{Y}^i &= \frac{\partial \tilde{H}_N}{\partial p}\Big(Y^i, P^i; X(t_n + c_i\Delta t), \dot{X}(t_n + c_i\Delta t)\Big), \\
\dot{P}^i &= -\frac{\partial \tilde{H}_N}{\partial y}\Big(Y^i, P^i; X(t_n + c_i\Delta t), \dot{X}(t_n + c_i\Delta t)\Big), \\
Y^i &= y^n + \Delta t \sum_{j=1}^{s} a_{ij}\dot{Y}^j, \qquad P^i = p^n + \Delta t \sum_{j=1}^{s} \bar{a}_{ij}\dot{P}^j, \\
y^{n+1} &= y^n + \Delta t \sum_{i=1}^{s} b_i\dot{Y}^i, \qquad p^{n+1} = p^n + \Delta t \sum_{i=1}^{s} \bar{b}_i\dot{P}^i,
\end{aligned}
\tag{4.1.17}
$$

where Y^i, $\dot{Y}^i$, P^i, $\dot{P}^i$ are the internal stages and Δt is the integration timestep. Let us apply the same partitioned Runge-Kutta method to (4.1.15). In order to compute the internal stages Q^i, $\dot{Q}^i$ of the X variable we use the state-space form approach, that is, we demand that the constraints and their time derivatives be satisfied (see [26]). The new step value X^{n+1} is computed by solving the constraints as well. The resulting numerical scheme is thus

$$
\begin{aligned}
\dot{Y}^i &= \frac{\partial \tilde{H}_N}{\partial p}\Big(Y^i, P^i; Q^i, \dot{Q}^i\Big), \qquad \dot{P}^i = -\frac{\partial \tilde{H}_N}{\partial y}\Big(Y^i, P^i; Q^i, \dot{Q}^i\Big), \\
Y^i &= y^n + \Delta t \sum_{j=1}^{s} a_{ij}\dot{Y}^j, \qquad P^i = p^n + \Delta t \sum_{j=1}^{s} \bar{a}_{ij}\dot{P}^j, \\
0 &= g(Y^i, Q^i), \qquad 0 = \frac{\partial g}{\partial y}(Y^i, Q^i)\,\dot{Y}^i + \frac{\partial g}{\partial X}(Y^i, Q^i)\,\dot{Q}^i, \\
y^{n+1} &= y^n + \Delta t \sum_{i=1}^{s} b_i\dot{Y}^i, \qquad p^{n+1} = p^n + \Delta t \sum_{i=1}^{s} \bar{b}_i\dot{P}^i, \\
0 &= g(y^{n+1}, X^{n+1}).
\end{aligned}
\tag{4.1.18}
$$

We have the following trivial observation.

Proposition 4.1.4. *If $X(t)$ is defined to be a C^1 interpolation of the internal stages Q^i, $\dot{Q}^i$ at times $t_n + c_i\Delta t$ (that is, if the values $X(t_n + c_i\Delta t)$, $\dot{X}(t_n + c_i\Delta t)$ coincide with Q^i, $\dot{Q}^i$), then the schemes (4.1.17) and (4.1.18) give the same numerical approximations y^n, p^n to the exact solution $y(t)$, $p(t)$.*

Intuitively, Proposition 4.1.4 states that we can apply a symplectic partitioned Runge-Kutta method to the DAE system (4.1.15), which solves both for $X(t)$ and $(y(t), p(t))$, and

the result will be the same as if we performed a symplectic integration of the Hamiltonian system (4.1.14) for $(y(t), p(t))$ with a *known* $X(t)$.

4.1.4 Example

To illustrate these ideas let us consider the Lagrangian density

$$\mathcal{L}(\phi, \phi_X, \phi_t) = \frac{1}{2}\phi_t^2 - W(\phi_X). \tag{4.1.19}$$

The reparametrized Lagrangian (4.1.2) takes the form

$$\tilde{L}[\varphi, \varphi_t, t] = \int_0^{X_{max}} \left[\frac{1}{2} X_x \Big(\varphi_t - \frac{\varphi_x}{X_x} X_t\Big)^2 - W\Big(\frac{\varphi_x}{X_x}\Big) X_x\right] dx. \tag{4.1.20}$$

Let $N = 1$ and $\phi_L = \phi_R = 0$. Then

$$\varphi(x,t) = y_1(t)\eta_1(x), \qquad X(x,t) = X_1(t)\eta_1(x) + X_{max}\,\eta_2(x). \tag{4.1.21}$$

The semi-discrete Lagrangian is

$$\begin{aligned}\tilde{L}_N(y_1, \dot{y}_1, t) =& \frac{X_1(t)}{6}\left(\dot{y}_1 - \frac{y_1}{X_1(t)}\dot{X}_1(t)\right)^2 + \frac{X_{max} - X_1(t)}{6}\left(\dot{y}_1 + \frac{y_1}{X_{max} - X_1(t)}\dot{X}_1(t)\right)^2 \\ & - W\left(\frac{y_1}{X_1(t)}\right)X_1(t) - W\left(-\frac{y_1}{X_{max} - X_1(t)}\right)\big(X_{max} - X_1(t)\big).\end{aligned} \tag{4.1.22}$$

The Legendre transform gives $p_1 = \partial \tilde{L}_N / \partial \dot{y}_1 = X_{max}\dot{y}_1/3$, hence the semi-discrete Hamiltonian is

$$\begin{aligned}\tilde{H}_N(y_1, p_1; X_1, \dot{X}_1) =& \frac{3}{2X_{max}}p_1^2 - \frac{1}{6}\frac{X_{max}\dot{X}_1^2}{X_1(X_{max} - X_1)}y_1^2 \\ & + W\Big(\frac{y_1}{X_1}\Big)X_1 + W\Big(-\frac{y_1}{X_{max} - X_1}\Big)(X_{max} - X_1).\end{aligned} \tag{4.1.23}$$

The corresponding DAE system is

$$\begin{aligned}
\dot{y}_1 &= \frac{3}{X_{max}} p_1, \\
\dot{p}_1 &= \frac{1}{3} \frac{X_{max} \dot{X}_1^2}{X_1 (X_{max} - X_1)} y_1 - W'\Big(\frac{y_1}{X_1}\Big) + W'\Big(-\frac{y_1}{X_{max} - X_1}\Big), \\
0 &= g_1(y_1, X_1).
\end{aligned} \tag{4.1.24}$$

This system is to be solved for the unknown functions $y_1(t)$, $p_1(t)$, and $X_1(t)$. It is of index 1, because we have three unknown functions and only two differential equations—the algebraic equation has to be differentiated once in order to obtain a missing ODE.

4.1.5 Backward error analysis

As argued in Section 2.2.3, the true power of symplectic integration of Hamiltonian equations is revealed through backward error analysis: it can be shown that a symplectic integrator for a Hamiltonian system with the Hamiltonian $H(q,p)$ defines the *exact* flow for a nearby Hamiltonian system, whose Hamiltonian can be expressed as the asymptotic series

$$\mathscr{H}(q,p) = H(q,p) + \Delta t H_2(q,p) + \Delta t^2 H_3(q,p) + \dots \tag{4.1.25}$$

As a consequence, under some additional assumptions, symplectic numerical schemes nearly conserve the original Hamiltonian $H(q,p)$ over exponentially long time intervals. See [23] for details.

Let us briefly review the results of backward error analysis for the integrator (4.1.18). Suppose $g(y,X)$ satisfies the assumptions of the Implicit Function Theorem. Then, at least locally, we can solve the constraint $X = h(y)$. The Hamiltonian DAE system (4.1.15) can be then written as the following (implicit) ODE system for y and p

$$\begin{aligned}
\dot{y} &= \frac{\partial \tilde{H}_N}{\partial p}\Big(y, p; h(y), h'(y)\dot{y}\Big), \\
\dot{p} &= -\frac{\partial \tilde{H}_N}{\partial y}\Big(y, p; h(y), h'(y)\dot{y}\Big).
\end{aligned} \tag{4.1.26}$$

Since we used the state-space formulation, the numerical scheme (4.1.18) is equivalent to

applying the same partitioned Runge-Kutta method to (4.1.26), that is, we have $Q^i = h(Y^i)$ and $\dot{Q}^i = h'(Y^i)\dot{Y}^i$. We computed the corresponding modified equation for several symplectic methods, namely Gauss and Lobatto IIIA-IIIB quadratures (see Section 2.2.2). Unfortunately, none of the quadratures resulted in a form akin to (4.1.26) for some modified Hamiltonian function $\tilde{\mathscr{H}}_N$ related to $\tilde{H}_N$ by a series similar to (4.1.25). This hints at the fact that we should not expect this integrator to show excellent energy conservation over long integration times. One could also consider the implicit ODE system (4.1.16), which has an obvious triple partitioned structure, and apply a different Runge-Kutta method to each variable y, p, and X. Although we did not pursue this idea further, it seems unlikely it would bring a desirable result.

We therefore conclude that the control-theoretic strategy, while yielding a perfectly legitimate numerical method, does not take full advantage of the underlying geometric structures. Let us point out that, while we used a variational discretization of the governing physical PDE, the mesh equations were coupled in a manner that is typical of the existing r-adaptive methods (see Section 3.3 and [7], [28]). We now turn our attention to a second approach, which offers a novel way of coupling the mesh equations to the physical equations.

4.2 Lagrange multiplier approach to r-adaptation

As we saw in Section 4.1, discretization of the variational principle alone is not sufficient if we would like to accurately capture the geometric properties of the physical system described by (4.0.1). In this section we propose a new technique of coupling the mesh equations to the physical equations. Our idea is based on the observation that in r-adaptation the number of mesh points is constant, therefore we can treat them as pseudo-particles, and we can incorporate their dynamics into the variational principle. We show that this strategy results in integrators that much better preserve the energy of the considered system.

4.2.1 Reparametrized Lagrangian

In this approach, we treat $X(x,t)$ as an independent field, that is, another degree of freedom, and we are going to treat the 'modified' action (4.0.3) as a functional of both φ and X: $\tilde{S} = \tilde{S}[\varphi, X]$. For the purpose of the derivations below, we assume that $\varphi(.,t)$ and $X(.,t)$ are continuous and piecewise C^1. One could consider the closure of this space in the

topology of either Hilbert or Banach space of sufficiently integrable functions and interpret differentiation in a sufficiently weak sense, but this functional-analytic aspect is of little importance for the developments in this section. We refer the interested reader to [12] and [14]. As in Section 4.1.1, let $\xi(X,t)$ be the function such that $\xi(.,t) = X(.,t)^{-1}$, that is, $\xi(X(x,t),t) = x$. Then $\tilde{S}[\varphi, X] = S[\varphi(\xi(X,t),t)]$. We begin with two propositions and one corollary which will be important for the rest of our exposition.

Proposition 4.2.1. *Extremizing $S[\phi]$ with respect to ϕ is equivalent to extremizing $\tilde{S}[\varphi, X]$ with respect to both φ and X.*

Proof. The variational derivatives of S and $\tilde{S}$ are related by the formula

$$\begin{aligned} \delta_1\tilde{S}[\varphi,X]\cdot\delta\varphi(x,t) &= \delta S[\varphi(\xi(X,t),t)]\cdot\delta\varphi(\xi(X,t),t), \\ \delta_2\tilde{S}[\varphi,X]\cdot\delta X(x,t) &= \delta S[\varphi(\xi(X,t),t)]\cdot\Big(-\frac{\varphi_x(\xi(X,t),t)}{X_x(\xi(X,t),t)}\delta X(\xi(X,t),t)\Big), \end{aligned} \tag{4.2.1}$$

where δ_1 and δ_2 denote differentiation with respect to the first and second argument, respectively. Suppose $\phi(X,t)$ extremizes $S[\phi]$, i.e., $\delta S[\phi]\cdot\delta\phi = 0$ for all variations $\delta\phi$. Choose an arbitrary $X(x,t)$, such that $X(.,t)$ is a (sufficiently smooth) homeomorphism, and define $\varphi(x,t) = \phi(X(x,t),t)$. Then by the formula above we have $\delta_1\tilde{S}[\varphi,X] = 0$ and $\delta_2\tilde{S}[\varphi,X] = 0$, so the pair (φ, X) extremizes $\tilde{S}$. Conversely, suppose the pair (φ, X) extremizes $\tilde{S}$, that is, $\delta_1\tilde{S}[\varphi,X]\cdot\delta\varphi = 0$ and $\delta_2\tilde{S}[\varphi,X]\cdot\delta X = 0$ for all variations $\delta\varphi$ and δX. Since we assume $X(.,t)$ is a homeomorphism, we can define $\phi(X,t) = \varphi(\xi(X,t),t)$. Note that an arbitrary variation $\delta\phi(X,t)$ induces the variation $\delta\varphi(x,t) = \delta\phi(X(x,t),t)$. Then we have $\delta S[\phi]\cdot\delta\phi = \delta_1\tilde{S}[\varphi,X]\cdot\delta\varphi = 0$ for all variations $\delta\phi$, so $\phi(X,t)$ extremizes $S[\phi]$.

□

Proposition 4.2.2. *The equation $\delta_2\tilde{S}[\varphi,X] = 0$ is implied by the equation $\delta_1\tilde{S}[\varphi,X] = 0$.*

Proof. As we saw in the proof of Proposition 4.2.1, the condition $\delta_1\tilde{S}[\varphi,X]\cdot\delta\varphi = 0$ implies $\delta S = 0$. By (4.2.1), this in turn implies $\delta_2\tilde{S}[\varphi,X]\cdot\delta X = 0$ for all δX. Note that this argument cannot be reversed: $\delta_2\tilde{S}[\varphi,X]\cdot\delta X = 0$ does not imply $\delta S = 0$ when $\varphi_x = 0$.

□

Corollary 4.2.3. *The field theory described by $\tilde{S}[\varphi, X]$ is degenerate and the solutions to the Euler-Lagrange equations are not unique.*

4.2.2 Spatial Finite Element discretization

The Lagrangian of the 'reparametrized' theory $\tilde{L} : Q \times G \times W \times Z \longrightarrow \mathbb{R}$

$$\tilde{L}[\varphi, X, \varphi_t, X_t] = \int_0^{X_{max}} \mathcal{L}\Big(\varphi, \frac{\varphi_x}{X_x}, \varphi_t - \frac{\varphi_x X_t}{X_x}\Big) X_x \, dx \tag{4.2.2}$$

has the same form as (4.1.2) (we only treat it as a functional of X and X_t as well), where Q, G, W, and Z are spaces of continuous and piecewise C^1 functions, as mentioned before. We again let $\Delta x = X_{max}/(N+1)$, and define the uniform mesh $x_i = i \cdot \Delta x$ for $i = 0, 1, ..., N+1$. Define the finite element spaces

$$Q_N = G_N = W_N = Z_N = \text{span}(\eta_0, ..., \eta_{N+1}), \tag{4.2.3}$$

where we used the finite elements (4.1.6). We have $Q_N \subset Q$, $G_N \subset G$, $W_N \subset W$, $Z_N \subset Z$. In addition to (4.1.9) we also consider

$$X(x) = \sum_{i=0}^{N+1} X_i \eta_i(x), \qquad \dot{X}(x) = \sum_{i=0}^{N+1} \dot{X}_i \eta_i(x). \tag{4.2.4}$$

The numbers $(y_i, X_i, \dot{y}_i, \dot{X}_i)$ thus form natural (global) coordinates on $Q_N \times G_N \times W_N \times Z_N$. We again consider the restricted Lagrangian $\tilde{L}_N = \tilde{L}|_{Q_N \times G_N \times W_N \times Z_N}$. In the chosen coordinates

$$\tilde{L}_N(y_1, ..., y_N, X_1, ..., X_N, \dot{y}_1, ..., \dot{y}_N, \dot{X}_1, ..., \dot{X}_N) = \tilde{L}\Big[\varphi(x), X(x), \dot{\varphi}(x), \dot{X}(x)\Big], \tag{4.2.5}$$

where $\varphi(x)$, $X(x)$, $\dot{\varphi}(x)$, $\dot{X}(x)$ are defined by (4.1.9) and (4.2.4). Once again, we refrain from writing y_0, y_{N+1}, $\dot{y}_0$, $\dot{y}_{N+1}$, X_0, X_{N+1}, $\dot{X}_0$, and $\dot{X}_{N+1}$ as arguments of $\tilde{L}_N$ in the remainder of this section, as those are not actual degrees of freedom.

4.2.3 Invertibility of the Legendre Transform

For simplicity, let us restrict our considerations to Lagrangian densities of the form

$$\mathcal{L}(\phi, \phi_X, \phi_t) = \frac{1}{2}\phi_t^2 - R(\phi_X, \phi). \tag{4.2.6}$$

We chose a kinetic term that is most common in applications. The corresponding 'reparametrized' Lagrangian is

$$\tilde{L}[\varphi, X, \varphi_t, X_t] = \int_0^{X_{max}} \frac{1}{2} X_x \Big(\varphi_t - \frac{\varphi_x}{X_x} X_t\Big)^2 dx - \dots, \tag{4.2.7}$$

where we kept only the terms that involve the velocities φ_t and X_t. The semi-discrete Lagrangian becomes

$$\begin{aligned}\tilde{L}_N = \sum_{i=0}^{N} \frac{X_{i+1} - X_i}{6} \Big[\Big(\dot{y}_i - \frac{y_{i+1} - y_i}{X_{i+1} - X_i} \dot{X}_i\Big)^2 + \Big(\dot{y}_i - \frac{y_{i+1} - y_i}{X_{i+1} - X_i} \dot{X}_i\Big)\Big(\dot{y}_{i+1} - \frac{y_{i+1} - y_i}{X_{i+1} - X_i} \dot{X}_{i+1}\Big) \\ + \Big(\dot{y}_{i+1} - \frac{y_{i+1} - y_i}{X_{i+1} - X_i} \dot{X}_{i+1}\Big)^2 \Big] - \dots\end{aligned} \tag{4.2.8}$$

Let us define the conjugate momenta via the Legendre Transform (see Section 2.3)

$$p_i = \frac{\partial \tilde{L}_N}{\partial \dot{y}_i}, \qquad S_i = \frac{\partial \tilde{L}_N}{\partial \dot{X}_i}, \qquad i = 1, 2, ..., N. \tag{4.2.9}$$

This can be written as

$$\begin{pmatrix} p_1 \\ S_1 \\ \vdots \\ p_N \\ S_N \end{pmatrix} = \tilde{M}_N(y, X) \cdot \begin{pmatrix} \dot{y}_1 \\ \dot{X}_1 \\ \vdots \\ \dot{y}_N \\ \dot{X}_N \end{pmatrix}, \tag{4.2.10}$$

where the $2N \times 2N$ mass matrix $\tilde{M}_N(y, X)$ has the following block tridiagonal structure

$$\tilde{M}_N(y,X) = \begin{pmatrix} A_1 & B_1 & & & & \\ B_1 & A_2 & B_2 & & & \\ & B_2 & A_3 & B_3 & & \\ & & \ddots & \ddots & \ddots & \\ & & & \ddots & \ddots & B_{N-1} \\ & & & & B_{N-1} & A_N \end{pmatrix}, \tag{4.2.11}$$

with the 2×2 blocks

$$A_i = \begin{pmatrix} \frac{1}{3}\delta_{i-1} + \frac{1}{3}\delta_i & -\frac{1}{3}\delta_{i-1}\gamma_{i-1} - \frac{1}{3}\delta_i\gamma_i \\ -\frac{1}{3}\delta_{i-1}\gamma_{i-1} - \frac{1}{3}\delta_i\gamma_i & \frac{1}{3}\delta_{i-1}\gamma_{i-1}^2 + \frac{1}{3}\delta_i\gamma_i^2 \end{pmatrix}, \qquad B_i = \begin{pmatrix} \frac{1}{6}\delta_i & -\frac{1}{6}\delta_i\gamma_i \\ -\frac{1}{6}\delta_i\gamma_i & \frac{1}{6}\delta_i\gamma_i^2 \end{pmatrix}, \tag{4.2.12}$$

where

$$\delta_i = X_{i+1} - X_i, \qquad \gamma_i = \frac{y_{i+1} - y_i}{X_{i+1} - X_i}. \tag{4.2.13}$$

From now on we will always assume $\delta_i > 0$, as we demand that $X(x) = \sum_{i=0}^{N+1} X_i \eta_i(x)$ be a homeomorphism. We also have

$$\det A_i = \frac{1}{9}\delta_{i-1}\delta_i(\gamma_{i-1} - \gamma_i)^2. \tag{4.2.14}$$

Proposition 4.2.4. *The mass matrix $\tilde{M}_N(y,X)$ is non-singular almost everywhere (as a function of the y_i's and X_i's) and singular iff $\gamma_{i-1} = \gamma_i$ for some i.*

Proof. We are going to compute the determinant of $\tilde{M}_N(y,X)$ by transforming (4.2.11) into a block upper triangular form by zeroing the blocks B_i below the diagonal. Let us start with the block B_1. We use linear combinations of the first two rows of the mass matrix to zero the elements of the block B_1 below the diagonal. Suppose $\gamma_0 = \gamma_1$. Then it is easy to see that the first two rows of the mass matrix are not linearly independent, so the determinant of the mass matrix is zero. Assume $\gamma_0 \neq \gamma_1$. Then by (4.2.14) the block A_1 is invertible. We multiply the first two rows of the mass matrix by $B_1 A_1^{-1}$ and subtract the result from the third and fourth rows. This zeroes the block B_1 below the diagonal and replaces the block A_2 by

$$C_2 = A_2 - B_1 A_1^{-1} B_1. \tag{4.2.15}$$

We now zero the block B_2 below the diagonal in a similar fashion. After $n-1$ steps of this procedure the mass matrix is transformed into

$$\begin{pmatrix} C_1 & B_1 & & & & & \\ & C_2 & B_2 & & & & \\ & & \ddots & \ddots & & & \\ & & & C_n & B_n & & \\ & & & B_n & A_{n+1} & \ddots & \\ & & & & \ddots & \ddots & B_{N-1} \\ & & & & & B_{N-1} & A_N \end{pmatrix}. \tag{4.2.16}$$

In a moment we are going to see that C_n is singular iff $\gamma_{n-1} = \gamma_n$ and in that case the two rows of the matrix above that contain C_n and B_n are linearly dependent, thus making the mass matrix singular. Suppose $\gamma_{n-1} \neq \gamma_n$, so that C_n is invertible. In the next step of our procedure the block A_{n+1} is replaced by

$$C_{n+1} = A_{n+1} - B_n C_n^{-1} B_n. \tag{4.2.17}$$

Together with the condition $C_1 = A_1$ this gives us a recurrence. By induction on n we find that

$$C_n = \begin{pmatrix} \frac{1}{4}\delta_{n-1} + \frac{1}{3}\delta_n & -\frac{1}{4}\delta_{n-1}\gamma_{n-1} - \frac{1}{3}\delta_n\gamma_n \\ -\frac{1}{4}\delta_{n-1}\gamma_{n-1} - \frac{1}{3}\delta_n\gamma_n & \frac{1}{4}\delta_{n-1}\gamma_{n-1}^2 + \frac{1}{3}\delta_n\gamma_n^2 \end{pmatrix} \tag{4.2.18}$$

and

$$\det C_i = \frac{1}{12}\delta_{i-1}\delta_i(\gamma_{i-1} - \gamma_i)^2, \tag{4.2.19}$$

which justifies our assumptions on the invertibility of the blocks C_i. We can now express the determinant of the mass matrix as $\det C_1 \cdot \ldots \cdot \det C_N$. The final formula is

$$\det \tilde{M}_N(y, X) = \frac{\delta_0 \delta_1^2 \ldots \delta_{N-1}^2 \delta_N}{9 \cdot 12^{N-1}} (\gamma_0 - \gamma_1)^2 \ldots (\gamma_{N-1} - \gamma_N)^2. \tag{4.2.20}$$

We see that the mass matrix becomes singular iff $\gamma_{i-1} = \gamma_i$ for some i, and this condition defines a measure zero subset of $\mathbb{R}^{2N}$.

□

Remark I. This result shows that the finite-dimensional system described by the semi-discrete Lagrangian (4.2.8) is non-degenerate almost everywhere. This means that, unlike in the continuous case, the Euler-Lagrange equations corresponding to the variations of the y_i's and X_i's are independent of each other (almost everywhere), and the equations corresponding to the X_i's are in fact necessary for the correct description of the dynamics. This can also be seen in a more general way. Owing to the fact we are considering a finite element approximation, the semi-discrete action functional $\tilde{S}_N$ is simply a restriction of $\tilde{S}$, and therefore formulas (4.2.1) still hold. The corresponding Euler-Lagrange equations take the form

$$\begin{aligned} \delta_1 \tilde{S}[\varphi, X] \cdot \delta\varphi(x,t) &= 0, \\ \delta_2 \tilde{S}[\varphi, X] \cdot \delta X(x,t) &= 0, \end{aligned} \tag{4.2.21}$$

which must hold for all variations $\delta\varphi(x,t) = \sum_{i=1}^{N} \delta y_i(t)\eta_i(x)$ and $\delta X(x,t) = \sum_{i=1}^{N} \delta X_i(t)\eta_i(x)$. Since we are working in a finite dimensional subspace, the second equation now does not follow from the first equation. To see this, consider a particular variation $\delta X(x,t) = \delta X_k(t)\eta_k(x)$ for some k, where $\delta X_k \not\equiv 0$. Then we have

$$-\frac{\varphi_x}{X_x}\delta X_k(t) = \begin{cases} -\gamma_{k-1}\,\delta X_k(t)\,\eta_k(x), & \text{if } x_{k-1} \le x \le x_k, \\ -\gamma_k\,\delta X_k(t)\,\eta_k(x), & \text{if } x_k \le x \le x_{k+1}, \\ 0, & \text{otherwise,} \end{cases} \tag{4.2.22}$$

which is discontinuous at $x = x_k$ and cannot be expressed as $\sum_{i=1}^{N} \delta y_i(t)\eta_i(x)$ for any $\delta y_i(t)$, unless $\gamma_{k-1} = \gamma_k$. Therefore, we cannot invoke the first equation to show that $\delta_2 \tilde{S}[\varphi, X] \cdot \delta X(x,t) = 0$. The second equation becomes independent.

Remark II. It is also instructive to realize what exactly happens when $\gamma_{k-1} = \gamma_k$. This means that locally in the interval $[X_{k-1}, X_{k+1}]$ the field $\phi(X,t)$ is a straight line with

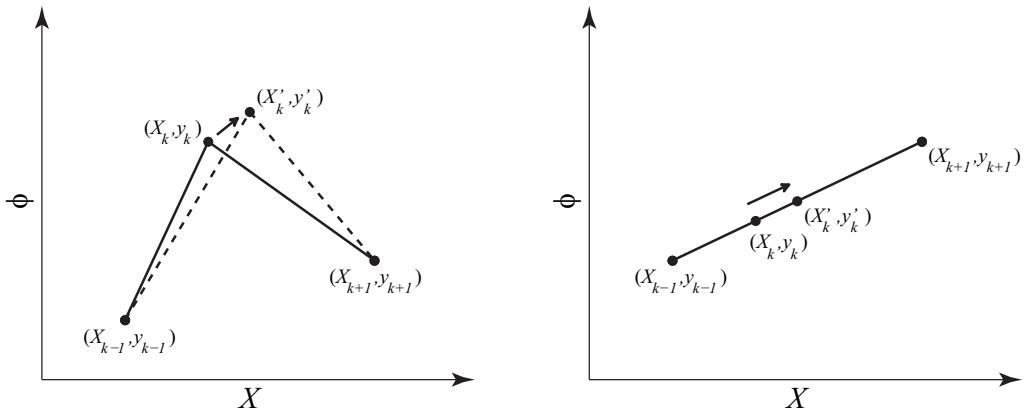

Figure 4.2.1: *Left:* If $\gamma_{k-1} \neq \gamma_k$, then any change to the middle point changes the local shape of $\phi(X,t)$. *Right:* If $\gamma_{k-1} = \gamma_k$, then there are infinitely many possible positions for (X_k, y_k) that reproduce the local linear shape of $\phi(X,t)$.

the slope γ_k. It also means that there are infinitely many values (X_k, y_k) that reproduce the same local shape of $\phi(X,t)$. This reflects the arbitrariness of $X(x,t)$ in the infinite-dimensional setting. In the finite element setting, however, this holds only when the points (X_{k-1}, y_{k-1}), (X_k, y_k) and (X_{k+1}, y_{k+1}) line up. Otherwise any change to the middle point changes the shape of $\phi(X,t)$. See Figure 4.2.1.

4.2.4 Existence and uniqueness of solutions

Since the Legendre Transform (4.2.10) becomes singular at some points, this raises a question about the existence and uniqueness of the solutions to the Euler-Lagrange equations (4.2.21). In this section we provide a partial answer to this problem. We will begin by computing the Lagrangian symplectic form (see Section 2.3)

$$\tilde{\Omega}_N = \sum_{i=1}^{N} dy_i \wedge dp_i + dX_i \wedge dS_i, \tag{4.2.23}$$

where p_i and S_i are given by (4.2.9). For notational convenience we will collectively denote $q = (y_1, X_1, ..., y_N, X_N)^T$ and $\dot{q} = (\dot{y}_1, \dot{X}_1, ..., \dot{y}_N, \dot{X}_N)^T$. Then in the ordered basis $(\frac{\partial}{\partial q_1}, ..., \frac{\partial}{\partial q_{2N}}, \frac{\partial}{\partial \dot{q}_1}, ..., \frac{\partial}{\partial \dot{q}_{2N}})$ the symplectic form can be represented by the matrix

$$\tilde{\Omega}_N(q, \dot{q}) = \begin{pmatrix} \tilde{\Delta}_N(q, \dot{q}) & \tilde{M}_N(q) \\ -\tilde{M}_N(q) & 0 \end{pmatrix}, \tag{4.2.24}$$

where the $2N \times 2N$ block $\tilde{\Delta}_N(q, \dot{q})$ has the further block tridiagonal structure

$$\tilde{\Delta}_N(q,\dot{q}) = \begin{pmatrix} \Gamma_1 & \Lambda_1 & & & & \\ -\Lambda_1^T & \Gamma_2 & \Lambda_2 & & & \\ & -\Lambda_2^T & \Gamma_3 & \Lambda_3 & & \\ & & \ddots & \ddots & \ddots & \\ & & & \ddots & \ddots & \Lambda_{N-1} \\ & & & & -\Lambda_{N-1}^T & \Gamma_N \end{pmatrix} \tag{4.2.25}$$

with the 2×2 blocks

$$\Gamma_i = \begin{pmatrix} 0 & -\frac{\dot{y}_{i+1}-\dot{y}_{i-1}}{3} - \frac{\dot{X}_{i-1}+2\dot{X}_i}{3}\gamma_{i-1} + \frac{2\dot{X}_i+\dot{X}_{i+1}}{3}\gamma_i \\ \frac{\dot{y}_{i+1}-\dot{y}_{i-1}}{3} + \frac{\dot{X}_{i-1}+2\dot{X}_i}{3}\gamma_{i-1} - \frac{2\dot{X}_i+\dot{X}_{i+1}}{3}\gamma_i & 0 \end{pmatrix},$$
$$\Lambda_i = \begin{pmatrix} -\frac{\dot{X}_i+\dot{X}_{i+1}}{2} & -\frac{\dot{y}_{i+1}-\dot{y}_i}{6} + \frac{\dot{X}_i+2\dot{X}_{i+1}}{3}\gamma_i \\ \frac{\dot{y}_{i+1}-\dot{y}_i}{6} + \frac{2\dot{X}_i+\dot{X}_{i+1}}{3}\gamma_i & -\frac{\dot{X}_i+\dot{X}_{i+1}}{2}\gamma_i^2 \end{pmatrix}. \tag{4.2.26}$$

In this form, it is easy to see that

$$\det \tilde{\Omega}_N(q,\dot{q}) = \Big(\det \tilde{M}_N(q)\Big)^2, \tag{4.2.27}$$

so the symplectic form is singular whenever the mass matrix is.

The energy corresponding to the Lagrangian (4.2.8) can be written as (see Section 2.3)

$$\tilde{E}_N(q,\dot{q}) = \frac{1}{2}\dot{q}^T \tilde{M}_N(q)\,\dot{q} + \sum_{k=0}^{N} \int_{x_k}^{x_{k+1}} R\Big(\gamma_k, y_k\eta_k(x) + y_{k+1}\eta_{k+1}(x)\Big)\frac{X_{k+1}-X_k}{\Delta x}\,dx. \tag{4.2.28}$$

In the chosen coordinates, $d\tilde{E}_N$ can be represented by the row vector $d\tilde{E}_N = (\partial\tilde{E}_N/\partial q_1, ..., \partial\tilde{E}_N/\partial\dot{q}_{2N})$. It turns out that

$$d\tilde{E}_N^T(q,\dot{q}) = \begin{pmatrix} \xi \\ \tilde{M}_N(q)\dot{q} \end{pmatrix}, \tag{4.2.29}$$

where the vector ξ has the following block structure

$$\xi = \begin{pmatrix} \xi_1 \\ \vdots \\ \xi_N \end{pmatrix}. \tag{4.2.30}$$

Each of these blocks has the form $\xi_k = (\xi_{k,1}, \xi_{k,2})^T$. Through basic algebraic manipulations and integration by parts, one finds that

$$\begin{aligned}
\xi_{k,1} = \quad & \frac{\dot{y}_{k+1}(2\dot{X}_{k+1} + \dot{X}_k) + \dot{y}_k(\dot{X}_{k+1} - \dot{X}_{k-1}) - \dot{y}_{k-1}(\dot{X}_k + 2\dot{X}_{k-1})}{6} \\
& + \frac{\dot{X}_k^2 + \dot{X}_k\dot{X}_{k-1} + \dot{X}_{k-1}^2}{3}\gamma_{k-1} - \frac{\dot{X}_{k+1}^2 + \dot{X}_{k+1}\dot{X}_k + \dot{X}_k^2}{3}\gamma_k \\
& + \frac{1}{\Delta x}\int_{x_{k-1}}^{x_k} \frac{\partial R}{\partial \phi_X}\Big(\gamma_{k-1}, y_{k-1}\eta_{k-1}(x) + y_k\eta_k(x)\Big)\,dx \\
& - \frac{1}{\Delta x}\int_{x_k}^{x_{k+1}} \frac{\partial R}{\partial \phi_X}\Big(\gamma_k, y_k\eta_k(x) + y_{k+1}\eta_{k+1}(x)\Big)\,dx \\
& + \frac{1}{\gamma_{k-1}}\Big[R(\gamma_{k-1}, y_k) - \frac{1}{\Delta x}\int_{x_{k-1}}^{x_k} R\Big(\gamma_{k-1}, y_{k-1}\eta_{k-1}(x) + y_k\eta_k(x)\Big)\,dx\Big] \\
& - \frac{1}{\gamma_k}\Big[R(\gamma_k, y_k) - \frac{1}{\Delta x}\int_{x_k}^{x_{k+1}} R\Big(\gamma_k, y_k\eta_k(x) + y_{k+1}\eta_{k+1}(x)\Big)\,dx\Big],
\end{aligned} \tag{4.2.31}$$

and

$$\begin{aligned}
\xi_{k,2} = \quad & \frac{\dot{y}_{k-1}^2 + \dot{y}_{k-1}\dot{y}_k - \dot{y}_k\dot{y}_{k+1} - \dot{y}_{k+1}^2}{6} \\
& - \frac{\dot{X}_k^2 + \dot{X}_k\dot{X}_{k-1} + \dot{X}_{k-1}^2}{6}\gamma_{k-1}^2 + \frac{\dot{X}_{k+1}^2 + \dot{X}_{k+1}\dot{X}_k + \dot{X}_k^2}{6}\gamma_k^2 \\
& - \frac{\gamma_{k-1}}{\Delta x}\int_{x_{k-1}}^{x_k} \frac{\partial R}{\partial \phi_X}\Big(\gamma_{k-1}, y_{k-1}\eta_{k-1}(x) + y_k\eta_k(x)\Big)\,dx \\
& + \frac{\gamma_k}{\Delta x}\int_{x_k}^{x_{k+1}} \frac{\partial R}{\partial \phi_X}\Big(\gamma_k, y_k\eta_k(x) + y_{k+1}\eta_{k+1}(x)\Big)\,dx \\
& + \frac{1}{\Delta x}\int_{x_{k-1}}^{x_k} R\Big(\gamma_{k-1}, y_{k-1}\eta_{k-1}(x) + y_k\eta_k(x)\Big)\,dx \\
& - \frac{1}{\Delta x}\int_{x_k}^{x_{k+1}} R\Big(\gamma_k, y_k\eta_k(x) + y_{k+1}\eta_{k+1}(x)\Big)\,dx.
\end{aligned} \tag{4.2.32}$$

We are now ready to consider the generalized Hamiltonian equation (see Section 2.3)

$$i_Z\tilde{\Omega}_N = d\tilde{E}_N, \tag{4.2.33}$$

which we solve for the vector field $Z = \sum_{i=1}^{2N} \alpha_i \, \partial/\partial q_i + \beta_i \, \partial/\partial \dot{q}_i$. In the matrix representation this equation takes the form

$$\tilde{\Omega}_N^T(q, \dot{q}) \cdot \begin{pmatrix} \alpha \\ \beta \end{pmatrix} = d\tilde{E}_N^T(q, \dot{q}). \tag{4.2.34}$$

Equations of this form are called (quasilinear) implicit ODEs (see [53], [55]). If the symplectic form is nonsingular in a neighborhood of $(q^{(0)}, \dot{q}^{(0)})$, then the equation can be solved directly via

$$Z = [\tilde{\Omega}_N^T(q, \dot{q})]^{-1} d\tilde{E}_N^T(q, \dot{q})$$

to obtain the standard explicit ODE form and standard existence/uniqueness theorems (Picard's, Peano's, etc.) of ODE theory can be invoked to show local existence and uniqueness of the flow of Z in a neighborhood of $(q^{(0)}, \dot{q}^{(0)})$. If, however, the symplectic form is singular at $(q^{(0)}, \dot{q}^{(0)})$, then there are two possibilities. The first case is

$$d\tilde{E}_N^T(q^{(0)}, \dot{q}^{(0)}) \notin \text{Range } \tilde{\Omega}_N^T(q^{(0)}, \dot{q}^{(0)}), \tag{4.2.35}$$

and it means there is no solution for Z at $(q^{(0)}, \dot{q}^{(0)})$. This type of singularity is called an *algebraic* one and it leads to so called *impasse points* (see [48]-[53], [55]).

The other case is

$$d\tilde{E}_N^T(q^{(0)}, \dot{q}^{(0)}) \in \text{Range } \tilde{\Omega}_N^T(q^{(0)}, \dot{q}^{(0)}), \tag{4.2.36}$$

and it means that there exists a nonunique solution Z at $(q^{(0)}, \dot{q}^{(0)})$. This type of singularity is called a *geometric* one. If $(q^{(0)}, \dot{q}^{(0)})$ is a limit of regular points of (4.2.34) (i.e., points where the symplectic form is nonsingular), then there might exist an integral curve of Z passing through $(q^{(0)}, \dot{q}^{(0)})$. See [48], [49], [50], [51], [52], [53], [55] for more details.

Proposition 4.2.5. *The singularities of the symplectic form $\tilde{\Omega}_N(q, \dot{q})$ are geometric.*

Proof. Suppose that the mass matrix (and thus the symplectic form) is singular at $(q^{(0)}, \dot{q}^{(0)})$. Using the block structures (4.2.24) and (4.2.29) we can write (4.2.34) as the system

$$-\tilde{\Delta}_N(q^{(0)},\dot{q}^{(0)})\,\alpha - \tilde{M}_N(q^{(0)})\,\beta = \xi,$$
$$\tilde{M}_N(q^{(0)})\,\alpha = \tilde{M}_N(q^{(0)})\,\dot{q}^{(0)}. \tag{4.2.37}$$

The second equation implies that there exists a solution $\alpha = \dot{q}^{(0)}$. In fact this is the only solution we are interested in, since it satisfies the second order condition: the Euler-Lagrange equations underlying the variationl principle are second order, so we are only interested in solutions of the form $Z = \sum_{i=1}^{2N} \dot{q}_i\,\partial/\partial q_i + \beta_i\,\partial/\partial\dot{q}_i$. The first equation can be rewritten as

$$\tilde{M}_N(q^{(0)})\,\beta = -\xi - \tilde{\Delta}_N(q^{(0)},\dot{q}^{(0)})\,\dot{q}^{(0)}. \tag{4.2.38}$$

Since the mass matrix is singular, we must have $\gamma_{k-1} = \gamma_k$ for some k. As we saw in Section 4.2.3, this means that the two rows of the k^{th} 'block row' of the mass matrix (i.e., the rows containing the blocks B_{k-1}, A_k and B_k) are not linearly independent. In fact, we have

$$(B_{k-1})_{2*} = -\gamma_k (B_{k-1})_{1*}, \qquad (A_k)_{2*} = -\gamma_k (A_k)_{1*}, \qquad (B_k)_{2*} = -\gamma_k (B_k)_{1*}, \tag{4.2.39}$$

where a_{m*} denotes the m^{th} row of the matrix a. Equation (4.2.38) will have a solution for β iff the RHS satisfies a similar scaling condition in the the k^{th} 'block element'. Using formulas (4.2.26), (4.2.31), and (4.2.32) we show that $-\xi - \tilde{\Delta}_N\,\dot{q}^{(0)}$ indeed has this property. Hence, $d\tilde{E}_N^T(q^{(0)},\dot{q}^{(0)}) \in \text{Range}\ \tilde{\Omega}_N^T(q^{(0)},\dot{q}^{(0)})$ and $(q^{(0)},\dot{q}^{(0)})$ is a geometric singularity. Moreover, since $\gamma_{k-1} = \gamma_k$ defines a hypersurface in $\mathbb{R}^{2N}\times\mathbb{R}^{2N}$, $(q^{(0)},\dot{q}^{(0)})$ is a limit of regular points. □

Remark I. Numerical time integration of the semi-discrete equations of motion (4.2.34) has to deal with the singularity points of the symplectic form. While there are some numerical algorithms allowing one to get past singular hypersurfaces (see [53]), it might not be very practical from the application point of view. Note that, unlike in the continuous case, the time evolution of the meshpoints X_i's is governed by the equations of motion, so

the user does not have any influence on how the mesh is adapted. More importantly, there is no built-in mechanism that would prevent mesh tangling. Some preliminary numerical experiments show that the mesh points eventually collapse when started with nonzero initial velocities.

Remark II. The singularities of the mass matrix (4.2.11) bear some similarities to the singularities of the mass matrices encountered in the Moving Finite Element method. In [44] and [43], the authors proposed introducing a small 'internodal' viscosity which penalizes the method for relative motion between the nodes and thus regularizes the mass matrix. A similar idea could be applied in our case: one could add some small ε kinetic terms to the Lagrangian (4.2.8) in order to regularize the Legendre Transform. In light of the remark made above, we did not follow this idea further, and decided to take a different route instead, as described in the following sections. However, investigating further similarities between our variational approach and the Moving Finite Element method might be worthwhile. There also might be some connection to the r-adaptive method presented in [68]: the evolution of the mesh in that method is also set by the equations of motion, although the authors considered a different variational principle and different theoretical reasoning to justify the validity of their approach.

4.2.5 Constraints and adaptation strategy

As we saw in Section 4.2.4, upon discretization we lose the arbitrariness of $X(x,t)$ and the evolution of $X_i(t)$ is governed by the equations of motion, while we still want to be able to select a desired mesh adaptation strategy, like (3.2.8). This could be done by augmenting the Lagrangian (4.2.8) with Lagrange multipliers corresponding to each constraint g_i (see Section 2.5.1). However, it is not obvious that the dynamics of the constrained system as defined would reflect in any way the behavior of the approximated system (4.2.6). We are going to show that the constraints can be added via Lagrange multipliers already at the continuous level (4.2.6), and the continuous system as defined can be then discretized to arrive at (4.2.8) with the desired adaptation constraints.

4.2.5.1 Global constraint

As mentioned before, eventually we would like to impose the constraints

$$g_i(y_1, ..., y_N, X_1, ..., X_N) = 0, \qquad i = 1, ..., N \tag{4.2.40}$$

on the semi-discrete system (4.2.8). Let us assume that $g : \mathbb{R}^{2N} \longrightarrow \mathbb{R}^N$, $g = (g_1, ..., g_N)^T$ is C^1 and 0 is a regular value of g, so that (4.2.40) defines a submanifold. To see how these constraints can be introduced at the continuous level, let us select uniformly distributed points $x_i = i \cdot \Delta x$, $i = 0, ..., N+1$, $\Delta x = X_{max}/(N+1)$ and demand that the constraints

$$g_i\Big(\varphi(x_1, t), ..., \varphi(x_N, t), X(x_1, t), ..., X(x_N, t)\Big) = 0, \qquad i = 1, ..., N \tag{4.2.41}$$

be satisfied by $\varphi(x, t)$ and $X(x, t)$. One way of imposing these constraints is solving the system

$$\begin{aligned} &\delta_1 \tilde{S}[\varphi, X] \cdot \delta\varphi(x, t) = 0 \qquad \text{for all } \delta\varphi(x, t), \\ &g_i\Big(\varphi(x_1, t), ..., \varphi(x_N, t), X(x_1, t), ..., X(x_N, t)\Big) = 0, \qquad i = 1, ..., N. \end{aligned} \tag{4.2.42}$$

This system consists of one Euler-Lagrange equation that corresponds to extremizing $\tilde{S}$ with respect to φ (we saw in Section 4.2.1 that the other Euler-Lagrange equation is not independent) and a set of constraints enforced at some pre-selected points x_i. Note, that upon finite element discretization on a mesh coinciding with the pre-selected points this system reduces to the approach presented in Section 4.1: we minimize the discrete action with respect to the y_i's only, and supplement the resulting equations with the constraints (4.2.40).

Another way that we want to explore consists in using Lagrange multipliers. Define the auxiliary action functional

$$\tilde{S}_C[\varphi, X, \lambda_k] = \tilde{S}[\varphi, X] - \sum_{i=1}^{N} \int_0^{T_{max}} \lambda_i(t) \cdot g_i\Big(\varphi(x_1, t), ..., \varphi(x_N, t), X(x_1, t), ..., X(x_N, t)\Big)\, dt. \tag{4.2.43}$$

We are going to assume that the Lagrange multipliers $\lambda_i(t)$ are at least continuous in time. According to the method of Lagrange multipliers (see Section 2.5.1), we seek the stationary

points of $\tilde{S}_C$. This leads to the following system of equations

$$\begin{aligned}
\delta_1\tilde{S}[\varphi,X]\cdot\delta\varphi(x,t)-\sum_{i=1}^{N}\sum_{j=1}^{N}\int_0^{T_{max}}\lambda_i(t)\,\frac{\partial g_i}{\partial y_j}\,\delta\varphi(x_j,t)\,dt=0 \qquad &\text{for all } \delta\varphi(x,t),\\
\delta_2\tilde{S}[\varphi,X]\cdot\delta X(x,t)-\sum_{i=1}^{N}\sum_{j=1}^{N}\int_0^{T_{max}}\lambda_i(t)\,\frac{\partial g_i}{\partial X_j}\,\delta X(x_j,t)\,dt=0 \qquad &\text{for all } \delta X(x,t),\\
g_i\Big(\varphi(x_1,t),...,\varphi(x_N,t),X(x_1,t),...,X(x_N,t)\Big)=0, \qquad &i=1,...,N, \quad (4.2.44)
\end{aligned}$$

where for clarity we suppressed writing the arguments of $\frac{\partial g_i}{\partial y_j}$ and $\frac{\partial g_i}{\partial X_j}$.

Equation (4.2.42) is more intuitive, because we directly use the arbitrariness of $X(x,t)$, and simply restrict it further by imposing constraints. It is not immediately obvious how solutions of (4.2.42) and (4.2.44) relate to each other. We would like both systems to be 'equivalent' in some sense, or at least their solution sets to overlap. Let us investigate this issue in more detail.

Suppose (φ,X) satisfy (4.2.42). Then it is quite trivial to see that $(\varphi,X,\lambda_1,...,\lambda_N)$ such that $\lambda_k\equiv 0$ satisfy (4.2.44): the second equation is implied by the first one and the other equations coincide with those of (4.2.42). At this point it should be obvious that system (4.2.44) may have more solutions for φ and X than system (4.2.42).

Proposition 4.2.6. *The only solutions* $(\varphi,X,\lambda_1,...,\lambda_N)$ *to* (4.2.44) *that satisfy* (4.2.42) *as well are those with* $\lambda_k\equiv 0$ *for all* k.

Proof. Suppose $(\varphi,X,\lambda_1,...,\lambda_N)$ satisfy both (4.2.42) and (4.2.44). System (4.2.42) implies that $\delta_1\tilde{S}\cdot\delta\varphi=0$ and $\delta_2\tilde{S}\cdot\delta X=0$. Using this in system (4.2.44) gives

$$\begin{aligned}
\sum_{j=1}^{N}\int_0^{T_{max}}dt\,\delta\varphi(x_j,t)\sum_{i=1}^{N}\lambda_i(t)\,\frac{\partial g_i}{\partial y_j}=0 \qquad &\text{for all } \delta\varphi(x,t),\\
\sum_{j=1}^{N}\int_0^{T_{max}}dt\,\delta X(x_j,t)\sum_{i=1}^{N}\lambda_i(t)\,\frac{\partial g_i}{\partial X_j}=0 \qquad &\text{for all } \delta X(x,t). \quad (4.2.45)
\end{aligned}$$

In particular, this has to hold for variations $\delta\varphi$ and δX such that $\delta\varphi(x_j,t)=\delta X(x_j,t)=\nu(t)\cdot\delta_{kj}$, where $\nu(t)$ is an arbitrary continuous function of time. If we further assume that for all $x\in[0,X_{max}]$ the functions $\varphi(x,.)$ and $X(x,.)$ are continuous, both $\sum_{i=1}^{N}\lambda_i(t)\,\frac{\partial g_i}{\partial y_k}$ and $\sum_{i=1}^{N}\lambda_i(t)\,\frac{\partial g_i}{\partial X_k}$ are continuous and we get

$$Dg\Big(\varphi(x_1,t),...,\varphi(x_N,t),X(x_1,t),...,X(x_N,t)\Big)^T\cdot\lambda(t)=0 \tag{4.2.46}$$

for all t, where $\lambda=(\lambda_1,...,\lambda_N)^T$, and the $N\times 2N$ matrix $Dg=\left[\frac{\partial g_i}{\partial y_k}\ \frac{\partial g_i}{\partial X_k}\right]_{i,k=1,...,N}$ is the derivative of g. Since we assumed that 0 is a regular value of g and the constraint $g=0$ is satisfied by φ and X, we have that for all t the matrix Dg has full rank—that is, there exists a nonsingular $N\times N$ submatrix Ξ. Then the equation $\Xi^T\lambda(t)=0$ implies $\lambda\equiv 0$.

□

We see that considering Lagrange multipliers in (4.2.43) makes sense at the continuous level. We can now perform a finite element discretization. The auxiliary Lagrangian $\tilde{L}_C:Q\times G\times W\times Z\times\mathbb{R}^N\longrightarrow\mathbb{R}$ corresponding to (4.2.43) can be written as

$$\tilde{L}_C[\varphi,X,\varphi_t,X_t,\lambda_k]=\tilde{L}[\varphi,X,\varphi_t,X_t]-\sum_{i=1}^{N}\lambda_i\cdot g_i\Big(\varphi(x_1),...,\varphi(x_N),X(x_1),...,X(x_N)\Big), \tag{4.2.47}$$

where $\tilde{L}$ is the Lagrangian of the unconstrained theory and has been defined by (4.2.2). Let us choose a uniform mesh coinciding with the pre-selected points x_i. As in Section 4.2.2, we consider the restriction $\tilde{L}_{CN}=\tilde{L}_C|_{Q_N\times G_N\times W_N\times Z_N\times\mathbb{R}^N}$ and we get

$$\tilde{L}_{CN}(y_i,X_j,\dot{y}_k,\dot{X}_l,\lambda_m)=\tilde{L}_N(y_i,X_j,\dot{y}_k,\dot{X}_l)-\sum_{i=1}^{N}\lambda_i\cdot g_i(y_1,...,y_N,X_1,...,X_N). \tag{4.2.48}$$

We see that the semi-discrete Lagrangian $\tilde{L}_{CN}$ is obtained from the semi-discrete Lagrangian $\tilde{L}_N$ by adding the constraints g_i directly at the semi-discrete level, which is exactly what we set out to do at the beginning of this section. However, in the semi-discrete setting we cannot expect the Lagrange multipliers to vanish for solutions of interest. This is because there is no semi-discrete counterpart of Proposition 4.2.6. On one hand, the semi-discrete version of (4.2.42) (that is, the approach presented in Section 4.1) does not imply that $\delta_2\tilde{S}\cdot\delta X=0$, so the above proof will not work. On the other hand, if we supplement (4.2.42) with the equation corresponding to variations of X, then the finite element discretization will not have solutions, unless the constraint functions are integrals of motion of the system described by $\tilde{L}_N(y_i,X_j,\dot{y}_k,\dot{X}_l)$, which generally is not the case. Nonetheless, it is reasonable

to expect that if the continuous system (4.2.42) has a solution, then the Lagrange multipliers of the semi-discrete system (4.2.48) should remain small.

Defining constraints by Equations (4.2.41) allowed us to use the same finite element discretization for both $\tilde{L}$ and the constraints, and to prove some correspondence between the solutions of (4.2.42) and (4.2.44). However, constraints (4.2.41) are global in the sense that they depend on the values of the fields φ and X at different points in space. Moreover, these constraints do not determine unique solutions to (4.2.42) and (4.2.44), which is a little cumbersome when discussing multisymplecticity (see Chapter 5).

4.2.5.2 Local constraint

In Section 3.2 we discussed how some adaptation constraints of interest can be derived from certain partial differential equations based on the equidistribution principle, for instance equation (3.2.7). We can view these PDEs as local constraints that only depend on pointwise values of the fields φ, X, and their spatial derivatives. Let $G = G(\varphi, X, \varphi_x, X_x, \varphi_{xx}, X_{xx}, ...)$ represent such a local constraint. Then, similarly to (4.2.42), we can write our control-theoretic strategy from Section 4.1 as

$$\begin{aligned} &\delta_1 \tilde{S}[\varphi, X] \cdot \delta\varphi(x,t) = 0 \qquad \text{for all } \delta\varphi(x,t), \\ &G(\varphi, X, \varphi_x, X_x, \varphi_{xx}, X_{xx}, ...) = 0. \end{aligned} \tag{4.2.49}$$

Note that higher-order derivatives of the fields may require the use of higher degree basis functions than the ones in (4.1.6), or of finite differences instead.

The Lagrange multiplier approach consists in defining the auxiliary Lagrangian (see Section 2.5.1)

$$\tilde{L}_C[\varphi, X, \varphi_t, X_t, \lambda] = \tilde{L}[\varphi, X, \varphi_t, X_t] - \int_0^{X_{max}} \lambda(x) \cdot G(\varphi, X, \varphi_x, X_x, \varphi_{xx}, X_{xx}, ...)\, dx. \tag{4.2.50}$$

Suppose that the pair (φ, X) satisfies (4.2.49). Then, much like in Section 4.2.5.1, one can easily check that the triple $(\varphi, X, \lambda \equiv 0)$ satisfies the Euler-Lagrange equations associated with (4.2.50). However, an analog of Proposition 4.2.6 does not seem to be very interesting

in this case, therefore we are not proving it here.

Introducing the constraints this way is convenient, because the Lagrangian (4.2.50) then represents a constrained multisymplectic field theory with a local constraint, which makes the analysis of multisymplecticity easier (see Chapter 5). The disadvantage is that discretization of (4.2.50) requires mixed methods. We are going to use the linear finite elements (4.1.6) to discretize $\tilde{L}[\varphi, X, \varphi_t, X_t]$, but the constraint term will be approximated via finite differences. This way we again obtain the semi-discrete Lagrangian (4.2.48), where g_i represents the discretization of G at the point $x = x_i$.

In summary, the methods presented in Section 4.2.5.1 and Section 4.2.5.2 both lead to the same semi-discrete Lagrangian, but have different theoretical advantages.

4.2.6 DAE formulation of the equations of motion

The Lagrangian (4.2.48) can be written as

$$\tilde{L}_{CN}(q, \dot{q}, \lambda) = \frac{1}{2}\dot{q}^T \tilde{M}_N(q)\, \dot{q} - R_N(q) - \lambda^T g(q), \tag{4.2.51}$$

where

$$R_N(q) = \sum_{k=0}^{N} \int_{x_k}^{x_{k+1}} R\Big(\gamma_k, y_k \eta_k(x) + y_{k+1}\eta_{k+1}(x)\Big) \frac{X_{k+1} - X_k}{\Delta x}\, dx. \tag{4.2.52}$$

The Euler-Lagrange equations thus take the form (see Section 2.5.1)

$$\begin{aligned} \dot{q} &= u, \\ \tilde{M}_N(q)\, \dot{u} &= f(q, u) - Dg(q)^T \lambda, \\ g(q) &= 0, \end{aligned} \tag{4.2.53}$$

where

$$f_k(q, u) = -\frac{\partial R_N}{\partial q_k} + \sum_{i,j=1}^{2N} \Big(\frac{1}{2} \frac{\partial (\tilde{M}_N)_{ij}}{\partial q_k} - \frac{\partial (\tilde{M}_N)_{ki}}{\partial q_j} \Big) u_i u_j. \tag{4.2.54}$$

System (4.2.53) is to be solved for the unknown functions $q(t)$, $u(t)$, and $\lambda(t)$. This is a DAE system of index 3, since we are lacking a differential equation for $\lambda(t)$ and the

constraint equation has to be differentiated three times in order to express $\dot{\lambda}$ as a function of q, u, and λ, provided that certain regularity conditions are satisfied. Let us determine these conditions. Differentiate the constraint equation twice with respect to time to obtain the acceleration level constraint

$$Dg(q)\,\dot{u} = h(q,u), \tag{4.2.55}$$

where

$$h_k(q,u) = -\sum_{i,j=1}^{2N} \frac{\partial^2 g_k}{\partial q_i \partial q_j} u_i u_j. \tag{4.2.56}$$

We can then write (4.2.55) and the second equation of (4.2.53) together as

$$\begin{pmatrix} \tilde{M}_N(q) & Dg(q)^T \\ Dg(q) & 0 \end{pmatrix} \begin{pmatrix} \dot{u} \\ \lambda \end{pmatrix} = \begin{pmatrix} f(q,u) \\ h(q,u) \end{pmatrix}. \tag{4.2.57}$$

If we could solve this equation for $\dot{u}$ and λ in terms of q and u, then we could simply differentiate the expression for λ one more time to obtain the missing differential equation, thus showing system (4.2.53) is of index 3. System (4.2.57) is solvable if its matrix is invertible. Hence, for system (4.2.53) to be of index 3, the following condition

$$\det \begin{pmatrix} \tilde{M}_N(q) & Dg(q)^T \\ Dg(q) & 0 \end{pmatrix} \neq 0 \tag{4.2.58}$$

has to be satisfied for all q, or at least in a neighborhood of the points satisfying $g(q) = 0$. Note that with suitably chosen constraints this condition allows the mass matrix to be singular.

We would like to perform time integration of this mechanical system using the symplectic (variational) Lobatto IIIA-IIIB quadratures for constrained systems (see Section 2.5.2 and [23], [26], [31], [32], [41]). However, due to the singularity of the Runge-Kutta coefficient matrices (a_{ij}) and $(\bar{a}_{ij})$ for the Lobatto IIIA and IIIB schemes (see Table 2.4, Table 2.5 and Table 2.6), the assumption (4.2.58) does not guarantee that these quadratures define a unique numerical solution: the mass matrix would need to be invertible. To circumvent this numerical obstacle we resort to a trick described in [32]. We embed our mechanical system in a higher dimensional configuration space by adding slack degrees of freedom r and $\dot{r}$, and

form the augmented Lagrangian $\tilde{L}_N^A$ by modifying the kinetic term of $\tilde{L}_N$ to read

$$\tilde{L}_N^A(q,r,\dot{q},\dot{r}) = \frac{1}{2}\begin{pmatrix} \dot{q}^T & \dot{r}^T \end{pmatrix} \cdot \begin{pmatrix} \tilde{M}_N(q) & Dg(q)^T \\ Dg(q) & 0 \end{pmatrix} \cdot \begin{pmatrix} \dot{q} \\ \dot{r} \end{pmatrix} - R_N(q). \tag{4.2.59}$$

Assuming (4.2.58), the augmented system has a non-singular mass matrix. If we multiply out the terms we obtain simply

$$\tilde{L}_N^A(q,r,\dot{q},\dot{r}) = \tilde{L}_N(q,\dot{q}) + \dot{r}^T Dg(q)\,\dot{q}. \tag{4.2.60}$$

This formula in fact holds for general Lagrangians, not only for (4.2.8). In addition to $g(q) = 0$ we further impose the constraint $r = 0$. Then the augmented constrained Lagrangian takes the form

$$\tilde{L}_{CN}^A(q,r,\dot{q},\dot{r},\lambda,\mu) = \tilde{L}_N(q,\dot{q}) + \dot{r}^T Dg(q)\,\dot{q} - \lambda^T g(q) - \mu^T r. \tag{4.2.61}$$

The corresponding Euler-Lagrange equations are

$$\begin{aligned} \dot{q} &= u, \\ \dot{r} &= w, \\ \tilde{M}_N(q)\,\dot{u} + Dg(q)^T\,\dot{w} &= f(q,u) - Dg(q)^T\,\lambda, \\ Dg(q)\,\dot{u} &= h(q,u) - \mu, \\ g(q) &= 0, \\ r &= 0. \end{aligned} \tag{4.2.62}$$

It is straightforward to verify that $r(t) = 0$, $w(t) = 0$, $\mu(t) = 0$ is the exact solution, and the remaining equations reduce to (4.2.53), that is, the evolution of the augmented system coincides with the evolution of the original system, by construction. The advantage is that the augmented system is now regular, and we can readily apply the Lobatto IIIA-IIIB method for constrained systems to compute a numerical solution. It should be intuitively

clear that this numerical solution will approximate the solution of (4.2.53) as well. What is not immediately obvious is whether a variational integrator based on (4.2.60) can be interpreted as a variational integrator based on $\tilde{L}_N$. This can be elegantly justified with the help of exact constrained discrete Lagrangians (see Section 2.5.2 and Section 2.4.2). Let $\mathcal{N} \subset Q_N \times G_N$ be the constraint submanifold defined by $g(q) = 0$. The exact constrained discrete Lagrangian $\tilde{L}_N^{C,E} : \mathcal{N} \times \mathcal{N} \longrightarrow \mathbb{R}$ is defined by

$$\tilde{L}_N^{C,E}\big(q^{(1)}, q^{(2)}\big) = \int_0^{\Delta t} \tilde{L}_N\big(q(t), \dot{q}(t)\big)\, dt, \tag{4.2.63}$$

where $q(t)$ is the solution to the constrained Euler-Lagrange equations (4.2.53), such that it satisfies the boundary conditions $q(0) = q^{(1)}$ and $q(\Delta t) = q^{(2)}$. Note that $\mathcal{N} \times \{0\} \subset (Q_N \times G_N) \times \mathbb{R}^N$ is the constraint submanifold defined by $g(q) = 0$ and $r = 0$. Since necessarily $r^{(1)} = r^{(2)} = 0$, we can define the exact augmented constrained discrete Lagrangian $\tilde{L}_N^{A,C,E} : \mathcal{N} \times \mathcal{N} \longrightarrow \mathbb{R}$ by

$$\tilde{L}_N^{A,C,E}\big(q^{(1)}, q^{(2)}\big) = \int_0^{\Delta t} \tilde{L}_N^{A}\big(q(t), r(t), \dot{q}(t), \dot{r}(t)\big)\, dt, \tag{4.2.64}$$

where $q(t)$, $r(t)$ are the solutions to the augmented constrained Euler-Lagrange equations (4.2.62), such that the boundary conditions $q(0) = q^{(1)}$, $q(\Delta t) = q^{(2)}$, and $r(0) = r(\Delta t) = 0$ are satisfied.

Proposition 4.2.7. *The exact discrete Lagrangians $\tilde{L}_N^{A,C,E}$ and $\tilde{L}_N^{C,E}$ are equal.*

Proof. Let $q(t)$ and $r(t)$ be the solutions to (4.2.62) such that the boundary conditions $q(0) = q^{(1)}$, $q(\Delta t) = q^{(2)}$, and $r(0) = r(\Delta t) = 0$ are satisfied. As argued before, we in fact have $r(t) = 0$ and $q(t)$ satisfies (4.2.53) as well. By (4.2.60) we have

$$\tilde{L}_N^{A}\big(q(t), r(t), \dot{q}(t), \dot{r}(t)\big) = \tilde{L}_N\big(q(t), \dot{q}(t)\big)$$

for all $t \in [0, \Delta t]$, and consequently $\tilde{L}_N^{A,C,E} = \tilde{L}_N^{C,E}$.

□

This means that any discrete Lagrangian $\tilde{L}_d : (Q_N \times G_N) \times \mathbb{R}^N \times (Q_N \times G_N) \times \mathbb{R}^N \longrightarrow \mathbb{R}$ that approximates $\tilde{L}_N^{A,C,E}$ to order s also approximates $\tilde{L}_N^{C,E}$ to the same order, that is, a variational integrator for (4.2.62), in particular our Lobatto IIIA-IIIB scheme, is also a

variational integrator for (4.2.53).

Backward error analysis. The advantage of the Lagrange multiplier approach is the fact that upon spatial discretization we deal with a constrained mechanical system. Backward error analysis of symplectic/variational numerical schemes for such systems shows that the modified equations also describe a constrained mechanical system for a nearby Hamiltonian (see [23]). Therefore, we expect the Lagrange multiplier strategy to demonstrate better performance in terms of energy conservation than the control-theoretic strategy. The Lagrange multiplier approach makes better use of the geometry underlying the field theory we consider, the key idea being to *treat the reparametrization field* $X(x,t)$ *as an additional dynamical degree of freedom on equal footing with* $\varphi(x,t)$.

Chapter 5

R-adaptive multisymplectic integrators

In Chapter 4 we took the view of infinite dimensional manifolds of fields as configuration spaces, and presented a way to construct space-adaptive variational integrators in that formalism. We essentially applied symplectic integrators to semi-discretized Lagrangian field theories. In this chapter we show how r-adaptive integrators can be described in the more general framework of multisymplectic geometry (see Section 2.6). In particular we show that some of the integrators obtained in Chapter 4 can be interpreted as multisymplectic variational integrators (see Section 2.7). Multisymplectic geometry provides a covariant formalism for the study of field theories in which time and space are treated on equal footing, as a conseqence of which multisymplectic variational integrators allow for more general discretizations of spacetime, such that, for instance, each element of space may be integrated with a different timestep (see [36]).

5.1 Analysis of the control-theoretic approach

Continuous setting

We are now going to discuss a multisymplectic setting for the approach presented in Section 4.1. Let the computational spacetime be $\mathcal{X} = \mathbb{R} \times \mathbb{R}$ with coordinates (t, x) and consider the trivial configuration bundle $Y = \mathcal{X} \times \mathbb{R}$ with coordinates (t, x, y). Let $\mathcal{U} = [0, T_{max}] \times [0, X_{max}]$, and let our scalar field be represented by a section $\tilde{\varphi} : \mathcal{U} \longrightarrow Y$ with the coordinate representation $\tilde{\varphi}(t, x) = (t, x, \varphi(t, x))$. Let (t, x, y, v_t, v_x) denote local coordinates on J^1Y. In these coordinates the first jet prolongation of $\tilde{\varphi}$ is represented

by $j^1\tilde{\varphi}(t,x) = (t,x,\varphi(t,x),\varphi_t(t,x),\varphi_x(t,x))$. Then the Lagrangian density (4.1.3) can be viewed as a mapping $\tilde{\mathcal{L}} : J^1Y \longrightarrow \mathbb{R}$. The corresponding action (4.0.3) can now be expressed as

$$\tilde{S}[\tilde{\varphi}] = \int_{\mathcal{U}} \tilde{\mathcal{L}}\big(j^1\tilde{\varphi}\big)\, dt \wedge dx. \tag{5.1.1}$$

Just like in Section 4.1, let us for the moment assume that the function $X : \mathcal{U} \longrightarrow [0, X_{max}]$ is known, so that we can view $\tilde{\mathcal{L}}$ as being time and space dependent. The dynamics is obtained by extremizing $\tilde{S}$ with respect to $\tilde{\varphi}$, that is, by solving for $\tilde{\varphi}$ such that

$$\frac{d}{d\lambda}\bigg|_{\lambda=0} \tilde{S}[\eta_Y^\lambda \circ \tilde{\varphi}] = 0 \tag{5.1.2}$$

for all η_Y^λ that keep the boundary conditions on $\partial\mathcal{U}$ fixed, where $\eta_Y^\lambda : Y \longrightarrow Y$ is the flow of a vertical vector field V on Y (see Section 2.6). Therefore, for an *a priori* known $X(t,x)$ the multisymplectic form formula (2.6.9) is satisfied for solutions of (5.1.2).

Consider the additional bundle $\pi_{\mathcal{XB}} : \mathcal{B} = \mathcal{X} \times [0, X_{max}] \longrightarrow \mathcal{X}$ whose sections $\tilde{X} : \mathcal{U} \longrightarrow \mathcal{B}$ represent our diffeomorphisms. Let $\tilde{X}(t,x) = (t,x,X(t,x))$ denote a local coordinate representation, and assume $X(t,.)$ is a diffeomorphism. Then define $\tilde{Y} = Y \oplus \mathcal{B}$. We have $J^k\tilde{Y} \cong J^kY \oplus J^k\mathcal{B}$. In Section 4.2.5.2 we argued that the moving mesh partial differential equation (3.2.4) can be interpreted as a local constraint on the fields $\tilde{\varphi}$, $\tilde{X}$ and their spatial derivatives. This constraint can be represented by a function $G : J^k\tilde{Y} \longrightarrow \mathbb{R}$. Sections $\tilde{\varphi}$ and $\tilde{X}$ satisfy the constraint if $G(j^k\tilde{\varphi}, j^k\tilde{X}) = 0$. Therefore our control-theoretic strategy expressed in equations (4.2.49) can be rewritten as

$$\begin{aligned} \frac{d}{d\lambda}\bigg|_{\lambda=0} \tilde{S}[\eta_Y^\lambda \circ \tilde{\varphi}] &= 0, \\ G(j^k\tilde{\varphi}, j^k\tilde{X}) &= 0, \end{aligned} \tag{5.1.3}$$

for all η_Y^λ, as previously defined. Let us argue how to interpret the notion of multisymplecticity for this problem. Intuitively, multisymplecticity should be understood in a sense similar to Proposition 4.1.3. We first solve the problem (5.1.3) for $\tilde{\varphi}$ and $\tilde{X}$, given some initial and boundary conditions. Then we substitute this $\tilde{X}$ into the problem (5.1.2). Let $\mathcal{P}$ be the set of solutions to this problem. Naturally, $\tilde{\varphi} \in \mathcal{P}$. The multisymplectic form formula

(2.6.9) will be satisfied for all fields in $\mathcal{P}$, but the constraint $G = 0$ will be satisfied only for $\tilde{\varphi}$.

Discretization

Discretize the computational spacetime $\mathbb{R}\times\mathbb{R}$ by picking the discrete set of points $t_j = j\cdot\Delta t$, $x_i = i\cdot\Delta x$, and define $\mathcal{X} = \{(j,i)\,|\,j,i \in \mathbb{Z}\}$. Let $\mathcal{X}^{\square}$ and $\mathcal{X}^{\square\!\square}$ be the set of rectangles and 6-tuples in $\mathcal{X}$, respectively. The discrete configuration bundle is $Y = \mathcal{X}\times\mathbb{R}$, and for convenience of notation let the elements of the fiber Y_{ji} be denoted by y_i^j. Let $\mathcal{U} = \{(j,i)\,|\,j = 0,1,\ldots,M{+}1,\ i = 0,1,\ldots,N{+}1\}$, where $\Delta x = X_{max}/(N{+}1)$ and $\Delta t = T_{max}/(M{+}1)$. Suppose we have a discrete Lagrangian $\tilde{L}: J^1Y \longrightarrow \mathbb{R}$ and the corresponding discrete action $\tilde{S}$ that approximates (5.1.1), where we assume that $X(t,x)$ is known and of the form (4.1.7). A variational integrator is obtained by solving

$$\left.\frac{d}{d\lambda}\right|_{\lambda=0} \tilde{S}[\tilde{\varphi}_\lambda] = 0 \tag{5.1.4}$$

for a discrete section $\tilde{\varphi}: \mathcal{U} \longrightarrow Y$, as described in Section 2.7. This integrator is multisymplectic, i.e., the discrete multisymplectic form formula (2.7.4) is satisfied.

Example: Midpoint rule. In (4.1.17) consider the 1-stage symplectic partitioned Runge-Kutta method with the coefficients $a_{11} = \bar{a}_{11} = c_1 = 1/2$ and $b_1 = \bar{b}_1 = 1$. This method is often called the *midpoint rule* and is a 2-nd order member of the Gauss family of quadratures (see Section 2.2.2). It can be easily shown (see [23], [41]) that the discrete Lagrangian (4.1.12) for this method is given by

$$\tilde{L}_d(t_j, y^j, t_{j+1}, y^{j+1}) = \Delta t\cdot\tilde{L}_N\left(\frac{y^j + y^{j+1}}{2}, \frac{y^{j+1} - y^j}{\Delta t}, t_j + \frac{1}{2}\Delta t\right), \tag{5.1.5}$$

where $\Delta t = t_{j+1} - t_j$ and $y^j = (y_1^j, \ldots, y_N^j)$. Using (4.1.2) and (4.1.10) we can write

$$\tilde{L}_d(t_j, y^j, t_{j+1}, y^{j+1}) = \sum_{i=0}^{N} \tilde{L}\big(y_i^j, y_{i+1}^j, y_{i+1}^{j+1}, y_i^{j+1}\big), \tag{5.1.6}$$

where we defined the discrete Lagrangian $\tilde{L}: J^1Y \longrightarrow \mathbb{R}$ by the formula

$$\tilde{L}(y_i^j, y_{i+1}^j, y_{i+1}^{j+1}, y_i^{j+1}) = \Delta t \int_{x_i}^{x_{i+1}} \tilde{\mathcal{L}}\left(\bar{\varphi}(x), \bar{\varphi}_x(x), \bar{\varphi}_t(x), x, t_j + \frac{1}{2}\Delta t\right) dx \tag{5.1.7}$$

with

$$\begin{aligned}
\bar{\varphi}(x) &= \frac{y_i^j + y_i^{j+1}}{2}\eta_i(x) + \frac{y_{i+1}^j + y_{i+1}^{j+1}}{2}\eta_{i+1}(x), \\
\bar{\varphi}_x(x) &= \frac{1}{2}\frac{y_{i+1}^j - y_i^j}{\Delta x} + \frac{1}{2}\frac{y_{i+1}^{j+1} - y_i^{j+1}}{\Delta x}, \\
\bar{\varphi}_t(x) &= \frac{y_i^{j+1} - y_i^j}{\Delta t}\eta_i(x) + \frac{y_{i+1}^{j+1} - y_{i+1}^j}{\Delta t}\eta_{i+1}(x).
\end{aligned} \tag{5.1.8}$$

Given the Lagrangian density $\tilde{\mathcal{L}}$ as in (4.1.3), and assuming $X(t,x)$ is known, one can evaluate the integral in (5.1.7) explicitly. It is now a straightforward calculation to show that the discrete variational principle (5.1.4) for the discrete Lagrangian $\tilde{L}$ as defined is equivalent to the Discrete Euler-Lagrange equations (2.4.2) for $\tilde{L}_d$, and consequently to (4.1.17).

This shows that the 2-nd order Gauss method applied to (4.1.17) defines a multisymplectic method in the sense of formula (2.7.4). However, for other symplectic partitioned Runge-Kutta methods of interest to us, namely the 4-th order Gauss and the 2-nd/4-th order Lobatto IIIA-IIIB methods (see Section 2.2.2), it is not possible to isolate a discrete Lagrangian $\tilde{L}$ that would only depend on four values y_i^j, y_{i+1}^j, y_{i+1}^{j+1}, y_i^{j+1}. The mentioned methods have more internal stages, and the equations (4.1.17) couple them in a nontrivial way. Effectively, at any given time step the internal stages depend on all the values $y_1^j, \ldots, y_N^j$ and $y_1^{j+1}, \ldots, y_N^{j+1}$, and it it not possible to express the discrete Lagrangian (4.1.12) as a sum similar to (5.1.6). The resulting integrators are still variational, since they are derived by applying the discrete variational principle (5.1.4) to some discrete action $\tilde{S}$, but this action cannot be expressed as the sum of $\tilde{L}$ over all rectangles. Therefore, these integrators are not multisymplectic, at least not in the sense of formula (2.7.4).

Constraints. Let the additional bundle be $\mathcal{B} = \mathcal{X} \times [0, X_{max}]$, and denote by X_j^n the elements of the fiber $\mathcal{B}_{ji}$. Define $\tilde{Y} = Y \oplus \mathcal{B}$. We have $J^k\tilde{Y} \cong J^kY \oplus J^k\mathcal{B}$. Suppose $G : J^k\tilde{Y} \longrightarrow \mathbb{R}$ represents a discretization of the continuous constraint. For instance, one

can enforce a uniform mesh by defining $G : J^1\tilde{Y} \to \mathbb{R}$, $G(j^1\tilde{\varphi}, j^1\tilde{X}) = X_x - 1$ at the continuous level. The discrete counterpart will be defined on the discrete jet bundle $J^1\tilde{Y}$ by the formula

$$G(y_i^j, y_{i+1}^j, y_{i+1}^{j+1}, y_i^{j+1}, X_i^j, X_{i+1}^j, X_{i+1}^{j+1}, X_i^{j+1}) = \frac{X_{i+1}^j - X_i^j}{\Delta x} - 1. \tag{5.1.9}$$

Arc-length equidistribution can be realized by enforcing (3.2.7), that is, $G : J_0^2\tilde{Y} \to \mathbb{R}$, $G(j_0^2\tilde{\varphi}, j_0^2\tilde{X}) = \alpha^2\varphi_x\varphi_{xx} + X_xX_{xx}$. The discrete counterpart will be defined on the discrete subbundle $J_0^2\tilde{Y}$ by the formula

$$G(y_{\square^l}, X_{\square^r}) = \alpha^2(y_{\square^3} - y_{\square^2})^2 + (X_{\square^3} - X_{\square^2})^2 - \alpha^2(y_{\square^2} - y_{\square^1})^2 - (X_{\square^2} - X_{\square^1})^2, \tag{5.1.10}$$

where for convenience we used the notation introduced in (2.7.8), and $l, r = 1, \ldots, 6$. Note that (5.1.10) coincides with (3.2.8). In fact, g_i in (3.2.8) is nothing else but G computed on an element of $J_0^2\tilde{Y}$ over the base 6-tuple $\square$ such that $\square^2 = (j, i)$. The only difference is that in (3.2.8) we assumed g_i might depend on *all* the field values at a given time step, while G only takes arguments *locally*, i.e., it depends on *at most* 6 field values on a given 6-tuple.

A numerical scheme is now obtained by simultaneously solving the discrete Euler-Lagrange equations (2.7.3) resulting from (5.1.4) and the equation $G = 0$. If we know y_i^{j-1}, X_i^{j-1}, y_i^j, and X_i^j for $i = 1, \ldots, N$, this system of equations allows us to solve for y_i^{j+1}, X_i^{j+1}. This numerical scheme is multisymplectic in the sense similar to Proposition 4.1.4. If we take $X(t, x)$ to be a sufficiently smooth interpolation of the values X_i^j and substitute it in the problem (5.1.4), then the resulting multisymplectic integrator will yield the same numerical values y_i^{j+1}.

5.2 Analysis of the Lagrange multiplier approach

Continuous setting

We now turn to describing the Lagrange multiplier approach in a multisymplectic setting. Just like in Section 5.1, let the computational spacetime be $\mathcal{X} = \mathbb{R} \times [0, X_{max}]$ with coordinates (t, x), and consider the trivial configuration bundles $\pi_{\mathcal{X}Y} : Y = \mathcal{X} \times \mathbb{R} \longrightarrow \mathcal{X}$ and $\pi_{\mathcal{X}\mathcal{B}} : \mathcal{B} = \mathcal{X} \times [0, X_{max}] \longrightarrow \mathcal{X}$. Let our scalar field be represented by a section $\tilde{\varphi} : \mathcal{X} \longrightarrow Y$ with the coordinate representation $\tilde{\varphi}(t, x) = (t, x, \varphi(t, x))$, and our diffeomorphism by a

section $\tilde{X} : \mathcal{X} \longrightarrow \mathcal{B}$ with the local representation $\tilde{X}(t,x) = (t, x, X(t,x))$. Let the total configuration bundle be $\tilde{Y} = Y \oplus \mathcal{B}$. Then the Lagrangian density (4.1.3) can be viewed as a mapping $\tilde{\mathcal{L}} : J^1\tilde{Y} \cong J^1Y \oplus J^1\mathcal{B} \longrightarrow \mathbb{R}$. The corresponding action (4.0.3) can now be expressed as

$$\tilde{S}[\tilde{\varphi}, \tilde{X}] = \int_{\mathcal{U}} \tilde{\mathcal{L}}\big(j^1\tilde{\varphi}, j^1\tilde{X}\big)\, dt \wedge dx, \tag{5.2.1}$$

where $\mathcal{U} = [0, T_{max}] \times [0, X_{max}]$. As before, the MMPDE constraint can be represented by a function $G : J^k\tilde{Y} \longrightarrow \mathbb{R}$. Two sections $\tilde{\varphi}$ and $\tilde{X}$ satisfy the constraint if

$$G(j^k\tilde{\varphi}, j^k\tilde{X}) = 0. \tag{5.2.2}$$

Vakonomic formulation. We now face the problem of finding the right equations of motion. We want to extremize the action functional (5.2.1) in some sense, subject to the constraint (5.2.2). Note that the constraint is essentially *nonholonomic*, as it depends on the derivatives of the fields. Assuming G is a submersion, $G = 0$ defines a submanifold of $J^k\tilde{Y}$, but this submanifold will not in general be the k-th jet of any subbundle of $\tilde{Y}$. Two distinct approaches are possible here. One could follow the *Lagrange-d'Alembert principle* and take variations of $\tilde{S}$ first, but choosing variations V (vertical vector fields on $\tilde{Y}$) such that the jet prolongations j^kV are tangent to the submanifold $G = 0$, and then enforce the constraint $G = 0$. On the other hand, one could consider the *variational nonholonomic* problem (also called *vakonomic*), and minimize $\tilde{S}$ over the set of all sections $(\tilde{\varphi}, \tilde{X})$ that satisfy the constraint $G = 0$, that is, enforce the constraint before taking the variations. If the constraint is holonomic, both approaches yield the same equations of motion. However, if the constraint is nonholonomic, the resulting equations are in general different. Which equations are correct is really a matter of experimental verification. It has been established that the Lagrange-d'Alembert principle gives the right equations of motion for nonholonomic mechanical systems, whereas the vakonomic setting is appropriate for optimal control problems (see [3], [4], [5]).

We are going to argue that the vakonomic approach is the right one in our case. In Proposition 4.2.1 we showed that in the unconstrained case extremizing $S[\phi]$ with respect to ϕ was equivalent to extremizing $\tilde{S}[\tilde{\varphi}, \tilde{X}]$ with respect to $\tilde{\varphi}$, and in Proposition 4.2.2

we showed that extremizing with respect to $\tilde{X}$ did not yield new information. This is because there was no restriction on the fields $\tilde{\varphi}$ and $\tilde{X}$, and for any given $\tilde{X}$ there was a one-to-one correspondence between ϕ and $\tilde{\varphi}$ given by the formula $\varphi(t,x) = \phi(t, X(t,x))$, so extremizing over all possible $\tilde{\varphi}$ was equivalent to extremizing over all possible ϕ. Now, let $\mathcal{N}$ be the set of all smooth sections $(\tilde{\varphi}, \tilde{X})$ that satisfy the constraint (5.2.2) such that $X(t,.)$ is a diffeomorphism for all t. It should be intuitively clear that under appropriate assumptions on the mesh density function ρ, for any given smooth function $\phi(t,X)$, equation (3.2.4) together with $\varphi(t,x) = \phi(t, X(t,x))$ define a unique pair $(\tilde{\varphi}, \tilde{X}) \in \mathcal{N}$ (since our main purpose here is to only justify the application of the vakonomic approach, we do not attempt to specify those analytic assumptions precisely). Conversely, any given pair $(\tilde{\varphi}, \tilde{X}) \in \mathcal{N}$ defines a unique function ϕ through the formula $\phi(t,X) = \varphi(t, \xi(t,X))$, where $\xi(t,.) = X(t,.)^{-1}$, as in Section 4.2.1. Given this one-to-one correspondence and the fact that $S[\phi] = \tilde{S}[\tilde{\varphi}, \tilde{X}]$ by definition, we see that extremizing S with respect to all smooth ϕ is equivalent to extremizing $\tilde{S}$ over all smooth sections $(\tilde{\varphi}, \tilde{X}) \in \mathcal{N}$. We conclude that the vakonomic approach is appropriate in our case, since it follows from Hamilton's principle for the original, physically meaningful, action functional S.

Let us also note that our constraint depends on spatial derivatives only. Therefore, in the setting presented in Chapter 4 it can be considered holonomic, as it restricts the infinite-dimensional configuration manifold of fields that we used as our configuration space. In that case it is valid to use Hamilton's principle and minimize the action functional over the set of all allowable fields, i.e., those that satisfy the constraint $G = 0$. We did that by considering the augmented instantaneous Lagrangian (4.2.50).

In order to minimize $\tilde{S}$ over the set of sections satisfying the constraint (5.2.2) we will use the bundle-theoretic version of the Lagrange multiplier theorem, which we cite below after [40].

Theorem 5.2.1 (**Lagrange multiplier theorem**). *Let $\pi_{\mathcal{M},\mathcal{E}} : \mathcal{E} \longrightarrow \mathcal{M}$ be an inner product bundle over a smooth manifold $\mathcal{M}$, Ψ a smooth section of $\pi_{\mathcal{M},\mathcal{E}}$, and $h : \mathcal{M} \longrightarrow \mathbb{R}$ a smooth function. Setting $\mathcal{N} = \Psi^{-1}(0)$, the following are equivalent:*

1. *$\sigma \in \mathcal{N}$ is an extremum of $h|_{\mathcal{N}}$,*

2. *there exists an extremum $\bar{\sigma} \in \mathcal{E}$ of $\bar{h} : \mathcal{E} \longrightarrow \mathbb{R}$ such that $\pi_{\mathcal{M},\mathcal{E}}(\bar{\sigma}) = \sigma$,*

where $\bar{h}(\bar{\sigma}) = h(\pi_{\mathcal{M},\mathcal{E}}(\bar{\sigma})) - \left\langle \bar{\sigma}, \Psi(\pi_{\mathcal{M},\mathcal{E}}(\bar{\sigma})) \right\rangle_{\mathcal{E}}$.

Let us briefly review the ideas presented in [40], adjusting the notation to our problem, and generalizing when necessary. Let

$$C^{\infty}_{\mathcal{U}}(\tilde{Y}) = \{\sigma = (\tilde{\varphi}, \tilde{X}) : \mathcal{U} \subset \mathcal{X} \longrightarrow \tilde{Y}\} \tag{5.2.3}$$

be the set of smooth sections of $\pi_{\mathcal{X}\tilde{Y}}$ on $\mathcal{U}$. Then $\tilde{S} : C^{\infty}_{\mathcal{U}}(\tilde{Y}) \longrightarrow \mathbb{R}$ can be identified with h in Theorem 5.2.1, where $\mathcal{M} = C^{\infty}_{\mathcal{U}}(\tilde{Y})$. Furthermore, define the trivial bundle

$$\pi_{\mathcal{X}\mathcal{V}} : \mathcal{V} = \mathcal{X} \times \mathbb{R} \longrightarrow \mathcal{X}, \tag{5.2.4}$$

and let $C^{\infty}_{\mathcal{U}}(\mathcal{V})$ be the set of smooth sections $\tilde{\lambda} : \mathcal{U} \longrightarrow \mathcal{V}$, which represent our Lagrange multipliers, and in local coordinates have the representation $\tilde{\lambda}(t,x) = (t, x, \lambda(t,x))$. The set $C^{\infty}_{\mathcal{U}}(\mathcal{V})$ is an inner product space with $\langle \tilde{\lambda}_1, \tilde{\lambda}_2 \rangle = \int_{\mathcal{U}} \lambda_1 \lambda_2 \, dt \wedge dx$. Take

$$\mathcal{E} = C^{\infty}_{\mathcal{U}}(\tilde{Y}) \times C^{\infty}_{\mathcal{U}}(\mathcal{V}). \tag{5.2.5}$$

This is an inner product bundle over $C^{\infty}_{\mathcal{U}}(\tilde{Y})$ with the inner product defined by

$$\left\langle (\sigma, \tilde{\lambda}_1), (\sigma, \tilde{\lambda}_2) \right\rangle_{\mathcal{E}} = \langle \tilde{\lambda}_1, \tilde{\lambda}_2 \rangle. \tag{5.2.6}$$

We now have to construct a smooth section $\Psi : C^{\infty}_{\mathcal{U}}(\tilde{Y}) \longrightarrow \mathcal{E}$ that will realize our constraint (5.2.2). Define the fiber-preserving mapping $\tilde{G} : J^k\tilde{Y} \longrightarrow \mathcal{V}$ such that for $\vartheta \in J^k\tilde{Y}$

$$\tilde{G}(\vartheta) = \left(\pi_{\mathcal{X},J^k\tilde{Y}}(\vartheta), G(\vartheta)\right). \tag{5.2.7}$$

For instance, for $k = 1$, in local coordinates we have $\tilde{G}(t,x,y,v_t,v_x) = (t, x, G(t,x,y,v_t,v_x))$. Then we can define

$$\Psi(\sigma) = (\sigma, \tilde{G} \circ j^k\sigma). \tag{5.2.8}$$

The set of allowable sections $\mathcal{N} \subset C^{\infty}_{\mathcal{U}}(\tilde{Y})$ is now defined by $\mathcal{N} = \Psi^{-1}(0)$. That is, $(\tilde{\varphi}, \tilde{X}) \in \mathcal{N}$ provided that $G(j^k\tilde{\varphi}, j^k\tilde{X}) = 0$.

The augmented action functional $\tilde{S}_C : \mathcal{E} \longrightarrow \mathbb{R}$ is now given by

$$\tilde{S}_C[\bar{\sigma}] = \tilde{S}[\pi_{\mathcal{M},\mathcal{E}}(\bar{\sigma})] - \left\langle \bar{\sigma}, \Psi(\pi_{\mathcal{M},\mathcal{E}}(\bar{\sigma})) \right\rangle_{\mathcal{E}}, \tag{5.2.9}$$

or denoting $\bar{\sigma} = (\tilde{\varphi}, \tilde{X}, \tilde{\lambda})$

$$\begin{aligned}
\tilde{S}_C[\tilde{\varphi}, \tilde{X}, \tilde{\lambda}] &= \tilde{S}[\tilde{\varphi}, \tilde{X}] - \left\langle \tilde{\lambda}, \tilde{G} \circ (j^k\tilde{\varphi}, j^k\tilde{X}) \right\rangle \\
&= \int_{\mathcal{U}} \tilde{\mathcal{L}}\big(j^1\tilde{\varphi}, j^1\tilde{X}\big)\, dt \wedge dx - \int_{\mathcal{U}} \lambda(t,x)\, G(j^k\tilde{\varphi}, j^k\tilde{X})\, dt \wedge dx \\
&= \int_{\mathcal{U}} \Big[\tilde{\mathcal{L}}\big(j^1\tilde{\varphi}, j^1\tilde{X}\big) - \lambda(t,x)\, G(j^k\tilde{\varphi}, j^k\tilde{X})\Big]\, dt \wedge dx.
\end{aligned} \tag{5.2.10}$$

Theorem 5.2.1 states, that if $(\tilde{\varphi}, \tilde{X}, \tilde{\lambda})$ is an extremum of $\tilde{S}_C$, then $(\tilde{\varphi}, \tilde{X})$ extremizes $\tilde{S}$ over the set $\mathcal{N}$ of sections satisfying the constraint $G = 0$. Note that using the multisymplectic formalism we obtained the same result as (4.2.50) in the instantaneous formulation, where we could treat G as a holonomic constraint. The dynamics is obtained by solving for a triple $(\tilde{\varphi}, \tilde{X}, \tilde{\lambda})$ such that

$$\left.\frac{d}{d\epsilon}\right|_{\epsilon=0} \tilde{S}_C[\eta_Y^\epsilon \circ \tilde{\varphi}, \eta_{\mathcal{B}}^\epsilon \circ \tilde{X}, \eta_{\mathcal{V}}^\epsilon \circ \tilde{\lambda}] = 0 \tag{5.2.11}$$

for all η_Y^ϵ, $\eta_{\mathcal{B}}^\epsilon$, $\eta_{\mathcal{V}}^\epsilon$ that keep the boundary conditions on $\partial\mathcal{U}$ fixed, where η^ϵ denotes the flow of vertical vector fields on respective bundles.

Note that we can define $\tilde{Y}_C = Y \oplus \mathcal{B} \oplus \mathcal{V}$ and $\tilde{\mathcal{L}_C} : J^k\tilde{Y}_C \longrightarrow \mathbb{R}$ by setting $\tilde{\mathcal{L}_C} = \tilde{\mathcal{L}} - \lambda \cdot G$, i.e., we can consider a k-th order field theory. If $k = 1, 2$ then an appropriate multisymplectic form formula in terms of the fields $\tilde{\varphi}$, $\tilde{X}$, and $\tilde{\lambda}$ will hold. Presumably, this can be generalized for $k > 2$ using the techniques put forth in [34]. However, it is an interesting question whether there exists any multisymplectic form formula defined in terms of $\tilde{\varphi}$, $\tilde{X}$, and objects on $J^k\tilde{Y}$ only. It appears to be an open problem. This would be the multisymplectic analog of the fact that the flow of a constrained mechanical system is symplectic on the constraint submanifold of the configuration space (see Section 2.5.1).

Discretization

Let us use the same discretization as discussed in Section 5.1. Assume we have a discrete Lagrangian $\tilde{L} : J^1\tilde{Y} \longrightarrow \mathbb{R}$, the corresponding discrete action $\tilde{S}[\tilde{\varphi}, \tilde{X}]$, and a discrete constraint $G : J^1\tilde{Y} \longrightarrow \mathbb{R}$ or $G : J^2_0\tilde{Y} \longrightarrow \mathbb{R}$. Note that $\tilde{S}$ is essentially a function of $2MN$

variables, and we want to extremize it subject to the set of algebraic constraints $G = 0$. The standard Lagrange multiplier theorem proved in basic calculus textbooks applies here. However, let us work out a discrete counterpart of the formalism introduced at the continuous level. This will facilitate the discussion of the discrete notion of multisymplecticity. Let

$$C_{\mathcal{U}}(\tilde{Y}) = \{\sigma = (\tilde{\varphi}, \tilde{X}) : \mathcal{U} \subset \mathcal{X} \longrightarrow \tilde{Y}\} \tag{5.2.12}$$

be the set of discrete sections of $\pi_{\mathcal{X}\tilde{Y}} : \tilde{Y} \longrightarrow \mathcal{X}$. Similarly, define the discrete bundle $\mathcal{V} = \mathcal{X} \times \mathbb{R}$ and let $C_{\mathcal{U}_0}(\mathcal{V})$ be the set of discrete sections $\tilde{\lambda} : \mathcal{U}_0 \longrightarrow \mathcal{V}$ representing the Lagrange multipliers, where $\mathcal{U}_0 \subset \mathcal{U}$ is defined below. Let $\tilde{\lambda}(j,i) = (j,i,\lambda(j,i))$ with $\lambda_i^j \equiv \lambda(j,i)$ be the local representation. The set $C_{\mathcal{U}_0}(\mathcal{V})$ is an inner product space with $\langle \tilde{\lambda}, \tilde{\mu} \rangle = \sum_{(j,i)\in\mathcal{U}_0} \lambda_i^j \mu_i^j$. Take $\mathcal{E} = C_{\mathcal{U}}(\tilde{Y}) \times C_{\mathcal{U}_0}(\mathcal{V})$. Just like at the continuous level, $\mathcal{E}$ is an inner product bundle. However, at the discrete level it is more convenient to define the inner product on $\mathcal{E}$ in a slightly modified way. Since there are some nuances in the notation, let us consider the cases $k = 1$ and $k = 2$ separately.

Case k=1. Let $\mathcal{U}_0 = \{(j,i) \in \mathcal{U} \,|\, j \leq M, i \leq N\}$. Define the trivial bundle $\hat{\mathcal{V}} = \mathcal{X}^{\square} \times \mathbb{R}$ and let $C_{\mathcal{U}^{\square}}(\hat{\mathcal{V}})$ be the set of all sections of $\hat{\mathcal{V}}$ defined on $\mathcal{U}^{\square}$. For a given section $\tilde{\lambda} \in C_{\mathcal{U}_0}(\mathcal{V})$ we define its extension $\hat{\lambda} \in C_{\mathcal{U}^{\square}}(\hat{\mathcal{V}})$ by

$$\hat{\lambda}(\square) = \big(\square, \lambda(\square^1)\big), \tag{5.2.13}$$

that is, $\hat{\lambda}$ assigns to the square $\square$ the value that $\tilde{\lambda}$ takes on the *first* vertex of that square. Note that this operation is invertible: given a section of $C_{\mathcal{U}^{\square}}(\hat{\mathcal{V}})$ we can uniquely determine a section of $C_{\mathcal{U}_0}(\mathcal{V})$. We can define the inner product

$$\langle \hat{\lambda}, \hat{\mu} \rangle = \sum_{\square \subset \mathcal{U}} \lambda(\square^1)\mu(\square^1). \tag{5.2.14}$$

One can easily see that we have $\langle \hat{\lambda}, \hat{\mu} \rangle = \langle \tilde{\lambda}, \tilde{\mu} \rangle$, so by a slight abuse of notation we can use the same symbol $\langle ., . \rangle$ for both inner products. It will be clear from the context which definition should be invoked. We can now define an inner product on the fibers of $\mathcal{E}$ as

$$\Big\langle (\sigma, \tilde{\lambda}), (\sigma, \tilde{\mu}) \Big\rangle_{\mathcal{E}} = \langle \hat{\lambda}, \hat{\mu} \rangle = \langle \tilde{\lambda}, \tilde{\mu} \rangle. \tag{5.2.15}$$

Let us now construct a section $\Psi : C_{\mathcal{U}}(\tilde{Y}) \longrightarrow \mathcal{E}$ that will realize our discrete constraint G. First, in analogy to (5.2.7), define the fiber-preserving mapping $\tilde{G} : J^1\tilde{Y} \longrightarrow \hat{\mathcal{V}}$ such that

$$\tilde{G}(y_{\square^l}, X_{\square^r}) = \big(\square, G(y_{\square^l}, X_{\square^r})\big), \tag{5.2.16}$$

where $l, r = 1, 2, 3, 4$. We now define Ψ by requiring that for $\sigma \in C_{\mathcal{U}}(\tilde{Y})$ the extension (5.2.13) of $\Psi(\sigma)$ is given by

$$\hat{\Psi}(\sigma) = (\sigma, \tilde{G} \circ j^1\sigma). \tag{5.2.17}$$

The set of allowable sections $\mathcal{N} \subset C_{\mathcal{U}}(\tilde{Y})$ is now defined by $\mathcal{N} = \Psi^{-1}(0)$—that is, $(\tilde{\varphi}, \tilde{X}) \in \mathcal{N}$ provided that $G(j^1\tilde{\varphi}, j^1\tilde{X}) = 0$ for all $\square \in \mathcal{U}^{\square}$. The augmented discrete action $\tilde{S}_C : \mathcal{E} \longrightarrow \mathbb{R}$ is therefore

$$\begin{aligned}
\tilde{S}_C[\sigma, \tilde{\lambda}] &= \tilde{S}[\sigma] - \Big\langle (\sigma, \tilde{\lambda}), \Psi(\sigma) \Big\rangle_{\mathcal{E}} \\
&= \tilde{S}[\sigma] - \Big\langle \hat{\lambda}, \tilde{G} \circ j^1\sigma \Big\rangle \\
&= \sum_{\square \subset \mathcal{U}} \tilde{L}(j^1\sigma) - \sum_{\square \subset \mathcal{U}} \lambda(\square^1) G(j^1\sigma) \\
&= \sum_{\square \subset \mathcal{U}} \Big(\tilde{L}(j^1\sigma) - \lambda(\square^1) G(j^1\sigma) \Big).
\end{aligned} \tag{5.2.18}$$

By the standard Lagrange multiplier theorem, if $(\tilde{\varphi}, \tilde{X}, \tilde{\lambda})$ is an extremum of $\tilde{S}_C$, then $(\tilde{\varphi}, \tilde{X})$ is an extremum of $\tilde{S}$ over the set $\mathcal{N}$ of sections satisfying the constraint $G = 0$. The discrete Hamilton principle can be expressed as

$$\left. \frac{d}{d\epsilon} \right|_{\epsilon=0} \tilde{S}_C[\tilde{\varphi}_\epsilon, \tilde{X}_\epsilon, \tilde{\lambda}_\epsilon] = 0 \tag{5.2.19}$$

for all vector fields V on Y, W on $\mathcal{B}$, and Z on $\mathcal{V}$ that keep the boundary conditions on $\partial\mathcal{U}$ fixed, where $\tilde{\varphi}_\epsilon(j, i) = F_\epsilon^{V_{ji}}(\tilde{\varphi}(j, i))$ and $F_\epsilon^{V_{ji}}$ is the flow of V_{ji} on $\mathbb{R}$, and similarly for $\tilde{X}_\epsilon$ and $\tilde{\lambda}_\epsilon$. The discrete Euler-Lagrange equations can be conveniently computed if in (5.2.19) one focuses on some $(j, i) \in \operatorname{int}\mathcal{U}$. With the convention $\tilde{\varphi}(j, i) = y_i^j$, $\tilde{X}(j, i) = X_i^j$, $\tilde{\lambda}(j, i) = \lambda_i^j$,

we write the terms of $\tilde{S}_C$ containing y_i^j, X_i^j and λ_i^j explicitly as

$$\begin{aligned}
\tilde{S}_C = \ldots &+ \tilde{L}\big(y_i^j, y_{i+1}^j, y_{i+1}^{j+1}, y_i^{j+1}, X_i^j, X_{i+1}^j, X_{i+1}^{j+1}, X_i^{j+1}\big) \\
&+ \tilde{L}\big(y_{i-1}^j, y_i^j, y_i^{j+1}, y_{i-1}^{j+1}, X_{i-1}^j, X_i^j, X_i^{j+1}, X_{i-1}^{j+1}\big) \\
&+ \tilde{L}\big(y_{i-1}^{j-1}, y_i^{j-1}, y_i^j, y_{i-1}^j, X_{i-1}^{j-1}, X_i^{j-1}, X_i^j, X_{i-1}^j\big) \\
&+ \tilde{L}\big(y_i^{j-1}, y_{i+1}^{j-1}, y_{i+1}^j, y_i^j, X_i^{j-1}, X_{i+1}^{j-1}, X_{i+1}^j, X_i^j\big) \\
&+ \lambda_i^j G\big(y_i^j, y_{i+1}^j, y_{i+1}^{j+1}, y_i^{j+1}, X_i^j, X_{i+1}^j, X_{i+1}^{j+1}, X_i^{j+1}\big) \\
&+ \lambda_{i-1}^j G\big(y_{i-1}^j, y_i^j, y_i^{j+1}, y_{i-1}^{j+1}, X_{i-1}^j, X_i^j, X_i^{j+1}, X_{i-1}^{j+1}\big) \\
&+ \lambda_{i-1}^{j-1} G\big(y_{i-1}^{j-1}, y_i^{j-1}, y_i^j, y_{i-1}^j, X_{i-1}^{j-1}, X_i^{j-1}, X_i^j, X_{i-1}^j\big) \\
&+ \lambda_i^{j-1} G\big(y_i^{j-1}, y_{i+1}^{j-1}, y_{i+1}^j, y_i^j, X_i^{j-1}, X_{i+1}^{j-1}, X_{i+1}^j, X_i^j\big) + \ldots
\end{aligned} \tag{5.2.20}$$

The discrete Euler-Lagrange equations (see Section 2.7) are obtained by differentiating with respect to y_i^j, X_i^j, and λ_i^j, and can be written compactly as

$$\sum_{\substack{l,\square \\ (j,i)=\square^l}} \left[\frac{\partial \tilde{L}}{\partial y^l}(y_{\square^1}, \ldots, y_{\square^4}, X_{\square^1}, \ldots, X_{\square^4}) + \right.$$
$$\left. + \lambda_{\square^1} \frac{\partial G}{\partial y^l}(y_{\square^1}, \ldots, y_{\square^4}, X_{\square^1}, \ldots, X_{\square^4}) \right] = 0,$$

$$\sum_{\substack{l,\square \\ (j,i)=\square^l}} \left[\frac{\partial \tilde{L}}{\partial X^l}(y_{\square^1}, \ldots, y_{\square^4}, X_{\square^1}, \ldots, X_{\square^4}) + \right.$$
$$\left. + \lambda_{\square^1} \frac{\partial G}{\partial X^l}(y_{\square^1}, \ldots, y_{\square^4}, X_{\square^1}, \ldots, X_{\square^4}) \right] = 0,$$

$$G\big(y_i^j, y_{i+1}^j, y_{i+1}^{j+1}, y_i^{j+1}, X_i^j, X_{i+1}^j, X_{i+1}^{j+1}, X_i^{j+1}\big) = 0 \tag{5.2.21}$$

for all $(j,i) \in \operatorname{int}\mathcal{U}$. If we know y_i^{j-1}, X_i^{j-1}, y_i^j, X_i^j, and λ_i^{j-1} for $i = 1, \ldots, N$, this system of equations allows us to solve for y_i^{j+1}, X_i^{j+1}, and λ_i^j.

Note that we can define $\tilde{Y}_C = Y \oplus \mathcal{B} \oplus \mathcal{V}$, and the augmented Lagrangian $\tilde{L}_C : J^1\tilde{Y}_C \longrightarrow \mathbb{R}$ by setting

$$\tilde{L}_C(j^1\tilde{\varphi}, j^1\tilde{X}, j^1\tilde{\lambda}) = \tilde{L}(j^1\tilde{\varphi}, j^1\tilde{X}) - \lambda(\square^1) \cdot G(j^1\tilde{\varphi}, j^1\tilde{X}), \tag{5.2.22}$$

that is, we can consider an unconstrained field theory in terms of the fields $\tilde{\varphi}$, $\tilde{X}$, and $\tilde{\lambda}$. Then the solutions of (5.2.21) satisfy the multisymplectic form formula (2.7.4) in terms of objects defined on $J^1\tilde{Y}_C$.

Case k=2. Let $\mathcal{U}_0 = \{(j,i) \in \mathcal{U} \,|\, j \leq M, 1 \leq i \leq N\}$. Define the trivial bundle $\hat{\mathcal{V}} = \mathcal{X}^{\square} \times \mathbb{R}$ and let $C_{\mathcal{U}^{\square}}(\hat{\mathcal{V}})$ be the set of all sections of $\hat{\mathcal{V}}$ defined on $\mathcal{U}^{\square}$. For a given section $\tilde{\lambda} \in C_{\mathcal{U}_0}(\mathcal{V})$ we define its extension $\hat{\lambda} \in C_{\mathcal{U}^{\square}}(\hat{\mathcal{V}})$ by

$$\hat{\lambda}(\square) = \big(\square, \lambda(\square^2)\big), \tag{5.2.23}$$

that is, $\hat{\lambda}$ assigns to the 6-tuple $\square$ the value that $\tilde{\lambda}$ takes on the *second* vertex of that 6-tuple. Like before, this operation is invertible. We can define the inner product

$$\langle \hat{\lambda}, \hat{\mu} \rangle = \sum_{\square \subset \mathcal{U}} \lambda(\square^2)\mu(\square^2) \tag{5.2.24}$$

and the inner product on $\mathcal{E}$ as in (5.2.15). Define the fiber-preserving mapping $\tilde{G} : J_0^2\tilde{Y} \longrightarrow \hat{\mathcal{V}}$ such that

$$\tilde{G}(y_{\square^l}, X_{\square^r}) = \big(\square, G(y_{\square^l}, X_{\square^r})\big), \tag{5.2.25}$$

where $l, r = 1, \ldots, 6$. We now define Ψ by requiring that for $\sigma \in C_{\mathcal{U}}(\tilde{Y})$ the extension (5.2.23) of $\Psi(\sigma)$ is given by

$$\hat{\Psi}(\sigma) = (\sigma, \tilde{G} \circ j_0^2\sigma). \tag{5.2.26}$$

Again, the set of allowable sections is $\mathcal{N} = \Psi^{-1}(0)$. That is, $(\tilde{\varphi}, \tilde{X}) \in \mathcal{N}$ provided that $G(j_0^2\tilde{\varphi}, j_0^2\tilde{X}) = 0$ for all $\square \in \mathcal{U}^{\square}$. The augmented discrete action $\tilde{S}_C : \mathcal{E} \longrightarrow \mathbb{R}$ is therefore

$$\begin{aligned}\tilde{S}_C[\sigma,\tilde{\lambda}] &= \tilde{S}[\sigma] - \Big\langle (\sigma,\tilde{\lambda}), \Psi(\sigma)\Big\rangle_{\mathcal{E}} \\ &= \tilde{S}[\sigma] - \Big\langle \hat{\lambda}, \tilde{G}\circ j_0^2\sigma\Big\rangle \\ &= \sum_{\square\subset\mathcal{U}} \tilde{L}(j^1\sigma) - \sum_{\square\!\square\subset\mathcal{U}} \lambda(\square\!\square^2) G(j_0^2\sigma). \end{aligned} \tag{5.2.27}$$

By writing out the terms involving y_i^j, X_i^j, and λ_i^j explicitly, as in (5.2.20), and invoking the discrete Hamilton principle (5.2.19), one obtains the discrete Euler-Lagrange equations, which can be compactly expressed as

$$\begin{aligned}&\sum_{\substack{l,\square\\(j,i)=\square^l}} \frac{\partial\tilde{L}}{\partial y^l}(y_{\square^1},\dots,y_{\square^4},X_{\square^1},\dots,X_{\square^4}) + \\ &\qquad + \sum_{\substack{l,\square\!\square\\(j,i)=\square\!\square^l}} \lambda_{\square\!\square^2}\frac{\partial G}{\partial y^l}(y_{\square\!\square^1},\dots,y_{\square\!\square^6},X_{\square\!\square^1},\dots,X_{\square\!\square^6}) = 0,\end{aligned}$$

$$\begin{aligned}&\sum_{\substack{l,\square\\(j,i)=\square^l}} \frac{\partial\tilde{L}}{\partial X^l}(y_{\square^1},\dots,y_{\square^4},X_{\square^1},\dots,X_{\square^4}) + \\ &\qquad + \sum_{\substack{l,\square\!\square\\(j,i)=\square\!\square^l}} \lambda_{\square\!\square^2}\frac{\partial G}{\partial X^l}(y_{\square\!\square^1},\dots,y_{\square\!\square^6},X_{\square\!\square^1},\dots,X_{\square\!\square^6}) = 0,\end{aligned}$$

$$G\big(y_{i-1}^j, y_i^j, y_{i+1}^j, y_{i+1}^{j+1}, y_i^{j+1}, y_{i-1}^{j+1}, X_{i-1}^j, X_i^j, X_{i+1}^j, X_{i+1}^{j+1}, X_i^{j+1}, X_{i-1}^{j+1}\big) = 0 \tag{5.2.28}$$

for all $(j,i)\in \operatorname{int}\mathcal{U}$. If we know y_i^{j-1}, X_i^{j-1}, y_i^j, X_i^j, and λ_i^{j-1} for $i=1,\dots,N$, this system of equations allows us to solve for y_i^{j+1}, X_i^{j+1}, and λ_i^j.

Let us define the extension $\tilde{L}_{\text{ext}} : J_0^2\tilde{Y} \longrightarrow \mathbb{R}$ of the Lagrangian density $\tilde{L}$ by setting

$$\tilde{L}_{\text{ext}}(y_{\square\!\square^1},\dots,X_{\square\!\square^6}) = \begin{cases} \tilde{L}(y_{\square^1},\dots,X_{\square^4}) & \text{if } \square\!\square^2 = (j,0),(j,N+1),\\ & \text{where } \square = \square\!\square\cap\mathcal{U},\\ \frac{1}{2}\sum_{\square\subset\square\!\square}\tilde{L}(y_{\square^1},\dots,X_{\square^4}) & \text{otherwise.}\end{cases} \tag{5.2.29}$$

Let us also set $G(y_{\square^1},\dots,X_{\square^4}) = 0$ if $\square^2 = (j,0),(j,N+1)$. Define $\mathcal{A} = \{\square \,|\, \square^2, \square^5 \in \mathcal{U}\}$. Then (5.2.27) can be written as

$$\tilde{S}_C[\sigma,\tilde{\lambda}] = \sum_{\square\in\mathcal{A}} \Big[\tilde{L}_{\text{ext}}(j_0^2\sigma) - \lambda(\square^2)G(j_0^2\sigma)\Big] = \sum_{\square\in\mathcal{A}} \tilde{L}_C(j_0^2\sigma, j_0^2\tilde{\lambda}), \tag{5.2.30}$$

where the last equality defines the augmented Lagrangian $\tilde{L}_C : J_0^2\tilde{Y}_C \longrightarrow \mathbb{R}$ for $\tilde{Y}_C = Y \oplus \mathcal{B} \oplus \mathcal{V}$. Therefore, we can consider an unconstrained second-order field theory in terms of the fields $\tilde{\varphi}$, $\tilde{X}$, and $\tilde{\lambda}$, and the solutions of (5.2.28) will satisfy a discrete multisymplectic form formula very similar to the one proved in [34]. The only difference is the fact that the authors analyzed a discretization of the Camassa-Holm equation, and were able to consider an even smaller subbundle of the second jet of the configuration bundle. As a result, it was sufficient for them to consider a discretization based on squares $\square$ rather than 6-tuples $\square$. In our case there will be six discrete 2-forms $\Omega^l_{\tilde{L}_C}$ for $l = 1,\dots,6$ instead of just four.

Remark. In both cases we showed that our discretization leads to integrators that are multisymplectic on the augmented jets $J^k\tilde{Y}_C$. However, just like in the continuous setting, it is an interesting problem whether there exists a discrete multisymplectic form formula in terms of objects defined on $J^k\tilde{Y}$ only.

Example: Trapezoidal rule. Consider the semi-discrete Lagrangian (4.2.8). We can use the trapezoidal rule to define the discrete Lagrangian (4.1.11) as

$$\begin{aligned}\tilde{L}_d(y^j,X^j,y^{j+1},X^{j+1}) = \frac{\Delta t}{2}\tilde{L}_N\left(y^j,X^j,\frac{y^{j+1}-y^j}{\Delta t},\frac{X^{j+1}-X^j}{\Delta t}\right)\\ + \frac{\Delta t}{2}\tilde{L}_N\left(y^{j+1},X^{j+1},\frac{y^{j+1}-y^j}{\Delta t},\frac{X^{j+1}-X^j}{\Delta t}\right),\end{aligned} \tag{5.2.31}$$

where $y^j = (y_1^j,\dots,y_N^j)$ and $X^j = (X_1^j,\dots,X_N^j)$. The constrained version (see Section 2.5.2 and [41]) of the Discrete Euler-Lagrange equations takes the form

$$D_2\tilde{L}_d(q^{j-1},q^j)+D_1\tilde{L}_d(q^j,q^{j+1})=Dg(q^j)^T\lambda^j,$$
$$g(q^{j+1})=0, \tag{5.2.32}$$

where for brevity $q^j=(y_1^j,X_1^j,\dots,y_N^j,X_N^j)$, $\lambda^j=(\lambda_1^j,\dots,\lambda_N^j)$, and g is an adaptation constraint, for instance (3.2.8). If q^{j-1}, q^j are known, then (5.2.32) can be used to compute q^{j+1} and λ^j. It is easy to verify that the condition (4.2.58) is enough to ensure solvability of (5.2.32), assuming the time step Δt is sufficiently small, so there is no need to introduce slack degrees of freedom as in (4.2.59). If the mass matrix (4.2.11) was constant and nonsingular, then (5.2.32) would result in the SHAKE algorithm, or in the RATTLE algorithm if one passes to the position-momentum formulation (see [23], [41]).

Using (4.2.2) and (4.2.5) we can write

$$\tilde{L}_d(y^j,X^j,y^{j+1},X^{j+1})=\sum_{i=0}^{N}\tilde{L}\big(y_i^j,y_{i+1}^j,y_{i+1}^{j+1},y_i^{j+1},X_i^j,X_{i+1}^j,X_{i+1}^{j+1},X_i^{j+1}\big), \tag{5.2.33}$$

where we defined the discrete Lagrangian $\tilde{L}:J^1\tilde{Y}\longrightarrow\mathbb{R}$ by the formula

$$\begin{aligned}\tilde{L}\Big(y_i^j,y_{i+1}^j,y_{i+1}^{j+1},y_i^{j+1},X_i^j,X_{i+1}^j,X_{i+1}^{j+1},X_i^{j+1}\Big)=\\ \frac{\Delta t}{2}\int_{x_i}^{x_{i+1}}\tilde{\mathcal{L}}\Big(\bar{\varphi}^j(x),\bar{X}^j(x),\bar{\varphi}_x^j(x),\bar{X}_x^j(x),\bar{\varphi}_t(x),\bar{X}_t(x)\Big)\,dx\\ +\frac{\Delta t}{2}\int_{x_i}^{x_{i+1}}\tilde{\mathcal{L}}\Big(\bar{\varphi}^{j+1}(x),\bar{X}^{j+1}(x),\bar{\varphi}_x^{j+1}(x),\bar{X}_x^{j+1}(x),\bar{\varphi}_t(x),\bar{X}_t(x)\Big)\,dx\end{aligned} \tag{5.2.34}$$

with

$$\begin{aligned}\bar{\varphi}^j(x)&=y_i^j\eta_i(x)+y_{i+1}^j\eta_{i+1}(x),\\ \bar{\varphi}_x^j(x)&=\frac{y_{i+1}^j-y_i^j}{\Delta x},\\ \bar{\varphi}_t(x)&=\frac{y_i^{j+1}-y_i^j}{\Delta t}\eta_i(x)+\frac{y_{i+1}^{j+1}-y_{i+1}^j}{\Delta t}\eta_{i+1}(x),\end{aligned} \tag{5.2.35}$$

and similarly for $\bar{X}(x)$. Given the Lagrangian density $\tilde{\mathcal{L}}$ as in (4.2.7), one can compute the integrals in (5.2.34) explicitly. Suppose that the adaptation constraint g has a 'local' structure, for instance

$$g_i(y^j, X^j) = G(y_i^j, y_{i+1}^j, y_{i+1}^{j+1}, y_i^{j+1}, X_i^j, X_{i+1}^j, X_{i+1}^{j+1}, X_i^{j+1}), \tag{5.2.36}$$

as in (5.1.9) or

$$g_i(y^j, X^j) = G(y_{\square^l}, X_{\square^r}), \qquad \text{where } \square^2 = (j, i), \tag{5.2.37}$$

as in (5.1.10). It is straightforward to show that (5.2.21) or (5.2.28) are equivalent to (5.2.32), that is, the variational integrator defined by (5.2.32) is also multisymplectic.

For reasons similar to the ones pointed out in Section 5.1, the 2-nd and 4-th order Lobatto IIIA-IIIB methods that we used for our numerical computations are not multisymplectic.

Chapter 6

Numerical experiments

We applied the methods discussed in the previous chapters to the Sine-Gordon equation. This interesting model arises in many physical applications. For instance, it governs the propagation of dislocations in crystals, the evolution of magnetic flux in a long Josephson-junction transmission line, or the modulation of a weakly unstable baroclinic wave packet in a two-layer fluid. It also has applications in the description of one-dimensional organic conductors, one-dimensional ferromagnets, liquid crystals, or in particle physics as a model for baryons (see [11], [54]).

6.1 The Sine-Gordon equation

The Sine-Gordon equation takes the form

$$\frac{\partial^2\phi}{\partial t^2} - \frac{\partial^2\phi}{\partial X^2} + \sin\phi = 0, \tag{6.1.1}$$

and describes the dynamics of the (1+1)-dimensional scalar field theory with the Lagrangian density

$$\mathcal{L}(\phi, \phi_X, \phi_t) = \frac{1}{2}\phi_t^2 - \frac{1}{2}\phi_X^2 - (1 - \cos\phi). \tag{6.1.2}$$

The Sine-Gordon equation has interesting soliton solutions. A single soliton traveling at the speed v is given by

$$\phi_S(X,t) = 4\arctan\left[\exp\left(\frac{X - X_0 - vt}{\sqrt{1-v^2}}\right)\right]. \tag{6.1.3}$$

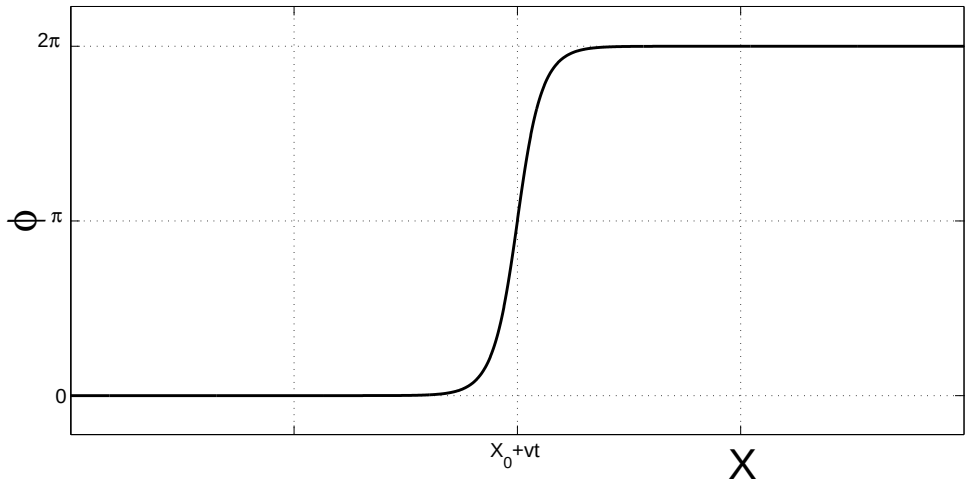

Figure 6.1.1: The single-soliton solution of the Sine-Gordon equation.

It is depicted in Figure 6.1.1. The backscattering of two solitons, each traveling with the velocity v, is described by the formula

$$\phi_{SS}(X,t) = 4\arctan\left[\frac{v\sinh(\frac{X}{\sqrt{1-v^2}})}{\cosh(\frac{vt}{\sqrt{1-v^2}})}\right]. \tag{6.1.4}$$

It is depicted in Figure 6.1.2. Note that if we restrict $X \geq 0$, then this formula also gives a single-soliton solution satisfying the boundary condition $\phi(0,t) = 0$, that is, a soliton bouncing from a rigid wall.

6.2 Generating consistent initial conditions

Suppose we specify the following initial conditions

$$\begin{aligned} \phi(X,0) &= a(X), \\ \phi_t(X,0) &= b(X), \end{aligned} \tag{6.2.1}$$

and assume they are consistent with the boundary conditions (4.0.2). In order to determine appropriate consistent initial conditions for (4.1.15) and (4.2.62) we need to solve several equations. First we solve for the y_i's and X_i's. We have $y_0 = \phi_L$, $y_{N+1} = \phi_R$, $X_0 = 0$, $X_{N+1} = X_{max}$. The rest are determined by solving the system

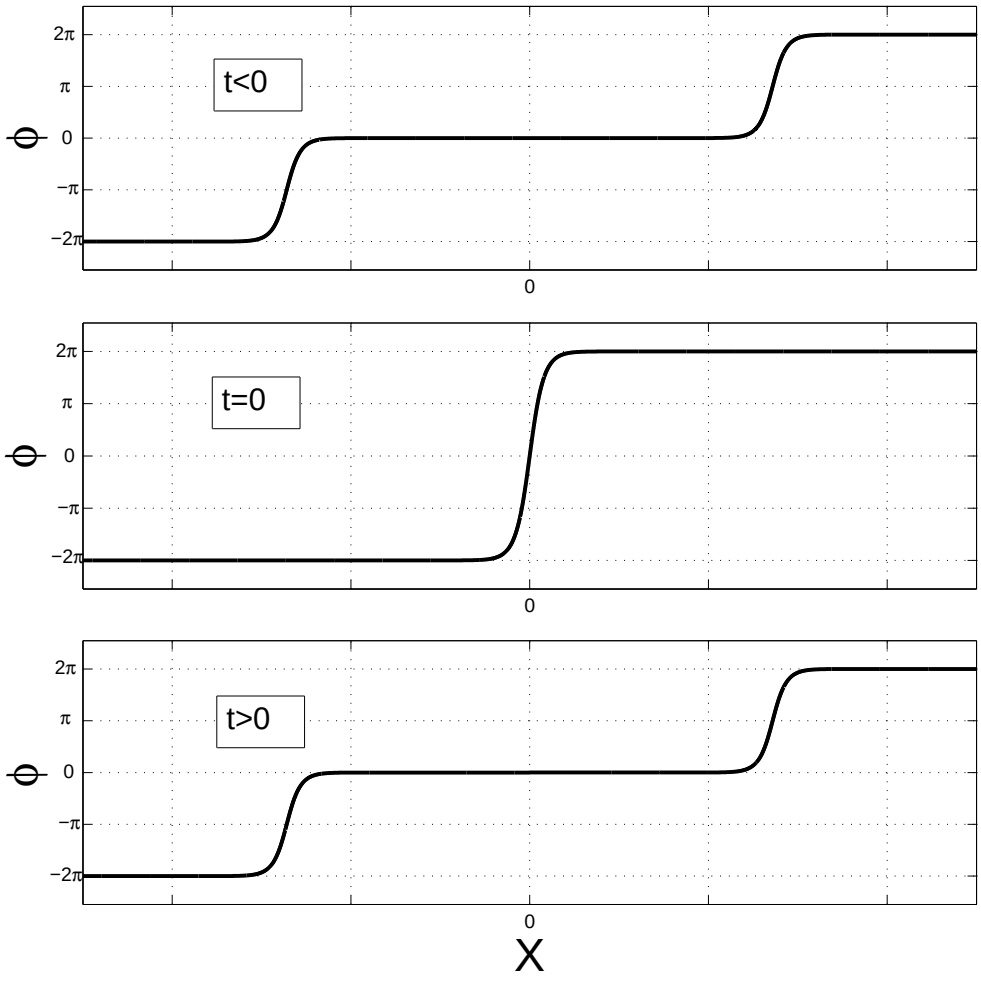

Figure 6.1.2: The two-soliton solution of the Sine-Gordon equation.

$$
\begin{aligned}
y_i &= a(X_i), \\
0 &= g_i(y_1, \ldots, y_N, X_1, \ldots, X_N),
\end{aligned}
\tag{6.2.2}
$$

for $i = 1, \ldots, N$. This is a system of $2N$ nonlinear equations for $2N$ unknowns. We solve it using Newton's method. Note, however, that we do not *a priori* know good starting points for Newton's iterations. If our initial guesses are not close enough to the desired solution, the iterations may converge to the wrong solution or may not converge at all. In our computations we used the constraints (3.2.8). We found that a very simple variant of a homotopy continuation method worked very well in our case. Note that for $\alpha = 0$ the set of constraints (3.2.8) generates a uniform mesh. In order to solve (6.2.2) for some $\alpha > 0$, we split $[0, \alpha]$ into d subintervals by picking $\alpha_k = (k/d) \cdot \alpha$ for $k = 1, \ldots, d$. We then solved (6.2.2) with α_1 using the uniformly spaced mesh points $X_i^{(0)} = (i/(N+1)) \cdot X_{max}$ as our initial guess, resulting in $X_i^{(1)}$ and $y_i^{(1)}$. Then we solved (6.2.2) with α_2 using $X_i^{(1)}$ and $y_i^{(1)}$ as the initial guesses, resulting in $X_i^{(2)}$ and $y_i^{(2)}$. Continuing in this fashion, we got $X_i^{(d)}$ and $y_i^{(d)}$ as the numerical solution to (6.2.2) for the original value of α. Note that for more complicated initial conditions and constraint functions, predictor-corrector methods should be used—see [1] for more information. Another approach to solving (6.2.2) could be based on relaxation methods (see [7], [28]).

Next, we solve for the initial values of the velocities $\dot{y}_i$ and $\dot{X}_i$. Since $\varphi(x,t) = \phi(X(x,t),t)$, we have $\varphi_t(x,t) = \phi_X(X(x,t),t)X_t(x,t) + \phi_t(X(x,t),t)$. We also require that the velocities be consistent with the constraints. Hence the linear system

$$
\begin{aligned}
\dot{y}_i &= a'(X_i)\dot{X}_i + b(X_i), \qquad\qquad i = 1, \ldots, N \\
0 &= \frac{\partial g}{\partial y}(y, X)\dot{y} + \frac{\partial g}{\partial X}(y, X)\dot{X}.
\end{aligned}
\tag{6.2.3}
$$

This is a system of $2N$ linear equations for the $2N$ unknowns $\dot{y}_i$ and $\dot{X}_i$, where $y = (y_1, \ldots, y_N)$ and $X = (X_1, \ldots, X_N)$. We can use those velocities to compute the initial values of the conjugate momenta. For the control-theoretic approach we use $p_i = \partial \tilde{L}_N / \partial \dot{y}_i$, as in Section 4.1.3, and for the Lagrange multiplier approach we use (4.2.10). In addition,

for the Lagrange multiplier approach we also have the initial values for the slack variables $r_i = 0$ and their conjugate momenta $B_i = \partial \tilde{L}_N^A / \partial \dot{r}_i = 0$. It is also useful to use (4.2.57) to compute the initial values of the Lagrange multipliers λ_i that can be used as initial guesses in the first iteration of the Lobatto IIIA-IIIB algorithm. The initial guesses for the slack Lagrange multipliers are trivially $\mu_i = 0$.

6.3 Convergence

In order to test the convergence of our methods as the number of mesh points N is increased, we considered a single soliton bouncing from two rigid walls at $X = 0$ and $X = X_{max} = 25$. We imposed the boundary conditions $\phi_L = 0$ and $\phi_R = 2\pi$, and as initial conditions we used (6.1.3) with $X_0 = 12.5$ and $v = 0.9$. It is possible to obtain the exact solution to this problem by considering a multi-soliton solution to (6.1.1) on the whole real line. Such a solution can be obtained using a Bäcklund transformation (see [11], [54]). However, the formulas quickly become complicated and, technically, one would have to consider an infinite number of solitons. Instead, we constructed a nearly exact solution by approximating the boundary interactions with (6.1.4):

$$\phi_{exact}(X,t) = \begin{cases} \phi_{SS}\big(X - X_{max}, t - (4n+1)T\big) + 2\pi & \text{if } t \in \big[4nT, (4n+2)T\big), \\ \phi_{SS}\big(X, t - (4n+3)T\big) & \text{if } t \in \big[(4n+2)T, (4n+4)T\big), \end{cases} \tag{6.3.1}$$

where n is an integer number, and T satisfies $\phi_{SS}(X_{max}/2, T) = \pi$ (we numerically found $T \approx 13.84$). Given how fast (6.1.3) and (6.1.4) approach its asymptotic values, one may check that (6.3.1) can be considered exact to machine precision.

We performed numerical integration with the constant time step $\Delta t = 0.01$ up to the time $T_{max} = 50$. For the control-theoretic strategy we used the 1-stage and 2-stage Gauss method (2-nd and 4-th order respectively), and the 2-stage and 3-stage Lobatto IIIA-IIIB method (also 2-nd/4-th order). For the Lagrange multiplier strategy we used the 2-stage and 3-stage Lobatto IIIA-IIIB method for constrained mechanical systems (2-nd/4-th order). See Section 2.2.2, Section 2.5.2, and [23], [24], [26] for more information about the mentioned symplectic Runge-Kutta methods. We used the constraints (3.2.8) based on the generalized arclength density (3.2.6). We chose the scaling parameter to be $\alpha = 2.5$, so that

approximately half of the available mesh points were concentrated in the area of high gradient. A few example solutions are presented in Figure 6.3.1-6.3.4. Note that the Lagrange multiplier strategy was able to accurately capture the motion of the soliton with merely 17 mesh points (that is, $N = 15$). The trajectories of the mesh points for several simulations are depicted in Figure 6.3.6 and Figure 6.3.7. An example solution computed on a uniform mesh is depicted in Figure 6.3.5.

For the convergence test, we performed simulations for several N in the range 15-127. For comparison, we also computed solutions on a uniform mesh for N in the range 15-361. The numerical solutions were compared against the solution (6.3.1). The L^∞ errors are depicted in Figure 6.3.8. The L^∞ norms were evaluated over all nodes and over all time steps. Note that in case of a uniform mesh the spacing between the nodes is $\Delta x = X_{max}/(N+1)$, therefore the errors are plotted versus $(N+1)$. The Lagrange multiplier strategy proved to be more accurate than the control-theoretic strategy. As the number of mesh points is increased, the uniform mesh solution becomes quadratically convergent, as expected, since we used linear finite elements for spatial discretization. The control-theoretic strategy also shows near quadratic convergence, whereas the Lagrange multiplier method seems to converge slightly slower. While there are very few analytical results regarding the convergence of r-adaptive methods, it has been observed that the rate of convergence depends on several factors, including the chosen mesh density function. Our results are consistent with the convergence rates reported in [2] and [67]. Both papers deal with the viscous Burgers' equation, but consider different initial conditions. Computations with the arclength density function converged only linearly in [2], but quadratically in [67].

Throughout all simulations the ratio $\kappa = \Delta X_{max}/\Delta X_{min}$ of the largest and smallest spacing between the mesh points was on average $\kappa \approx 12$, reaching $\kappa \approx 21$ when the soliton bounced off of the walls.

6.4 Energy conservation

As we pointed out in Section 2.2.3, the true power of variational and symplectic integrators for mechanical systems lies in their excellent conservation of energy and other integrals of motion, even when a big time step is used. In order to test the energy behavior of our methods, we performed simulations of the Sine-Gordon equation over longer time intervals.

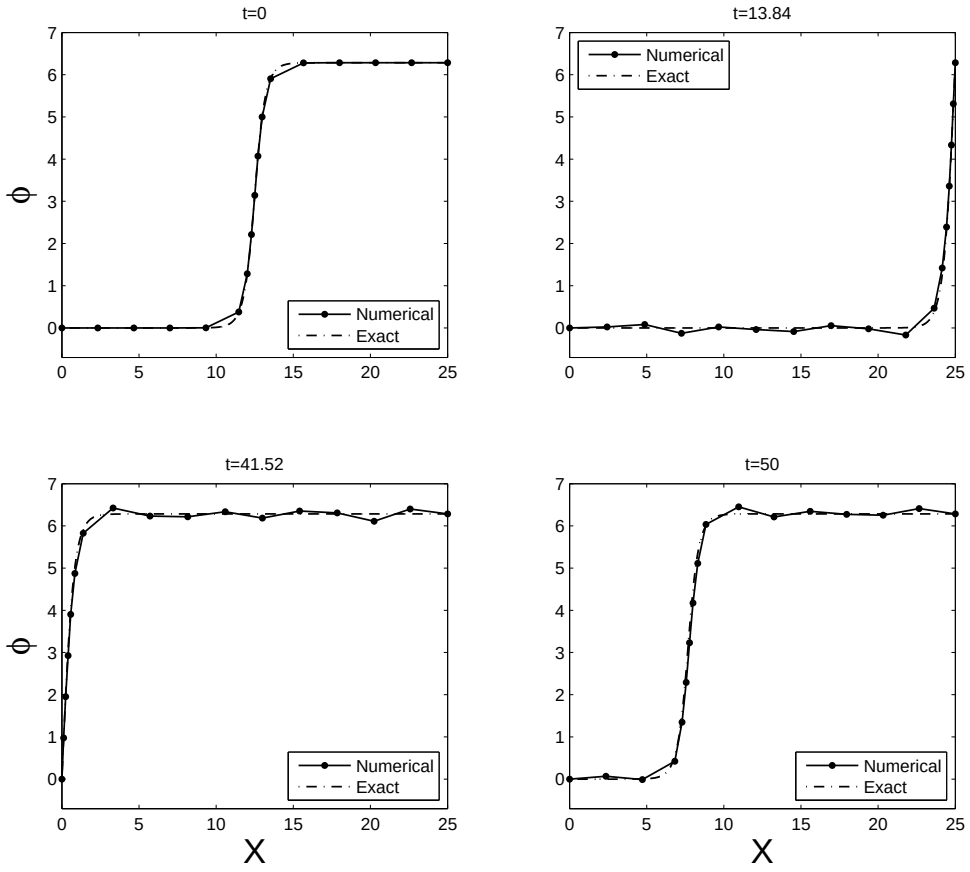

Figure 6.3.1: The single-soliton solution obtained with the Lagrange multiplier strategy for $N = 15$. Integration in time was performed using the 4-th order Lobatto IIIA-IIIB scheme for constrained mechanical systems. The soliton moves to the right with the initial velocity $v = 0.9$, bounces from the right wall at $t = 13.84$, and starts moving to the left wall with the velocity $v = -0.9$, from which it bounces at $t = 41.52$.

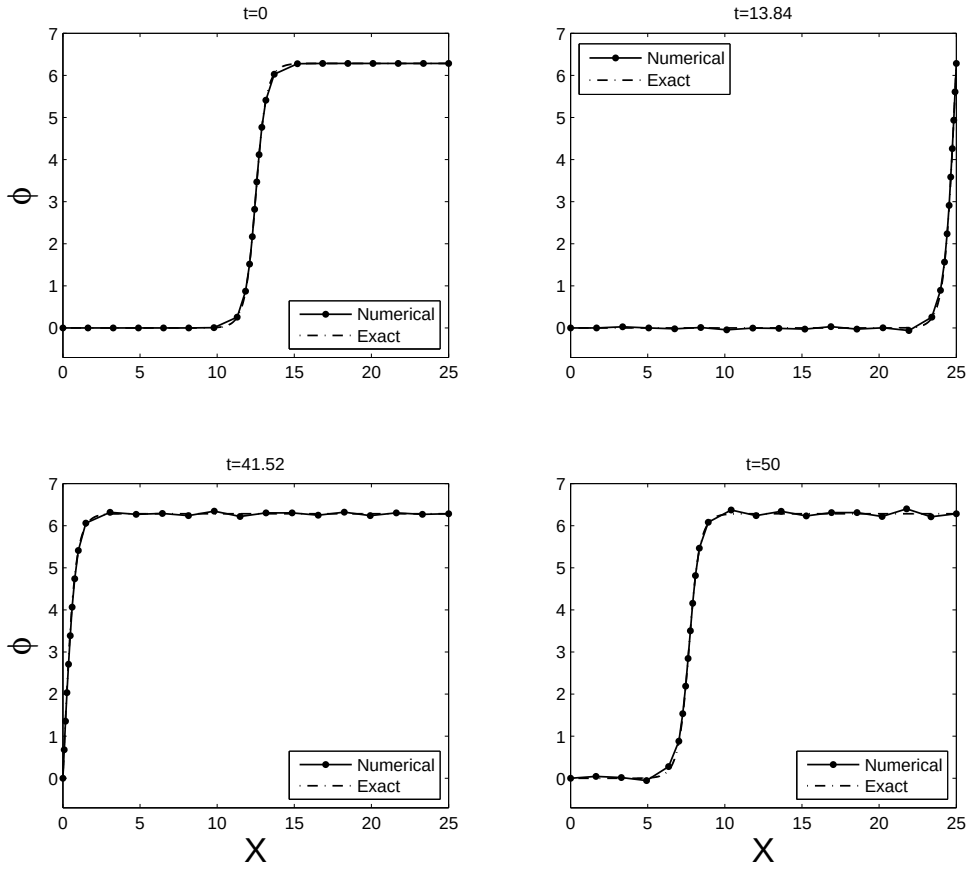

Figure 6.3.2: The single-soliton solution obtained with the Lagrange multiplier strategy for $N = 22$. Integration in time was performed using the 4-th order Lobatto IIIA-IIIB scheme for constrained mechanical systems.

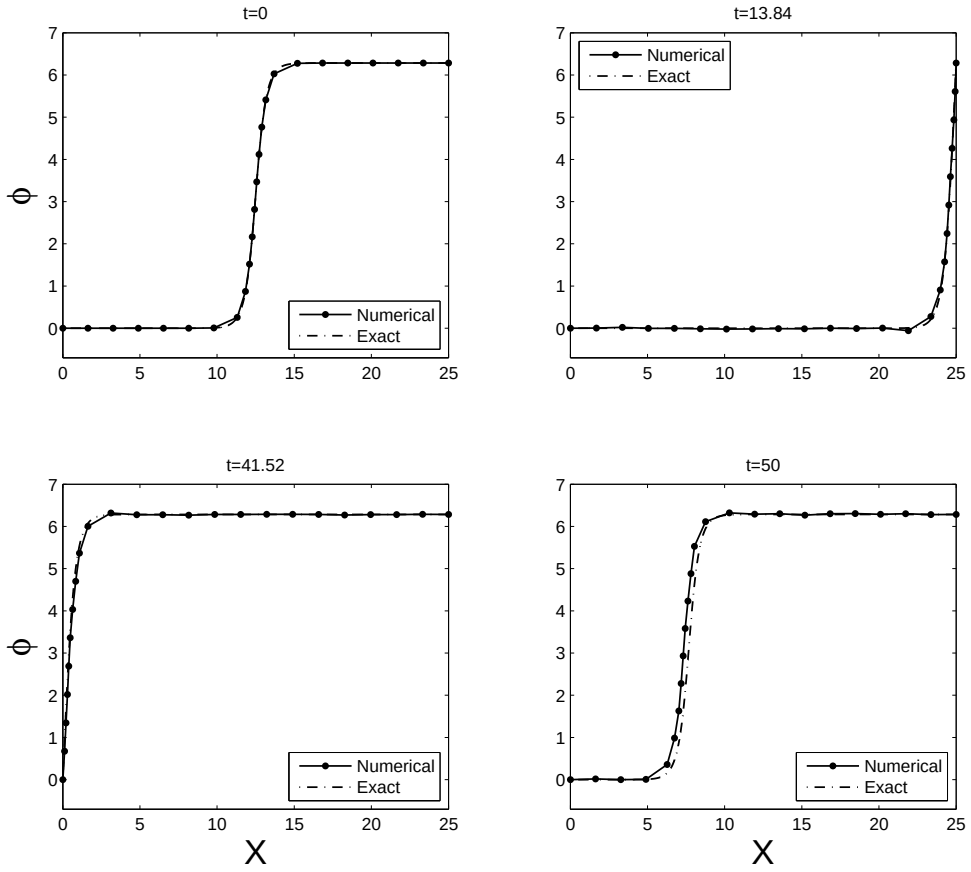

Figure 6.3.3: The single-soliton solution obtained with the control-theoretic strategy for $N = 22$. Integration in time was performed using the 4-th order Gauss scheme. Integration with the 4-th order Lobatto IIIA-IIIB yields a very similar level of accuracy.

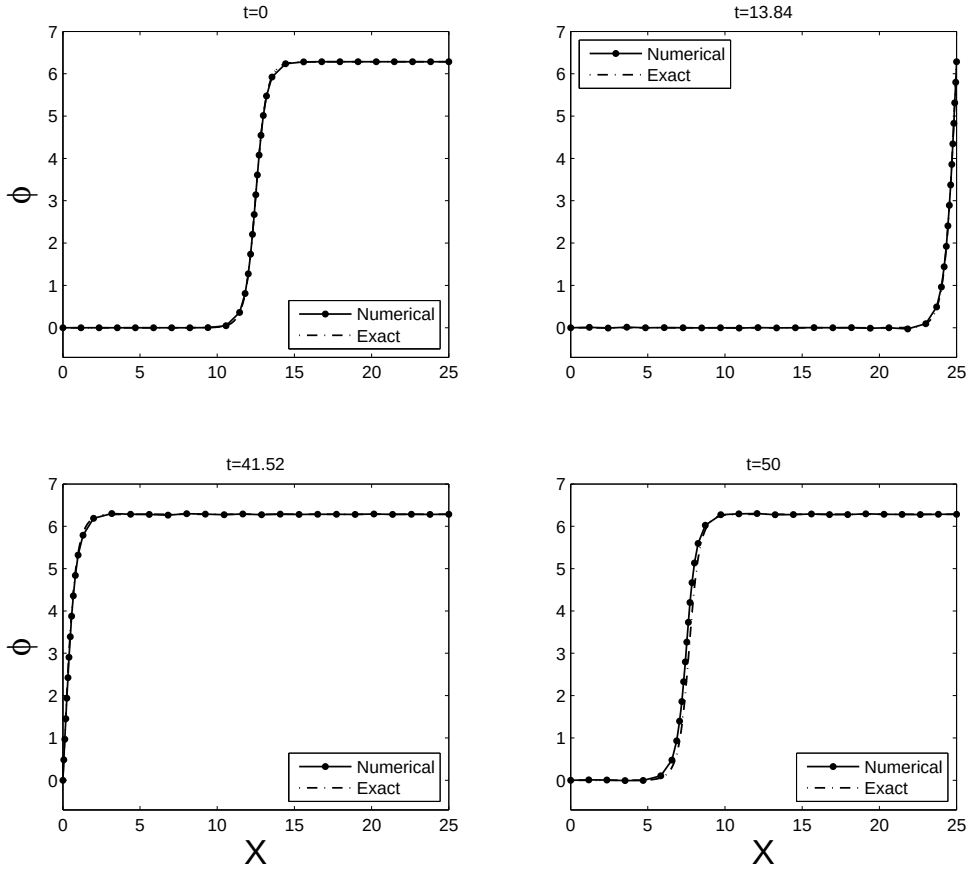

Figure 6.3.4: The single-soliton solution obtained with the control-theoretic strategy for $N = 31$. Integration in time was performed using the 4-th order Gauss scheme. Integration with the 4-th order Lobatto IIIA-IIIB yields a very similar level of accuracy.

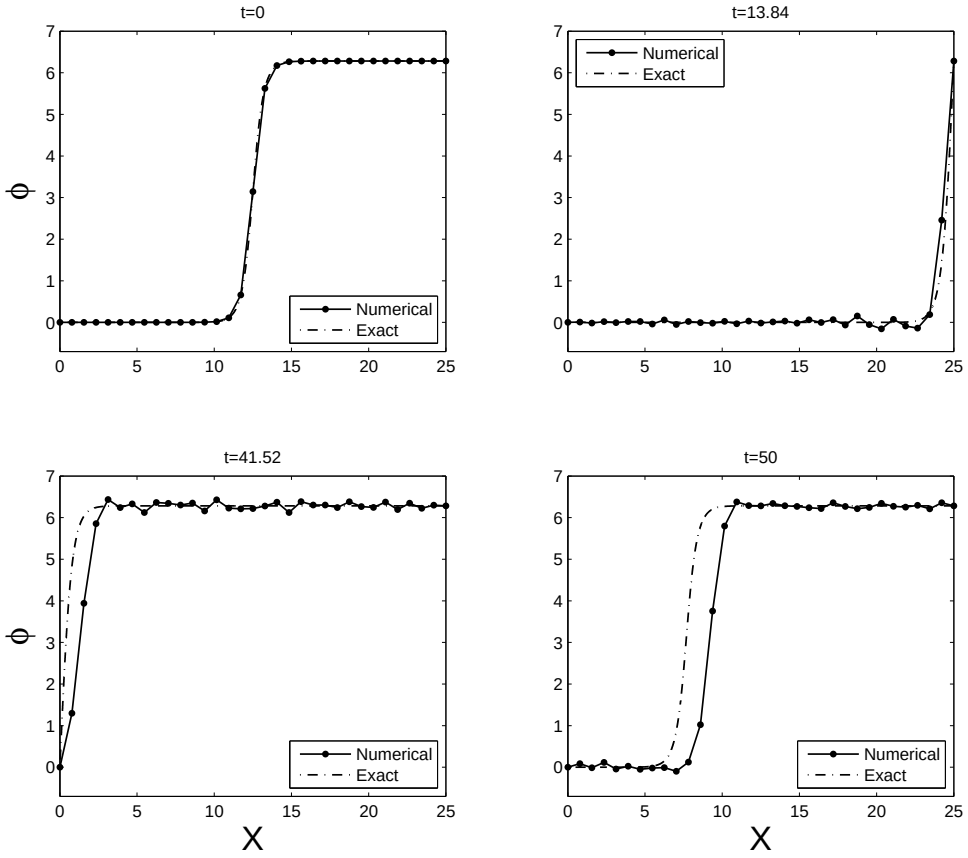

Figure 6.3.5: The single-soliton solution computed on a uniform mesh with $N = 31$. Integration in time was performed using the 4-th order Gauss scheme. Integration with the 4-th order Lobatto IIIA-IIIB yields a very similar level of accuracy.

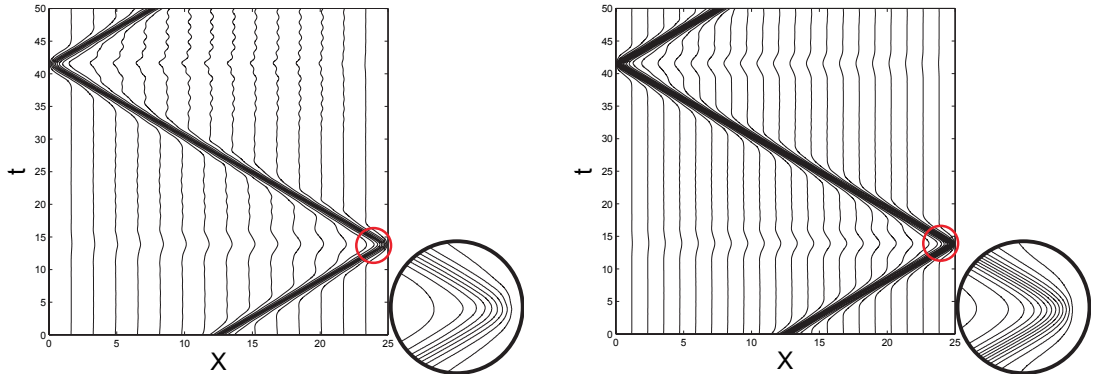

Figure 6.3.6: The mesh point trajectories (with zoomed-in insets) for the Lagrange multiplier strategy for $N = 22$ (left) and $N = 31$ (right). Integration in time was performed using the 4-th order Lobatto IIIA-IIIB scheme for constrained mechanical systems.

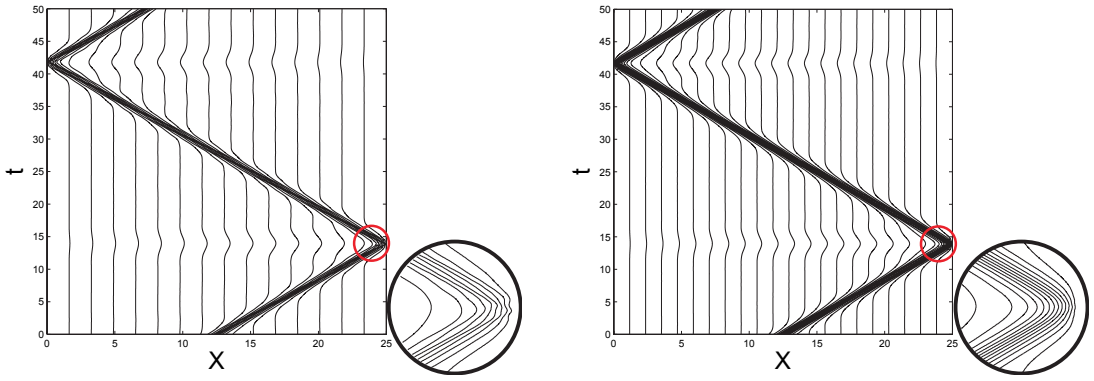

Figure 6.3.7: The mesh point trajectories (with zoomed-in insets) for the control-theoretic strategy for $N = 22$ (left) and $N = 31$ (right). Integration in time was performed using the 4-th order Gauss scheme. Integration with the 4-th order Lobatto IIIA-IIIB yields a very similar result.

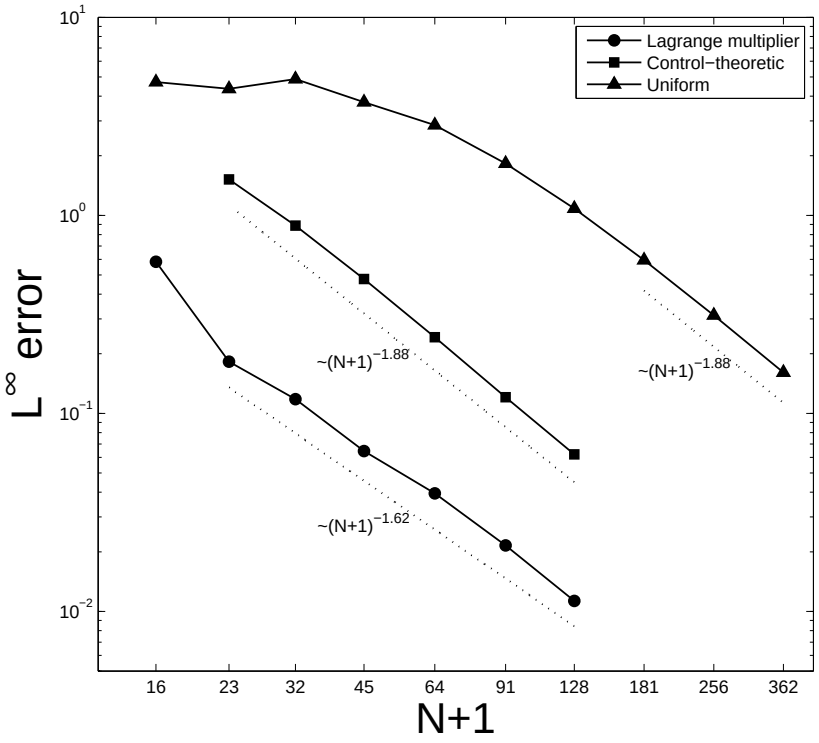

Figure 6.3.8: Comparison of the convergence rates of the discussed methods. Integration in time was performed using the 4-th order Lobatto IIIA-IIIB method for constrained systems in the case of the Lagrange multiplier strategy, and the 4-th order Gauss scheme in the case of both the control-theoretic strategy and the uniform mesh simulation. The 4-th order Lobatto IIIA-IIIB scheme for the control-theoretic strategy and the uniform mesh simulation yields a very similar level of accuracy. Also, using 2-nd order integrators gives very similar error plots.

We considered two solitons bouncing from each other and from two rigid walls at $X = 0$ and $X_{max} = 25$. We imposed the boundary conditions $\phi_L = -2\pi$ and $\phi_R = 2\pi$, and as initial conditions we used $\phi(X, 0) = \phi_{SS}(X - 12.5, -5)$ with $v = 0.9$. We ran our computations on a mesh consisting of 27 nodes ($N = 25$). Integration was performed with the time step $\Delta t = 0.05$, which is rather large for this type of simulations. The scaling parameter in (3.2.8) was set to $\alpha = 1.5$, so that approximately half of the available mesh points were concentrated in the areas of high gradient. An example solution is presented in Figure 6.4.1.

The exact energy of the two-soliton solution can be computed using (4.1.4). It is possible to compute that integral explicitly to obtain $E = 16/\sqrt{1 - v^2} \approx 36.71$. The energy associated with the semi-discrete Lagrangian (4.2.8) can be expressed by the formula

$$E_N = \frac{1}{2}\dot{q}^T \tilde{M}_N(q)\, \dot{q} + R_N(q), \tag{6.4.1}$$

where R_N was defined in (4.2.52), and for our Sine-Gordon system is given by

$$R_N(q) = \sum_{k=0}^{N} \left[\frac{1}{2}\left(\frac{y_{k+1} - y_k}{X_{k+1} - X_k} \right)^2 + 1 - \frac{\sin y_{k+1} - \sin y_k}{y_{k+1} - y_k} \right] (X_{k+1} - X_k), \tag{6.4.2}$$

and M_N is the mass matrix (4.2.11). The energy E_N is an approximation to (4.1.4) if the field $\phi(X, t)$ is sampled at the nodes $X_0, \ldots, X_{N+1}$, and then piecewise linearly approximated. In fact, for $N = 25$ and the initial conditions described above, we have the exact value $E_N \approx 35.58354$. We used a time discretization of (6.4.1) to compute the energy of our numerical solutions.

The energy plots for the Lagrange multiplier strategy are depicted in Figure 6.4.2. We can see that the energy stays nearly constant in the presented time interval, showing only mild oscillations, which are reduced as higher order of integration in time is used. The energy plots for the control-theoretic strategy are depicted in Figure 6.4.3. In this case the discrete energy is more erratic and not nearly as preserved. Moreover, the symplectic Gauss and Lobatto methods show virtually the same energy behavior as the non-symplectic Radau IIA method, which is known for its excellent stability properties when applied to stiff differential equations (see [26]). It seems that we do not gain much by performing symplectic integration in this case. It is consistent with our observations in Section 4.1.5, and shows that the control-theoretic strategy does not take full advantage of the underlying geometry.

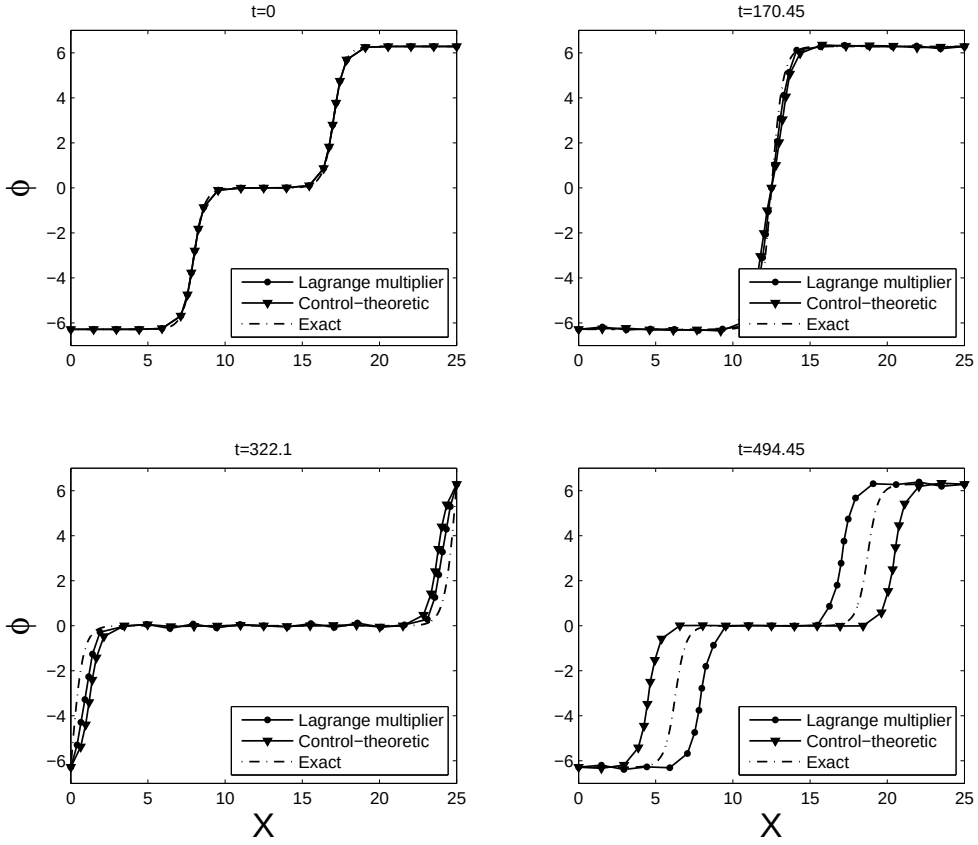

Figure 6.4.1: The two-soliton solution obtained with the control-theoretic and Lagrange multiplier strategies for $N = 25$. Integration in time was performed using the 4-th order Gauss quadrature for the control-theoretic approach, and the 4-th order Lobatto IIIA-IIIB quadrature for constrained mechanical systems in the case of the Lagrange multiplier approach. The solitons initially move towards each other with the velocities $v = 0.9$, then bounce off of each other at $t = 5$ and start moving towards the walls, from which they bounce at $t = 18.79$. The solitons bounce off of each other again at $t = 32.57$. This solution is periodic in time with the period $T_{period} = 27.57$. The nearly exact solution was constructed in a similar fashion as (6.3.1). As the simulation progresses, the Lagrange multiplier solution gets ahead of the exact solution, whereas the control-theoretic solution lags behind.

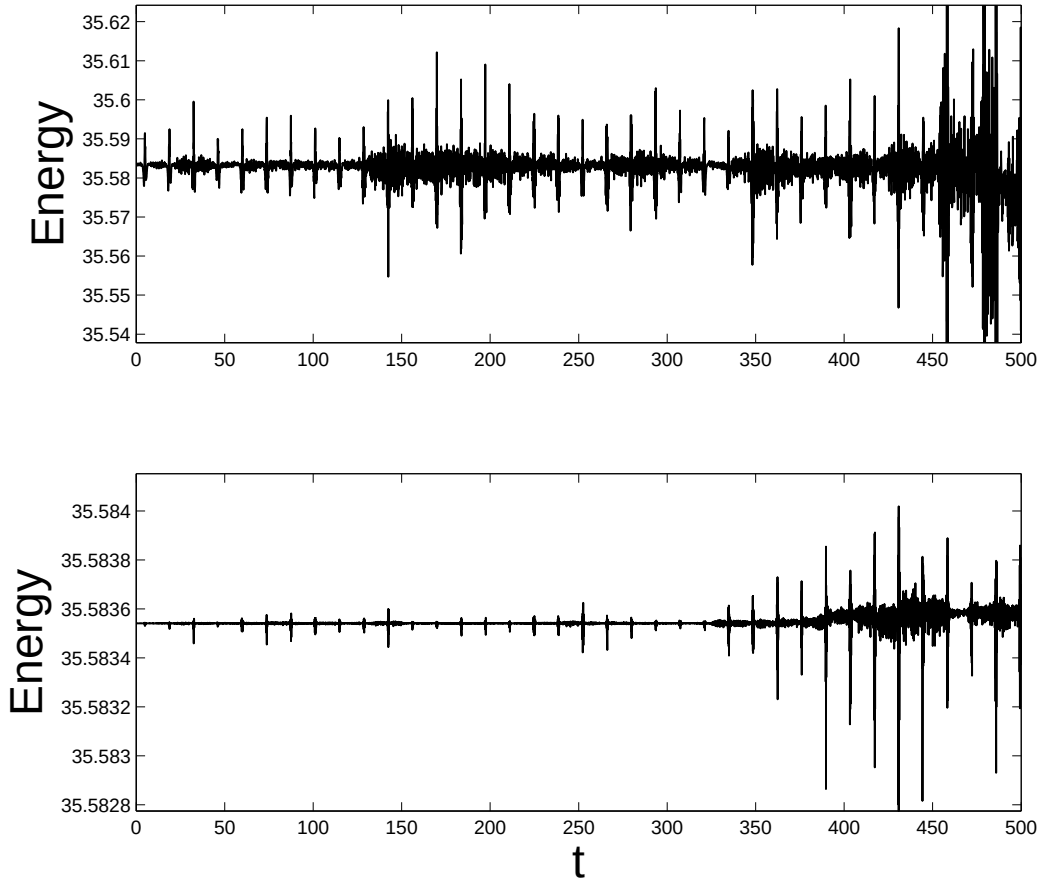

Figure 6.4.2: The discrete energy E_N for the Lagrange multiplier strategy. Integration in time was performed with the 2-nd (top) and 4-th (bottom) order Lobatto IIIA-IIIB method for constrained mechanical systems. The spikes correspond to the times when the solitons bounced off of each other or of the walls. Note that the numerical energy oscillates around the exact value $E_N \approx 35.58354$.

As we did not use adaptive time-stepping, and did not implement any mesh smoothing techniques (see Section 3.2.2), the quality of the mesh deteriorated with time in all the simulations, eventually leading to mesh crossing, i.e., two mesh points collapsing or crossing each other. The control-theoretic strategy, even though less accurate, retained good mesh quality longer, with the break-down time $T_{break} > 1000$, as opposed to $T_{break} \sim 600$ in the case of the Lagrange multiplier approach (both using a rather large constant time step). We discuss extensions to our approach for increased robustness in Chapter 8.

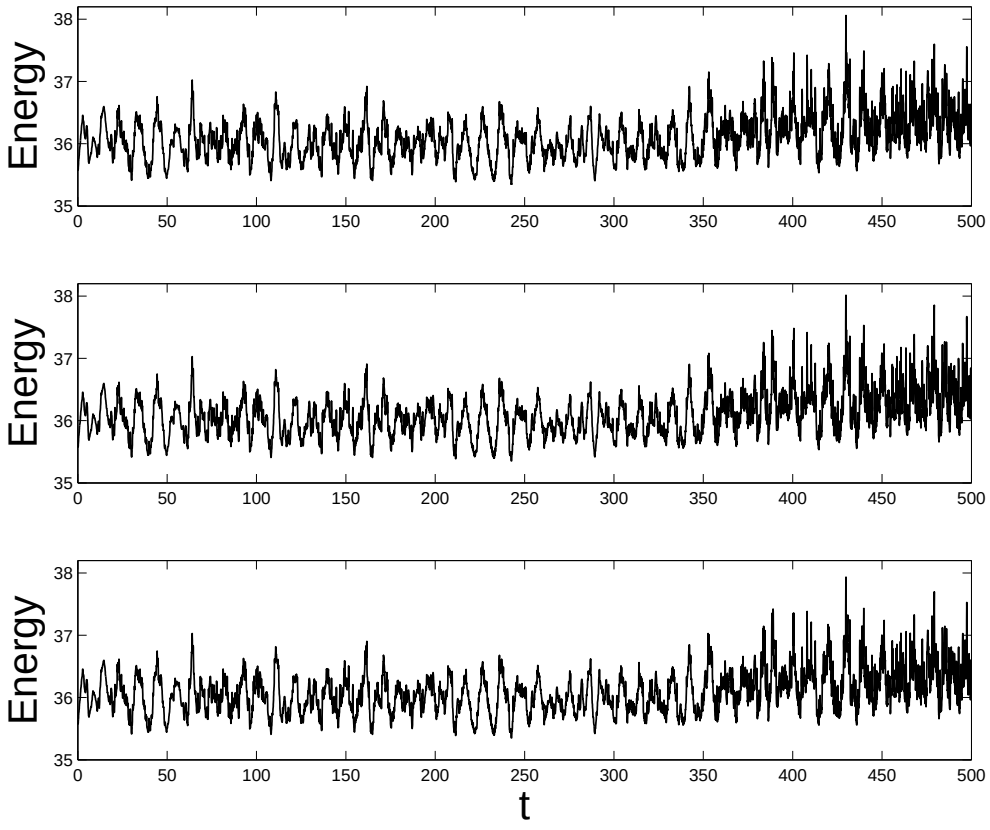

Figure 6.4.3: The discrete energy E_N for the control-theoretic strategy. Integration in time was performed with the 4-th order Gauss (top), 4-th order Lobatto IIIA-IIIB (middle), and non-symplectic 5-th order Radau IIA (bottom) methods.

6.5 Computational cost

The main goal of this work is to design space-adaptive variational integrators. We focused our attention on the analysis of the geometric aspects of such integrators, and their conservation and convergence properties. We were less concerned about the efficiency of our computations, and in fact we made little effort to optimize our codes. However, for completeness, in this section we present a preliminary analysis of the computational cost of our algorithms. We caution the reader that we implemented our algorithms in Mathematica 8.0.4.0. Nevertheless, each of our implementations used a very similar level of optimization, so we believe that our comparative cost analysis below is instructive.

We performed a cost analysis of the computations presented in Section 6.3. We investigated the average CPU time needed to perform one time step of the control-theoretic and Lagrange multiplier strategies, and the uniform mesh simulations. For concreteness we focused on the computations that used 4-th order integration in time. In the case of the Lagrange multiplier strategy, the most computationally expensive operation at each time step is solving the nonlinear system (2.5.11) corresponding to the augmented semi-discrete Lagrangian (4.2.60). For the control-theoretic strategy, at each time step one needs to solve the nonlinear system (4.1.18). Finally, in the case of the computations on a uniform mesh, the most expensive step is solving the nonlinear system (2.4.17). The average CPU times needed to perform those operations are depicted in Figure 6.5.1. We see that the computational time scales linearly with the number of mesh points N, as expected. The deviation from linearity for larger N is likely caused by Mathematica's memory management.

Even this simple analysis leads to interesting conclusions. The Lagrange multiplier strategy introduces additional variables and additional internal stages. As a consequence, the resulting nonlinear equations one needs to solve at each time step are much more complicated than in the case of uniform mesh computations. One could expect that this would make this approach too costly and inefficient. However, it turns out that the Lagrange multiplier strategy outperforms both the control-theoretic strategy and uniform mesh computations. The Lagrange multiplier strategy with $N = 15$ yields a similar level of accuracy as computations on a uniform mesh with $N = 180$ (cf. Figure 6.3.8). However, one step of the Lagrange multiplier strategy takes on average 0.5241s, whereas the uniform mesh simulation requires 1.1965s when the 4-th order Gauss method is used, and 1.6584s when the

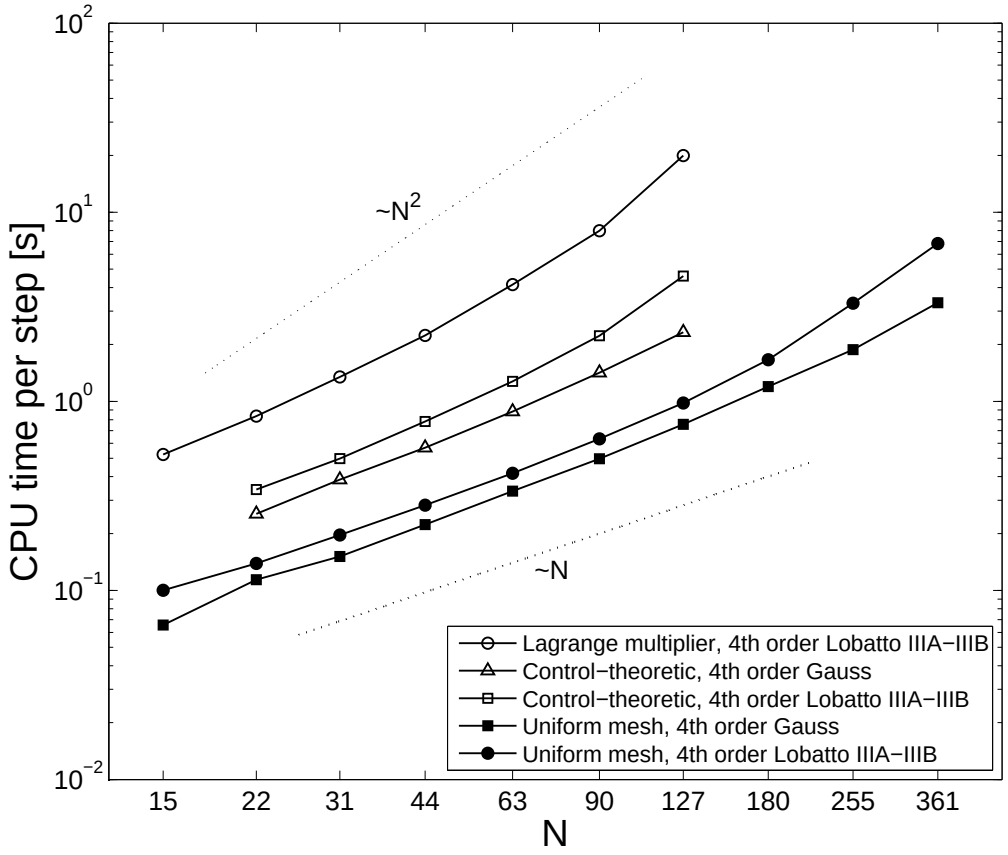

Figure 6.5.1: The average CPU time (in seconds) required to perform one time step of the computations.

4-th order Lobatto IIIA-IIIB method is used. Similarly, the Lagrange multiplier strategy with $N = 31$ yields a comparable level of accuracy as the control-theoretic strategy with $N = 90$. However, one step of the Lagrange multiplier strategy takes 1.3447s, whereas one step of the control-theoretic strategy requires 1.418s when the 4-th order Gauss method is used, and 2.2247s when the 4-th order Lobatto IIIA-IIIB method is used. The Lagrange multiplier strategy has the added benefit of nearly preserving energy. Let us also note that the control-theoretic strategy itself outperforms uniform mesh computations. For instance, for $N = 22$ the control theoretic strategy gives a more accurate solution than a uniform mesh simulation for $N = 90$, but one step of the control-theoretic strategy takes 0.2542s (4-th order Gauss) and 0.3417s (4-th order Lobatto IIIA-IIIB), whereas the uniform mesh simulation requires 0.4975s and 0.6333s, respectively.

We used Newton's method (by means of Mathematica's `FindRoot` function) to solve the aforementioned nonlinear systems of equations. The efficiency of the nonlinear solve can be greatly improved by using the simplified Newton iterations appropriate for implicit Runge-Kutta methods (see [26]) and by taking advantage of the banded structure of the Jacobians for the systems in question.

Chapter 7

Lagrangians linear in velocities

In Chapter 4 we proposed two general ways to construct r-adaptive variational integrators for Lagrangian field theories, but we specialized our considerations to Lagrangian densities of the form (4.2.6). As a result, the corresponding semi-discrete Lagrangian (4.2.8) was quadratic in velocities and non-degenerate almost everywhere, and consequently we were able to apply standard techniques of variational integration. There are, however, many interesting degenerate field theories whose Lagrangian densities are linear in ϕ_t, for instance the nonlinear Schrödinger, KdV, or Camassa-Holm equations. The semi-discrete Lagrangians for these theories will be linear in velocities, and little is known about variational integration of such systems (see [56], [65]). This is our main motivation for constructing higher-order variational integrators for Lagrangians linear in velocities. However, this topic is also interesting on its own, as there are many situations in which such Lagrangians arise—see Chapter 1. Therefore, even though related to the previous parts of the thesis, this chapter is independent and stands on its own.

Outline of the chapter

This chapter is organized as follows. In Section 7.1 we introduce a proper geometric setup and discuss the properties of systems linear in velocities which are important for further analysis of numerical integrators. In Section 7.2 we analyze the general properties of variational integrators and point out how the relevant theory differs from the non-degenerate case. In Section 7.3 we introduce variational partitioned Runge-Kutta methods and discuss their relation to numerical integration of differential-algebraic systems. In Section 7.4 we present the results of our numerical experiments for Kepler's problem, a system of two interacting vortices, and the Lotka-Volterra model.

7.1 Geometric setup

Let Q be the configuration manifold and TQ its tangent bundle. Throughout this chapter we will assume that the dimension of the configuration manifold $\dim Q = n$ is even. We will further assume Q is a vector space and by a slight abuse of notation we will denote by q both an element of Q and the vector of its coordinates $q = (q^1, \ldots, q^n)$ in a local chart on Q. It will be clear from the context which definition is invoked. Consider the Lagrangian $L : TQ \longrightarrow \mathbb{R}$ given by

$$L(v_q) = \langle \alpha, v_q \rangle - H(q), \tag{7.1.1}$$

where $\alpha : Q \longrightarrow T^*Q$ is a smooth one-form, $H : Q \longrightarrow \mathbb{R}$ is the Hamiltonian, and $v_q \in T_qQ$. Let $(q^\mu, \dot{q}^\mu)$ denote canonical coordinates on TQ, where $\mu = 1, \ldots, n$. In these coordinates we can consider

$$L(q, \dot{q}) = \alpha_\mu(q)\, \dot{q}^\mu - H(q), \tag{7.1.2}$$

where summation over repeated Greek indices is implied.

7.1.1 Equations of motion

The Lagrangian (7.1.1) is degenerate, since the associated Legendre transform (see Section 2.3)

$$\mathbb{F}L : TQ \ni v_q \longrightarrow \alpha_q \in T^*Q \tag{7.1.3}$$

is not invertible. The local representation of the Legendre transform is

$$\mathbb{F}L(q^\mu, \dot{q}^\mu) = \left(q^\mu, \frac{\partial L}{\partial \dot{q}^\mu} \right) = \big(q^\mu, \alpha_\mu(q) \big), \tag{7.1.4}$$

that is,

$$p_\mu = \alpha_\mu(q), \tag{7.1.5}$$

where (q^μ, p_μ) denote canonical coordinates on T^*Q. The dynamics is defined by the action

functional

$$S[q(t)] = \int_a^b L\big(q(t), \dot{q}(t)\big)\, dt \tag{7.1.6}$$

and Hamilton's principle, which seeks the curves $q(t)$ such that the functional $S[q(t)]$ is stationary under variations of $q(t)$ with fixed endpoints, i.e., we seek $q(t)$ such that

$$dS[q(t)] \cdot \delta q(t) = \frac{d}{d\epsilon}\bigg|_{\epsilon=0} S[q_\epsilon(t)] = 0 \tag{7.1.7}$$

for all $\delta q(t)$ with $\delta q(a) = \delta q(b) = 0$, where $q_\epsilon(t)$ is a smooth family of curves satisfying $q_0 = q$ and $\frac{d}{d\epsilon}\big|_{\epsilon=0} q_\epsilon = \delta q$. The resulting Euler-Lagrange equations

$$M_{\mu\nu}(q)\, \dot{q}^\nu = \partial_\mu H(q) \tag{7.1.8}$$

form a system of *first-order* ODEs, where we assume that the even-dimensional antisymmetric matrix $M_{\mu\nu}(q) = \partial_\mu \alpha_\nu(q) - \partial_\nu \alpha_\mu(q)$ is invertible for all $q \in Q$. Without loss of generality we can further assume that the coordinate mapping $p_\mu = \alpha_\mu(q)$ is invertible and the inverse is smooth: if the Jacobian $\partial \alpha_\mu / \partial q^\nu$ is singular, we can redefine $\alpha_\mu(q) \to \alpha_\mu(q) + b_\mu(q^\mu)$, where $b_\mu(q^\mu)$ are arbitrary functions; the Euler-Lagrange equations remain the same, and with the right choice of the functions $b_\mu(q^\mu)$ the redefined Jacobian can be made nonsingular. Let $B = M^{-1}$. Then (7.1.8) can be equivalently written as the Poisson system

$$\dot{q}^\mu = B^{\mu\nu}(q)\, \partial_\nu H(q). \tag{7.1.9}$$

The Euler-Lagrange equations (7.1.8) can also be formulated as the implicit 'Hamiltonian' system (see Section 2.3)

$$\begin{aligned} p_\mu &= \alpha_\mu(q), \\ \dot{p}_\mu &= \partial_\mu \alpha_\nu(q)\, \dot{q}^\nu - \partial_\mu H(q). \end{aligned} \tag{7.1.10}$$

Since the Lagrangian L is degenerate, (7.1.10) is an index 1 DAE system, rather than a Hamiltonian ODE system: the Legendre transform is an algebraic equation and has to be

differentiated once with respect to time in order to turn this system into (7.1.8). This reflects the fact that the evolution of the considered degenerate system takes place on the *primary constraint* $N = \mathbb{F}L(TQ) \subsetneq T^*Q$. It is easy to see that the primary constraint N is (locally) diffeomorphic to the configuration manifold Q, where the diffeomorphism $\eta : Q \ni q \longrightarrow \alpha_q \in N$ is locally, in the coordinates on T^*Q, given by

$$\eta(q) = (q, \alpha(q)), \tag{7.1.11}$$

where by a slight abuse of notation $\alpha(q) = (\alpha_1(q), \ldots, \alpha_n(q))$. This shows that q^μ can also be used as local coordinates on N. Note that η is simply the restriction of α to N, i.e., $\eta = \alpha|_{Q \longrightarrow N}$.

7.1.2 Symplectic forms

The spaces Q, TQ, T^*Q and N can be equipped with several symplectic or pre-symplectic forms. It is instructive to investigate the relationships between them in order to later avoid confusion regarding the sense in which variational integrators for Lagrangians linear in velocities are symplectic. On the configuration space Q we can define the two-form

$$\Omega = -d\alpha, \tag{7.1.12}$$

which in local coordinates can be expressed as

$$\Omega = -d\alpha_\mu \wedge dq^\mu = -M_{\mu\nu}(q)\, dq^\mu \otimes dq^\nu. \tag{7.1.13}$$

The two-form Ω is symplectic if it is nondegenerate, i.e., if the matrix $M_{\mu\nu}$ is invertible for all q.

The cotangent bundle T^*Q is equipped with the canonical Cartan one-form $\tilde{\Theta} : T^*Q \longrightarrow T^*T^*Q$, which is intrinsically defined by the formula (see Section 2.1)

$$\tilde{\Theta}(\omega) = (\pi_{T^*Q})^* \omega \tag{7.1.14}$$

for any $\omega \in T^*Q$, where $\pi_{T^*Q} : T^*Q \longrightarrow Q$ is the cotangent bundle projection. In canonical coordinates we have

$$\tilde{\Theta} = p_\mu dq^\mu. \tag{7.1.15}$$

We further have the canonical symplectic two-form

$$\tilde{\Omega} = -d\tilde{\Theta} = dq^\mu \wedge dp_\mu. \tag{7.1.16}$$

The symplectic forms Ω and $\tilde{\Omega}$ are related by

$$\Omega = \alpha^* \tilde{\Omega}. \tag{7.1.17}$$

This follows from the simple calculation

$$\alpha^* \tilde{\Theta} \cdot v_q = \tilde{\Theta}(\alpha_q) \cdot T\alpha(v_q) = \alpha_q \cdot T\pi_{T^*Q} \circ T\alpha(v_q) = \alpha_q \cdot T(\pi_{T^*Q} \circ \alpha)(v_q) = \alpha_q \cdot v_q, \tag{7.1.18}$$

where we used (7.1.14) and the fact that $\pi_{T^*Q} \circ \alpha = \mathrm{id}_Q$. Hence $\alpha^* \tilde{\Theta} = \alpha$, and taking the exterior derivative on both sides we obtain (7.1.17).

Using the Legendre transform (7.1.3) we can define the Lagrangian two-form $\tilde{\Omega}_L$ on TQ by $\tilde{\Omega}_L = \mathbb{F}L^* \tilde{\Omega}$ (see Section 2.3), which in canonical coordinates $(q^\mu, \dot{q}^\mu)$ is given by

$$\tilde{\Omega}_L = dq^\mu \wedge d\alpha_\mu = -M_{\mu\nu}(q)\, dq^\mu \otimes dq^\nu. \tag{7.1.19}$$

The Lagrangian form $\tilde{\Omega}_L$ is only pre-symplectic, because it is degenerate. Noting that $\mathbb{F}L = \alpha \circ \pi_{TQ}$, where $\pi_{TQ} : TQ \longrightarrow Q$ is the tangent bundle projection, we can relate Ω and $\tilde{\Omega}_L$ through the formula

$$\tilde{\Omega}_L = (\pi_{TQ})^* \alpha^* \tilde{\Omega} = (\pi_{TQ})^* \Omega. \tag{7.1.20}$$

The symplectic structure on N can be introduced in two ways: by pushing forward Ω from Q, or pulling back $\tilde{\Omega}$ from T^*Q. Both ways are equivalent

$$\tilde{\Omega}_N = \eta_* \Omega = i^* \tilde{\Omega}, \tag{7.1.21}$$

where $i : N \longrightarrow T^*Q$ is the inclusion map. This follows from the calculation

$$\eta_* \Omega = (\eta^{-1})^* \alpha^* \tilde{\Omega} = (\alpha \circ \eta^{-1})^* \tilde{\Omega} = i^* \tilde{\Omega}, \tag{7.1.22}$$

where we used $\alpha = i \circ \eta$. If we use q^μ as coordinates on N, then the local representation of $\tilde{\Omega}_N$ will be given by (7.1.13).

7.1.3 Symplectic flows

Let $\varphi_t : Q \longrightarrow Q$ denote the flow of (7.1.8) or (7.1.9). This flow is symplectic on Q, that is

$$\varphi_t^* \Omega = \Omega. \tag{7.1.23}$$

This fact can be proven by considering the Hamiltonian or Poisson properties of Equation (7.1.8) or Equation (7.1.9) (see [23], [38]). It also follows directly from the action principle (7.1.7) (see [56]).

Since the Lagrangian (7.1.1) is degenerate, the dynamics of the system is defined on Q rather than TQ. However, we can obtain the associated flow on TQ through lifting φ_t by its tangent map $T\varphi_t : TQ \longrightarrow TQ$. This flow preserves the Lagrangian two-form

$$(T\varphi_t)^* \tilde{\Omega}_L = \tilde{\Omega}_L. \tag{7.1.24}$$

This can be seen from the calculation

$$(T\varphi_t)^* \tilde{\Omega}_L = (T\varphi_t)^* (\pi_{TQ})^* \Omega = (\pi_{TQ} \circ T\varphi_t)^* \Omega = (\varphi_t \circ \pi_{TQ})^* \Omega = (\pi_{TQ})^* \varphi_t^* \Omega = \tilde{\Omega}_L, \tag{7.1.25}$$

where we used (7.1.20), (7.1.23), and the property $\pi_{TQ} \circ T\varphi_t = \varphi_t \circ \pi_{TQ}$.

The flow φ_t induces the flow $\tilde{\varphi}_t : N \longrightarrow N$ in a natural way as

$$\tilde{\varphi}_t = \eta \circ \varphi_t \circ \eta^{-1}. \tag{7.1.26}$$

This flow is symplectic on N, i.e.,

$$\tilde{\varphi}_t^* \tilde{\Omega}_N = \tilde{\Omega}_N, \tag{7.1.27}$$

which can be established through the simple calculation

$$\tilde{\varphi}_t^* \tilde{\Omega}_N = (\eta \circ \varphi_t \circ \eta^{-1})^* \eta_* \Omega = (\eta^{-1})^* \varphi_t^* \eta^* (\eta^{-1})^* \Omega = \eta_* \varphi_t^* \Omega = \tilde{\Omega}_N, \tag{7.1.28}$$

where we used (7.1.21) and (7.1.23). The flow $\tilde{\varphi}_t$ can be interpreted as the symplectic flow for the 'Hamiltonian' DAE (7.1.10).

7.2 Veselov discretization and Discrete Mechanics

7.2.1 Discrete Mechanics and exact discrete Lagrangian

For a Veselov-type discretization we consider the discrete state space $Q \times Q$, as discussed in Section 2.4.1. Suppose we have a regular discrete Lagrangian $L_d : Q \times Q \longrightarrow \mathbb{R}$. Then the evolution of the discrete system is governed by the discrete Euler-Lagrange equations (2.4.2).

To relate discrete and continuous mechanics it is necessary to introduce a timestep $h \in \mathbb{R}$. If the continuous Lagrangian L is non-degenerate, it is possible to define a particular choice of discrete Lagrangian which gives an exact correspondence between discrete and continuous systems (see Section 2.4.2 and [41]), the so-called *exact discrete Lagrangian*

$$L_d^E(q, \bar{q}) = \int_0^h L\big(q_E(t), \dot{q}_E(t)\big)\, dt, \tag{7.2.1}$$

where $q_E(t)$ is the solution to the continuous Euler-Lagrange equations associated with L such that it satisfies the boundary conditions $q_E(0) = q$ and $q_E(h) = \bar{q}$. Note, however, that in the case of a regular Lagrangian the associated Euler-Lagrange equations are second order, therefore boundary value problems are solvable, at least for sufficiently small h and $\bar{q}$ sufficiently close to q. In the case of the Lagrangian (7.1.1) the associated Euler-Lagrange equations (7.1.8) are first order in time, therefore we have the freedom to choose an initial condition either at $t = 0$ or $t = h$, but not both. An exact discrete Lagrangian analogous to (7.2.1) cannot thus be defined on whole $Q \times Q$. We will therefore assume the following definition:

Definition 7.2.1. *Let* $\Gamma(\varphi_h) = \big\{\big(q, \varphi_h(q)\big) \in Q \times Q\big\}$ *be the graph of* φ_h. *The exact discrete Lagrangian* $L_d^E : \Gamma(\varphi_h) \longrightarrow \mathbb{R}$ *for the Lagrangian* (7.1.1) *is*

$$L_d^E(q,\bar{q}) = \int_0^h L\big(q_E(t),\dot{q}_E(t)\big)\,dt, \tag{7.2.2}$$

where $q_E(t)$ *is the solution to* (7.1.8) *that satisfies the initial condition* $q_E(0) = q$.

Note that in this definition we automatically have $q_E(h) = \bar{q}$.

7.2.2 Singular perturbation problem

As mentioned, the purpose of introducing an exact discrete Lagrangian is to establish an exact correspondence between the continuous and discrete systems. For a regular Lagrangian L and its exact discrete Lagrangian L_d^E, one can show that the exact discrete Hamiltonian map $\tilde{F}_{L_d^E}$ is equal to $\tilde{\varphi}_h$, where $\tilde{\varphi}_t$ is the symplectic flow for the Hamiltonian system associated with L (cf. Theorem 2.4.3). The problem is that the exact discrete Lagrangian (7.2.2) is not defined on the whole space $Q \times Q$, so the discrete Euler-Lagrange equations (2.4.2) do not make sense, and it is not entirely clear how to define the associated discrete Lagrangian map $F_{L_d^E}$. One possible way to deal with this issue is to consider a singular perturbation problem. Assume that Q is a Riemannian manifold equipped with the nondegenerate scalar product $\langle\!\langle .,. \rangle\!\rangle$. Define the ϵ-regularized Lagrangian

$$L^\epsilon(v_q) = \frac{\epsilon}{2}\langle\!\langle v_q, v_q \rangle\!\rangle + \langle \alpha, v_q \rangle - H(q), \tag{7.2.3}$$

or in coordinates

$$L^\epsilon(q,\dot{q}) = \frac{\epsilon}{2}\, g_{\mu\nu}\,\dot{q}^\mu\,\dot{q}^\nu + \alpha_\mu(q)\,\dot{q}^\mu - H(q), \tag{7.2.4}$$

where $g_{\mu\nu}$ denotes the local coordinates of the metric tensor. Without loss of generality assume that in the chosen coordinates $g_{\mu\mu} = 1$ and $g_{\mu\nu} = 0$ if $\mu \neq \nu$. For $\epsilon > 0$ this Lagrangian is nondegenerate and the Legendre transform $\mathbb{F}L^\epsilon : TQ \longrightarrow T^*Q$ is given by

$$\mathbb{F}L(q^\mu,\dot{q}^\mu) = \big(q^\mu, g_{\mu\nu}\,\dot{q}^\nu + \alpha_\mu(q)\big), \tag{7.2.5}$$

that is,

$$p_\mu = \epsilon\, g_{\mu\nu}\, \dot{q}^\nu + \alpha_\mu(q). \tag{7.2.6}$$

The Euler-Lagrange equations

$$\epsilon\, g_{\mu\nu}\, \ddot{q}^\nu = M_{\mu\nu}(q)\, \dot{q}^\nu - \partial_\mu H(q) \tag{7.2.7}$$

are second order. The corresponding Hamiltonian equations (in implicit form; see Section 2.3) are

$$\begin{aligned} p_\mu &= \epsilon\, g_{\mu\nu}\, \dot{q}^\nu + \alpha_\mu(q), \\ \dot{p}_\mu &= \partial_\mu \alpha_\nu(q)\, \dot{q}^\nu - \partial_\mu H(q). \end{aligned} \tag{7.2.8}$$

There is no reason to expect that the solutions of (7.2.7) or (7.2.8) unconditionally approximate the solutions of (7.1.8) or (7.1.10), respectively. The equations (7.2.8) form a system of first-order ordinary differential equations, and therefore it is possible to specify arbitrary initial conditions $q(0) = q_{init}$ and $p(0) = p_{init}$, whereas initial conditions for (7.1.10) have to satisfy the algebraic constraint $p_{init} = \alpha(q_{init})$. Under certain restrictive analytic assumptions, for some singular perturbation problems it is possible to show that, in order to satisfy the initial conditions, the solutions initially develop a steep boundary layer, but then rapidly converge to the solution of the corresponding DAE system (see [26]). On the other hand, for other singular perturbation problems, when the initial conditions do not satisfy the algebraic constraint, it may happen that the solutions do not converge to the solution of the DAE, but instead rapidly oscillate (see [37], [53]). We expect the latter behavior for (7.2.8), as will be demonstrated by a simple example in Section 7.2.4. Since our main goal here is to show how the notion of a discrete Legendre transform can be introduced for the exact discrete Lagrangian (7.2.2), we will make two intuitive, although nontrivial, assumptions. We refer the interested reader to [26] and [37] for techniques that can be used to prove these statements rigorously.

Assumption 7.2.2. *Let* $\big(q(t), p(t)\big)$ *and* $\big(q^\epsilon(t), p^\epsilon(t)\big)$ *be the unique smooth solutions of* (7.1.10) *and* (7.2.8) *on the interval* $[0, T]$ *satisfying the initial conditions* $q(0) = q_{init}$, $q^\epsilon(0) =$

q_{init}, and $p^\epsilon(0) = p_{init}$, where $p_{init} = \alpha(q_{init})$. Then $q^\epsilon(t) \longrightarrow q(t)$, $p^\epsilon(t) \longrightarrow p(t)$ and $\dot{q}^\epsilon(t) \longrightarrow \dot{q}(t)$, $\dot{p}^\epsilon(t) \longrightarrow \dot{p}(t)$ uniformly on $[0,T]$ as $\epsilon \longrightarrow 0^+$.

Assumption 7.2.3. *Let $q(t)$ be the unique smooth solution of (7.1.8) on the interval $[0,T]$ satisfying the initial condition $q(0) = q_{init}$, and let $q^\epsilon(t)$ be the unique smooth solution of (7.2.7) on the interval $[0,T]$ satisfying the boundary conditions $q^\epsilon(0) = q_{init}$, $q^\epsilon(T) = q_{final}$, where $q_{final} = q(T)$. Then $q^\epsilon(t) \longrightarrow q(t)$ and $\dot{q}^\epsilon(t) \longrightarrow \dot{q}(t)$ uniformly on $[0,T]$ as $\epsilon \longrightarrow 0^+$.*

With these assumption one can easily see that

$$L_d^E(q,\bar{q}) = \lim_{\epsilon\to 0^+} L_d^{\epsilon,E}(q,\bar{q}), \tag{7.2.9}$$

where $L_d^{\epsilon,E}$ is the exact discrete Lagrangian for (7.2.3).

7.2.3 Exact discrete Legendre Transform

Since L^ϵ is regular, $L_d^{\epsilon,E}$ is properly defined on the whole space $Q \times Q$ (or at least in a neighborhood of $\Gamma(\varphi_h)$) and the associated exact discrete Legendre transforms satisfy the properties (see Section 2.4.3 and [41])

$$\begin{aligned}
\mathbb{F}^+ L_d^{\epsilon,E}(q,\bar{q}) &= \mathbb{F}L^\epsilon\big(q_E^\epsilon(h), \dot{q}_E^\epsilon(h)\big) = (\bar{q}, \epsilon\dot{\bar{q}}^\epsilon + \alpha(\bar{q})),\\
\mathbb{F}^- L_d^{\epsilon,E}(q,\bar{q}) &= \mathbb{F}L^\epsilon\big(q_E^\epsilon(0), \dot{q}_E^\epsilon(0)\big) = (q, \epsilon\dot{q}^\epsilon + \alpha(q)),
\end{aligned} \tag{7.2.10}$$

where $q_E^\epsilon(t)$ is the solution to the regularized Euler-Lagrange equations (7.2.7) satisfying the boundary conditions $q_E^\epsilon(0) = q$ and $q_E^\epsilon(h) = \bar{q}$, and we denoted $\dot{q}^\epsilon = \dot{q}_E^\epsilon(0)$, $\dot{\bar{q}}^\epsilon = \dot{q}_E^\epsilon(h)$. In the spirit of (7.2.9), we can assume the following definitions of the exact discrete Legendre transforms $\mathbb{F}^\pm L_d^E : \Gamma(\varphi_h) \longrightarrow T^*Q$

$$\begin{aligned}
\mathbb{F}^+ L_d^E(q,\bar{q}) &= \lim_{\epsilon\to 0^+} \mathbb{F}^+ L_d^{\epsilon,E}(q,\bar{q}) = (\bar{q}, \alpha(\bar{q})),\\
\mathbb{F}^- L_d^E(q,\bar{q}) &= \lim_{\epsilon\to 0^+} \mathbb{F}^- L_d^{\epsilon,E}(q,\bar{q}) = (q, \alpha(q)),
\end{aligned} \tag{7.2.11}$$

where $\epsilon\dot{q}^\epsilon \longrightarrow 0$ and $\epsilon\dot{\bar{q}}^\epsilon \longrightarrow 0$ by uniform convergence of $\dot{q}_E^\epsilon(t)$. Note that $\mathbb{F}^\pm L_d^E = \alpha \circ \pi^\pm$, where $\pi^+ : \Gamma(\varphi_h) \ni (q,\bar{q}) \longrightarrow \bar{q} \in Q$ and $\pi^- : \Gamma(\varphi_h) \ni (q,\bar{q}) \longrightarrow q \in Q$ are projections (both

$\pi^{\pm}$ are diffeomorphisms). This is a close analogy to $\mathbb{F}L = \alpha \circ \pi_{TQ}$ (see Section 7.1). We also note the property

$$\begin{aligned} \mathbb{F}^{+}L_d^E(q,\bar{q}) &= \mathbb{F}L\big(q_E(h), \dot{q}_E(h)\big), \\ \mathbb{F}^{-}L_d^E(q,\bar{q}) &= \mathbb{F}L\big(q_E(0), \dot{q}_E(0)\big), \end{aligned} \tag{7.2.12}$$

where $q_E(t)$ is the solution of (7.1.8) satisfying the initial condition $q_E(0) = q$. This further indicates that our definition of the exact discrete Legendre transforms is sensible. Note that $\mathbb{F}^{\pm}L_d^E(\Gamma(\varphi_h)) = N$. It is convenient to redefine $\mathbb{F}^{\pm}L_d^E : \Gamma(\varphi_h) \longrightarrow N$, that is, $\mathbb{F}^{\pm}L_d^E = \eta \circ \pi^{\pm}$, so that both transforms are diffeomorphisms between $\Gamma(\varphi_h)$ and N.

The discrete Euler-Lagrange equations for L_d^E can be obtained as the limit of the discrete Euler-Lagrange equations for $L_d^{\epsilon,E}$, that is, one can substitute $L_d^{\epsilon,E}$ in (2.4.5) and take the limit $\epsilon \longrightarrow 0^+$ on both sides to obtain

$$\mathbb{F}^{+}L_d^E(q_{k-1}, q_k) = \mathbb{F}^{-}L_d^E(q_k, q_{k+1}). \tag{7.2.13}$$

This equation implicitly defines the exact discrete Lagrangian map $F_{L_d^E} : \Gamma(\varphi_h) \ni (q_{k-1}, q_k) \longrightarrow (q_k, q_{k+1}) \in \Gamma(\varphi_h)$, which, given our definitions, necessarily takes the form $F_{L_d^E}(q_{k-1}, q_k) = (q_k, \varphi_h(q_k))$. Using the discrete Legendre transforms $\mathbb{F}^{\pm}L_d^E$, we can define the corresponding exact discrete 'Hamiltonian' map $\tilde{F}_{L_d^E} : N \longrightarrow N$ as $\tilde{F}_{L_d^E} = \mathbb{F}^{\pm}L_d^E \circ F_{L_d^E} \circ (\mathbb{F}^{\pm}L_d^E)^{-1}$. The simple calculation

$$\tilde{F}_{L_d^E} = \eta \circ \pi^{\pm} \circ F_{L_d^E} \circ (\pi^{\pm})^{-1} \circ \eta^{-1} = \eta \circ \varphi_h \circ \eta^{-1} = \tilde{\varphi}_h \tag{7.2.14}$$

shows that the discrete 'Hamiltonian' map associated with the exact discrete Lagrangian L_d^E is equal to the 'Hamiltonian' flow $\tilde{\varphi}_h$ for (7.1.10), i.e., the evolution of the discrete systems described by L_d^E coincides with the evolution of the continuous system described by L at times $t_k = kh$, $k = 0, 1, 2, \ldots$

7.2.4 Example

Let us illustrate these ideas with a very simple example for which analytic solutions are known. Let $Q = \mathbb{R}^2$ and let (x, y) denote local coordinates on Q. The tangent bundle is

$TQ = \mathbb{R}^2 \times \mathbb{R}^2$, and the induced local coordinates are $(x, y, \dot{x}, \dot{y})$. Consider the Lagrangian

$$L(x, y, \dot{x}, \dot{y}) = \frac{1}{2} y\dot{x} - \frac{1}{2} x\dot{y}. \tag{7.2.15}$$

The corresponding Euler-Lagrange equations (7.1.8) are simply

$$\begin{aligned} \dot{x} &= 0, \\ \dot{y} &= 0, \end{aligned} \tag{7.2.16}$$

so the flow $\varphi_t : Q \longrightarrow Q$ is the identity, i.e., $\varphi_t(x, y) = (x, y)$. Let (x, y, p_x, p_y) denote canonical coordinates on the cotangent bundle $T^*Q \cong \mathbb{R}^2 \times \mathbb{R}^2$. The Legendre transform is

$$\mathbb{F}L(x, y, \dot{x}, \dot{y}) = \Big(x, y, \frac{1}{2} y, -\frac{1}{2} x\Big). \tag{7.2.17}$$

Let h be a timestep. Note $\Gamma(\varphi_h) = \{(x, y, x, y) \,|\, (x, y) \in Q\}$. The exact discrete Lagrangian (7.2.2) is therefore

$$L_d^E(x, y, x, y) = 0. \tag{7.2.18}$$

Let us now consider the ϵ-regularized Lagrangian

$$L^\epsilon(x, y, \dot{x}, \dot{y}) = \frac{\epsilon}{2}\dot{x}^2 + \frac{\epsilon}{2}\dot{y}^2 + \frac{1}{2} y\dot{x} - \frac{1}{2} x\dot{y}. \tag{7.2.19}$$

The corresponding Euler-Lagrange equations (7.2.7) take the form

$$\begin{aligned} \epsilon\ddot{x} + \dot{y} &= 0, \\ \epsilon\ddot{y} + \dot{x} &= 0. \end{aligned} \tag{7.2.20}$$

One can easily verify analytically that

$$x^\epsilon(t) = \frac{1}{2}\left[(x_i + x_f) - (y_f - y_i)\cot\frac{T}{2\epsilon}\right] + \frac{1}{2}\left[(y_f - y_i) + (x_f - x_i)\cot\frac{T}{2\epsilon}\right]\sin\frac{t}{\epsilon}$$
$$- \frac{1}{2}\left[(x_f - x_i) - (y_f - y_i)\cot\frac{T}{2\epsilon}\right]\cos\frac{t}{\epsilon},$$
$$y^\epsilon(t) = \frac{1}{2}\left[(y_i + y_f) + (x_f - x_i)\cot\frac{T}{2\epsilon}\right] - \frac{1}{2}\left[(x_f - x_i) - (y_f - y_i)\cot\frac{T}{2\epsilon}\right]\sin\frac{t}{\epsilon}$$
$$- \frac{1}{2}\left[(y_f - y_i) + (x_f - x_i)\cot\frac{T}{2\epsilon}\right]\cos\frac{t}{\epsilon}, \qquad (7.2.21)$$

is the solution to (7.2.20) satisfying the boundary conditions $(x^\epsilon(0), y^\epsilon(0)) = (x_i, y_i)$ and $(x^\epsilon(T), y^\epsilon(T)) = (x_f, y_f)$. Note that if $x_i \neq x_f$ or $y_i \neq y_f$, then as $\epsilon \longrightarrow 0^+$ this solution is rapidly oscillatory and not convergent. However, if $(x_f, y_f) = \varphi_T(x_i, y_i) = (x_i, y_i)$ (cf. Assumption 7.2.3) then we have

$$x^\epsilon(t) = x_i,$$
$$y^\epsilon(t) = y_i, \qquad (7.2.22)$$

and this solution converges uniformly (in this simple example it is in fact equal) to the solution of (7.2.16) with the same initial condition. We can also find an analytic expression for the exact discrete Lagrangian (7.2.1) associated with (7.2.19) as

$$L_d^{\epsilon,E}(x, y, \bar{x}, \bar{y}) = \frac{\bar{x}y - x\bar{y}}{2} + \frac{(\bar{x} - x)^2 + (\bar{y} - y)^2}{4}\cot\frac{T}{2\epsilon}. \qquad (7.2.23)$$

Restricting the domain to $\Gamma(\varphi_h)$ we get $L_d^{\epsilon,E}(x, y, x, y) = 0$, and comparing to (7.2.18) we verify that (7.2.9) indeed holds. The discrete Legendre transforms (2.4.4) associated with $L_d^{\epsilon,E}$ take the form

$$\mathbb{F}^+L_d^{\epsilon,E}(x, y, \bar{x}, \bar{y}) = \left(\bar{x}, \bar{y}, \frac{y}{2} + \frac{\bar{x} - x}{2}\cot\frac{T}{2\epsilon}, -\frac{x}{2} + \frac{\bar{y} - y}{2}\cot\frac{T}{2\epsilon}\right),$$
$$\mathbb{F}^-L_d^{\epsilon,E}(x, y, \bar{x}, \bar{y}) = \left(x, y, \frac{\bar{y}}{2} + \frac{\bar{x} - x}{2}\cot\frac{T}{2\epsilon}, -\frac{\bar{x}}{2} + \frac{\bar{y} - y}{2}\cot\frac{T}{2\epsilon}\right). \qquad (7.2.24)$$

Restricting the domain to $\Gamma(\varphi_h)$ and taking the limit $\epsilon \longrightarrow 0^+$ as in (7.2.11), we can define

the exact discrete Legendre transforms associated with (7.2.18)

$$\begin{aligned}\mathbb{F}^+L_d^E(x,y,x,y) &= \Big(x,y,\frac{y}{2},-\frac{x}{2}\Big),\\ \mathbb{F}^-L_d^E(x,y,x,y) &= \Big(x,y,\frac{y}{2},-\frac{x}{2}\Big).\end{aligned} \tag{7.2.25}$$

Comparing with (7.2.17), we see that the property (7.2.12) is satisfied, which replicates the analogous property for regular Lagrangians.

7.2.5 Variational error analysis

For a given continuous system described by the Lagrangian L, a variational integrator is constructed by choosing a discrete Lagrangian L_d which approximates the exact discrete Lagrangian L_d^E. We can define the order of accuracy of the discrete Lagrangian in a way similar to that for discrete Lagrangians resulting from regular continuous Lagrangians (see Section 2.4.2 and [41]).

Definition 7.2.4. *A discrete Lagrangian $L_d : Q \times Q \longrightarrow \mathbb{R}$ is of order r if there exists an open subset $U \subset Q$ with compact closure and constants $C > 0$ and $\bar{h} > 0$ such that*

$$\Big|L_d\big(q(0),q(h)\big) - L_d^E\big(q(0),q(h)\big)\Big| \leq Ch^{r+1} \tag{7.2.26}$$

for all solutions $q(t)$ of the Euler-Lagrange equations (7.1.8) with initial conditions $q(0) \in U$ and for all $h \leq \bar{h}$.

We will always assume that the discrete Lagrangian L_d is non-degenerate, so that the discrete Euler-Lagrange equations (2.4.2) can be solved for q_{k+1}. This defines the discrete Lagrangian map $F_{L_d} : Q \times Q \longrightarrow Q \times Q$ and the associated discrete Hamiltonian map $\tilde{F}_{L_d} : T^*Q \longrightarrow T^*Q$, as explained in Section 2.4.1. Of particular interest is the rate of convergence of $\tilde{F}_{L_d}$ to $\tilde{\varphi}_h$. One usually considers a *local error* (error made after one step) and a *global error* (error made after many steps). We will assume the following definitions, which are appropriate for the differential-algebraic systems (see Section 2.2.1 and [23], [24], [26], [41]).

Definition 7.2.5. *A discrete Hamiltonian map $\tilde{F}_{L_d}$ is of order r if there exists an open set $U \subset N$ and constants $C > 0$ and $\bar{h} > 0$ such that*

$$\left\|\tilde{F}_{L_d}(q,p) - \tilde{\varphi}_h(q,p)\right\| \leq Ch^{r+1} \tag{7.2.27}$$

for all $(q,p) \in U$ *and* $h \leq \bar{h}$.

Definition 7.2.6. *A discrete Hamiltonian map* $\tilde{F}_{L_d}$ *is convergent of order* r *if there exists an open set* $U \subset N$ *and constants* $C > 0$, $\bar{h} > 0$, *and* $\bar{T} > 0$ *such that*

$$\left\|(\tilde{F}_{L_d})^K(q,p) - \tilde{\varphi}_T(q,p)\right\| \leq Ch^{r+1}, \tag{7.2.28}$$

where $h = T/K$, *for all* $(q,p) \in U$, $h \leq \bar{h}$, *and* $T \leq \bar{T}$.

If the Lagrangian L is regular, then one can show that a discrete Lagrangian L_d is of order r if and only if the corresponding Hamiltonian map $\tilde{F}_{L_d}$ is of order r (see Section 2.4.2 and [41]). Also, the associated Hamiltonian equations are a set of ordinary differential equations, and under some smoothness assumptions one can show that if $\tilde{F}_{L_d}$ is of order r, then it is also convergent of order r (see Section 2.2.1 and [24]). However, in the case of the Lagrangian (7.1.1) it is not true in general—both the order of the discrete Lagrangian and the local order of the discrete Hamiltonian map may be different than the actual global order of convergence (see [26], [22]), as will be demonstrated in Section 7.3.

Example: Midpoint Rule. In a simple example we will demonstrate that the variational order of accuracy of a discretization method is unaffected by a degeneracy of a Lagrangian L. In order to calculate the order of a discrete Lagrangian L_d, we can expand $L_d(q(0), q(h))$ in a Taylor series in h and compare it to the analogous expansion for L_d^E. If the two expansions agree up to r terms, then L_d is of order r. Expanding $q(t)$ in a Taylor series about $t = 0$ and substituting it in (7.2.2), we get the expression

$$L_d^E\big(q(0),q(h)\big) = hL + \frac{h^2}{2}\left(\frac{\partial L}{\partial q}\dot{q} + \frac{\partial L}{\partial \dot{q}}\ddot{q}\right) + \frac{h^3}{6}\left(\frac{\partial L}{\partial q}\ddot{q} + \frac{\partial L}{\partial \dot{q}}\dddot{q} + \dot{q}^T\frac{\partial^2 L}{\partial q^2}\dot{q} + 2\dot{q}^T\frac{\partial^2 L}{\partial q \partial \dot{q}}\ddot{q} + \ddot{q}^T\frac{\partial^2 L}{\partial \dot{q}^2}\ddot{q}\right) + o(h^3), \tag{7.2.29}$$

where we denoted $q = q(0)$, $\dot{q} = \dot{q}(0)$, etc., and the Lagrangian L and its derivatives are computed at $(q, \dot{q})$. For the Lagrangian (7.1.1) the values of $\dot{q}$, $\ddot{q}$, $\dddot{q}$ are determined by differentiating (7.1.8) sufficiently many times and substituting the initial condition $q(0)$. Note that in the case of regular Lagrangians the value of $\dot{q}$ is determined by the boundary

conditions $q(0)$, $q(h)$, and the higher-order derivatives by differentiating the corresponding Euler-Lagrange equations, but apart from that the expression (7.2.29) remains qualitatively unaffected.

The *midpoint rule* is an integrator obtained by defining the discrete Lagrangian

$$L_d(q,\bar{q}) = hL\Big(\frac{q+\bar{q}}{2}, \frac{\bar{q}-q}{h}\Big). \tag{7.2.30}$$

Calculating the expansion in h gives

$$\begin{aligned} L_d\big(q(0),q(h)\big) = hL &+ \frac{h^2}{2}\left(\frac{\partial L}{\partial q}\dot{q} + \frac{\partial L}{\partial \dot{q}}\ddot{q}\right) \\ &+ h^3\left(\frac{1}{4}\frac{\partial L}{\partial q}\ddot{q} + \frac{1}{6}\frac{\partial L}{\partial \dot{q}}\dddot{q} + \frac{1}{8}\dot{q}^T\frac{\partial^2 L}{\partial q^2}\dot{q} + \frac{1}{4}\dot{q}^T\frac{\partial^2 L}{\partial q \partial \dot{q}}\ddot{q} + \frac{1}{8}\ddot{q}^T\frac{\partial^2 L}{\partial \dot{q}^2}\ddot{q}\right) + o(h^3). \end{aligned} \tag{7.2.31}$$

Comparing this to (7.2.29) shows that the discrete Lagrangian defined by the midpoint rule is second order regardless of the degeneracy of L. However, as mentioned before, if L is degenerate we cannot conclude about the global order of convergence of the corresponding discrete Hamiltonian map. The midpoint rule can be formulated as a Runge-Kutta method, namely the 1-stage Gauss method (see Section 2.2.2). We discuss Gauss and other Runge-Kutta methods and their convergence properties in more detail in Section 7.3. Note that low-order variational integrators for Lagrangians (7.1.1) based on the midpoint rule have been studied in [56] and [65] in the context of the dynamics of point vortices.

7.3 Variational partitioned Runge-Kutta methods

7.3.1 VPRK methods as PRK methods for the 'Hamiltonian' DAE

To construct higher-order variational integrators one may consider a class of partitioned Runge-Kutta (PRK) methods. Variational partitioned Runge-Kutta (VPRK) methods for regular Lagrangians are described in [23] and [41] (see also Section 2.4.3). In this section we show how VPRK methods can be applied to systems described by Lagrangians such as (7.1.1). As in the case of regular Lagrangians, we will construct an s-stage variational partitioned Runge-Kutta integrator for the Lagrangian (7.1.1) by considering the discrete

Lagrangian

$$L_d(q,\bar{q}) = h\sum_{i=1}^{s} b_i L(Q_i,\dot{Q}_i), \tag{7.3.1}$$

where the internal stages Q_i, $\dot{Q}_i$, $i = 1,\dots,s$, satisfy the relation

$$Q_i = q + h\sum_{j=1}^{s} a_{ij}\dot{Q}_j, \tag{7.3.2}$$

and are chosen so that the right-hand side of (7.3.1) is extremized under the constraint

$$\bar{q} = q + h\sum_{i=1}^{s} b_i\dot{Q}_i. \tag{7.3.3}$$

A variational integrator is then obtained by forming the corresponding discrete Euler-Lagrange equations (2.4.2).

Theorem 7.3.1. *The s-stage variational partitioned Runge-Kutta method based on the discrete Lagrangian* (7.3.1) *with the coefficients a_{ij} and b_i is equivalent to the following partitioned Runge-Kutta method applied to the 'Hamiltonian' DAE* (7.1.10)*:*

$$P^i = \alpha(Q_i), \qquad i = 1,\dots,s, \tag{7.3.4a}$$

$$\dot{P}^i = [D\alpha(Q_i)]^T\dot{Q}_i - DH(Q_i), \qquad i = 1,\dots,s, \tag{7.3.4b}$$

$$Q_i = q + h\sum_{j=1}^{s} a_{ij}\dot{Q}_j, \qquad i = 1,\dots,s, \tag{7.3.4c}$$

$$P^i = p + h\sum_{j=1}^{s} \bar{a}_{ij}\dot{P}^j, \qquad i = 1,\dots,s, \tag{7.3.4d}$$

$$\bar{q} = q + h\sum_{j=1}^{s} b_j\dot{Q}_j, \tag{7.3.4e}$$

$$\bar{p} = p + h\sum_{j=1}^{s} b_j\dot{P}^j, \tag{7.3.4f}$$

where the coefficients satisfy the condition

$$b_i\bar{a}_{ij} + b_j a_{ji} = b_i b_j, \qquad \forall i,j = 1,\dots,s, \tag{7.3.5}$$

and (q,p) denote the current values of position and momentum, $(\bar{q},\bar{p})$ denote the respective

values at the next time step, $D\alpha = (\partial\alpha_\mu/\partial q^\nu)_{\mu,\nu=1,\dots,n}$, $DH = (\partial H/\partial q^\mu)_{\mu=1,\dots,n}$, *and* Q_i, $\dot{Q}_i$, P^i, $\dot{P}^i$ *are the internal stages, with* $Q_i = (Q_i^\mu)_{\mu=1,\dots,n}$, *and similarly for the others.*

Proof. See Theorem VI.6.4 in [23] or Theorem 2.6.1 in [41]. The proof is essentially identical. The only qualitative difference is the fact that in our case the Lagrangian (7.1.1) is degenerate, so the corresponding Hamiltonian system is in fact the index 1 differential-algebraic system (7.1.10) rather than a typical system of ordinary differential equations. See also Section 2.4.3.

□

Existence and uniqueness of the numerical solution. Given q and p, one can use Equations (7.3.4) to compute the new position $\bar{q}$ and momentum $\bar{p}$. First, one needs to solve (7.3.4a)-(7.3.4d) for the internal stages Q_i, $\dot{Q}_i$, P^i, and $\dot{P}^i$. This is a system of $4sn$ equations for $4sn$ variables, but one has to make sure these equations are independent, so that a unique solution exists. One may be tempted to calculate the Jacobian of this system for $h = 0$, and then use the Implicit Function Theorem. This approach, however, has a certain difficulty. Even if we start with consistent initial values (q_0, p_0), the numerical solution (q_k, p_k) for $k > 0$ will only approximately satisfy the algebraic constraint, so $Q_i = q$ and $P^i = p$ cannot be assumed to be the solution of (7.3.4a)-(7.3.4d) for $h = 0$, and consequently, the Implicit Function Theorem will not yield a useful result. Let us therefore regard q and p as h-dependent, as they result from the previous iterations of the method with the timestep h. If the method is convergent, it is reasonable to expect that $p - \alpha(q)$ is small and converges to zero as h is refined. The following approach was inspired by Theorem 4.1 in [22].

Theorem 7.3.2. *Let* H *and* α *be smooth in an* h*-independent neighborhood* U *of* q *and let the matrix*

$$W(\xi_1, \dots, \xi_s) = (\bar{\mathcal{A}} \otimes I_n)\{D\alpha^T\} - (\mathcal{A} \otimes I_n)\{D\alpha\} \tag{7.3.6}$$

be invertible with the inverse bounded in U^s*, i.e., there exists* $C > 0$ *such that*

$$\left\| W^{-1}(\xi_1, \dots, \xi_s) \right\| \le C, \qquad \forall (\xi_1, \dots, \xi_s) \in U^s, \tag{7.3.7}$$

where $\mathcal{A} = (a_{ij})_{i,j=1,\dots,s}$, $\bar{\mathcal{A}} = (\bar{a}_{ij})_{i,j=1,\dots,s}$, I_n *is the* $n \times n$ *identity matrix, and* $\{D\alpha\}$ *denotes the block diagonal matrix*

$$\{D\alpha\}(\xi_1, \dots, \xi_s) = \bigoplus_{i=1}^{s} D\alpha(\xi_i) = \text{blockdiag}\big(D\alpha(\xi_1), \dots, D\alpha(\xi_s)\big). \tag{7.3.8}$$

Suppose also that (q, p) *satisfy*

$$p - \alpha(q) = O(h). \tag{7.3.9}$$

Then there exists $\bar{h} > 0$ *such that the nonlinear system* (7.3.4a)-(7.3.4d) *has a solution for* $h \le \bar{h}$. *The solution is locally unique and satisfies*

$$Q_i - q = O(h), \qquad P^i - p = O(h), \qquad \dot{Q}_i = O(1), \qquad \dot{P}^i = O(1). \tag{7.3.10}$$

Proof. Substitute (7.3.4c) and (7.3.4d) in (7.3.4a) and (7.3.4b) to obtain

$$\begin{aligned} 0 &= \alpha(Q_i) - p - h \sum_{j=1}^{s} \bar{a}_{ij} \dot{P}^j, \\ \dot{P}^i &= D\alpha^T(Q_i)\dot{Q}_i - DH(Q_i), \end{aligned} \tag{7.3.11}$$

for $i = 1, \dots, s$, where for notational convenience we left the Q_i's as arguments of α, $D\alpha^T$ and DH, but we keep in mind they are defined by (7.3.4c), so that (7.3.11) is a nonlinear system for $\dot{Q}_i$ and $\dot{P}^i$. Let us consider the homotopy

$$\begin{aligned} 0 &= \alpha(Q_i) - p - h \sum_{j=1}^{s} \bar{a}_{ij} \dot{P}^j - (\tau - 1)\big(p - \alpha(q)\big), \\ \dot{P}^i &= D\alpha^T(Q_i)\dot{Q}_i - DH(Q_i) - (\tau - 1)DH(q), \end{aligned} \tag{7.3.12}$$

for $i = 1, \dots, s$. It is easy to see that for $\tau = 0$ the system (7.3.12) has the solution $\dot{Q}_i = 0$ and $\dot{P}^i = 0$, and for $\tau = 1$ it is equivalent to (7.3.11). Let us treat $\dot{Q}_i$ and $\dot{P}^i$ as functions of τ, and differentiate (7.3.12) with respect to this parameter. The resulting ODE system can be written as

$$\{D\alpha\}(\mathcal{A}\otimes I_n)\frac{d\dot{Q}}{d\tau} - \bar{\mathcal{A}}\otimes I_n\frac{d\dot{P}}{d\tau} = \frac{1}{h}\mathbb{1}_s\otimes\big(p-\alpha(q)\big), \tag{7.3.13a}$$

$$\frac{d\dot{P}}{d\tau} = \Big(\{D\alpha^T\} + h\{B\}(\mathcal{A}\otimes I_n)\Big)\frac{d\dot{Q}}{d\tau} - \mathbb{1}_s\otimes DH(q), \tag{7.3.13b}$$

where for compactness we introduced the following notations: $\dot{Q} = (\dot{Q}_1,\dots,\dot{Q}_s)^T$, similarly for $\dot{P}$; $\mathbb{1}_s = (1,\dots,1)^T$ is the s-dimensional vector of ones; $\{D\alpha\} = \{D\alpha\}(Q_1,\dots,Q_s)$, and similarly, $\{B\}$ denotes the block diagonal matrix

$$\{B\} = \text{blockdiag}\big(B(Q_1,\dot{Q}_1),\dots,B(Q_s,\dot{Q}_s)\big) \tag{7.3.14}$$

with $B(Q_i,\dot{Q}_i) = D^2\alpha_\beta(Q_i)\dot{Q}_i^\beta - D^2H(Q_i)$, where D^2 denotes the Hessian matrix of the respective function, and summation over β is implied. The system (7.3.13) is further simplified if we substitute (7.3.13b) in (7.3.13a). This way we obtain an ODE system for the variables $\dot{Q}$ of the form

$$\Big[(\bar{\mathcal{A}}\otimes I_n)\{D\alpha^T\} - \{D\alpha\}(\mathcal{A}\otimes I_n) + h(\bar{\mathcal{A}}\otimes I_n)\{B\}(\mathcal{A}\otimes I_n)\Big]\frac{d\dot{Q}}{d\tau} = (\bar{\mathcal{A}}\mathbb{1}_s)\otimes DH(q) - \frac{1}{h}\mathbb{1}_s\otimes\big(p-\alpha(q)\big). \tag{7.3.15}$$

Since α is smooth, we have

$$\Big[\{D\alpha\}(\mathcal{A}\otimes I_n)\Big]_{ij} = a_{ij}D\alpha(Q_i) = a_{ij}D\alpha(Q_j) + O(\delta) = \Big[(\mathcal{A}\otimes I_n)\{D\alpha\}\Big]_{ij} + O(\delta), \tag{7.3.16}$$

where $\|Q_i - Q_j\| \le \delta$ and δ is assumed small, but independent of h. Moreover, since α and H are smooth, the term $\{B\}$, as a function of $\dot{Q}$, is bounded in a neighborhood of 0. Therefore, we can write (7.3.15) as

$$\Big[W(Q_1,\dots,Q_s) + O(\delta) + O(h)\Big]\frac{d\dot{Q}}{d\tau} = (\bar{\mathcal{A}}\mathbb{1}_s)\otimes DH(q) - \frac{1}{h}\mathbb{1}_s\otimes\big(p-\alpha(q)\big). \tag{7.3.17}$$

By (7.3.7), for sufficiently small h and δ, the matrix $W(Q_1,\dots,Q_s) + O(\delta) + O(h)$ has a

bounded inverse, provided that $Q_1, \ldots, Q_s$ remain in U. Therefore, the ODE (7.3.17) with the initial condition $\dot{Q}(0) = 0$ has a unique solution $\dot{Q}(\tau)$ on a non-empty interval $[0, \bar{\tau})$, which can be extended until any of the corresponding $Q_i(\tau)$ leaves U. Let us argue that for a sufficiently small h we have $\bar{\tau} > 1$. Given (7.3.7) and (7.3.9), the ODE (7.3.17) implies that

$$\frac{d\dot{Q}}{d\tau} = O(1). \tag{7.3.18}$$

Therefore, we have

$$\dot{Q}(\tau) = \int_0^\tau \frac{d\dot{Q}}{d\zeta}\, d\zeta = O(\tau) \tag{7.3.19}$$

and further

$$Q_i(\tau) = q + O(\tau h) \tag{7.3.20}$$

for $\tau < \bar{\tau}$. This implies that all $Q_i(\tau)$ remain in U for $\tau \leq 1$ if h is sufficiently small. Consequently, the ODE (7.3.15) has a solution on the interval $[0, 1]$. Then $\dot{Q}_i(1)$ and $Q_i(1)$ satisfy the estimates (7.3.10), and are a solution to the nonlinear system (7.3.4a)-(7.3.4d). The corresponding $\dot{P}^i$ and P^i can be computed using (7.3.4b) and (7.3.4d), and the remaining estimates (7.3.10) can be proved using the fact that α and H are smooth. This completes the proof of the existence of a numerical solution to (7.3.4a)-(7.3.4d).

In order to prove local uniqueness, let us substitute the second equation of (7.3.11) in the first one to obtain a nonlinear system for $\dot{Q}_i$, namely

$$0 = \alpha(Q_i) - p - h \sum_{j=1}^{s} \bar{a}_{ij} \big(D\alpha^T(Q_j)\dot{Q}_j - DH(Q_j) \big), \tag{7.3.21}$$

for $i = 1, \ldots, s$, where we again left the Q_i's for notational convenience. Suppose there exists another solution $\dot{\tilde{Q}}_i$ that satisfies the estimates (7.3.10), and denote $\Delta\dot{Q}_i = \dot{\tilde{Q}}_i - \dot{Q}_i$. Based on the assumptions, we have $\Delta\dot{Q}_i = O(1)$, i.e., it is at least bounded as $h \longrightarrow 0$. We will show that for sufficiently small h we in fact have $\Delta\dot{Q}_i = 0$. Since $\dot{\tilde{Q}}_i$ satisfy (7.3.21), we have

$$0 = \alpha(\bar{Q}_i) - p - h\sum_{j=1}^{s} \bar{a}_{ij}\big(D\alpha^T(\bar{Q}_j)\dot{\bar{Q}}_j - DH(\bar{Q}_j)\big) \tag{7.3.22}$$

for $i = 1, \ldots, s$. Subtract (7.3.21) from (7.3.22), and linearize around $\dot{Q}_i$. Based on the fact that $\Delta\dot{Q}_i = O(1)$, and using the notation introduced before, we get

$$0 = h\Big[\{D\alpha\}(\mathcal{A}\otimes I_n) - (\bar{\mathcal{A}}\otimes I_n)\{D\alpha^T\}\Big]\Delta\dot{Q} + O(h^2\|\Delta\dot{Q}\|). \tag{7.3.23}$$

By a similar argument as before, for sufficiently small h the matrix $\Big[\{D\alpha\}(\mathcal{A}\otimes I_n) - (\bar{\mathcal{A}}\otimes I_n)\{D\alpha^T\}\Big]$ has a bounded inverse, therefore (7.3.23) implies $\Delta\dot{Q} = O(h\|\Delta\dot{Q}\|)$, that is,

$$\|\Delta\dot{Q}\| \le \tilde{C}h\|\Delta\dot{Q}\| \qquad \Longleftrightarrow \qquad (1-\tilde{C}h)\|\Delta\dot{Q}\| \le 0 \tag{7.3.24}$$

for some constant $\tilde{C} > 0$. Note that for $h < 1/\tilde{C}$ we have $(1 - \tilde{C}h) > 0$, and therefore $\|\Delta\dot{Q}\| = 0$, which completes the proof of the local uniqueness of a numerical solution to (7.3.4a)-(7.3.4d).

□

.

Remarks. The condition (7.3.7) may be tedious to verify, especially when the used Runge-Kutta method has many stages. However, this condition is significantly simplified in the following special cases.

1. For a non-partitioned Runge-Kutta method we have $\mathcal{A} = \bar{\mathcal{A}}$, and the condition (7.3.7) is satisfied if $\mathcal{A}$ is invertible, and the mass matrix $M(q) = D\alpha^T(q) - D\alpha(q)$, as defined in Section 7.1.1, is invertible in U and the inverse is bounded.

2. If $D\alpha$ is antisymmetric, then the condition (7.3.7) is satisfied if $(\mathcal{A} + \bar{\mathcal{A}})$ is invertible, and the matrix $D\alpha(q)$ is invertible in U and the inverse is bounded.

7.3.2 Linear $\alpha_\mu(q)$

An interesting special case is obtained if in some local chart on Q we have $\alpha_\mu(q) = -\frac{1}{2}\Lambda_{\mu\nu}q^\nu$ for some constant matrix Λ. Without loss of generality assume that Λ is invertible and

antisymmetric. The Lagrangian (7.1.2) then takes the form

$$L(q,\dot{q}) = -\frac{1}{2}\Lambda_{\mu\nu}\dot{q}^{\mu}q^{\nu} - H(q), \tag{7.3.25}$$

the Euler-Lagrange equations (7.1.8) become

$$\Lambda\dot{q} = DH(q), \tag{7.3.26}$$

and the 'Hamiltonian' DAE system (7.1.10) is

$$\begin{aligned} p &= -\frac{1}{2}\Lambda q, \\ \dot{p} &= \frac{1}{2}\Lambda\dot{q} - DH(q). \end{aligned} \tag{7.3.27}$$

Let us consider a special case of the method (7.3.4) with $a_{ij} = \bar{a}_{ij}$, i.e., a non-partitioned Runge-Kutta method. Applying it to (7.3.27) we get

$$P^i = -\frac{1}{2}\Lambda Q_i, \qquad i = 1,\dots,s, \tag{7.3.28a}$$

$$\dot{P}^i = \frac{1}{2}\Lambda\dot{Q}_i - DH(Q_i), \qquad i = 1,\dots,s, \tag{7.3.28b}$$

$$Q_i = q + h\sum_{j=1}^{s} a_{ij}\dot{Q}_j, \qquad i = 1,\dots,s, \tag{7.3.28c}$$

$$P^i = p + h\sum_{j=1}^{s} a_{ij}\dot{P}^j, \qquad i = 1,\dots,s, \tag{7.3.28d}$$

$$\bar{q} = q + h\sum_{j=1}^{s} b_j\dot{Q}_j, \tag{7.3.28e}$$

$$\bar{p} = p + h\sum_{j=1}^{s} b_j\dot{P}^j. \tag{7.3.28f}$$

Since Λ is antisymmetric and invertible, then by Theorem 7.3.2 the scheme (7.3.28) yields a unique numerical solution to (7.3.27) if the Runge-Kutta matrix $\mathcal{A} = (a_{ij})$ is invertible.

Theorem 7.3.3. *Suppose $\mathcal{A} = (a_{ij})$ is invertible and $p = -\frac{1}{2}\Lambda q$. Then the method* (7.3.28) *is equivalent to the same Runge-Kutta method applied to* (7.3.26).

Proof. Substitute (7.3.28c) and (7.3.28d) in (7.3.28a), and use the fact $p = -\frac{1}{2}\Lambda q$ to obtain

$$\sum_{j=1}^{s} a_{ij}\Big(\dot{P}^j + \frac{1}{2}\Lambda\dot{Q}_j\Big) = 0, \qquad i = 1, \dots, s. \tag{7.3.29}$$

Since $\mathcal{A}$ is invertible, this implies

$$\dot{P}^i = -\frac{1}{2}\Lambda\dot{Q}_i, \qquad i = 1, \dots, s. \tag{7.3.30}$$

Substituting this in (7.3.28b) yields

$$\Lambda\dot{Q}_i = DH(Q_i), \qquad i = 1, \dots, s. \tag{7.3.31}$$

Together with (7.3.28c) and (7.3.28e), this gives a Runge-Kutta method for (7.3.26). Moreover, substituting (7.3.30) and $p = -\frac{1}{2}\Lambda q$ in (7.3.28f), and using (7.3.28e), we show

$$\bar{p} = -\frac{1}{2}\Lambda q + h\sum_{j=1}^{s} b_j\Big(-\frac{1}{2}\Lambda\dot{Q}_j\Big) = -\frac{1}{2}\Lambda\bar{q}, \tag{7.3.32}$$

that is, $(\bar{q}, \bar{p})$ satisfy the algebraic constraint.

□

Corollary 7.3.4. *The numerical flow on T^*Q defined by* (7.3.28) *leaves the primary constraint N invariant, i.e., if $(q, p) \in N$, then $(\bar{q}, \bar{p}) \in N$.*

If the coefficients of the method (7.3.28) satisfy the condition (7.3.5), then (7.3.28) is a variational integrator and the associated discrete Hamiltonian map $\tilde{F}_{L_d}$ is symplectic on T^*Q, as explained in Section 2.4.1. Given Corollary 7.3.4, we further have:

Corollary 7.3.5. *If the coefficients a_{ij} and b_i in* (7.3.28) *satisfy the condition* (7.3.5)*, then the discrete Hamiltonian map $\tilde{F}_{L_d}$ associated with* (7.3.1) *is symplectic on the primary constraint N, that is, $\big(\tilde{F}_{L_d}\big|_N\big)^*\tilde{\Omega}_N = \tilde{\Omega}_N$.*

Convergence. Various Runge-Kutta methods and their classical orders of convergence, that is, orders of convergence when applied to (non-stiff) ordinary differential equations, are discussed in many textbooks on numerical analysis, for instance [24] and [26]. When applied to differential-algebraic equations, the order of convergence of a Runge-Kutta method may be reduced (see [6], [26], [53]). However, in the case of (7.3.27) Theorem 7.3.3 implies

that the classical order of convergence of non-partitioned Runge-Kutta methods (7.3.28) is retained.

Theorem 7.3.6. *A Runge-Kutta method with the coefficients a_{ij} and b_i applied to the DAE system* (7.3.27) *retains its classical order of convergence.*

Proof. Let r be the classical order of the considered Runge-Kutta method, $(q,p) \in N$ an initial condition, $(q_E(t), p_E(t))$ the exact solution to (7.3.27) such that $(q_E(0), p_E(0)) = (q,p)$, and (q_k, p_k) the numerical solution obtained by applying the method (7.3.28) iteratively k times with $(q_0, p_0) = (q,p)$. Theorem 7.3.3 states that the method (7.3.28) is equivalent to applying the same Runge-Kutta method to the ODE system (7.3.26). Hence, we obtain convergence of order r in the q variable, that is, for a fixed time $T > 0$ and an integer K such that $h = T/K$, we have the estimate

$$\|q_K - q(T)\| \leq Ch^{r+1} \tag{7.3.33}$$

for some constant $C > 0$ (cf. Definition 7.2.6). By Corollary 7.3.4 we know that $p_K = -\frac{1}{2}\Lambda q_K$, so we have the estimate

$$\|p_K - p(T)\| \leq \frac{1}{2}\|\Lambda\|\|q_K - q(T)\| \leq \frac{1}{2}\|\Lambda\|Ch^{r+1}, \tag{7.3.34}$$

which completes the proof, since $\|\Lambda\| < +\infty$.

□

Of particular interest to us are Runge-Kutta methods that satisfy the condition (7.3.5), for instance symplectic diagonally-implicit Runge-Kutta methods (DIRK) or Gauss collocation methods (see Section 2.2.2 and [23]). The s-stage Gauss method is of classical order $2s$ (cf. Theorem 2.2.5), therefore we have:

Corollary 7.3.7. *The s-stage Gauss collocation method applied to the DAE system* (7.3.27) *is convergent of order $2s$.*

As mentioned in Section 7.2.5, the midpoint rule is a 1-stage Gauss method, therefore it retains its classical second order of convergence.

Backward error analysis. The system (7.3.26) can be rewritten as the Poisson system

$$\dot{q} = \Lambda^{-1} DH(q) \tag{7.3.35}$$

with the structure matrix Λ^{-1} (see [38], [23]). The flow φ_t for this equation is a *Poisson map*, that is, it satisfies the property

$$D\varphi_t(q)\, \Lambda^{-1} \left[D\varphi_t(q)\right]^T = \Lambda^{-1}, \tag{7.3.36}$$

which is in fact equivalent to the symplecticity property (7.1.23) or (7.1.27) written in local coordinates on Q or N, respectively. Let $F_h : Q \longrightarrow Q$ represent the numerical flow defined by some numerical algorithm applied to (7.3.35). We say this flow is a *Poisson integrator* if

$$DF_h(q)\, \Lambda^{-1} \left[DF_h(q)\right]^T = \Lambda^{-1}. \tag{7.3.37}$$

The left-hand side of (7.3.36) can be regarded as a quadratic invariant of (7.3.35). By Theorem 7.3.3 the method (7.3.28) is equivalent to applying the same Runge-Kutta method to (7.3.35). If in addition its coefficients satisfy the condition (7.3.5), then it can be shown that the method preserves quadratic invariants (see Theorem IV.2.2 in [23]). Therefore, we have:

Corollary 7.3.8. *If $\mathcal{A} = (a_{ij})$ is invertible, the coefficients a_{ij} and b_i satisfy the condition* (7.3.5)*, and $p = -\frac{1}{2}\Lambda q$, then the method* (7.3.28) *is a Poisson integrator for* (7.3.35)*.*

As discussed in Section 2.2.3, symplectic numerical schemes nearly conserve the Hamiltonian over exponentially long time intervals, because their modified differential equations are also Hamiltonian. A similar result holds for Poisson integrators for Poisson systems: a Poisson integrator defines the exact flow for a nearby Poisson system, whose structure matrix is the same and whose Hamiltonian has the asymptotic expansion (2.2.12) (see Theorem IX.3.6 in [23]). Therefore, we expect the non-partitioned Runge-Kutta schemes (7.3.28) satisfying the condition (7.3.5) to demonstrate good preservation of the original Hamiltonian H. See Section 7.4 for numerical examples.

Partitioned Runge-Kutta methods do not seem to have special properties when applied to systems with linear $\alpha_\mu(q)$, therefore we describe them in the general case in Section 7.3.3.

7.3.3 Nonlinear $\alpha_\mu(q)$

When the coordinates $\alpha_\mu(q)$ are nonlinear functions of q, then the Runge-Kutta methods discussed in Section 7.3.2 lose some of their properties. A theorem similar to Theorem 7.3.3 cannot be proved, most of the Runge-Kutta methods (whether non-partitioned or partitioned) do not preserve the algebraic constraint $p = \alpha(q)$, i.e., the numerical solution does not stay on the primary constraint N, and therefore their order of convergence is reduced, unless they are *stiffly accurate*.

7.3.3.1 Runge-Kutta methods

Let us again consider non-partitioned methods with $a_{ij} = \bar{a}_{ij}$. Convergence results for some classical Runge-Kutta schemes of interest can be obtained by transforming (7.1.10) into a semi-explicit index 2 DAE system. Let us briefly review this approach. More details can be found in [22] and [26].

The system (7.1.10) can be written as the quasi-linear DAE

$$C(y)\dot{y} = f(y), \tag{7.3.38}$$

where $y = (q, p)$ and

$$C(y) = \begin{pmatrix} [D\alpha(q)]^T & -I_n \\ 0 & 0 \end{pmatrix}, \qquad f(y) = \begin{pmatrix} DH(q) \\ p - \alpha(q) \end{pmatrix}, \tag{7.3.39}$$

where I_n denotes the $n \times n$ identity matrix. Let us introduce a slack variable z and rewrite (7.3.38) as the index 2 DAE system

$$\dot{y} = z, \tag{7.3.40a}$$

$$0 = C(y)z - f(y). \tag{7.3.40b}$$

This is an index 2 system, because we have $4n$ dependent variables, but only $2n$ differential equations (7.3.40a), and some components of the algebraic equations (7.3.40b) have to be differentiated twice with respect to time in order to derive the missing differential equations for z. Note that $C(y)$ is a singular matrix of constant rank n, therefore it can be decomposed

(using Gauss elimination or the singular value decomposition) as

$$C(y) = S(y)\begin{pmatrix} I_n & 0 \\ 0 & 0 \end{pmatrix} T(y) \tag{7.3.41}$$

for some non-singular matrices $S(y)$ and $T(y)$. Since $\alpha(q)$ is assumed to be smooth, one can choose S and T so that they are also smooth (at least in a neighborhood of y). Pre-multiplying both sides of (7.3.40b) by $S^{-1}(y)$ turns the DAE (7.3.40) into

$$\dot{y}_1 = z_1, \tag{7.3.42a}$$

$$\dot{y}_2 = z_2, \tag{7.3.42b}$$

$$0 = T_{11}(y)\, z_1 + T_{12}(y)\, z_2 - \tilde{f}_1(y), \tag{7.3.42c}$$

$$0 = \tilde{f}_2(y), \tag{7.3.42d}$$

where we introduced the block structure $y = (y_1, y_2)$, $z = (z_1, z_2)$, and

$$T(y) = \begin{pmatrix} T_{11} & T_{12} \\ T_{21} & T_{22} \end{pmatrix}, \qquad S^{-1}(y)\, f(y) = \begin{pmatrix} \tilde{f}_1(y) \\ \tilde{f}_2(y) \end{pmatrix}. \tag{7.3.43}$$

Since $T(y)$ is invertible, without loss of generality, so is the block $T_{11}(y)$ (one can always permute the columns of $T(y)$). Let us compute z_1 from (7.3.42c) and substitute it in (7.3.42a). The resulting system,

$$\dot{y}_1 = \big(T_{11}(y)\big)^{-1}\big(\tilde{f}_1(y) - T_{12}(y) z_2\big), \tag{7.3.44a}$$

$$\dot{y}_2 = z_2, \tag{7.3.44b}$$

$$0 = \tilde{f}_2(y), \tag{7.3.44c}$$

has the form of a semi-explicit index 2 DAE

$$\begin{aligned} \dot{y} &= F(y, z_2), \\ 0 &= G(y), \end{aligned} \tag{7.3.45}$$

provided that

$$D_y G \, D_{z_2} F = -D_{y_1} \tilde{f}_2 \, T_{11}^{-1} \, T_{12} + D_{y_2} \tilde{f}_2 \tag{7.3.46}$$

has a bounded inverse.

It is an elementary exercise to show that the partitioned Runge-Kutta method (7.3.4) is invariant under the presented transformation, that is, it defines a numerically equivalent partitioned Runge-Kutta method for (7.3.44). Runge-Kutta methods for semi-explicit index 2 DAEs have been studied and some convergence results are available. Convergence estimates for the y component of (7.3.44) can be readily applied to the solution of (7.3.38).

As in Section 7.3.2, of particular interest to us are variational Runge-Kutta methods, i.e., methods satisfying the condition (7.3.5), for example Gauss collocation methods (see Section 2.2.2 and [23], [24]). However, in the case when $\alpha(q)$ is a nonlinear function, the solution generated by the Gauss methods does not stay on the primary constraint N and this affects their rate of convergence, as will be shown below. For comparison, we will also consider the Radau IIA methods (see Section 2.2.5 and [26]), which, although not variational/symplectic, are *stiffly accurate*, that is, their coefficients satisfy $a_{sj} = b_j$ for $j = 1, \ldots, s$, so the numerical value of the solution at the new time step is equal to the value of the last internal stage, and therefore the numerical solution stays on the submanifold N. We cite the following convergence rates for the y component of (7.3.45) after [26] and [22]:

- s-stage Gauss method—convergent of order $\begin{cases} s+1 & \text{for } s \text{ odd} \\ s & \text{for } s \text{ even} \end{cases}$,
- s-stage Radau IIA method—convergent of order $2s - 1$.

With the exception of the midpoint rule ($s = 1$), we see that the order of convergence of the Gauss methods is reduced. On the other hand, the Radau IIA methods retain their classical order $2s - 1$.

Symplecticity. Since the Gauss methods satisfy the condition (7.3.5), they generate a flow which preserves the canonical symplectic form $\tilde{\Omega}$ on T^*Q, as explained in Section 2.4.1. However, since the primary constraint N is not invariant under this flow, a result analogous to Corollary 7.3.5 does not hold, i.e., the flow is not symplectic on N.

7.3.3.2 Partitioned Runge-Kutta methods

In Section 7.4 we present numerical results for the Lobatto IIIA-IIIB methods (see Section 2.2.2 and [23]). Their numerical performance appears rather unattractive, therefore our theoretical results regarding partitioned Runge-Kutta methods are less complete. Below we summarize the experimental orders of convergence of the Lobatto IIIA-IIIB schemes that we observed in our numerical computations (see Figure 7.4.2, Figure 7.4.6 and Figure 7.4.10):

- 2-stage Lobatto IIIA-IIIB—inconsistent,
- 3-stage Lobatto IIIA-IIIB—convergent of order 2,
- 4-stage Lobatto IIIA-IIIB—convergent of order 2.

Comments regarding the symplecticity of these schemes are the same as for the Gauss methods in Section 7.3.3.1.

7.4 Numerical experiments

In this section we present the results of the numerical experiments we performed to test the methods discussed in Section 7.3. We consider Kepler's problem, the dynamics of planar point vortices, and the Lotka-Volterra model, and we show how each of these models can be formulated as a Lagrangian system linear in velocities.

7.4.1 Kepler's problem

A particle or a planet moving in a central potential in two dimensions can be described by the Hamiltonian

$$H(x, y, p_x, p_y) = \frac{1}{2}p_x^2 + \frac{1}{2}p_x^2 - \frac{1}{\sqrt{x^2 + y^2}} - H_0, \tag{7.4.1}$$

where (x, y) denotes the position of the planet and (p_x, p_y) its momentum; H_0 is an arbitrary constant. The corresponding Lagrangian can be obtained in the usual way as

$$L = p_x\dot{x} + p_y\dot{y} - H(x, y, p_x, p_y). \tag{7.4.2}$$

If one performs the standard Legendre transform $\dot{x} = \partial H/\partial p_x$, $\dot{y} = \partial H/\partial p_y$, then $L = L(x, y, \dot{x}, \dot{y})$ will take the usual nondegenerate form, quadratic in velocities. However, one can also introduce the variable $q = (x, y, p_x, p_y)$ and view $L = L(q, \dot{q})$ as (7.1.2), that is, a Lagrangian linear in velocities (see [15]). Comparing (7.4.2) and (7.3.25), we see that the corresponding Λ is singular. Without loss of generality we replace Λ with its antisymmetric part $(\Lambda - \Lambda^T)/2$, which is invertible, and consider the Lagrangian

$$L = \frac{1}{2}q^3\dot{q}^1 + \frac{1}{2}q^4\dot{q}^2 - \frac{1}{2}q^1\dot{q}^3 - \frac{1}{2}q^2\dot{q}^4 - H(q). \tag{7.4.3}$$

As a test problem we considered an elliptic orbit with eccentricity $e = 0.5$ and semi-major axis $a = 1$. We took the initial condition at the pericenter, i.e., $q^1_{init} = (1-e)a = 0.5$, $q^2_{init} = 0$, $q^3_{init} = 0$, $q^4_{init} = a\sqrt{(1+e)/(1-e)} \approx 1.73$. This is a periodic orbit with period $T_{period} = 2\pi$. A reference solution was computed by integrating (7.3.26) until the time $T = 7$ using Verner's method (a 6-th order explicit Runge-Kutta method; see Section 2.2.2 and [24]) with the small time step $h = 2 \times 10^{-7}$. The reference solution is depicted in Figure 7.4.1.

We solved the same problem using several of the methods discussed in Section 7.3 for a number of time steps ranging from $h = 3.5 \times 10^{-3}$ to $h = 3.5 \times 10^{-1}$. The value of the solutions at $T = 7$ was then compared against the reference solution. The max norm errors are depicted in Figure 7.4.2. We see that the rates of convergence of the Gauss and the 3-stage Radau IIA methods are consistent with Theorem 7.3.6 and Corollary 7.3.7. For the Lobatto IIIA-IIIB methods we observe a reduction of order. The 2-stage Lobatto IIIA-IIIB method turns out to be inconsistent and is not depicted in Figure 7.4.2. Both the 3- and 4-stage methods converge only quadratically, while their classical orders of convergence are 4 and 6, respectively.

We also investigated the long-time behavior of our integrators and conservation of the Hamiltonian. For convenience, we set $H_0 = -0.5$ in (7.4.1), so that $H = 0$ on the considered orbit. We applied the Gauss methods with the relatively large time step $h = 0.1$ and computed the numerical solution until the time $T = 5 \times 10^5$. Figure 7.4.3 shows that the Gauss

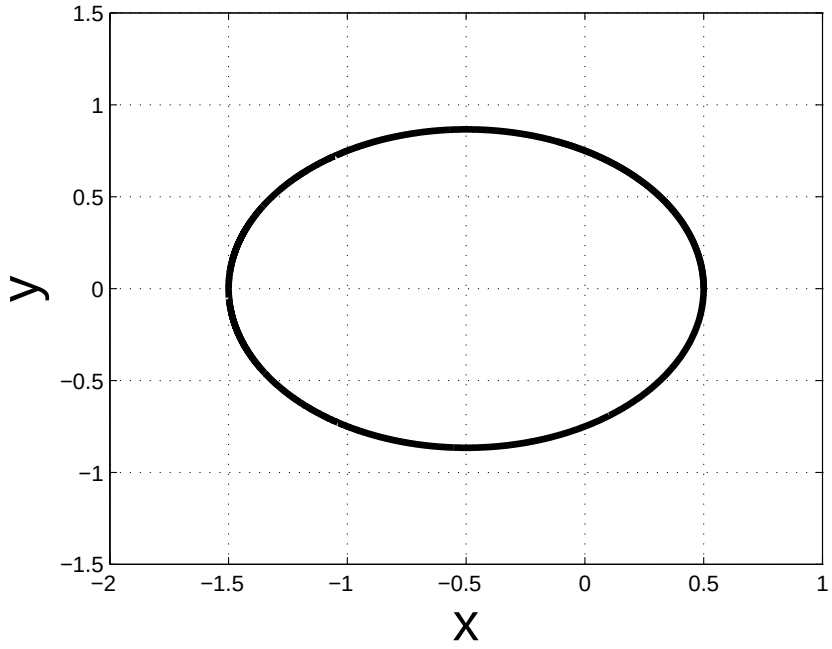

Figure 7.4.1: The reference solution for Kepler's problem computed by integrating (7.3.26) until the time $T = 7$ using Verner's method with the time step $h = 2 \times 10^{-7}$.

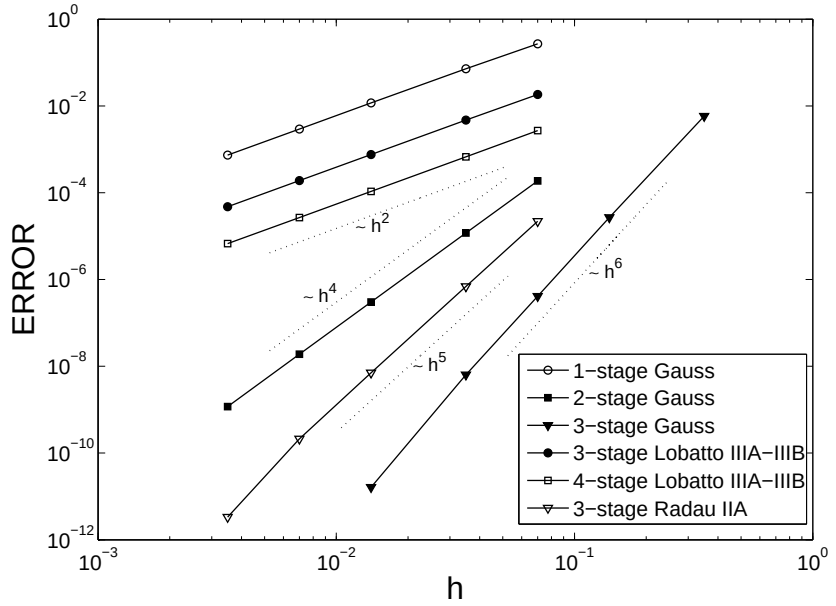

Figure 7.4.2: Convergence of several Runge-Kutta methods for Kepler's problem.

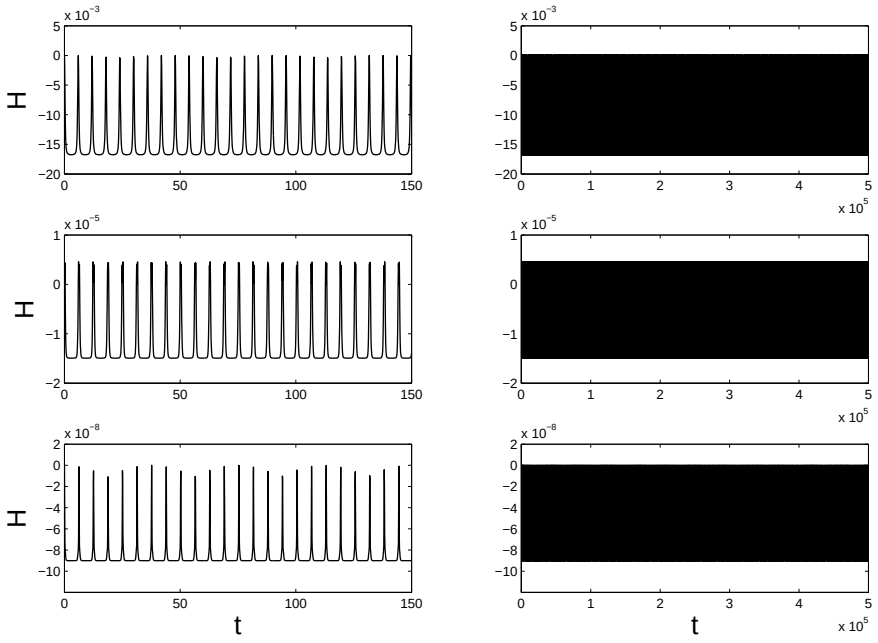

Figure 7.4.3: Hamiltonian conservation for the 1-stage (*top row*), 2-stage (*middle row*), and 3-stage (*bottom row*) Gauss methods applied to Kepler's problem with the time step $h = 0.1$ over the time interval $[0, 5 \times 10^5]$ (*right column*), with a close-up on the initial interval $[0, 150]$ shown in the *left column*.

integrators preserve the Hamiltonian very well, which is consistent with Corollary 7.3.8. We performed similar computations for the Lobatto IIIA-IIIB and Radau IIA methods, also with $h = 0.1$. The results are depicted in Figure 7.4.4. The 3- and 4-stage Lobatto IIIA-IIIB schemes result in instabilities, the planet's trajectory spirals down on the center of gravity, and the computations cannot be continued too far in time. The Hamiltonian shows major variations whose amplitude grows in time. The non-variational Radau IIA scheme yields an accurate solution, but it demonstrates a gradual energy dissipation.

7.4.2 Point vortices

Point vortices in the plane are another interesting example of a system with linear $\alpha_\mu(q)$ (see [45], [56], [65]). A system of K interacting point vortices in two dimensions can be described by the Lagrangian

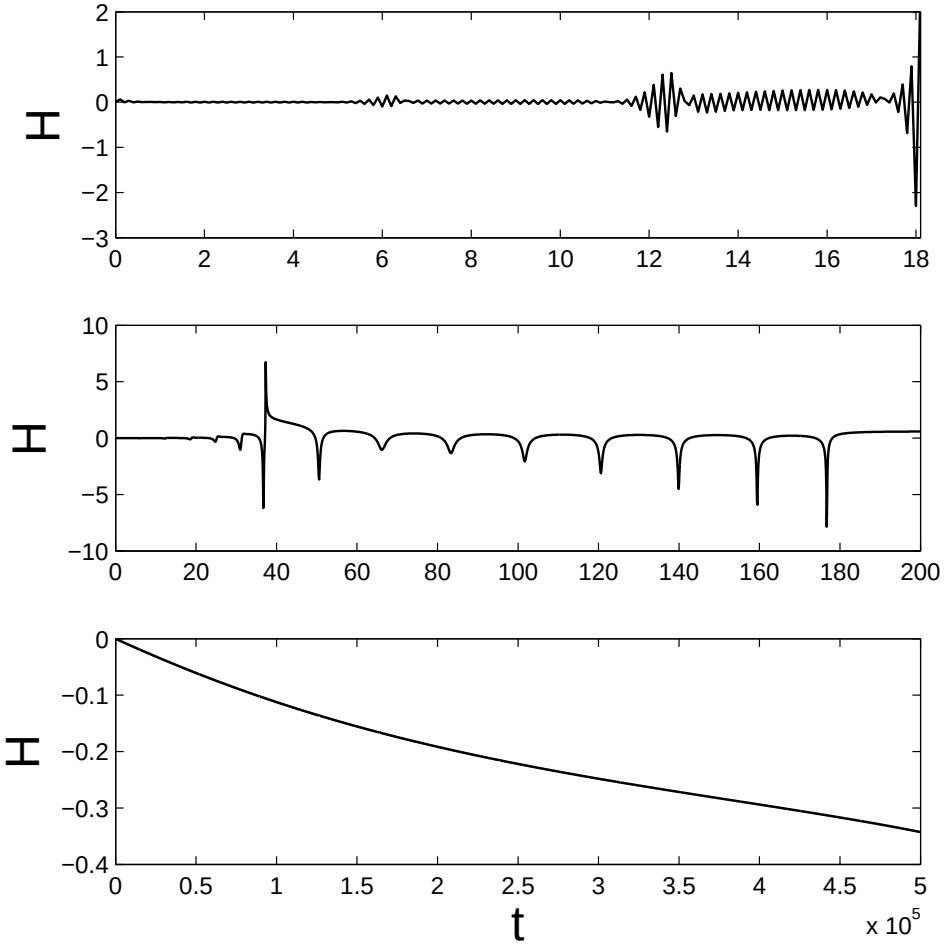

Figure 7.4.4: Hamiltonian for the numerical solution of Kepler's problem obtained with the 3- and 4-stage Lobatto IIIA-IIIB schemes (*top* and *middle*, respectively), and the non-variational Radau IIA method (*bottom*).

$$L(x_1, y_1, \ldots, x_K, y_K, \dot{x}_1, \dot{y}_1, \ldots, \dot{x}_K, \dot{y}_K) = \frac{1}{2}\sum_{i=1}^{K} \Gamma_i (x_i \dot{y}_i - y_i \dot{x}_i) - H(x_1, y_1, \ldots, x_K, y_K) \quad (7.4.4)$$

with the Hamiltonian

$$H(x_1, y_1, \ldots, x_K, y_K) = \frac{1}{4\pi}\sum_{i<j}^{K} \Gamma_i \Gamma_j \log\left((x_i - x_j)^2 + (y_i - y_j)^2\right) - H_0, \quad (7.4.5)$$

where (x_i, y_i) denotes the location of the i-th vortex and Γ_i its circulation, and H_0 is an arbitrary constant.

As a test problem we considered the system of $K = 2$ vortices with circulations $\Gamma_1 = 4$ and $\Gamma_2 = 2$, respectively, and distance $D = 1$ between them. The vortices rotate on concentric circles about their center of vorticity at $x_C = 0$ and $y_C = 0$. We took the initial condition at $x_1^{(0)} = \Gamma_2 D/(\Gamma_1 + \Gamma_2) \approx 0.33$, $y_1^{(0)} = 0$, $x_2^{(0)} = -\Gamma_1 D/(\Gamma_1 + \Gamma_2) \approx -0.67$ and $y_2^{(0)} = 0$. The analytic solution can be found (see [45]) as

$$\begin{aligned} x_1(t) &= \frac{\Gamma_2}{\Gamma_1 + \Gamma_2} D \cos \omega t, & x_2(t) &= -\frac{\Gamma_1}{\Gamma_1 + \Gamma_2} D \cos \omega t, \\ y_1(t) &= \frac{\Gamma_2}{\Gamma_1 + \Gamma_2} D \sin \omega t, & y_2(t) &= -\frac{\Gamma_1}{\Gamma_1 + \Gamma_2} D \sin \omega t, \end{aligned} \quad (7.4.6)$$

where $\omega = (\Gamma_1 + \Gamma_2)/(2\pi D^2)$. This is a periodic solution with period $T_{period} \approx 6.58$. See Figure 7.4.5.

We performed similar convergence tests as in Section 7.4.1. The value of the numerical solutions at time T=7 were compared against the exact solution (7.4.6). The max norm errors are depicted in Figure 7.4.6. The results are qualitatively the same as for Kepler's problem.

We set $H_0 = 0$ in (7.4.5), so that $H = 0$ for the considered solution. Figure 7.4.7 and Figure 7.4.8 show the behavior of the numerical Hamiltonian over a long integration interval. The 3- and 4-stage Lobatto IIIA-IIIB integrators performed better than for Kepler's problem. In the case of the Gauss methods the Hamiltonian stayed virtually constant—the visible minor erratic oscillations are the result of round-off errors. The Radau IIA scheme demonstrated a slow but systematic drift.

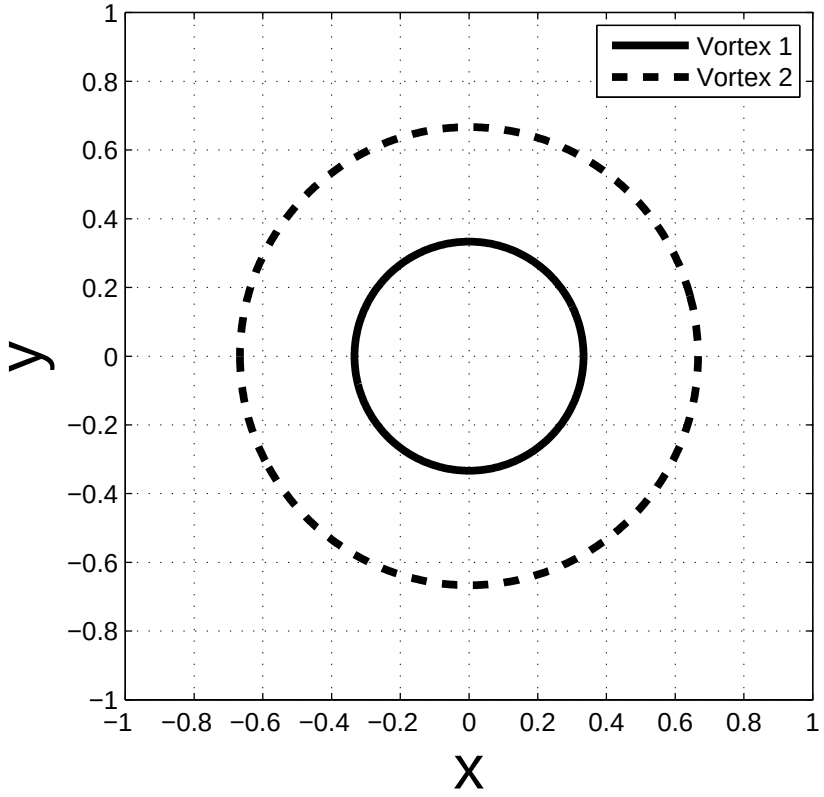

Figure 7.4.5: The circular trajectories of the two point vortices rotating about their vorticity center at $x_C = 0$ and $y_C = 0$.

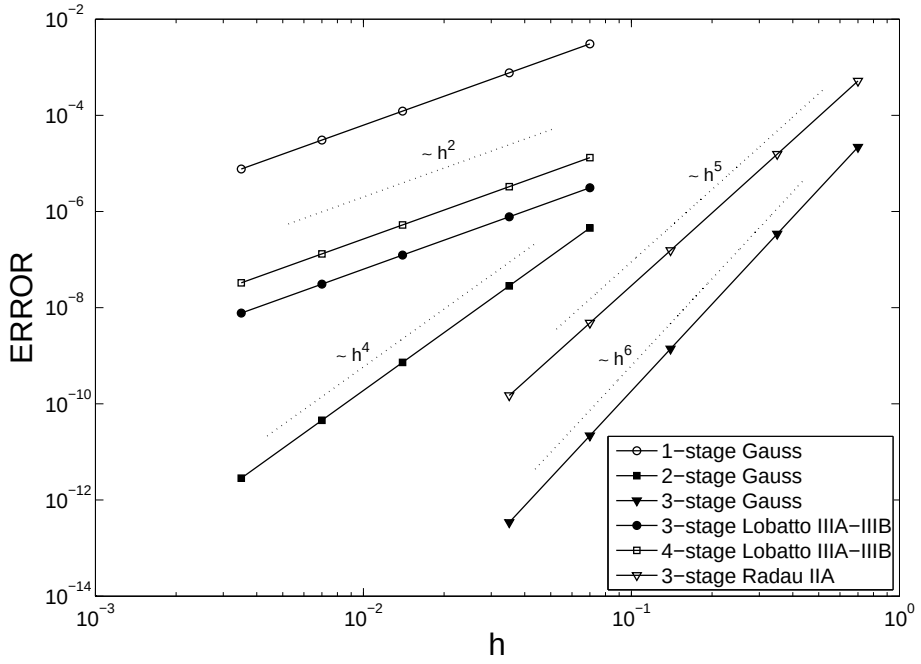

Figure 7.4.6: Convergence of several Runge-Kutta methods for the system of two point vortices.

7.4.3 Lotka-Volterra model

The dynamics of the growth of two interacting species can be modeled by the Lotka-Volterra equations

$$\begin{aligned} \dot{u} &= u(v-2), \\ \dot{v} &= v(1-u), \end{aligned} \tag{7.4.7}$$

where $u(t)$ denotes the number of predators and $v(t)$ the number of prey, and the constants 1 and 2 were chosen arbitrarily. These equations can be rewritten as the Poisson system

$$\begin{pmatrix} \dot{u} \\ \dot{v} \end{pmatrix} = \begin{pmatrix} 0 & uv \\ -uv & 0 \end{pmatrix} DH(u,v), \tag{7.4.8}$$

where the Hamiltonian is given by

$$H(u,v) = u - \log u + v - 2\log v - H_0 \tag{7.4.9}$$

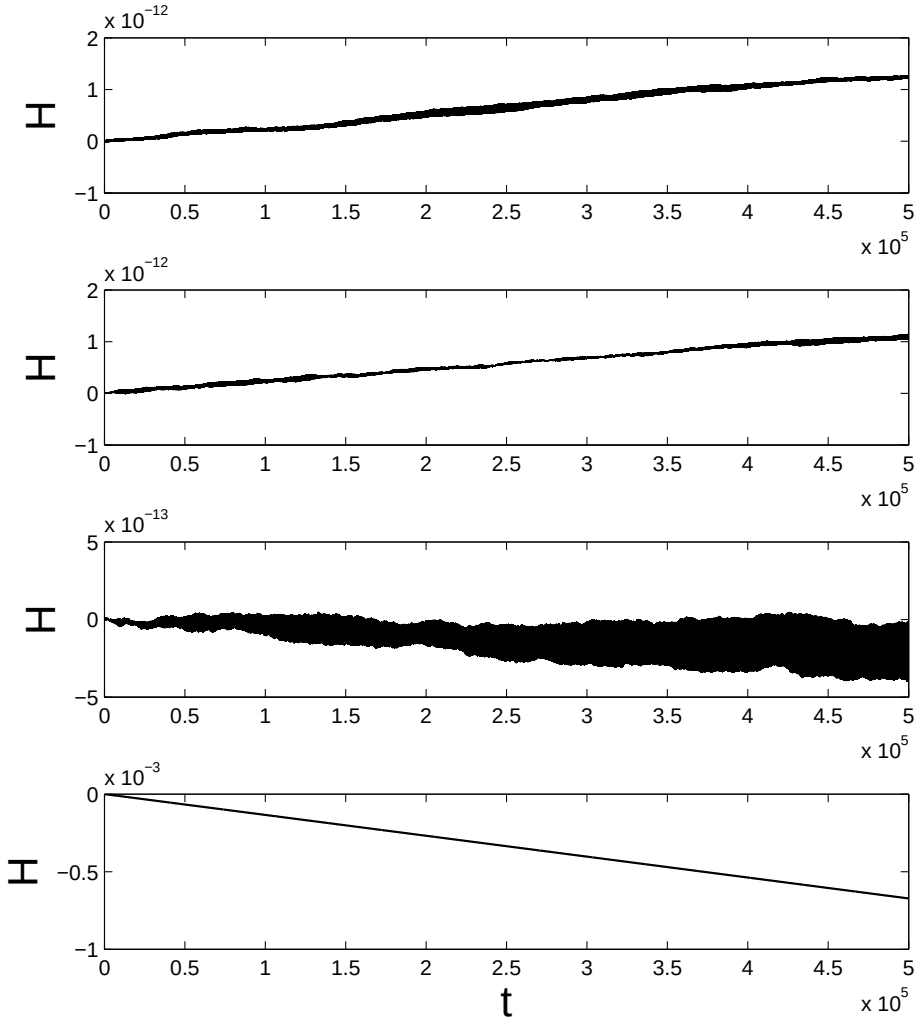

Figure 7.4.7: Hamiltonian for the 1-stage (*top*), 2-stage (*second*), and 3-stage (*third*) Gauss, and the 3-stage Radau IIA (*bottom*) methods applied to the system of two point vortices with the time step $h = 0.1$ over the time interval $[0, 5 \times 10^5]$.

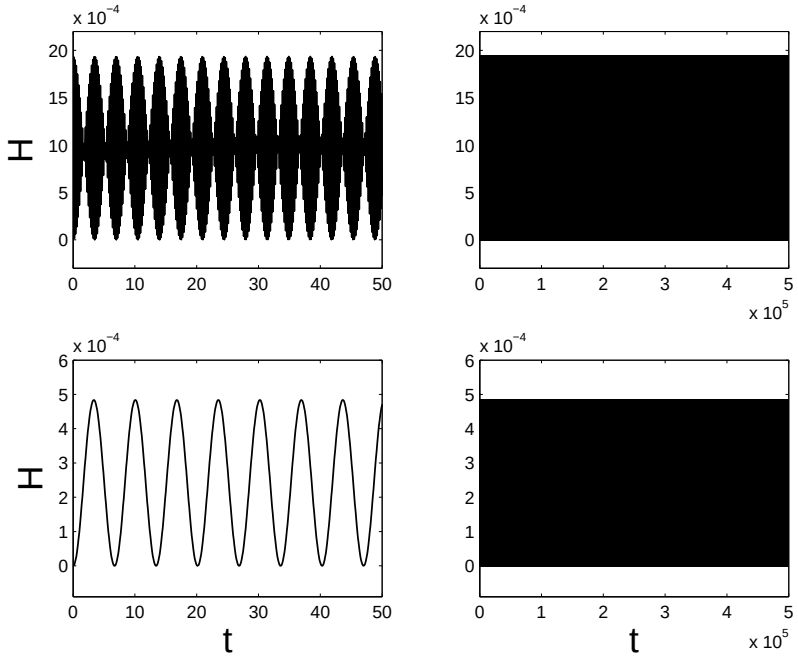

Figure 7.4.8: Hamiltonian conservation for the 3-stage (*top*) and 4-stage (*bottom*) Lobatto IIIA-IIIB methods applied to the system of two point vortices with the time step $h = 0.1$ over the time interval $[0, 5\times10^5]$ (*right column*), with a close-up on the initial interval $[0, 50]$ shown in the *left column*.

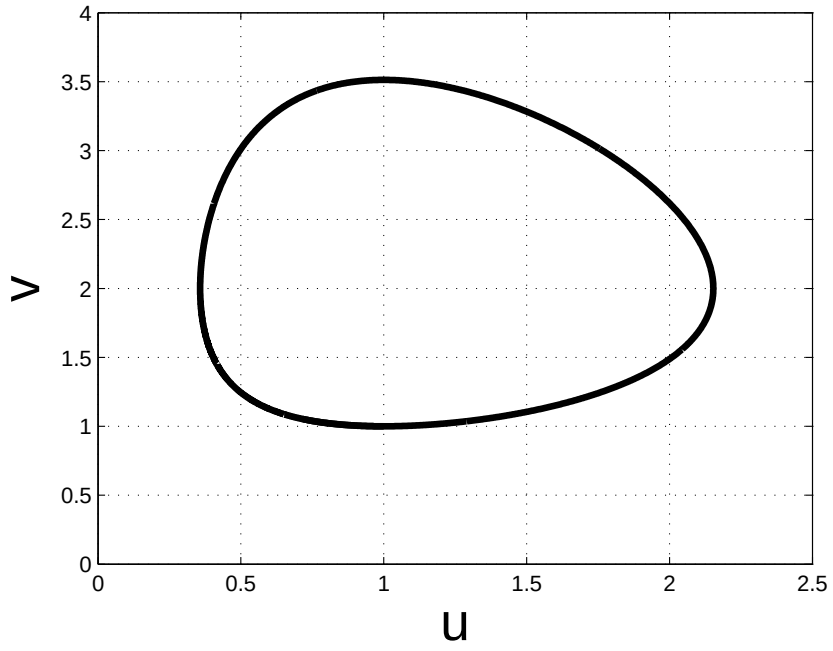

Figure 7.4.9: The reference solution for the Lotka-Volterra equations computed by integrating (7.3.26) until the time $T = 5$ using Verner's method with the time step $h = 10^{-7}$.

with an arbitraty constant H_0 (see [23]). Using an approach similar to the one presented in Section 7.4.1, one can easily verify that the Lagrangian

$$L(q, \dot{q}) = \left(\frac{\log q^2}{q^1} + q^2 \right) \dot{q}^1 + q^1 \dot{q}^2 - H(q) \tag{7.4.10}$$

reproduces the same equations of motion, where $q = (u, v)$. The coordinates $\alpha_\mu(q)$ (cf. Equation (7.1.2)) were chosen, so that the assumptions of Theorem 7.3.2 are satisfied for the considered Runge-Kutta methods.

As a test problem we considered the solution with the initial condition $q^1_{init} = 1$ and $q^2_{init} = 1$ (note that $q = (1, 2)$ is an equilibrium point). This is a periodic solution with period $T_{period} \approx 4.66$. A reference solution was computed by integrating (7.3.26) until the time $T = 5$, using Verner's method with the small time step $h = 10^{-7}$. The reference solution is depicted in Figure 7.4.9.

Convergence plots are shown in Figure 7.4.10. The convergence rates for the Gauss and Radau IIA methods are consistent with the theoretical results presented in Section 7.3.3.1—we see that the orders of the 2- and 3-stage Gauss schemes are reduced. The 2-stage Lobatto IIIA-IIIB scheme again proves to be inconsistent, and the 3- and 4-stage schemes converge

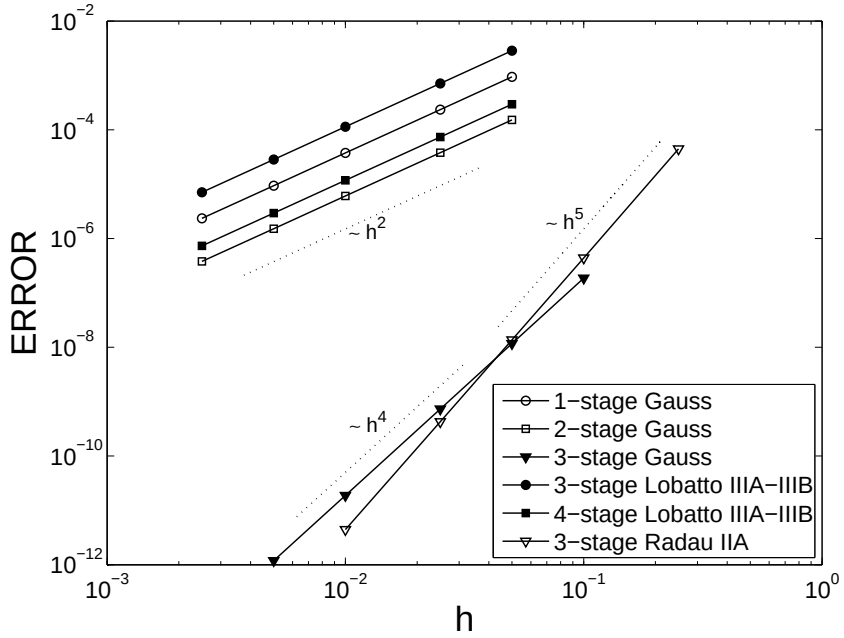

Figure 7.4.10: Convergence of several Runge-Kutta methods for the Lotka-Volterra model.

quadratically, just as in Section 7.4.1 and Section 7.4.2.

We performed another series of numerical experiments with the time step $h = 0.1$ to investigate the long time behavior of the considered integrators. The results are shown in Figure 7.4.11 and Figure 7.4.12. We set $H_0 = 2$ in (7.4.9), so that $H = 0$ for the considered solution. The 1- and 3-stage Gauss methods again show excellent Hamiltonian conservation over a long time interval. The 2-stage Gauss method, however, does not perform equally well—the Hamiltonian oscillates with an increasing amplitude over time, until the computations finally break down. The Lobatto IIIA-IIIB methods show similar problems as in Section 7.4.1. The non-variational Radau IIA method yields an accurate solution, but demonstrates a steady drift in the Hamiltonian.

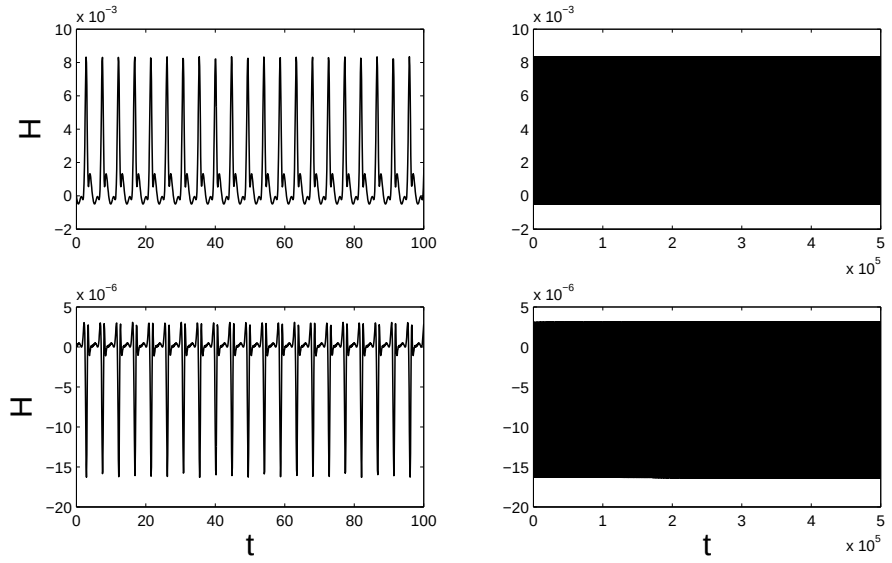

Figure 7.4.11: Hamiltonian conservation for the 1-stage (*top row*) and 3-stage (*bottom row*) Gauss methods applied to the Lotka-Volterra model with the time step $h = 0.1$ over the time interval $[0, 5\times10^5]$ (*right column*), with a close-up on the initial interval $[0, 100]$ shown in the *left column*.

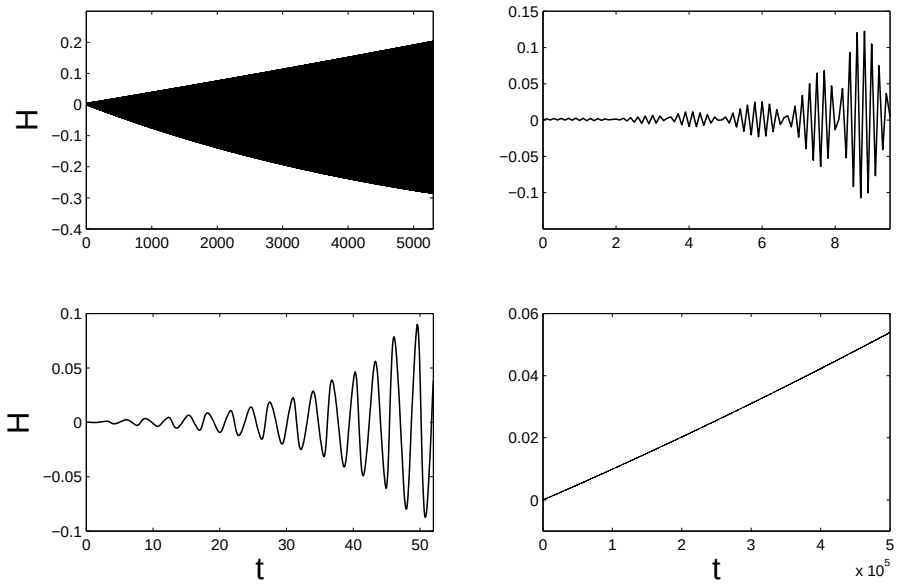

Figure 7.4.12: Hamiltonian for the numerical solution of the Lotka-Volterra model obtained with the 2-stage Guass method (*top left*), the 3- and 4-stage Lobatto IIIA-IIIB schemes (*top right* and *bottom left*, respectively), and the non-variational Radau IIA method (*bottom right*).

Chapter 8

Summary and future work

We have proposed two general ideas on how r-adaptive meshes can be applied in geometric numerical integration of Lagrangian partial differential equations. We have constructed several variational and multisymplectic integrators and discussed their properties. We have used the Sine-Gordon model and its solitonic solutions to test our integrators numerically.

We have also analyzed a class of degenerate systems described by Lagrangians that are linear in velocities, and presented a way to construct higher-order variational integrators for such systems. We have pointed out how the theory underlying variational integration is different from the non-degenerate case and we have made a connection with numerical integration of differential-algebraic equations. Finally, we have performed numerical experiments for several example models.

Our work can be extended in many directions. Interestingly, it also opens many questions in geometric mechanics and multisymplectic field theory. Addressing those questions will have a broader impact on the field of geometric numerical integration.

Non-hyperbolic equations

The special form of the Lagrangian density (4.2.6) we considered leads to a hyperbolic PDE, which poses a challenge to r-adaptive methods, as at each time step the mesh is adapted *globally* in response to *local* changes in the solution. *Causality* and the structure of the characteristic lines of hyperbolic systems make r-adaptation prone to instabilities and integration in time has to be performed carefully. The literature on r-adaptation almost entirely focuses on parabolic problems (see [7], [28] and references therein). Therefore, it would be interesting to apply our methods to PDEs that are first-order in time, for instance, the Korteweg-de Vries, Nonlinear Schrödinger, or Camassa-Holm equations. All

three equations are first-order in time and are not hyperbolic in nature. Moreover, all can be derived as Lagrangian field theories (see [8], [9], [10], [11], [16], [19], [34]). The Nonlinear Schrödinger equation has applications to optics and water waves, whereas the Korteweg-de Vries and Camassa-Holm equations were introduced as models for waves in shallow water. All equations possess interesting solitonic solutions. The purpose of r-adaptation would be to improve resolution, for instance, to track the motion of solitons by placing more mesh points near their centers and making the mesh less dense in the asymptotically flat areas.

Hamiltonian Field Theories

Variational multisymplectic integrators for field theories have been developed in the Lagrangian setting ([34], [39]). However, many interesting field theories are formulated in the Hamiltonian setting. They may not even possess a Lagrangian formulation. It would be interesting to construct Hamiltonian variational integrators for multisymplectic PDEs by generalizing the variational characterization of discrete Hamiltonian mechanics. This would allow one to handle Hamiltonian PDEs without the need for converting them to the Lagrangian framework. Recently Leok & Zhang [35] and Vankerschaver & Liao & Leok [66] have laid foundations for such integrators. It would also be interesting to see if the techniques we used in our work could be applied in order to construct r-adaptive Hamiltonian integrators.

Time adaptation based on local error estimates

One of the challenges of r-adaptation is that it requires solving differential-algebraic or stiff ordinary differential equations. This is because there are two different time scales present: one defined by the physics of the problem and one following from the strategy we use to adapt the mesh. Stiff ODEs and DAEs are known to require time integration with an adaptive step size control based on local error estimates (see [6], [26]). In our work we used constant time-stepping, as adaptive step size control is difficult to combine with geometric numerical integration. Classical step size control is based on past information only, time symmetry is destroyed and with it the qualitative properties of the method. Hairer & Söderlind [25] developed explicit, reversible, symmetry-preserving, adaptive step size selection algorithms for geometric integrators, but their method is not based on local error estimation, thus it is not useful for r-adaptation. Symmetric error estimators are considered in [32] and

some promising results are discussed. Hopefully, the ideas presented in those papers could be combined and generalized. The idea of Asynchronous Variational Integrators (see [36]) could also be useful here, as this would allow one to use a different time step for each cell of the mesh. The structure-preserving multiscale techniques proposed in [61] and [62] might also be of certain interest.

Constrained multisymplectic field theories

The multisymplectic form formula (2.6.9) was first introduced in [39]. The authors, however, consider only unconstrained field theories. In our work we start with the unconstrained field theory (4.0.1), but upon choosing an adaptation strategy represented by the constraint $G = 0$ we obtain a constrained theory, as described in Section 4.2 and Section 5.2. Moreover, this constraint is essentially nonholonomic, as it contains derivatives of the fields, and the equations of motion are obtained using the *vakonomic* approach (also called variational nonholonomic) rather than the Lagrange-d'Alembert principle. All that gives rise to many very interesting and general questions. Is there a multisymplectic form formula for such theories? Is it derived in a similar fashion? Do variational integrators obtained this way satisfy some discrete multisymplectic form formula? These issues have been touched upon in [40], but are by no means resolved.

Mesh smoothing and variational nonholonomic integrators

The major challenge of r-adaptive methods is *mesh crossing*, which occurs when two mesh points collapse or cross each other. In order to avoid mesh crossing and retain good mesh quality, mesh smoothing techniques were developed (see Section 3.2.2 and [7], [28]). They essentially attempt to regularize the exact equidistribution constraint $G = 0$ by replacing it with the condition $\epsilon\, \partial X/\partial t = G$, where ϵ is a small parameter. This can be interpreted as adding some attraction and repulsion pseudoforces between mesh points. If one applies the Lagrange multiplier approach to r-adaptation as described in Section 4.2, then upon finite element discretization one obtains a finite dimensional Lagrangian system with a nonholonomic constraint. This constraint is enforced using the vakonomic (nonholonomic variational) formulation. Variational integrators for systems with nonholonomic constraints have been developed mostly in the Lagrange-d'Alembert setting. Surprisingly, there seems to be virtually no literature regarding discrete vakonomic mechanics. In a recent paper, Gar-

cia & Fernandez & Rodrigo [17] address variational integrators for vakonomic systems. The ideas presented in that paper could be used to design structure-preserving mesh smoothing techniques.

Variational integrators for Lagrangians linear in velocities

In Section 7.4.3 we presented our numerical results for the Lotka-Volterra model, which is an example of a system for which the coordinate functions $\alpha_\mu(q)$ are nonlinear. The 1- and 3-stage Gauss methods performed exceptionally well and preserved the Hamiltonian over a very long integration time. It would be interesting to perform a backward error (or similar) analysis to check if this behavior is generic. If confirmed, our variational approach could provide a new way to construct geometric integrators for a broader class of Poisson systems.

It would also be interesting to further consider *constrained* systems with Lagrangians that are linear in velocities and construct associated higher-order variational integrators. This would allow one to generalize the space-adaptive methods presented in Chapter 4 and Chapter 5 to degenerate field theories, such as the nonlinear Schrödinger, KdV or Camassa-Holm equations.

Bibliography

[1] E. Allgower and K. Georg. *Introduction to Numerical Continuation Methods*. Classics in applied mathematics. Society for Industrial and Applied Mathematics, 2003.

[2] G. Beckett, J. Mackenzie, A. Ramage, and D. Sloan. On the numerical solution of one-dimensional PDEs using adaptive methods based on equidistribution. *Journal of Computational Physics*, 167(2):372 – 392, 2001.

[3] A. Bloch. *Nonholonomic Mechanics and Control*. Interdisciplinary Applied Mathematics. Springer, 2003.

[4] A. M. Bloch and P. E. Crouch. Optimal control, optimization, and analytical mechanics. In J. Baillieul and J. Willems, editors, *Mathematical Control Theory*, pages 268–321. Springer New York, 1999.

[5] A. M. Bloch, P. Krishnaprasad, J. E. Marsden, and R. M. Murray. Nonholonomic mechanical systems with symmetry. *Archive for Rational Mechanics and Analysis*, 136(1):21–99, 1996.

[6] K. Brenan, S. Campbell, and L. Petzold. *Numerical Solution of Initial-Value Problems in Differential-Algebraic Equations*. Classics in Applied Mathematics. Society for Industrial and Applied Mathematics, 1996.

[7] C. J. Budd, W. Huang, and R. D. Russell. Adaptivity with moving grids. *Acta Numerica*, 18:111–241, 2009.

[8] R. Camassa and D. D. Holm. An integrable shallow water equation with peaked solitons. *Phys. Rev. Lett.*, 71:1661–1664, 1993.

[9] R. Camassa, D. D. Holm, and J. Hyman. A new integrable shallow water equation. *Adv. App. Mech.*, 31:1–31, 1994.

[10] J.-B. Chen and M.-Z. Qin. A multisymplectic variational integrator for the nonlinear Schrödinger equation. *Numerical Methods for Partial Differential Equations*, 18(4):523–536, 2002.

[11] P. Drazin and R. Johnson. *Solitons: An Introduction*. Cambridge Computer Science Texts. Cambridge University Press, 1989.

[12] D. G. Ebin and J. Marsden. Groups of diffeomorphisms and the motion of an incompressible fluid. *Annals of Mathematics*, 92(1):102–163, 1970.

[13] T. Ergenç and B. Karasözen. Poisson integrators for Volterra lattice equations. *Applied Numerical Mathematics*, 56(6):879–887, 2006.

[14] L. Evans. *Partial Differential Equations*. Graduate studies in mathematics. American Mathematical Society, 2010.

[15] L. Faddeev and R. Jackiw. Hamiltonian reduction of unconstrained and constrained systems. *Physical Review Letters*, 60(17):1692–1694, 1988.

[16] E. Faou. *Geometric Numerical Integration and Schrödinger Equations*. Zurich lectures in advanced mathematics. European Mathematical Society, 2012.

[17] P. L. García, A. Fernández, and C. Rodrigo. Variational integrators in discrete vakonomic mechanics. *Revista de la Real Academia de Ciencias Exactas, Fisicas y Naturales. Serie A. Matematicas*, 106(1):137–159, 2012.

[18] M. Gotay. *Presymplectic manifolds, geometric constraint theory and the Dirac-Bergmann theory of constraints*. PhD thesis, University of Maryland, College Park, 1979.

[19] M. Gotay. A multisymplectic approach to the KdV equation. In *Differential Geometric Methods in Theoretical Physics*, volume 250, pages 295–305. NATO Advanced Science Institutes Series C: Mathematical and Physical Sciences, 1988.

[20] M. Gotay. A multisymplectic framework for classical field theory and the calculus of variations I: covariant Hamiltonian formulation. In M. Francavigila, editor, *Mechanics, analysis and geometry: 200 years after Lagrange*, pages 203–235. North-Holland, Amsterdam, 1991.

[21] M. Gotay, J. Isenberg, J. Marsden, and R. Montgomery. Momentum maps and classical relativistic fields. Part I: Covariant field theory. Unpublished, arXiv:physics/9801019, 1997.

[22] E. Hairer, C. Lubich, and M. Roche. *The numerical solution of differential-algebraic systems by Runge-Kutta methods*. Lecture Notes in Math. 1409. Springer Verlag, 1989.

[23] E. Hairer, C. Lubich, and G. Wanner. *Geometric Numerical Integration: Structure-Preserving Algorithms for Ordinary Differential Equations*. Springer Series in Computational Mathematics. Springer, New York, 2002.

[24] E. Hairer, S. Nørsett, and G. Wanner. *Solving Ordinary Differential Equations I: Non-stiff Problems*, volume 8 of *Springer Series in Computational Mathematics*. Springer, 2nd edition, 1993.

[25] E. Hairer and G. Söderlind. Explicit, time reversible, adaptive step size control. *SIAM J. Sci. Comput.*, 26(6):1838–1851, 2005.

[26] E. Hairer and G. Wanner. *Solving Ordinary Differential Equations II: Stiff and Differential-Algebraic Problems*, volume 14 of *Springer Series in Computational Mathematics*. Springer, 2nd edition, 1996.

[27] W. Huang, Y. Ren, and R. D. Russell. Moving mesh partial differential equations (MMPDEs) based on the equidistribution principle. *SIAM J. Numer. Anal.*, 31(3):709–730, June 1994.

[28] W. Huang and R. Russell. *Adaptive Moving Mesh Methods*, volume 174 of *Applied Mathematical Sciences*. Springer Verlag, 2011.

[29] W. Huang and R. D. Russell. Analysis of moving mesh partial differential equations with spatial smoothing. *SIAM J. Numer. Anal*, 31:709–730, 1997.

[30] W. Huang and R. D. Russell. Moving mesh strategy based on a gradient flow equation for two-dimensional problems. *SIAM J. Sci. Comp.*, 20(5):998–1015, 1999.

[31] L. Jay. Symplectic partitioned Runge-Kutta methods for constrained Hamiltonian systems. *SIAM Journal on Numerical Analysis*, 33(1):368–387, 1996.

[32] L. O. Jay. Structure preservation for constrained dynamics with super partitioned additive Runge–Kutta methods. *SIAM Journal on Scientific Computing*, 20(2):416–446, 1998.

[33] B. Karasözen. Poisson integrators. *Mathematical and Computer Modelling*, 40(11):1225–1244, 2004.

[34] S. Kouranbaeva and S. Shkoller. A variational approach to second-order multisymplectic field theory. *Journal of Geometry and Physics*, 35(4):333–366, 2000.

[35] M. Leok and J. Zhang. Discrete Hamiltonian variational integrators. *IMA Journal of Numerical Analysis*, 31(4):1497–1532, 2011.

[36] A. Lew, J. E. Marsden, M. Ortiz, and M. West. Asynchronous variational integrators. *Archive for Rational Mechanics and Analysis*, 167(2):85–146, 2003.

[37] C. Lubich. Integration of stiff mechanical systems by Runge-Kutta methods. *Zeitschrift für angewandte Mathematik und Physik ZAMP*, 44(6):1022–1053, 1993.

[38] J. Marsden and T. Ratiu. *Introduction to Mechanics and Symmetry*, volume 17 of *Texts in Applied Mathematics*. Springer Verlag, 1994.

[39] J. E. Marsden, G. W. Patrick, and S. Shkoller. Multisymplectic geometry, variational integrators, and nonlinear PDEs. *Communications in Mathematical Physics*, 199(2):351–395, 1998.

[40] J. E. Marsden, S. Pekarsky, S. Shkoller, and M. West. Variational methods, multisymplectic geometry and continuum mechanics. *Journal of Geometry and Physics*, 38(3):253–284, 2001.

[41] J. E. Marsden and M. West. Discrete mechanics and variational integrators. *Acta Numerica*, 10(1):357–514, 2001.

[42] R. I. McLachlan and G. R. W. Quispel. Geometric integrators for ODEs. *Journal of Physics A: Mathematical and General*, 39(19):5251–5285, 2006.

[43] K. Miller. Moving finite elements II. *SIAM Journal on Numerical Analysis*, 18(6):1033–1057, 1981.

[44] K. Miller and R. N. Miller. Moving finite elements I. *SIAM Journal on Numerical Analysis*, 18(6):1019–1032, 1981.

[45] P. Newton. *The N-Vortex Problem: Analytical Techniques*, volume 145 of *Applied Mathematical Sciences*. Springer Verlag, New York, 2001.

[46] H. Nijmeijer and A. van der Schaft. *Nonlinear Dynamical Control Systems*. Springer, New York, 1990.

[47] D. Pavlov, P. Mullen, Y. Tong, E. Kanso, J. E. Marsden, and M. Desbrun. Structure-preserving discretization of incompressible fluids. *Physica D: Nonlinear Phenomena*, 240(6):443–458, 2011.

[48] P. J. Rabier. Implicit differential equations near a singular point. *Journal of Mathematical Analysis and Applications*, 144(2):425–449, 1989.

[49] P. J. Rabier and W. C. Rheinboldt. A general existence and uniqueness theory for implicit differential-algebraic equations. *J. Diff. and Integral Equations*, 4:563–582, 1991.

[50] P. J. Rabier and W. C. Rheinboldt. A geometric treatment of implicit differential-algebraic equations. *Journal of Differential Equations*, 109(1):110–146, 1994.

[51] P. J. Rabier and W. C. Rheinboldt. On impasse points of quasilinear differential-algebraic equations. *J. Math. Anal. Appl.*, 181:429–454, 1994.

[52] P. J. Rabier and W. C. Rheinboldt. On the computation of impasse points of quasilinear differential-algebraic equations. *Mathematics of Computation*, 62(205):133–154, 1994.

[53] P. J. Rabier and W. C. Rheinboldt. Theoretical and numerical analysis of differential-algebraic equations. In P. G. Ciarlet and J.-L. Lion, editors, *Handbook of Numerical Analysis*, volume 8, pages 183–540. Elsevier Science B.V., 2002.

[54] R. Rajaraman. *Solitons and Instantons: An Introduction to Solitons and Instantons in Quantum Field Theory*. North-Holland personal library. North-Holland Publishing Company, Amsterdam, 1982.

[55] G. Reißig and H. Boche. On singularities of autonomous implicit ordinary differential equations. *Circuits and Systems I: Fundamental Theory and Applications, IEEE Transactions on*, 50(7):922–931, 2003.

[56] C. W. Rowley and J. E. Marsden. Variational integrators for degenerate Lagrangians, with application to point vortices. In *Decision and Control, 2002, Proceedings of the 41st IEEE Conference on*, volume 2, pages 1521–1527. IEEE, 2002.

[57] J. M. Sanz-Serna. Symplectic integrators for Hamiltonian problems: an overview. *Acta Numerica*, 1:243–286, 1992.

[58] D. Saunders. *The Geometry of Jet Bundles*, volume 142 of *London Mathematical Society Lecture Note Series*. Cambridge University Press, 1989.

[59] A. Stern, Y. Tong, M. Desbrun, and J. E. Marsden. Variational integrators for Maxwell's equations with sources. *PIERS Online*, 4(7):711–715, 2008.

[60] Y. B. Suris. Integrable discretizations for lattice system: local equations of motion and their Hamiltonian properties. *Reviews in Mathematical Physics*, 11(6):727–822, 1999.

[61] M. Tao, H. Owhadi, and J. E. Marsden. Non-intrusive and structure preserving multiscale integration of stiff ODEs, SDEs and Hamiltonian systems with hidden slow dynamics via flow averaging. *SIAM Multiscale Model. Simul.*, 8(4):1269–1324, 2010.

[62] M. Tao, H. Owhadi, and J. E. Marsden. Space-time FLAVORS: finite difference, multisymplectic, and pseudospectral integrators for multiscale PDEs. *Dyn. Partial Differ. Equ.*, 8(1):21–45, 2011.

[63] T. M. Tyranowski and M. Desbrun. R-adaptive multisymplectic and variational integrators. *IMA Journal of Numerical Analysis*, 2013. (submitted, arXiv:1303.6796).

[64] T. M. Tyranowski and M. Desbrun. Variational partitioned Runge-Kutta methods for Lagrangians linear in velocities. In preparation, 2013.

[65] J. Vankerschaver and M. Leok. A novel formulation of point vortex dynamics on the sphere: geometrical and numerical aspects. *J. Nonlin. Sci.*, 2012. (to appear, arXiv:1211.4560).

[66] J. Vankerschaver, C. Liao, and M. Leok. Generating functionals and Lagrangian PDEs. Unpublished, arXiv:1111.0280, 2011.

[67] A. Wacher. A comparison of the String Gradient Weighted Moving Finite Element method and a Parabolic Moving Mesh Partial Differential Equation method for solutions of partial differential equations. *Central European Journal of Mathematics*, 11(4):642–663, 2013.

[68] M. Zielonka, M. Ortiz, and J. Marsden. Variational r-adaption in elastodynamics. *International Journal for Numerical Methods in Engineering*, 74(7):1162–1197, 2008.